

# CHAPTER 4

## *Structural Features and Reactivity of (*sp*)PdCl<sub>2</sub>: A Model for Selectivity in the Oxidative Kinetic Resolution of Secondary Alcohols.*

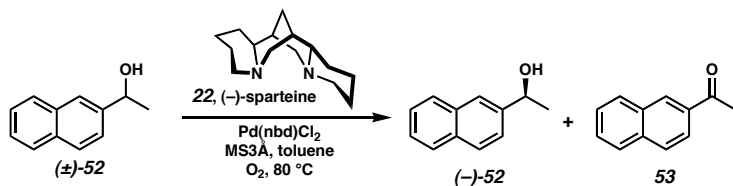
### 4.1 INTRODUCTION AND BACKGROUND

#### 4.1.1 *Introduction*

Palladium-catalyzed aerobic oxidation has been known for nearly a century since the discovery by Wieland that this metal could convert alcohols to aldehydes in aqueous media.<sup>1</sup> Modern developments to this reaction were initiated in 1977 by Schwartz and Blackburn, who reported that palladium(II) acetate and sodium acetate could aerobically oxidize alcohols to carbonyl compounds.<sup>2,3</sup> More recently, the Stoltz group has developed the enantioselective aerobic oxidation of secondary alcohols by palladium(II) and (–)-sparteine (**22**). An example of this transformation is shown in Scheme 4.1.1. While numerous improvements to oxidative kinetic resolution have been made, and the mechanism has been analyzed kinetically, there have been no reports detailing a structural model for asymmetric induction by (–)-sparteine (**22**) in these reactions.

Herein, we describe experiments that probe the origins of stereoselectivity in the oxidation and present a model for the absolute stereochemical outcome. This model is based on the reactivity and solid state structures of a series of palladium(II) complexes, including the first reported structure of a chiral palladium alkoxide relevant to this system. Calculations and studies of the diastereomers of (–)-sparteine (**22**) lend further support to our model, and highlight the alkaloid (–)-sparteine (**22**) as a unique ligand.

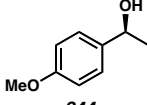
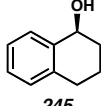
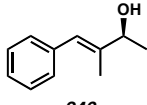
*Scheme 4.1.1*



#### 4.1.2 Background

Since the development of the oxidative kinetic resolution of secondary alcohols in our laboratories by graduate student Eric Ferreira,<sup>4</sup> several improvements have been made to the catalytic system through the work of graduate student Jeff Bagdanoff.<sup>5,6</sup> These results are summarized in Table 4.1.1 for three different substrates. The original conditions, which employ toluene, can be accelerated by the addition of cesium carbonate and *t*-butanol. The use of chloroform as a solvent permits reaction at a lower temperature, and facilitates the use of air as a reoxidant. Graduate students David Ebner and Daniel Caspi have carried out extensive studies of the substrate scope under these reaction conditions, and have employed the reaction in the synthesis of certain pharmaceutical intermediates.<sup>7</sup> Despite these advancements, we have been unable to find any ligand other than (–)-sparteine (**22**) capable of inducing selectivity in the reaction.<sup>8</sup>

Table 4.1.1 Oxidative kinetic resolution of secondary alcohols.

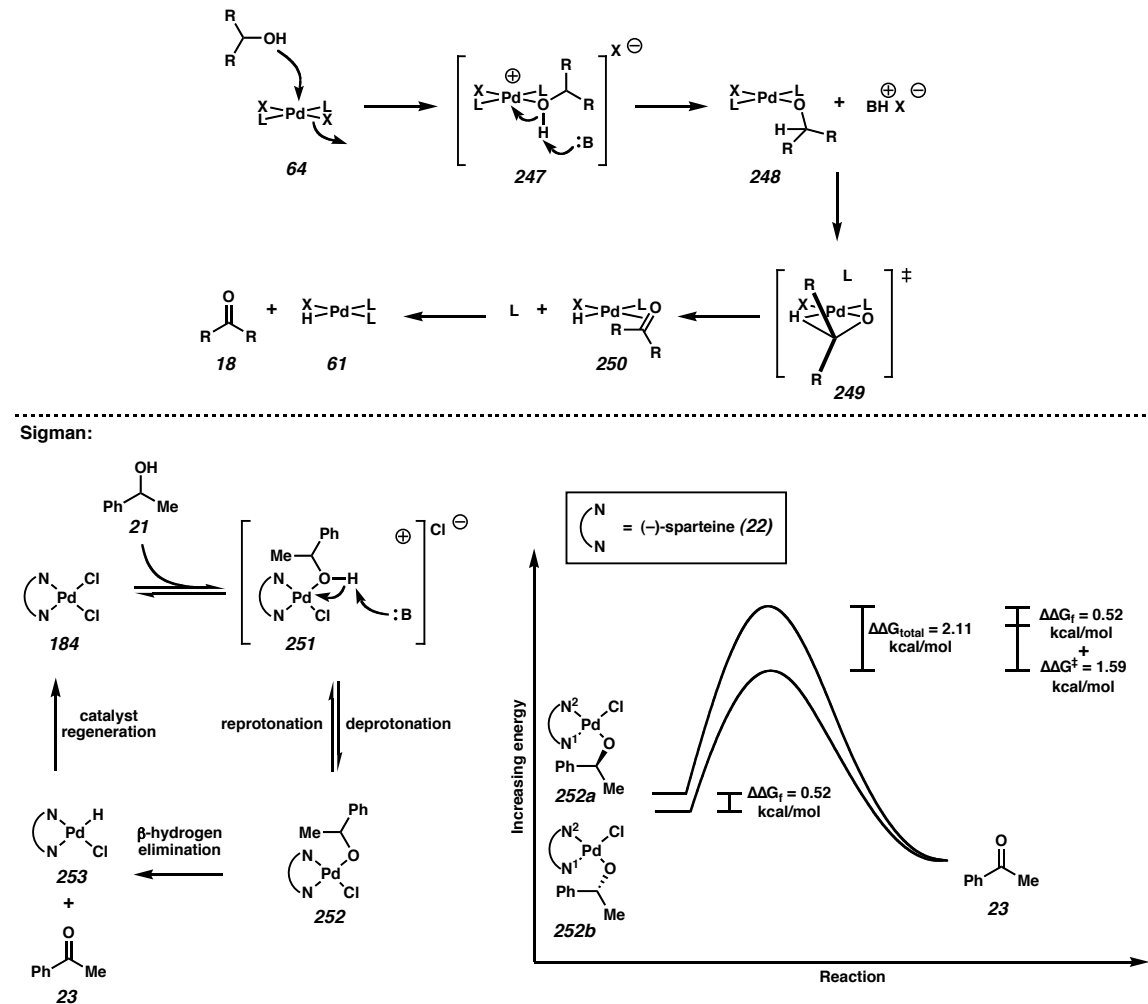
	$\text{Pd}(\text{nbd})\text{Cl}_2^{\text{a}}$ MS3Å (-)sparteine (22)			
	Original <sup>b</sup> $\text{O}_2$ , toluene 80 °C	Rate Accelerated <sup>c</sup> $\text{O}_2$ , toluene, 60 °C $\text{Cs}_2\text{CO}_3$ , <i>t</i> -BuOH	Chloroform / $\text{O}_2$ <sup>d</sup> $\text{O}_2$ , $\text{CHCl}_3$ , 23 °C $\text{Cs}_2\text{CO}_3$	Chloroform / Air <sup>e</sup> Air, $\text{CHCl}_3$ , 23 °C $\text{Cs}_2\text{CO}_3$
	96 h 67% conv 98% ee s = 12	9.5 h 67% conv 99.5% ee s = 15	48 h 63% conv 99.9% ee s = 27	24 h 62% conv 99.8% ee s = 25
	40 h 69% conv 99.8% ee s = 16	12 h 62% conv 99% ee s = 21	24 h 58% conv 98% ee s = 28	16 h 60% conv 99.6% ee s = 28
	120 h 70% conv 92% ee s = 6.6	12 h 65% conv 88% ee s = 7.5	48 h 63% conv 98.7% ee s = 18	44 h 65% conv 98.9% ee s = 16

<sup>a</sup> nbd = norbornadiene, s = selectivity factor, see Ref. 31. 500 mg MS3Å/mmol substrate was used for all four sets of conditions. <sup>b</sup> 5 mol% palladium catalyst, 0.20 equiv (–)-sparteine (22), 0.1 M in toluene. <sup>c</sup> 5 mol% palladium catalyst, 0.20 equiv (–)-sparteine (22), 0.5 equiv  $\text{Cs}_2\text{CO}_3$ , 1.5 equiv *t*-BuOH, 0.25 M in toluene. <sup>d</sup> 5 mol% palladium catalyst, 0.12 equiv (–)-sparteine (22), 0.40 equiv  $\text{Cs}_2\text{CO}_3$ , 0.25 M in  $\text{CHCl}_3$ . <sup>e</sup> (sp)PdCl<sub>2</sub> was used as catalyst (5 mol%). 0.07 equiv (–)-sparteine (22), 0.4 equiv  $\text{Cs}_2\text{CO}_3$ , 0.25 M in  $\text{CHCl}_3$ . Reactions were run open to air through a short drying tube of Drierite.

In general, the oxidation of alcohols to carbonyl compounds by palladium(II) most likely involves associative alcohol substitution at the palladium center (**64**), deprotonation of the resulting palladium alcohol complex (**247**) by base to form a palladium alkoxide (**248**), and  $\beta$ -hydrogen elimination to the carbonyl compound (**18**, Figure 4.1.1, top).<sup>9</sup> Sigman and coworkers have carried out extensive kinetic studies of the oxidative kinetic resolution using ((–)-sparteine)PdCl<sub>2</sub> (**184**, (sp)PdCl<sub>2</sub>), (–)-sparteine (**22**), and O<sub>2</sub>.<sup>10</sup> In their original publication, they report that  $\beta$ -hydrogen elimination is rate determining at high base concentration, and propose that the observed enantioselectivity results from a combination of the respective energy barriers for the elimination ( $\Delta G^{\ddagger}$ ) and the thermodynamic stabilities of the alkoxide complexes (**252a** and **252b**,  $\Delta G_f$ , Figure 4.1.1, bottom).<sup>10b</sup> A more recent publication from the same group has

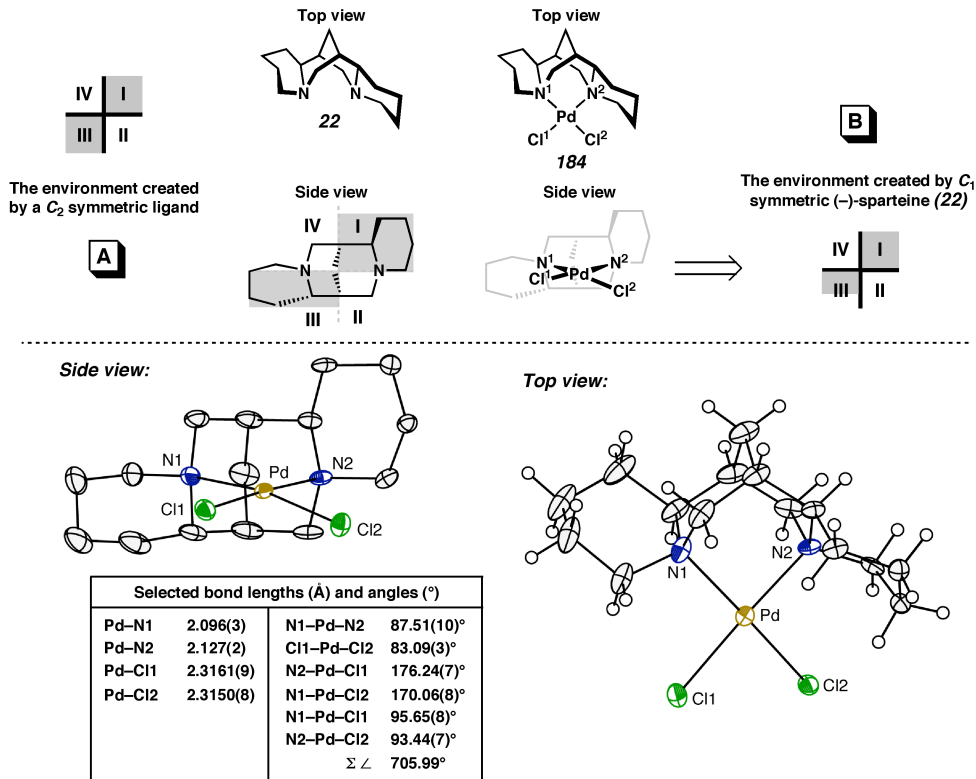
revised this original proposal, but maintains that  $\beta$ -hydrogen elimination from and reprotonation of the intermediate palladium alkoxide are the key kinetic influences on the selectivity.<sup>10a</sup> The alkoxide of the enantiomer that is oxidized (**252b**) undergoes  $\beta$ -hydrogen elimination more rapidly than the other (**252a**), and is reprotonated more slowly.

Figure 4.1.1 Alcohol oxidation by palladium.

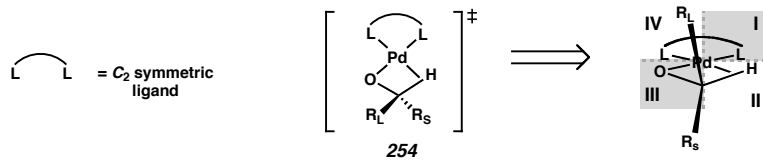


In this analysis **22** was treated as a  $C_2$  symmetric ligand.<sup>11</sup> Only two diastereomeric palladium alkoxides (**252a** and **252b**) are considered, in which the alkoxide is trans to N<sup>2</sup>. In fact, four diastereomers are possible, the remaining two arising from alkoxide

coordination trans to N<sup>1</sup> (not shown). Since the introduction of the DIOP ligand by Kagan in 1972,<sup>12</sup> C<sub>2</sub> symmetry has been a dominant guiding force in the design of improved ligands for enantioselective transition-metal catalyzed reactions. In this respect a C<sub>2</sub> symmetric scaffold offers distinct advantages: the presence of a symmetry axis reduces the number of competing diastereomeric reaction pathways, enables a more straightforward analysis of substrate–catalyst interactions, and simplifies mechanistic and structural studies.<sup>13</sup> The chiral scaffold of a C<sub>2</sub> symmetric ligand can be modeled by a quadrant diagram of the ligand–metal complex, in which quadrants I and III (or II and IV) are equivalently hindered (Figure 4.1.2A). (sp)PdCl<sub>2</sub> (**184**) can be mapped onto this quadrant diagram, but the hemispheres of this catalyst are clearly nonequivalent. As can be seen from the solid-state structure, Cl<sup>1</sup> and Cl<sup>2</sup> are located in different environments, due to the different steric influence of each of the flanking piperidine rings of (–)-sparteine (**22**).<sup>14</sup> Thus, it is perhaps more accurate to depict a quadrant diagram for (–)-sparteine (**22**) that has quadrant I fully blocked, but quadrant III only partially blocked (Figure 4.1.2B).

Figure 4.1.2 (*sp*)PdCl<sub>2</sub> (184).

Given the mechanism of the reaction, and that  $\beta$ -hydrogen elimination is a major component of enantiodifferentiation, it was also not obvious to us how a  $C_2$  symmetric ligand would induce asymmetry in this process. Figure 4.1.3 depicts the transition state for  $\beta$ -hydrogen elimination (see below, Section 4.3.1) imposed on a quadrant diagram for a  $C_2$  symmetric ligand. As the  $\beta$ -agostic interaction between the palladium center and the C–H atom approaches a full Pd–H bond, the transition state becomes more and more symmetrical. If the secondary carbon atom is aligned with the origin point of the quadrant diagram, in fact  $R_L$  and  $R_S$  are in identical steric environments.

Figure 4.1.3  $\beta$ -Hydrogen elimination with a  $C_2$  symmetric ligand.

Because (–)-sparteine (**22**) was the only effective ligand for the oxidative kinetic resolution, we became very interested in exploring the steric environment that **22** created in palladium complexes. The first question we chose to address was the extent to which the  $C_1$  symmetric (–)-sparteine (**22**) molecule mimics  $C_2$  symmetry when bound to  $\text{PdCl}_2$ . Reported in this chapter are the results of these investigations, which culminated in an experimentally derived model for the selectivity observed in the oxidative kinetic resolution of secondary alcohols. Further studies involving two other members of the lupin alkaloid family, (–)- $\alpha$ - and (+)- $\beta$ -isosparteine (**255** and **256**), completed this contribution to the rich history of an unusual molecule.<sup>15</sup>

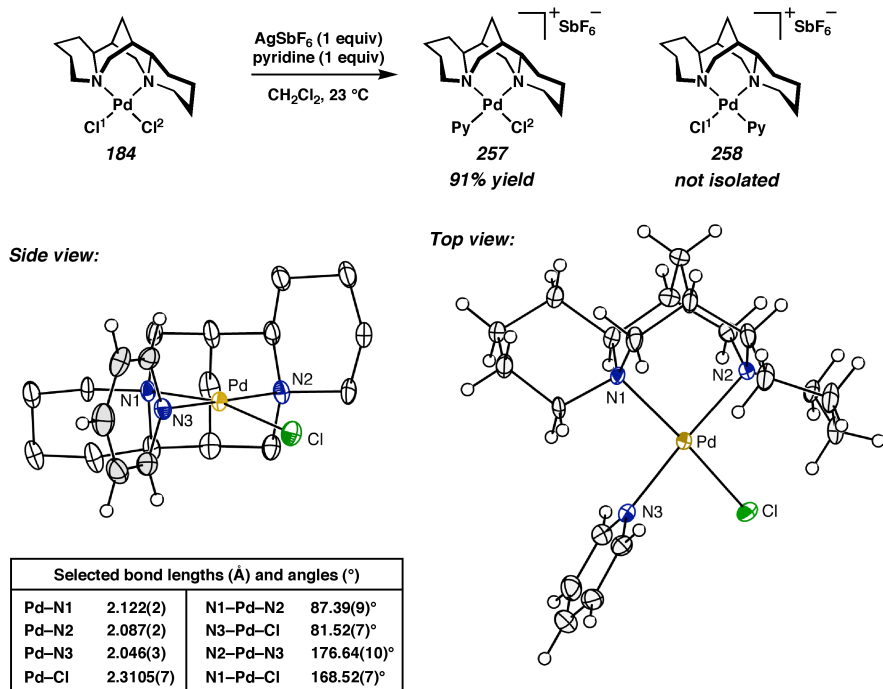
## 4.2 REACTIVITY AND STRUCTURAL STUDIES OF (–)-SPARTEINE PALLADIUM COMPLEXES.

### 4.2.1 The reactivity of (*sp*) $\text{PdCl}_2$ (**184**) with pyridine derivatives and their solid-state structures.

To experimentally test the degree to which the  $C_1$  symmetric ligand (–)-sparteine (**22**) approaches  $C_2$  symmetry, a series of substitution experiments were carried out on (*sp*) $\text{PdCl}_2$  (**184**). In the first experiment, **184** was treated with 1 equiv of  $\text{AgSbF}_6$  in the presence of pyridine (Scheme 4.2.1) at 25 °C in  $\text{CH}_2\text{Cl}_2$  to provide 91% yield of a crystalline product. We anticipated that if **22** behaved as a  $C_2$  symmetric ligand, two cationic pyridyl complexes (**257** and **258**) would form. In the event, one major complex

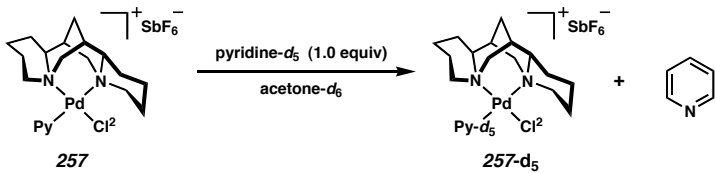
was observed by  $^1\text{H}$  and  $^{13}\text{C}$  NMR in acetone- $d_6$  along with a small amount of another compound.<sup>16</sup> The analysis of a single crystal by X-ray diffraction revealed complex **257**.<sup>17</sup> This was our first indication that (–)-sparteine (**22**) does not mimic  $C_2$  symmetry.

Scheme 4.2.1



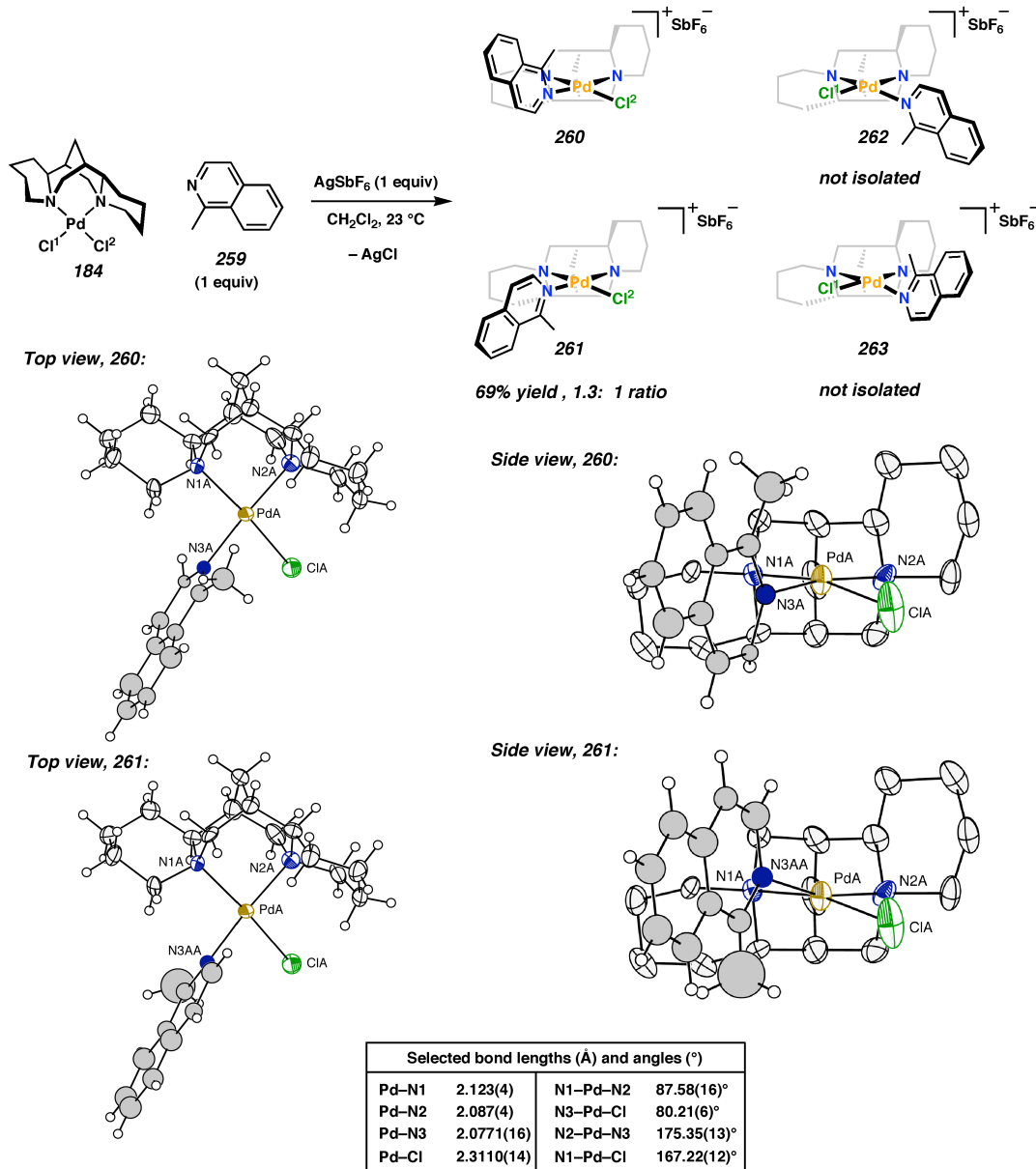
Although a solution state structural analysis was not carried out, we believe the major component in solution to be the same as that shown in Scheme 4.2.1, i.e., **257**. Treatment of the complex with pyridine- $d_5$  in acetone showed rapid deuterium incorporation and liberation of free pyridine at 25 °C (Scheme 4.2.2). It is unclear at this time what accounts for the minor component observed in solution. Observation of **257** by  $^1\text{H}$  NMR at 15 degree intervals from –60 °C to 45 °C in acetone- $d_6$  showed almost no change in the product ratio.

Scheme 4.2.2



We next investigated the reaction of **184** with a bulkier pyridine-related compound, 2-methyl isoquinoline (**259**, Scheme 4.2.3). Under the same reaction conditions, (sp)PdCl<sub>2</sub> (**184**) reacts with AgSbF<sub>6</sub> in the presence of **259** to produce a crystalline product in moderate yield. If (–)-sparteine (**22**) were exhibiting the properties of a C<sub>2</sub> symmetric ligand, we anticipated that four possible diastereomeric products could form, resulting from substitution at either Cl<sup>1</sup> or Cl<sup>2</sup> and the atropisomer at each position, but that two would dominate: **260** and **262**, or **261** and **263**. In the event, two major compounds are indeed observed by <sup>1</sup>H NMR in a 1.3:1 ratio in acetone-*d*<sub>6</sub> at 25 °C. However, on the basis of the outcome we observed in the reaction with pyridine, we considered the possibility that only Cl<sup>1</sup> was displaced, and that the two products arose instead from atropisomerism at that position. Analysis in the solid state by X-ray crystallography revealed only substitution of Cl<sup>1</sup>, with both orientations of the isoquinoline ligand related by a rotation of 180° around the Pd-N bond occupying the site.<sup>17,18</sup> This outcome provided further evidence against the possibility that **22** behaved with pseudo C<sub>2</sub> symmetry in this complex. In addition, the mixture of products indicated that the (sp)PdCl<sup>1</sup> fragment was not able to completely discriminate the prochiral faces of a planar molecule, albeit one with a steric environment analogous to that of acetophenone (**23**).

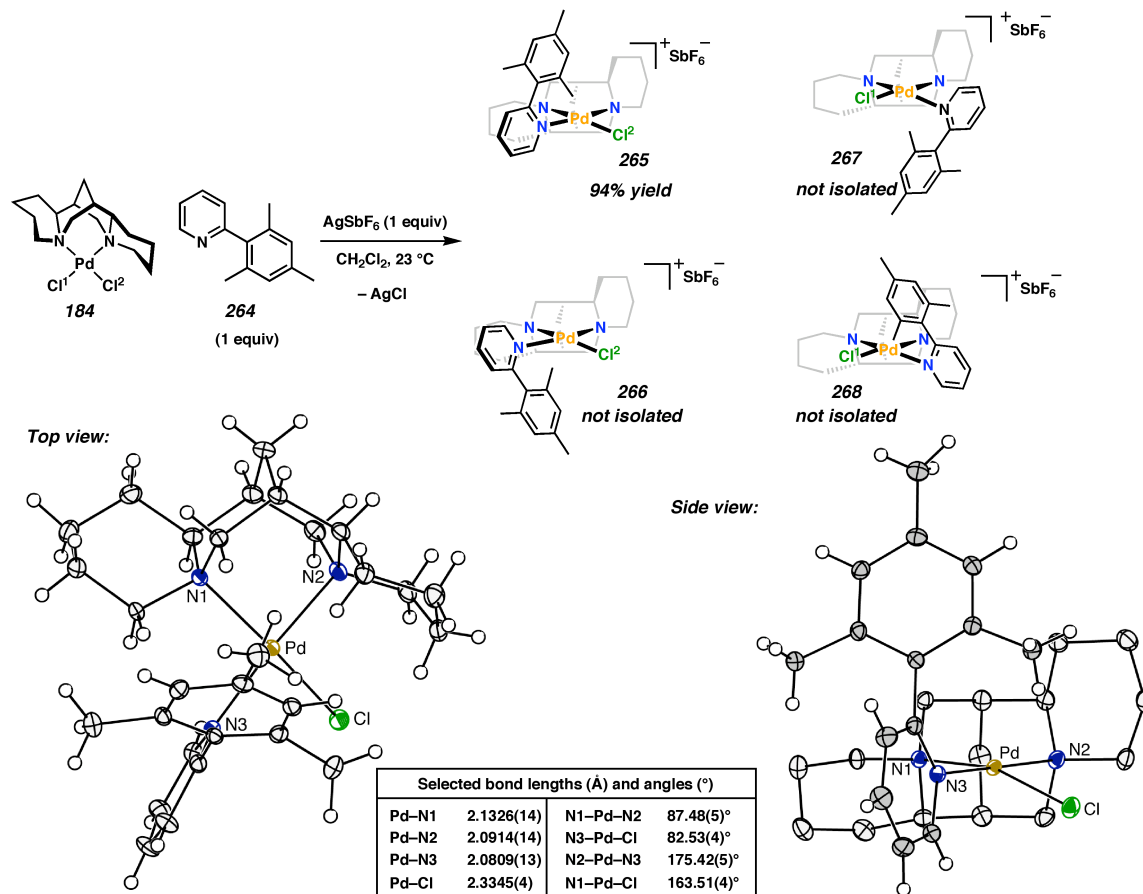
Scheme 4.2.3



In order to probe the steric environment of the (sp)PdCl fragment further, we turned to an even bulkier ligand, 2-mesityl pyridine (**264**). In this instance, under identical conditions to the syntheses of **257** and **260/261**, we observed a good yield of one major product out of four possible by  $^1\text{H}$  NMR in acetone- $d_6$  with approximately 5% of a minor component (Scheme 4.2.4). The presence of a single major product indicated that not

only had substitution occurred at a single site of the palladium center, but that a single atropisomer about the Pd–N bond was favored, for a suitably bulky ligand. X-ray crystallographic analysis showed that Cl<sup>1</sup> had been substituted as in **257** and **260/261**, and that the mesityl group resided exclusively in quadrant IV.<sup>17</sup>

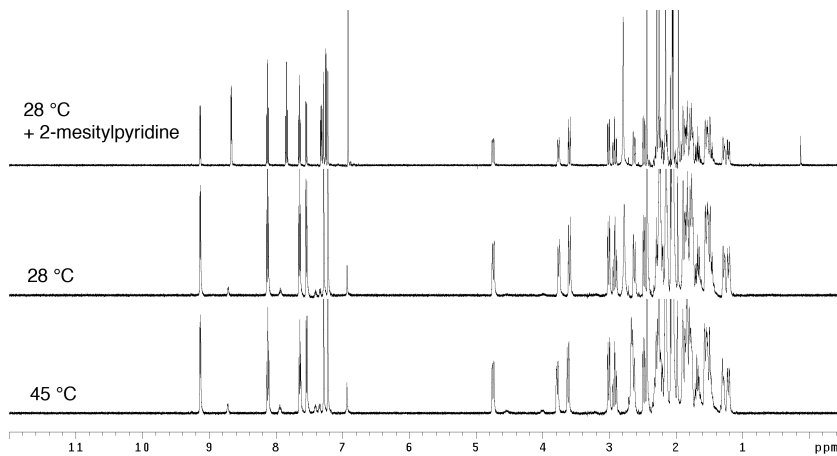
Scheme 4.2.4



The ratio of major and minor products observed in the <sup>1</sup>H NMR spectrum remained nearly unchanged from –60 °C to 45 °C in acetone-*d*<sub>6</sub>. The <sup>1</sup>H NMR spectra at 45 °C and 28 °C are shown in Figure 4.2.1. The addition of an equivalent of 2-mesitylpyridine (**264**) resulted in an increase in the minor peaks in the aryl region of the spectrum, and a disappearance of the minor peaks in the region from 1 to 5 ppm corresponding to

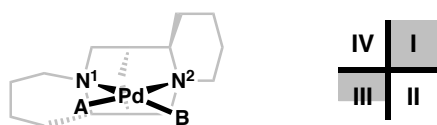
palladium-bound (–)-sparteine (**22**) (Figure 4.2.1, top spectrum). Thus, we believe the minor product observed by NMR to be dissociated ligand and an acetone•(sp)PdCl cation, and not any of the other possible positional or rotational isomers.

Figure 4.2.1  $^1\text{H}$  NMR spectra for **265**.



These ligand substitution experiments present convincing evidence that (–)-sparteine (**22**) does not mimic a  $C_2$  symmetric ligand when bound to  $\text{PdCl}_2$ , and provide information about the steric environment this ligand creates. The unique architecture favors substitution at site A on the palladium center, as depicted in Figure 4.2.2, and can sterically distinguish quadrants III and IV for sufficiently bulky unsymmetrical ligands. Most importantly, quadrants I and III are differentiated, unlike in a truly  $C_2$  symmetric ligand.

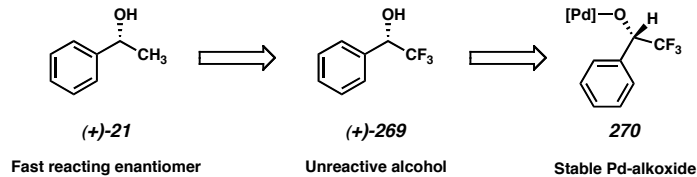
Figure 4.2.2 Quadrant diagram for (sp)Pd.



#### 4.2.2 The synthesis and reactivity of a palladium alkoxide as a model for an intermediate in the oxidative kinetic resolution.

To better understand the early stages of the oxidative kinetic resolution itself, we set out to synthesize an alkoxide complex relevant to our system. While numerous palladium alkoxides have been characterized, few bear  $\beta$ -hydrogen atoms due to the ease of  $\beta$ -hydrogen elimination.<sup>19</sup> A meaningful steric model for the prototypical oxidative kinetic resolution substrate 1-phenylethanol (**21**) is  $\alpha$ -(trifluoromethyl)benzyl alcohol **269** (Figure 4.2.3).<sup>20</sup> Under our kinetic resolution conditions,  $(\pm)$ -**269** does not react, presumably because the electron-withdrawing trifluoromethyl group disfavors the  $\beta$ -agostic interaction between the palladium atom and the benzylic C–H bond that precedes elimination. Thus, we hoped that a palladium-alkoxide complex of this alcohol would be relatively stable, and serve as a model of a relevant intermediate in the oxidation reaction. Ideally, such a complex could be used for reactivity studies as well. Alcohol  $(+)$ -**269**, which corresponds to the more reactive enantiomer of 1-phenylethanol  $((+)$ -**21**) in the resolution chemistry, was chosen as an initial target for palladium-alkoxide formation.

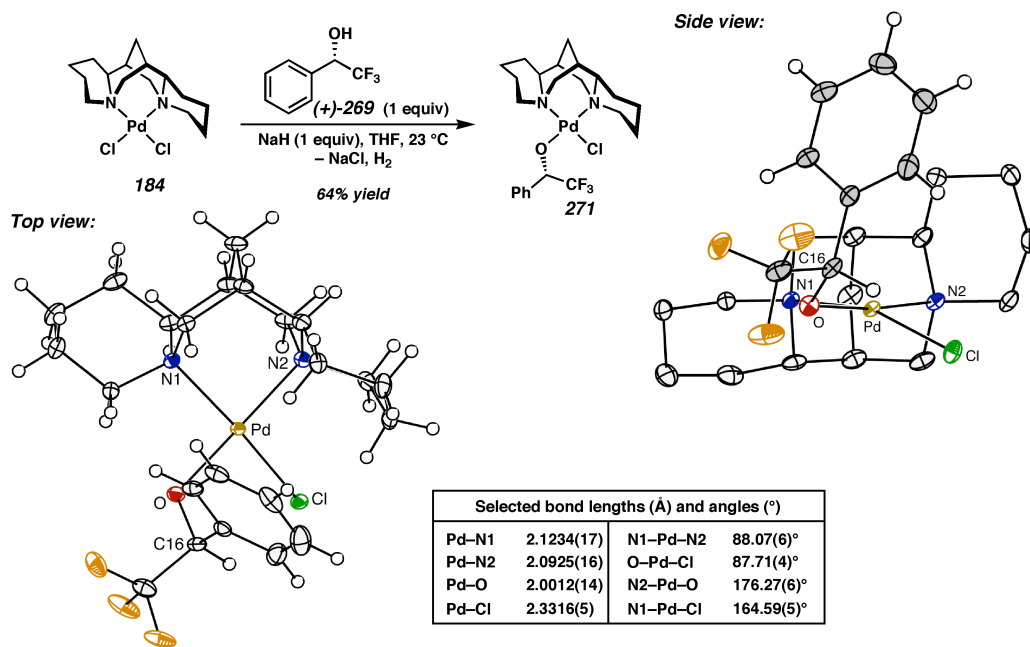
Figure 4.2.3 Rationale for a stable palladium alkoxide.



Treatment of complex **184** with the sodium alkoxide of  $(+)$ -**269** produced a 64% yield of recrystallized material that was one major product as observed by  $^1\text{H}$  NMR in  $\text{CD}_2\text{Cl}_2$  (Scheme 4.2.5). The compound was shown to alkoxide complex **271** by X-ray

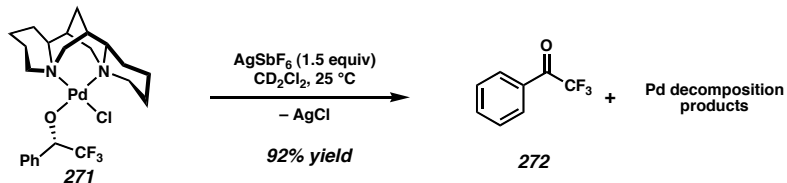
analysis.<sup>21</sup> A single atropisomer is observed and again substitution of Cl<sup>1</sup> occurs exclusively. The phenyl moiety is located in quadrant IV in an orientation similar to that of the mesityl group of complex **265**. In a manner similar to the cationic pyridyl complexes described above, the square plane of **271** is distorted such that Cl is displaced toward open quadrant II. In addition, the benzylic C–H bond is oriented toward the palladium center, and parallel to the distorted Pd–Cl bond.

Scheme 4.2.5



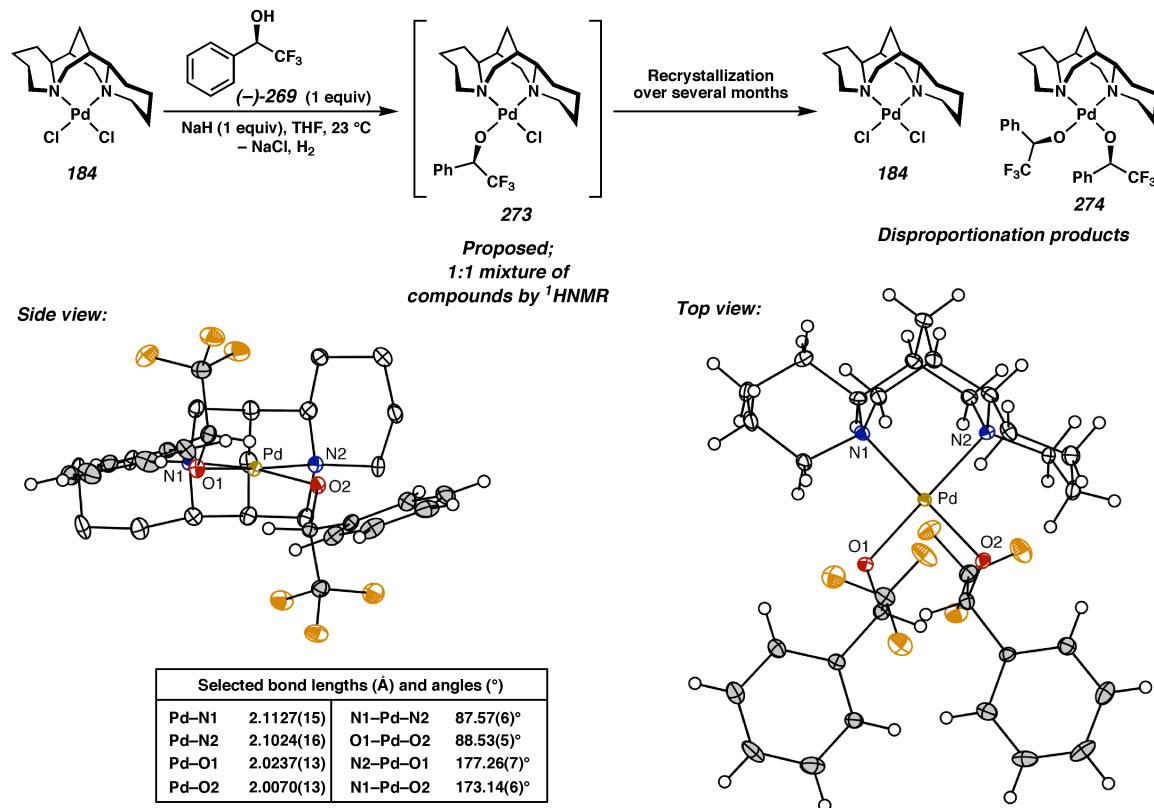
When **271** was treated with 1.5 equiv of AgSbF<sub>6</sub> in CD<sub>2</sub>Cl<sub>2</sub> at 25 °C immediate production of ketone **272** in 92% yield was observed (Scheme 4.2.6).<sup>22</sup> Unfortunately, thermolysis of **271** in toluene-*d*<sub>8</sub> has lead to only inconclusive results. Exposure of the alkoxide to air results in the formation of a single new product, which has thus far not been characterized.

Scheme 4.2.6



The synthesis of the other diastereomer of palladium alkoxide, arising from the opposite enantiomer of alcohol (*(–)*-**269**), was also pursued. Enantiodiscrimination is proposed to arise from the difference in rates of  $\beta$ -hydrogen elimination from each diastereomeric palladium alkoxide complex (see Section 4.1.2). Thus, we wished to examine the structure and reactivity of the less reactive diastereomer. When (*–*)-**269** was treated with sodium hydride and added to **184**, two major compounds were observed by  $^1\text{H}$  NMR in an approximately 1:1 ratio. This was our initial indication that the interaction between the (sp)PdCl fragment and the alcohol corresponding to the slow-reacting enantiomer of 1-phenylethanol (*(–)*-**269**) was more complicated than that for (*+*)-**269**. The products did not crystallize readily, and only after standing for a period of several months was a mixture of orange and yellow crystals obtained. X-ray analysis revealed the yellow crystals to be bisalkoxide **274**, the  $^1\text{H}$  NMR spectrum of which had changed from that for the original product mixture.<sup>21</sup> The orange crystals were dichloride complex **184**, also not observed in the original  $^1\text{H}$  NMR spectrum. We propose that the initially formed products are a mixture of unstable alkoxide atropisomers, which eventually disproportionate to **184** and **274**. However, it is not certain that rotation around the Pd–O bond would be slow enough to observe on the NMR timescale.

Scheme 4.2.7



It is unclear why alcohol **(-)-269** forms a more complex initial product mixture than the other enantiomer, or why disproportionation occurs. One possibility is that the aryl group, now oriented toward quadrant III, experiences a steric clash with  $\text{Cl}^2$ , which destabilizes the complex and leads to disproportionation.<sup>23</sup> Such an interaction could also lead to rotation around the Pd–O bond, giving rise to the mixture of products initially observed. In the bisalkoxide complex, the  $\text{N}^1\text{-Pd–O}^2$  angle is less acute than the corresponding  $\text{N}^1\text{-Pd–Cl}$  angle in monoalkoxide complex **271** ( $173.14^\circ$  vs  $164.59^\circ$ ), a geometry which perhaps can better accommodate a bulkier group in quadrant III. Further investigation into the complex of (sp)Pd with this enantiomer of alcohol is warranted,

especially to obtain insight into the reactivity of this other palladium alkoxide diastereomer.

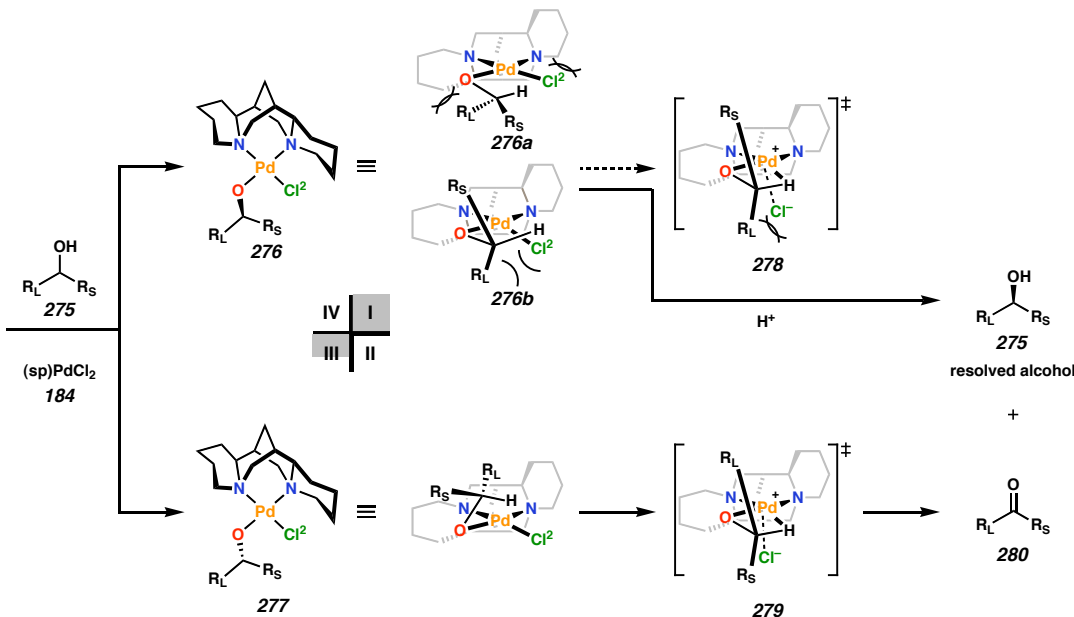
### 4.3 AN EXPERIMENTALLY DERIVED MODEL FOR THE STEREOSELECTIVITY OBSERVED IN THE OXIDATIVE KINETIC RESOLUTION

#### 4.3.1 *A description of the model.*

On the basis of the reactivity of (sp)PdCl<sub>2</sub> (**184**) and the structures of **257**, **260/261**, **265**, **271**, and **274**, we have proposed a general model for asymmetric induction in the palladium-catalyzed oxidative kinetic resolution of secondary alcohols.<sup>24</sup> Upon reaction of complex **1** with a racemic mixture of alcohol (**275**), Cl<sup>1</sup> is substituted preferentially over Cl<sup>2</sup> to form two diastereomeric palladium alkoxides (Figure 4.3.1, **276** and **277**). Either could be reprotonated leading to alcohol dissociation, or could undergo β-hydrogen elimination to afford ketone. Given the geometry of the solid state structure of palladium-alkoxide complex **271**, we propose that for the reactive diastereomer (**277**), the unsaturated moiety (R<sub>L</sub>) is located in open quadrant IV. In this geometry, the secondary C–H bond is positioned opposite the oblique Pd–Cl bond. The same orientation of R<sub>L</sub> in quadrant IV of the less reactive diastereomer **276** requires that the C–H bond point away from Pd (not shown). Alternatively, for diastereomer **276**, the C–H bond could approach from the opposite face of the square plane, as depicted by **276a**. This geometry, however, would be expected to induce destabilizing interactions between the alkoxide moiety and the piperidine ring in quadrant III, and between the chloride ligand and the piperidine ring in quadrant I. On the basis of the solid state structure of bisalkoxide **274**, we expect that unreactive diastereomer **276** likely has the

geometry shown in **276b**, although the disproportionation reaction described above (Scheme 4.2.7) indicates that it may be less stable than diastereomer **277**.

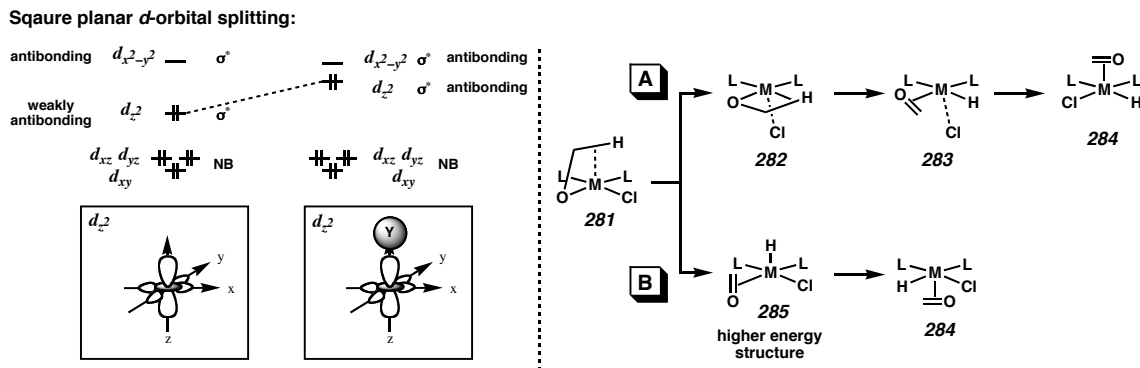
Figure 4.3.1 Model for selectivity in the oxidative kinetic resolution of secondary alcohols.



The transition state for  $\beta$ -hydrogen elimination (i.e., **278** or **279**) is expected to involve a developing cationic palladium species with 4-coordinate square planar geometry,<sup>25</sup> although calculations for this system have shown that  $\text{Cl}^-$  remains closely associated below the square plane (see below). A schematic representation of  $\beta$ -hydrogen elimination for our ligand set is shown in Figure 4.3.2. The C–H bond likely moves into the square plane by an associative substitution mechanism and displacement of the chloride ligand (**281**, Figure 4.3.2).  $\beta$ -Hydrogen elimination results in an intermediate possessing a hydride in a basal position (**283**). It is possible that  $\beta$ -hydrogen elimination could occur directly from an apical position (Figure 4.3.2, B). In this case, elimination would result in an apical hydride ligand (**285**). However, because the weakly antibonding  $d_{z^2}$  orbital of a square planar  $d_8$  complex is already filled, the introduction of

a  $\sigma$ -bonding apical ligand creates a fully antibonding interaction. Because hydride is a stronger  $\sigma$ -donor than chloride, apical  $\beta$ -hydrogen elimination would result in a higher-energy intermediate (**285**) than if chloride is forced into the apical position (**282**). In examples of  $\beta$ -hydrogen elimination from alkyl complexes, the hydride is delivered to a vacant orbital, and not a filled one. Furthermore, calculations by Hoffmann have shown that for five-coordinate, square pyramidal species, hydride ligands prefer to be basal.<sup>26</sup>

*Figure 4.3.2 Possibilities for  $\beta$ -hydrogen elimination.*



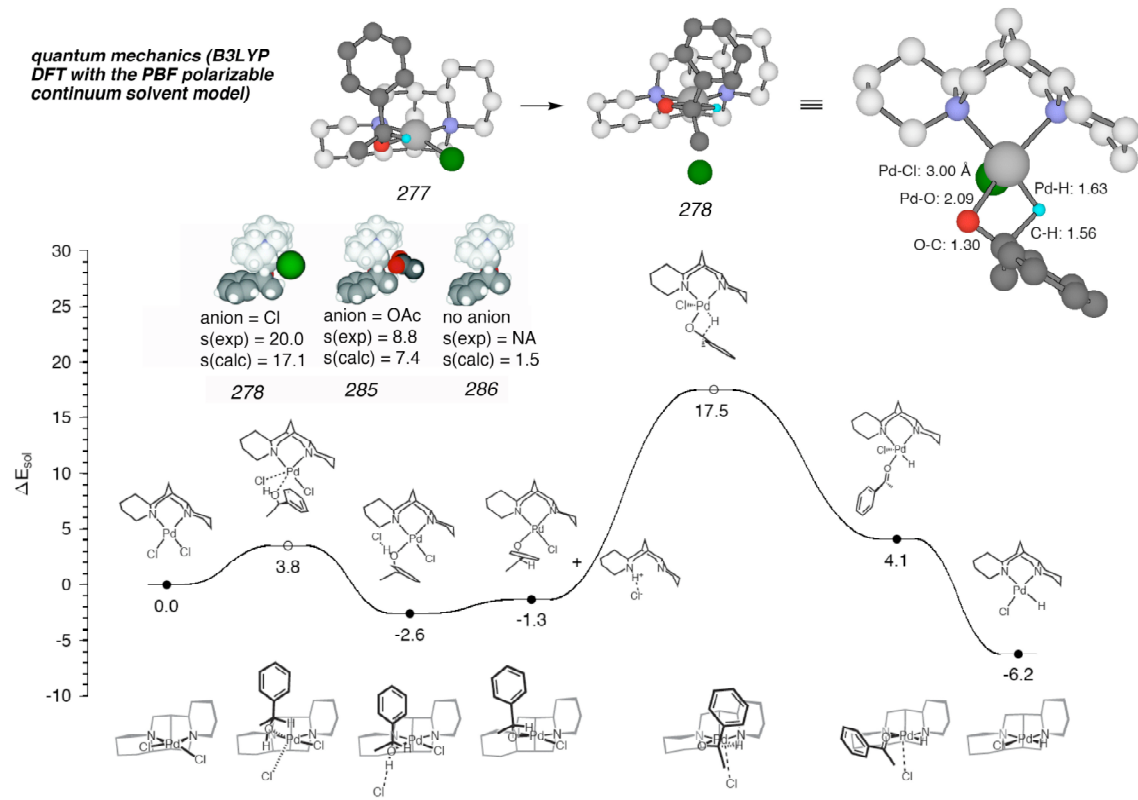
In structure **271**, and in **277** by analogy, the reactive C–H bond is poised to achieve the conformation for  $\beta$ -hydrogen elimination via **279** after displacement of  $\text{Cl}^2$  into quadrant II (Figure 4.3.1). This sequence of events minimizes potential steric interactions en route to ketone. In contrast, achievement of a similar conformation by diastereomer **276** would entail a destabilizing interaction between  $R_L$  and quadrant III or between  $\text{Cl}^2$  and quadrant I. Furthermore, and perhaps more importantly, a closely associated chloride ion in the apical position below the square plane could further disfavor the diastereomeric transition state (**278**) by steric crowding with  $R_L$ . Thus, **277** reacts to form ketone (**280**), while **276** protolytically dissociates to the observed enantiomer of resolved alcohol (**275**).

This model predicts the absolute stereochemical outcome of every (sp)PdCl<sub>2</sub> (**184**) catalyzed oxidative kinetic resolution performed to date.

#### 4.3.2 Calculations support the model.

Smith Nielsen, a graduate student in the Goddard group at Caltech, has carried out extensive calculations on the oxidative kinetic resolution catalyzed by (sp)PdCl<sub>2</sub> (**184**) that provide theoretical support to some of the conclusions described above.<sup>27</sup> Some of the results of these calculations are depicted in Figure 4.3.3. The high-level calculations determine the geometry of alkoxide intermediate **277** to be similar to that found in the solid-state structure of **271**, our model for this intermediate.  $\beta$ -Hydrogen elimination proceeds by displacement of the chloride anion by the benzylic C–H bond, although the chloride ion, while not fully bound, remains closely associated to the metal center in the transition state (**278**). Significantly, when the chloride ligand was left out of the calculation of the barriers to  $\beta$ -hydrogen elimination from each diastereomer, little difference was found, which indicates that the rates would be similar (**286**). Thus, the chloride anion appears to be essential to the selectivity.

Figure 4.3.3 Theoretical model for the oxidative kinetic resolution of secondary alcohols.



#### 4.3.3 The potential effect of the halide ligand on selectivity and reactivity.

On the basis of the experiments and calculations described above, we believe the chloride anion plays an essential role in communicating the chirality of (-)-sparteine (**22**) to the bound substrate. Table 4.3.1 compares the angles around the square plane determined from the solid-state structures for the (sp)Pd-derived complexes reported herein. The largest disparity among the complexes is in the N<sup>1</sup>–Pd–B, A–Pd–B and N<sup>1</sup>–Pd–A angles, while the other angles remain within three degrees of each other. The 2-mesityl pyridine cationic complex (**265**) and the monoalkoxide (**271**) are the most distorted, the sum of the six angles between ligands being 699.45° and 701.58°, respectively, compared to 720° in a perfect square plane and 657° for a tetrahedral

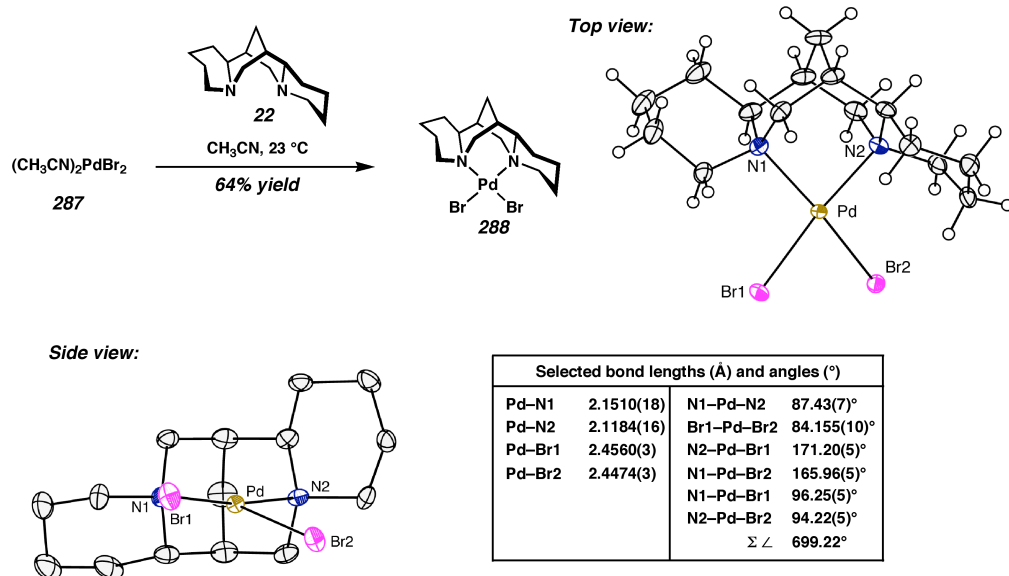
geometry. Because, as proposed,  $\text{Cl}^2$  remains close to the palladium atom throughout the reaction, it may effectively block quadrant II leaving only one quadrant open for substrate binding. In this way, the transition state for  $\beta$ -hydrogen elimination is further desymmetrized (see Figure 4.1.3).

Table 4.3.1 A comparison of bond angles in (sp)Pd complexes.

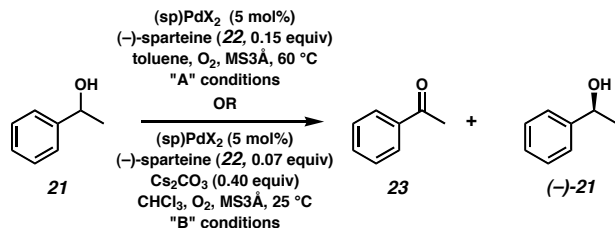
	$\text{A} = \text{Cl}$ $\text{B} = \text{Cl}$ 184	$\text{A} = \text{C}_6\text{H}_4\text{N}$ $\text{B} = \text{Cl}$ 257	$\text{A} = \text{C}_6\text{H}_4\text{N}$ $\text{B} = \text{Cl}$ 260/261	$\text{A} = \text{C}_6\text{H}_4\text{N}$ $\text{B} = \text{Cl}$ 265	$\text{A} = \text{o}-\text{CF}_3$ $\text{B} = \text{Cl}$ 271	$\text{A} = \text{o}-\text{CF}_3$ $\text{B} = \text{o}-\text{CF}_3$ 274
N1–Pd–B	170.06°	168.52°	167.22°	163.51°	164.59°	173.14°
N2–Pd–A	176.24°	176.64°	175.35°	175.42°	176.27°	177.26°
A–Pd–B	83.09°	81.52°	80.21°	82.53°	87.71°	88.53°
N1–Pd–N2	87.51°	87.39°	87.58°	87.48°	88.07°	87.57°
N1–Pd–A	95.65°	95.73°	96.85°	96.95°	89.78°	92.65°
N2–Pd–B	93.44°	95.67°	95.16°	93.56°	95.16°	91.57°
$\Sigma \angle$	705.99°	705.47°	702.37°	699.45°	701.58°	710.72°

If this proposed role for chloride is correct, then a larger, but still coordinating ligand at position B should improve selectivity in the kinetic resolution. To investigate this possibility, (sp)PdBr<sub>2</sub> (**288**) was pursued. Ligation of **22** to palladium precursor **287** occurred in moderate yield to provide **288** (Scheme 4.3.1). The molecular structure of **288** obtained by X-ray diffraction of a single crystal shows that the Pd–Br<sup>2</sup> bond is further distorted than the Pd–Cl<sup>2</sup> bond of **134**. The sum of the angles between the six ligands is 699.22°, which is comparable to the most tetrahedrally distorted complex containing a chloride at position B (**265**, Table 4.3.1).

Scheme 4.3.1



**288** was tested in the kinetic resolution reaction of 1-phenylethanol (**21**). The results for two sets of conditions are shown in Table 4.3.2 (entries 1 and 2). While these results are preliminary, high selectivities are obtained at rates 3 to 7 times faster than with (sp)PdCl<sub>2</sub> (**184**) for both sets of conditions (entries 3 and 4).<sup>4,5</sup> The effect of the bromide ligand appears to be rate acceleration without a loss in selectivity.

Table 4.3.2 Oxidative kinetic resolution with (sp)PdBr<sub>2</sub> (**288**).

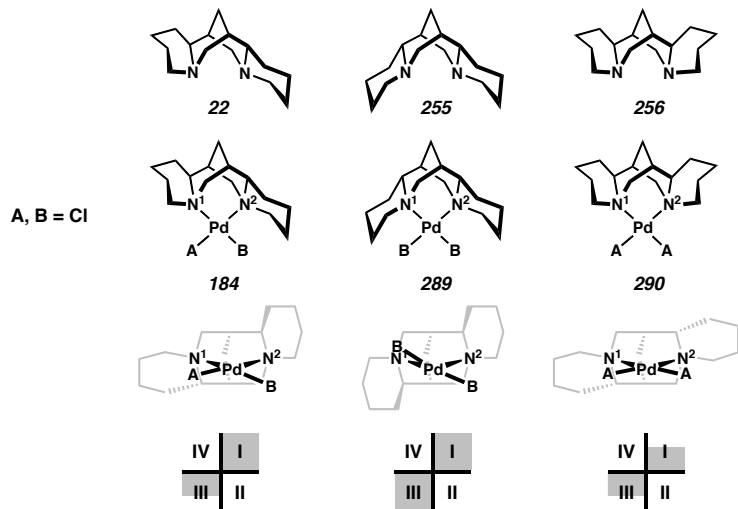
entry	X	Conditions	time	% conversion	%ee	s
1	Br	A	28 h	62	99	28
2	Br	B	6.5 h	56	93.6	22
3	Cl	A	96 h	60	98.7	23.1
4	Cl	B	48 h	60	99	31

## 4.4 THE PROPERTIES AND REACTIVITY OF $\alpha$ - AND $\beta$ -ISOSPARTEINE IN THE OXIDATIVE KINETIC RESOLUTION

### 4.4.1 *A structural comparison of the three sparteine diastereomers.*

Having developed our model for selectivity, our attention again turned to the issue of  $C_2$  symmetry. In particular, we were curious whether the  $C_2$  symmetric diastereomers of ( $-$ )-sparteine (**22**) would be more or less selective in the kinetic resolution. The  $\text{PdCl}_2$  complexes of the three diastereomers are shown in Figure 4.4.1 for comparison.<sup>28,29</sup> For ( $-$ )-sparteine (**22**), the reactions of **184** we have thus far observed have occurred primarily at site A, which we believe is the relevant site of substitution in the kinetic resolution reaction. For the ( $-$ )- $\alpha$ -isosparteine (**255**) complex (( $\alpha$ -isosp)PdCl<sub>2</sub>, **289**), reaction, if any, would be forced to occur at a B site, by analogy to **22**. That is, both anionic ligands of **289** would be in an environment identical to that of Cl<sup>2</sup> in (sp)PdCl<sub>2</sub> (**184**). On the other hand, for the ( $+$ )- $\beta$ -isosparteine (**256**) complex (( $\beta$ -isosp)PdCl<sub>2</sub>, **290**), in which both flanking piperidine rings are directed away from the metal center, only A sites are available. It was unclear to us what effect this would have on the rate of oxidation. If the  $C_1$  symmetry of ( $-$ )-sparteine (**22**) is essential to its unique selectivity in the kinetic resolution, a comparison of the three diastereomers would reveal this point.

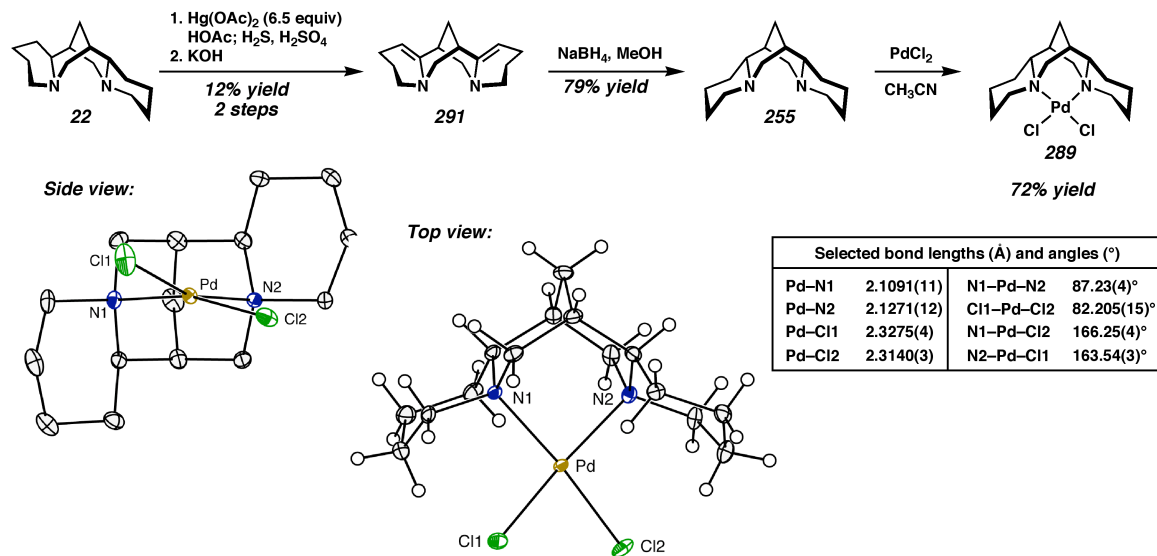
Figure 4.4.1 Comparison of the three sparteine diastereomers.



#### 4.4.2 (-)- $\alpha$ -Isosparteine as a ligand in the oxidative kinetic resolution.

(–)- $\alpha$ -Isosparteine (**255**) was prepared by the method of Leonard (Scheme 4.4.1).<sup>30</sup> Dehydrogenation with mercuric acetate and diastereoselective reduction of the resulting bisenamine **291** provides (–)- $\alpha$ -isosparteine (**255**). The ligand was complexed to palladium dichloride to give ( $\alpha$ -isosp)PdCl<sub>2</sub> (**289**), and a solid state structure was obtained by X-ray crystallography.<sup>21</sup> In this structure, both Pd–Cl bonds are deflected from planarity by the flanking piperidine rings of the sparteine ligand, and the sum of the six angles around the square plane is 693.72°, the smallest for our sparteine complexes thus far.

Scheme 4.4.1



The oxidative kinetic resolution of 1-phenylethanol (**21**), our prototypical substrate, was attempted under our standard conditions with 5 mol% of the catalyst (**289**) and 0.15 equiv of excess  $(-)\alpha$ -isosparteine (**255**) in toluene at 80 °C in the presence of  $\text{O}_2$  and MS3 $\text{\AA}$  (Table 4.4.1). The analogous reaction using **184** is shown for comparison. After 72 h, 33.6% conversion with 28.6% ee was obtained, for a selectivity factor (*s*) of 4.7 compared to *s* = 17.3 with (sp)PdCl<sub>2</sub> (**184**).<sup>31</sup>  $(-)\alpha$ -Isosparteine (**255**) appears to induce a much lower reactivity and selectivity in the kinetic resolution.

Table 4.4.1 Oxidative kinetic resolution with  $(\alpha\text{-isosp})\text{PdCl}_2$  (**289**).<sup>a</sup>

	$\xrightarrow[\text{toluene, O}_2, \text{MS3}\text{\AA}]{\text{catalyst (5 mol\%) ligand (0.15 equiv)}}$	
entry	catalyst	time
1 <sup>a</sup>	$(\alpha\text{-isosp})\text{PdCl}_2$	72 h
2 <sup>b</sup>	$(\text{sp})\text{PdCl}_2$	24 h
% conversion	%ee	<i>s</i>
33.6	28.6	4.7
58.1	93.2	17.3

<sup>a</sup> Data represent an average of two runs. <sup>b</sup> Data represent an average of three runs.

To account for any effect that free ligand may have on the selectivity, the kinetic resolution was carried out in the absence of excess ligand, but with cesium carbonate as a stoichiometric base (Table 4.4.2).<sup>32</sup> The reaction with ( $\alpha$ -isosp)PdCl<sub>2</sub> (**289**) as catalyst showed little conversion and almost no selectivity. While the selectivity for the reaction using (sp)PdCl<sub>2</sub> (**184**) without added ligand was also diminished, we believe this is a result of (–)-sparteine (**22**) decomplexation in the absence of excess ligand (see below).

Table 4.4.2 Oxidative kinetic resolution with ( $\alpha$ -isosp)PdCl<sub>2</sub> (**289**) and Cs<sub>2</sub>CO<sub>3</sub>.

entry	catalyst	time	% conversion	%ee	s
1 <sup>a</sup>	( $\alpha$ -isosp)PdCl <sub>2</sub> ( <b>289</b> )	12 h	17.3	4.96	1.7
2 <sup>a</sup>	(sp)PdCl <sub>2</sub> ( <b>184</b> )	12 h	36.2	35.2	6.0

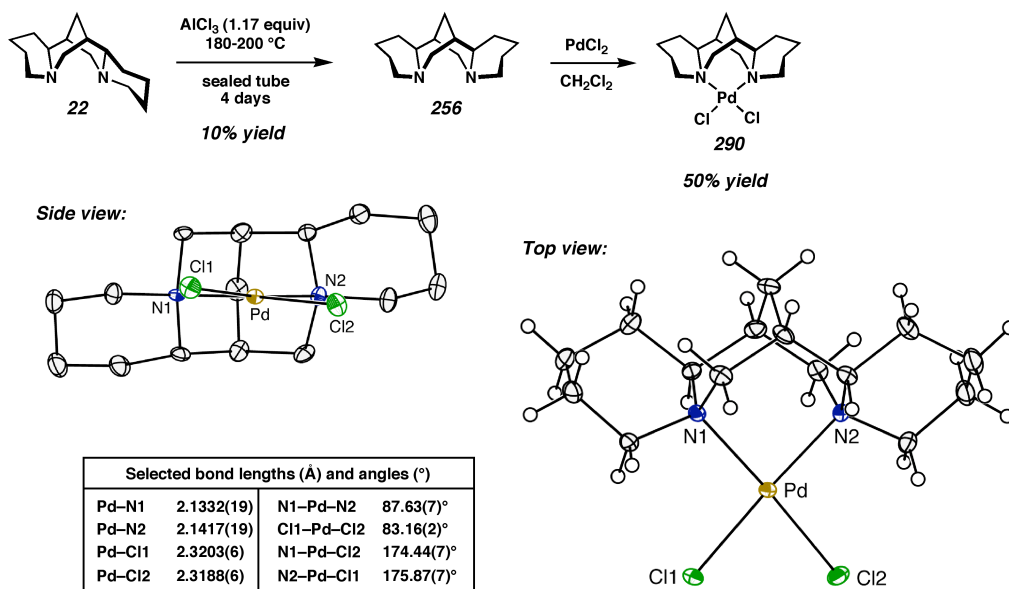
<sup>a</sup> Data represent an average of two runs.

The poor selectivity and low reactivity of ( $\alpha$ -isosp)PdCl<sub>2</sub> (**289**) in the kinetic resolution support our hypothesis that (–)-sparteine (**22**) is a uniquely effective ligand due to its  $C_1$  symmetry. While the increased steric bulk that (–)- $\alpha$ -isosparteine (**255**) provides close to the metal center could be expected to increase the steric interactions that control selectivity, it instead hampers even reactivity. In addition, no benefit is gained from the increased symmetry of the ligand, which stands in contrast to many asymmetric reactions in which a  $C_2$  symmetric ligand provides better selectivity.<sup>13</sup> These results also provide further indication that site A of the (sp)Pd fragment (Figure 4.4.1) is the relevant reactive site, and that a Curtin-Hammett situation seems unlikely to be operative in the reaction.

#### 4.4.3 (+)- $\beta$ -Isosparteine as a ligand in the oxidative kinetic resolution.

(+)- $\beta$ -Isosparteine (**256**) was prepared by the method of Winterfeld.<sup>33</sup> Thermolysis of (–)-sparteine (**22**) in the presence of 1.17 equiv of AlCl<sub>3</sub> at 180–200° in a sealed tube provided a mixture of all three sparteine diastereomers. Separation by column chromatography provided **256**.<sup>34</sup> Ligation to palladium dichloride was achieved in CH<sub>2</sub>Cl<sub>2</sub>,<sup>35</sup> and a solid-state structure of ( $\beta$ -isosp)PdCl<sub>2</sub> (**290**) was obtained by X-ray crystallography (Figure 4.4.2).<sup>21</sup> Without the steric intrusion of the trans quinolizidine ring system at the metal center, the complex is much more planar. The sum of the angles around the palladium atom is 710.68°, comparable to bisalkoxide **274**, and the closest to square planar geometry of any sparteine-derived complexes containing a chloride ligand.

Scheme 4.4.2



The results of the oxidative kinetic resolution of 1-phenylethanol (**21**) with ( $\beta$ -isosp)PdCl<sub>2</sub> (**290**) are shown in Table 4.4.3. Whether with excess ligand (entries 1 and 2)

or inorganic base (entry 3), there is essentially no selectivity. Reaction occurs more quickly than with ( $\alpha$ -isosp)PdCl<sub>2</sub> (**289**), but still more slowly than with (sp)PdCl<sub>2</sub> (**184**).

Table 4.4.3 Oxidative kinetic resolution with ( $\beta$ -isosp)PdCl<sub>2</sub> (**290**).<sup>a</sup>

entry	base	time	% conversion	%ee	s
1 <sup>a</sup>	(+)- $\beta$ -isosparteine ( <b>256</b> ) <sup>b</sup>	17 h	31%	4%	1.2
2 <sup>a</sup>	(+)- $\beta$ -isosparteine ( <b>256</b> ) <sup>b</sup>	23 h	42%	6%	1.3
3	Cs <sub>2</sub> CO <sub>3</sub> <sup>c</sup>	17 h	45%	6%	1.2

<sup>a</sup> Entries 1 and 2 are two different runs. <sup>b</sup> 0.15 equiv of ligand.

<sup>c</sup> 1 equiv of base.

( $\alpha$ -isosp)PdCl<sub>2</sub> (**289**) is likely a less-reactive catalyst because approach of the substrate and formation of the postulated palladium alkoxide intermediate is hindered by the additional steric bulk; reaction at site B of (sp)PdCl<sub>2</sub> (**184**) was never favored in the formation of cationic pyridine complexes. On the other hand, because ( $\beta$ -isosp)PdCl<sub>2</sub> (**290**) features two type A sites, it probably forms an alkoxide complex, but this is slower to undergo  $\beta$ -hydrogen elimination. This may be the case if a distorted Pd–Cl<sup>2</sup> bond is necessary for good reactivity; such distortion may facilitate displacement of Cl<sup>2</sup> to an axial position below the square plane by a C–H agostic interaction (Figure 4.3.2). Another possibility is that the more exposed palladium center can easily form a stable bisalkoxide that is resistant to  $\beta$ -hydrogen elimination.

These results provide strong evidence that the truly C<sub>2</sub> symmetric diastereomers of (–)-sparteine (**22**) are inferior ligands for the oxidative kinetic resolution in terms of both selectivity and reactivity. (–)-Sparteine (**22**) is perhaps uniquely effective for this reaction because it provides a highly specific steric environment at the palladium center.

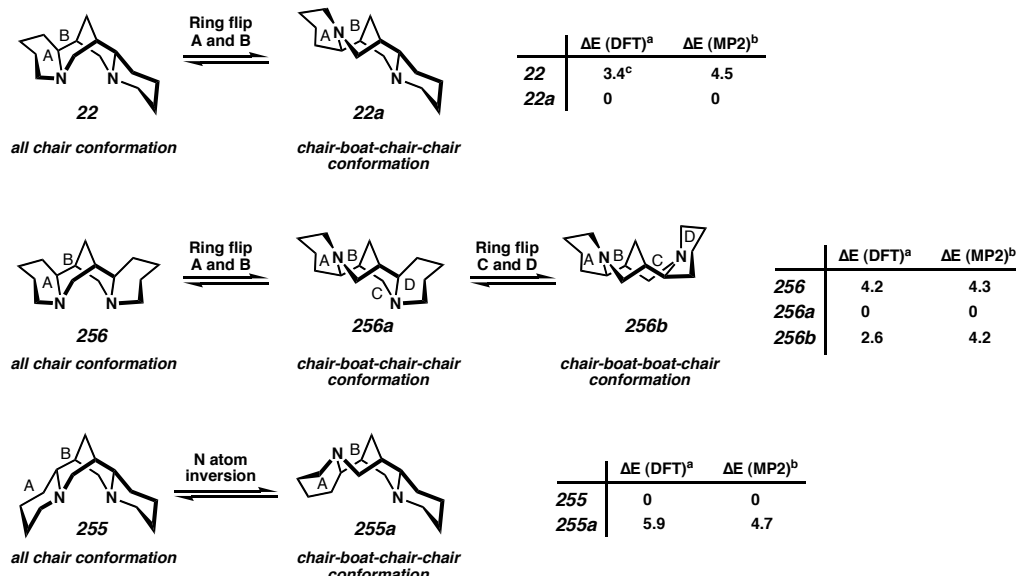
One coordination site is accessible to the substrate (site A, or quadrant IV), whereas the others contain the steric bulk necessary to desymmetrize the transition state enough to effect selectivity (Cl at site B, quadrants I and II). Unlike many catalytic enantioselective processes in which the chiral ligand blocks one face of a prochiral substrate from reaction, the oxidative kinetic resolution reaction *creates* a prochiral molecule. This unusual scenario seems to require a ligand environment more exotic than that provided by standard  $C_2$  symmetric ligands.<sup>36</sup>

#### 4.4.4. Ligand substitution experiments with $PPh_3$ and the three (*sparteine*) $PdCl_2$ complexes.

If a distorted Pd–Cl<sub>2</sub> bond is *necessary* for  $\beta$ -hydrogen elimination, the amount of reactivity observed with ( $\beta$ -isosp)PdCl<sub>2</sub> (**290**) may be due to dechelation and catalysis by a monocoordinated or unligated palladium species.<sup>35</sup> Indeed, the conformational flexibility of the sparteine diastereomers has been the subject of some study.<sup>37</sup> In a recent publication, Galasso and coworkers report their computations of the relative energies of different conformations of the three sparteine diastereomers in the gas phase and in solution (Figure 4.4.2).<sup>38</sup> For (–)-sparteine (**22**) in solution and in the gas phase, the species in which ring B is in a boat conformation is calculated to be 3-4 kcal more stable than the all-chair configuration (**22** vs **22a**). **22** and **22a** are related by ring flips of rings A and B. (+)- $\beta$ -Isosparteine (**256**) in solution is also more stable with ring B in a boat conformation (**256a**), and another double boat conformation (**256b**) is similar in energy to the all-chair geometry (**256**). In contrast, the all-chair conformation of (–)- $\alpha$ -isosparteine (**255**) is more stable by 4-6 kcal in the gas phase and in solution than the mono-boat species (**255a**). The A and B rings in **255** cannot ring flip to **255a** without

an inversion at a nitrogen atom. Thus,  $(-)\alpha$ -isosparteine (**255**) is the most rigid, followed by  $(-)$ -sparteine (**22**), and then  $(+)$ - $\beta$ -isosparteine (**256**) as the most conformationally flexible.

Figure 4.4.2 Theoretical study of the conformations of **22**, **255**, and **256**.



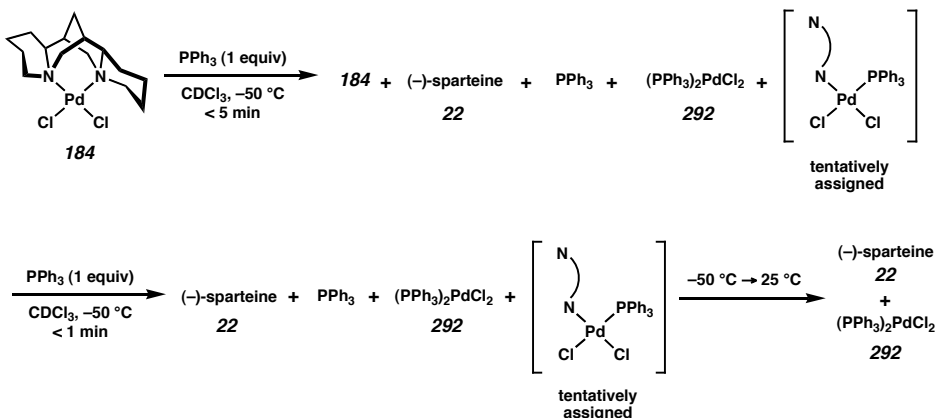
<sup>a</sup> DFT/B3LYP, 6-31+G(d,p) basis set with Gaussian 98. <sup>b</sup> Hartree-Fock second order Møller-Plesset perturbation theory calculations on the DFT optimized structures; DFT/BPW91, 6-31G(d,p) basis set. <sup>c</sup> kcal/mol.

If the propensity for **256** to undergo conformational changes results in dechelation, this property might account for the reactivity observed in the oxidation reaction with this ligand. While solid state structures of metal complexes of sparteine ligands always feature bidentate ligation,<sup>39</sup> the nature of the solution-state structure may be complicated by the weakness of alkyl amines as ligands and the availability of other sparteine conformations. To investigate this possibility, ligand substitution reactions with PPh<sub>3</sub> were observed qualitatively by NMR for the three sparteine complexes.

(sp)PdCl<sub>2</sub> (**184**) was examined first with the hopes of obtaining a reference point for comparison with ( $\beta$ -isosp)PdCl<sub>2</sub> (**290**, Scheme 4.4.3). Surprisingly, initial experiments indicated that substitution of  $(-)$ -sparteine (**22**) by 2 equiv of PPh<sub>3</sub> in CDCl<sub>3</sub> or CD<sub>2</sub>Cl<sub>2</sub> is

extremely rapid (< 5 min) even at -60 °C.<sup>40</sup> Addition of a single equivalent of PPh<sub>3</sub> to **184** at -50 °C in CDCl<sub>3</sub> led to an initial mixture of products that included **184**, (PPh<sub>3</sub>)<sub>2</sub>PdCl<sub>2</sub> (**292**), free (-)-sparteine (**22**), free PPh<sub>3</sub>, and an unidentified (sp)Pd derivative as observed by <sup>1</sup>H and <sup>31</sup>P NMR. Addition of a second equivalent of PPh<sub>3</sub> led to a complete disappearance of (sp)PdCl<sub>2</sub> (**184**), with the unidentified derivative still present. Subsequent warming to 25 °C produced a mixture of **292** and free (-)-sparteine (**22**). We hypothesize that the unidentified derivative possesses one phosphine ligand and a monocoordinated (-)-sparteine (**22**).<sup>41</sup> At this time we cannot rule out the possibility that PPh<sub>3</sub> displaces a chloride ligand initially. Further characterization of this intermediate is warranted; however, the rapidity of substitution even at low temperature suggests that it is facilitated by the conformational flexibility of (-)-sparteine (**22**).<sup>42,43</sup>

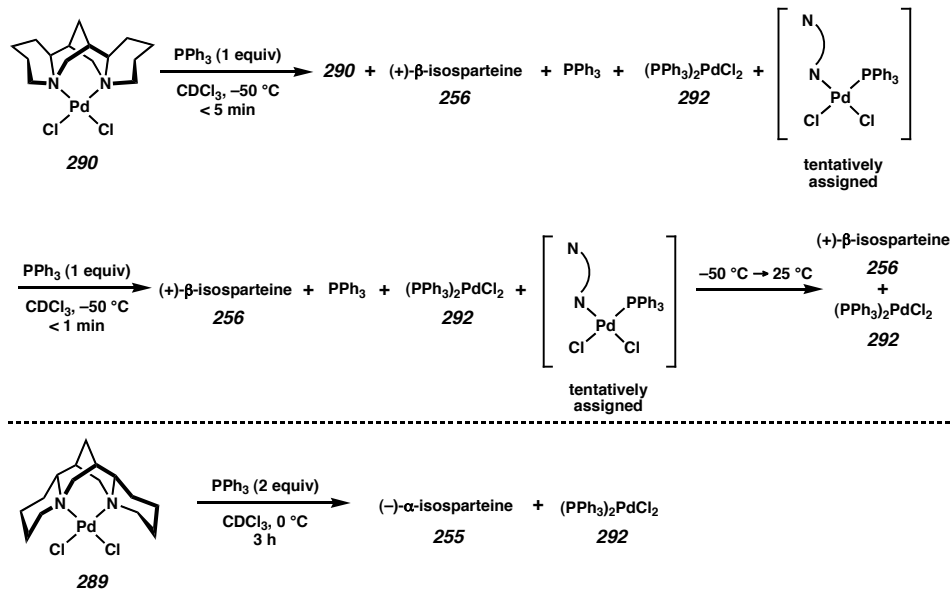
Scheme 4.4.3



Similar observations were made for the same reaction with ( $\beta$ -isosp)PdCl<sub>2</sub> (**290**) and ( $\alpha$ -isosp)PdCl<sub>2</sub> (**289**, Scheme 4.4.4). The reaction of **290** with first one, and then a second equivalent of PPh<sub>3</sub> was also too rapid to measure precisely at -50 °C. Nevertheless, a similar intermediate species was observed, which rapidly disappeared upon warming to -30 °C and then to 25 °C. While it is difficult to compare the rates of

reaction of **184** and **290**, qualitatively, (+)- $\beta$ -isosparteine (**256**) is displaced more rapidly, and the alkyl region of the spectrum is more fluxional. In contrast, the reaction of ( $\alpha$ -isosp)PdCl<sub>2</sub> (**289**) with 2 equiv of PPh<sub>3</sub> to produce (PPh<sub>3</sub>)<sub>2</sub>PdCl<sub>2</sub> (**292**) is measurable at 0 °C, and is complete in approximately 3 h. Because (-)- $\alpha$ -isosparteine (**255**) is the most rigid of the three ligands, this result supports the hypothesis that conformational flexibility promotes ligand substitution.<sup>44</sup>

Scheme 4.4.4



While the substitution experiments with PPh<sub>3</sub> and the palladium dichloride complexes of the three sparteine diastereomers are at this point highly qualitative, they provide a rough measure of the lability of each. Their respective qualitative substitution rates by PPh<sub>3</sub> are likely due to the relative conformational flexibility of the diastereomers (see Section 4.4.1) and the relative amounts of steric shielding of the palladium center. Further experiments in this area would be valuable on a fundamental level as well as for further understanding of reactions involving these ligands.

## 4.5 SUMMARY AND CONCLUSION

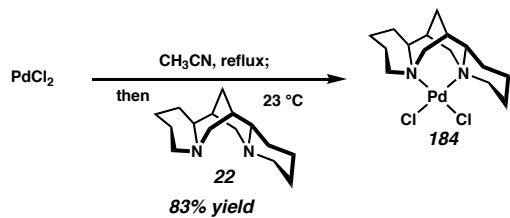
In conclusion, we have developed a model for the stereoselectivity in the Pd-catalyzed aerobic oxidative kinetic resolution of secondary alcohols. The model is based on the solid-state structures of coordination complexes and general reactivity trends of (sp)PdCl<sub>2</sub>. The first solid state structure of a non-racemic chiral palladium alkoxide is presented and further demonstrates the subtle steric influences of the ligand (–)-sparteine (**22**). High-level calculations support our model and emphasize the essential role that the halide ligand plays in selectivity. The *C*<sub>2</sub> symmetric diasteromers of (–)-sparteine (**22**), (–)-α-isosparteine (**255**) and (+)-β-isosparteine (**256**), were synthesized and investigated from a structural standpoint as well as in the oxidation reaction. Both were less selective and less reactive than (–)-sparteine (**22**), which supports the unusual conclusion that a *C*<sub>1</sub> symmetric ligand is uniquely effective for our oxidative kinetic resolution. Initial experiments into the substitution reactions of the palladium complexes of all three diastereomers hint at further interesting properties of these molecules that have yet to be elucidated. The lupine alkaloids never cease to fascinate.

## 4.6 EXPERIMENTAL SECTION

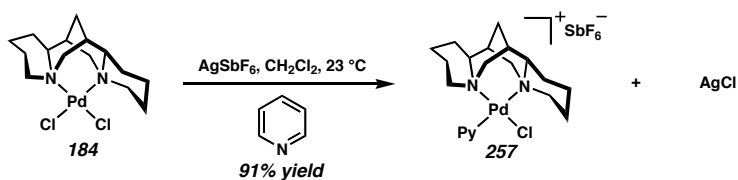
### 4.6.1 Materials and Methods.

Unless stated otherwise, reactions were conducted in flame-dried glassware under a nitrogen atmosphere with freshly distilled solvents. All commercially obtained reagents were used as received. Reaction temperatures were controlled by an IKAmag temperature modulator. Thin-layer chromatography (TLC) was conducted with E. Merck silica gel 60 F254 precoated plates (0.25 mm) and visualized via UV and anisaldehyde or potassium permanganate staining. ICN silica gel (particle size 0.032-0.063 mm) was used for flash column chromatography.  $^1\text{H}$ ,  $^{13}\text{C}$  and  $^{19}\text{F}$  NMR spectra were recorded on a Varian Mercury 300 spectrometer (at 300 MHz, 75 MHz, and 282 MHz, respectively) and are reported relative to  $\text{Me}_4\text{Si}$  ( $\delta$  0.0) for  $^1\text{H}$  and  $^{13}\text{C}$ , and to hexafluorobenzene ( $\delta$  -162.9) for  $^{19}\text{F}$ . Some  $^1\text{H}$ ,  $^{13}\text{C}$ , and all  $^{31}\text{P}$  NMR spectra were recorded on a Varian Inova 500 spectrometer (at 500 MHz, 125 MHz, and 121 MHz, respectively) and are reported relative to  $\text{Me}_4\text{Si}$  ( $\delta$  0.0) or  $\text{H}_3\text{PO}_4$  ( $\delta$  0.0) for  $^{31}\text{P}$  NMR. Data for  $^1\text{H}$  NMR spectra are reported as follows: chemical shift ( $\delta$  ppm), multiplicity, coupling constant (Hz) and integration. Data for  $^{13}\text{C}$  NMR spectra are reported in terms of chemical shift. Data for  $^2\text{H}$  NMR spectra are reported in terms of chemical shift. Variable temperature NMR experiments were recorded on a Varian Inova 500 spectrometer (at 500 MHz). IR spectra were recorded on a Perkin Elmer BXII spectrometer and are reported in frequency of absorption ( $\text{cm}^{-1}$ ). High resolution mass spectra were obtained from the California Institute of Technology Mass Spectral Facility.

**4.6.2 The preparation of palladium complexes of pyridine derivatives and the reactions thereof.**



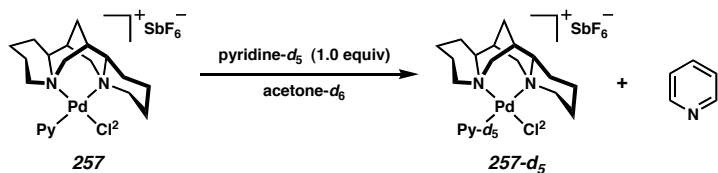
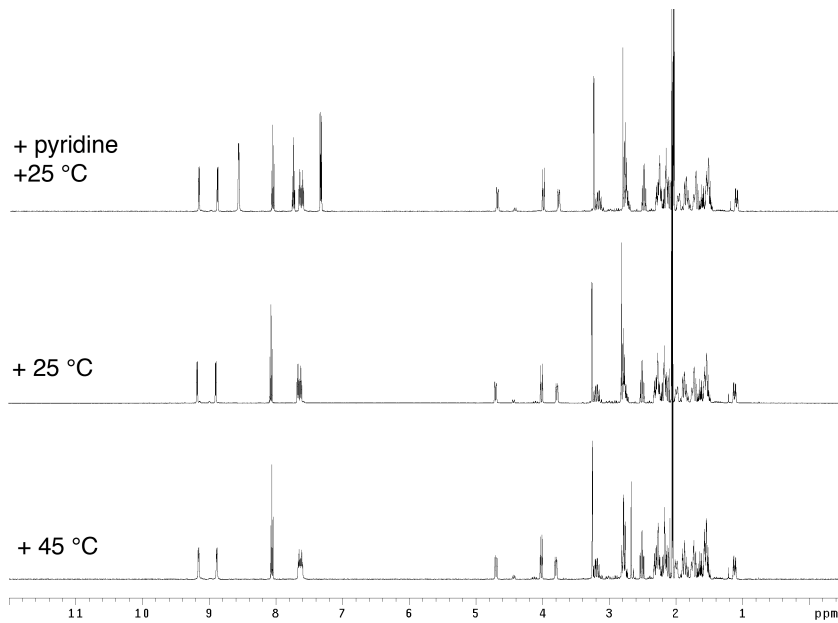
**(sp)PdCl<sub>2</sub> (184).** PdCl<sub>2</sub> (1.5 g, 8.46 mmol, 1.0 equiv) was suspended in CH<sub>3</sub>CN (40 mL) and refluxed under N<sub>2</sub> until formation of (CH<sub>3</sub>CN)<sub>2</sub>PdCl<sub>2</sub> was complete, as indicated by the change in color of the suspension from dark purple to yellow-orange. The mixture was allowed to cool to 23 °C at which time (–)-sparteine (**22**) (1.94 mL, 8.46 mmol, 1.0 equiv) was added. Upon stirring of the dark orange-red solution for 1 h under N<sub>2</sub>, an orange precipitate formed which was isolated via filtration in air. Trituration of the orange solid from CHCl<sub>3</sub> with Et<sub>2</sub>O resulted in **184** as a pale orange powder (2.89 g, 7.02 mmol, 83% yield) that was identical by NMR to previously published reports.<sup>6a</sup> A single crystal suitable for X-ray analysis was grown by slow evaporation from CDCl<sub>3</sub>.



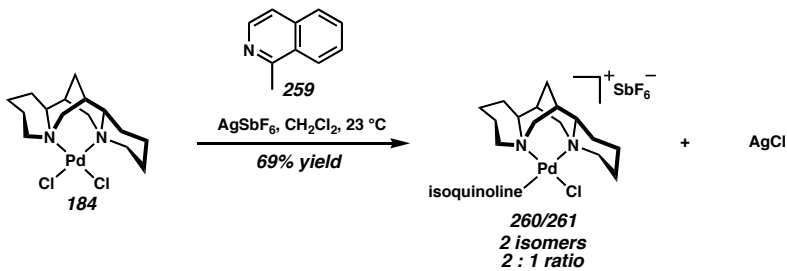
**[(sparteine)Pd(pyridine)Cl]<sup>+</sup>SbF<sub>6</sub><sup>-</sup> (257).** A Schlenk flask was charged with AgSbF<sub>6</sub> (125 mg, 0.364 mmol, 1.0 equiv) and (sp)PdCl<sub>2</sub> (**184**) (150 mg, 0.364 mmol, 1.0 equiv). Addition of pyridine (28 μL, 0.364 mmol, 1.0 equiv) via syringe followed immediately by CH<sub>2</sub>Cl<sub>2</sub> (10 mL) resulted in nearly instantaneous formation of an orange-yellow

solution and pale precipitate. After stirring for 1 h, silver chloride was removed by filtration through Celite in air. Concentration of the filtrate under vacuum yielded **257** as a yellow-orange solid which was recrystallized from acetone and pentane at –20 °C (229 mg, 0.331 mmol, 91% yield). Crystals suitable for X-ray diffraction were grown from acetone layered with pentane at 25 °C. In solution, approx. 10% of a minor component was observed.  $^1\text{H}$  NMR (300 MHz, acetone- $d_6$ )  $\delta$  9.16 (d,  $J$  = 4.9 Hz, 1H), 8.89 (d,  $J$  = 5.5 Hz, 1H), 8.06 (m, 1H), 7.67-7.59 (comp. m, 2H), 4.69 (dd,  $J$  = 12.1, 3.3 Hz, 1H), 4.00 (ddd,  $J$  = 13.2, 2.2, 2.2 Hz, 1H), 3.77 (ddd,  $J$  = 11.5, 1.7, 1.7 Hz, 1H), 3.24-2.82 (comp. m, 2H), 2.81-2.71 (comp. m, 2H), 2.48 (m, 1H), 2.33-1.48 (comp. m, 17H), 1.10 (m, 1H);  $^{13}\text{C}$  NMR (75 MHz, acetone- $d_6$ )  $\delta$  153.7, 152.7, 140.3, 127.7, 126.9, 69.9, 66.6, 66.0, 64.8, 63.7, 49.1, 35.4, 35.1, 31.3, 27.2, 27.0, 26.2, 24.8, 24.1, 21.1; Anal. calc'd for  $\text{C}_{20}\text{H}_{31}\text{ClF}_6\text{N}_3\text{PdSb}$ : C, 34.76; H, 4.52; N, 6.08. Found: C, 34.90; H, 4.64; N, 5.79; mp 127-130 °C dec.

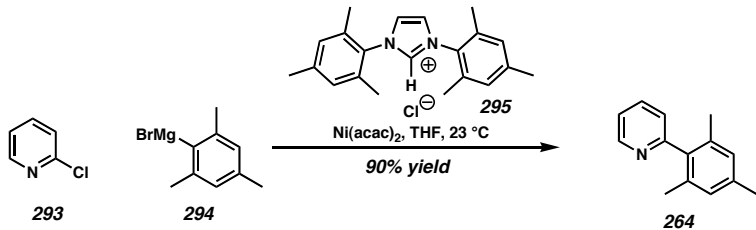
**Observation of **257** at variable temperatures.** **257** (12 mg, 0.017 mmol) was weighed into an NMR tube and dissolved in acetone- $d_6$  (0.700  $\mu\text{L}$ ). 500 MHz  $^1\text{H}$  NMR spectra were acquired from –60 °C to 45 °C at 15 °C intervals. One major complex, a minor set of peaks, and free pyridine were observable at all temperatures in approximately the same ratios, with significant broadening of the minor set of peaks at 45 °C. Addition of pyridine (1.37  $\mu\text{L}$ , 1.0 equiv) did not significantly change the product distribution. Refer to Figure 4.6.1 for the  $^1\text{H}$  NMR spectra.

Figure 4.6.1  $^1\text{H}$  NMR spectra of **257** at +45 °C, +25 °C and with 1 equiv added pyridine.

**Reaction of **257** with pyridine- $d_5$ .** **257** (11.3 mg, 0.016 mmol) was weighed into a sealable NMR tube and dissolved in acetone- $d_6$  (0.700 mL). A 500 MHz  $^1\text{H}$  NMR spectrum was acquired at 25 °C. Pyridine- $d_5$  (1.31  $\mu\text{L}$ , 0.016 mmol, 1 equiv) was added, and another spectrum was acquired. Pyridine- $d_5$  rapidly became incorporated into the complex (**257-d<sub>5</sub>**).

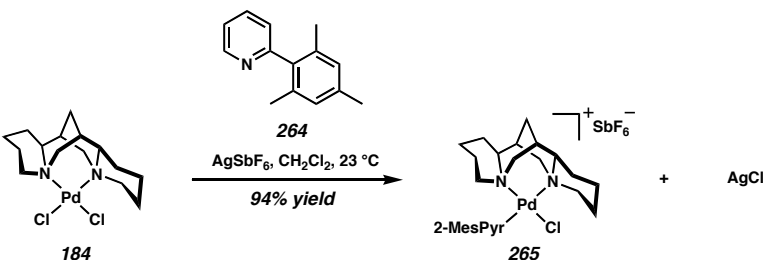


**[(sparteine)Pd(2-methylisoquinoline)Cl]<sup>+</sup>SbF<sub>6</sub><sup>-</sup> (260/261).** **260/261** was prepared according to the method described for **257** which afforded a yellow-orange solid (375 mg, 0.491 mmol, 69% yield). Crystals suitable for X-ray diffraction were grown by slow evaporation of a CH<sub>2</sub>Cl<sub>2</sub> solution of **260/261**. The <sup>1</sup>H NMR spectrum of the crystalline material showed a 1.3:1 mixture of products; the chemical shifts are reported together. <sup>1</sup>H NMR (300 MHz, CD<sub>2</sub>Cl<sub>2</sub>) δ 8.77 (d, *J* = 6.6 Hz, 1H), 8.52 (d, *J* = 6.6 Hz, 1H), 8.27-8.23 (m, 1H), 8.27-8.23 (m, 1H), 7.98-7.77 (comp. m, 4H). 7.98-7.77 (comp. m, 4H), 4.38 (d, *J* = 12.1 Hz, 1H), 4.36 (d, *J* = 12.1 Hz, 1H), 4.13 (ddd, *J* = 13.2, 2.2, 2.2 Hz, 1H), 4.01 (br. d, *J* = 13.7 Hz, 1H), 3.89 (s, 3H), 3.87-3.76 (comp. m, 2H), 3.87-3.76 (comp. m, 2H), 3.74 (s, 3H), 3.15-0.98 (comp. m, 22H), 3.15-0.93 (comp. m, 22H); <sup>13</sup>C NMR (75 MHz, CD<sub>2</sub>Cl<sub>2</sub>) δ 162.0, 161.8, 142.1, 141.4, 136.1, 136.0, 134.0, 133.9, 130.1, 130.0, 129.5, 128.8, 128.2, 128.1, 126.8, 126.7, 124.2, 123.4, 70.4, 70.4, 67.7, 67.2, 66.32, 66.29, 65.3, 64.3, 63.1, 49.74, 49.68, 35.1, 34.8, 34.7, 31.6, 30.9, 27.52, 27.46, 27.0, 26.8, 25.95, 25.92, 25.7, 24.62, 24.58, 24.56, 24.0, 23.9, 20.9, 20.8; Anal. calc'd for C<sub>25</sub>H<sub>35</sub>ClF<sub>6</sub>N<sub>3</sub>PdSb: C, 39.76; H, 4.67; N, 5.56. Found: C, 39.99; H, 4.41; N, 5.64. mp 115-120 °C dec.



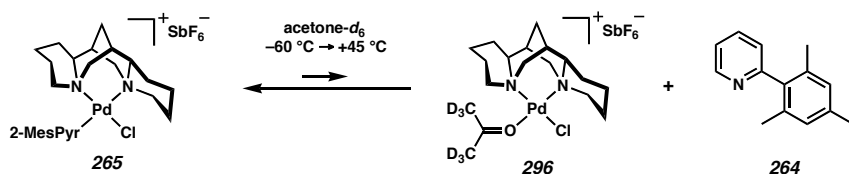
**2-Mesitylpyridine 264.** **264** was prepared by the modified procedure of Hermann et al.<sup>45</sup>

A Schlenk tube was charged with nickel(II) acetoacetone (103 mg, 0.40 mmol, 0.05 mol%), 1,3-bis(2,4,6-trimethylphenyl)-imidazolium chloride (**295**, 136 mg, 0.40 mmol, 0.05 mol%) and 2-chloropyridine (**293**, 757 µL, 8.0 mmol, 1.0 equiv) under argon. After addition of THF (8.0 mL), the pale green mixture was stirred for 15 min. Mesityl magnesium bromide (**294**, 1.83 mL, 2.0 M in THF, 12.0 mmol, 1.5 equiv) was transferred via cannula to the mixture, which immediately became dark brown. After stirring for 45 min, methanol (5 mL) was added and the mixture filtered over Celite and concentrated in vacuo. Flash column chromatography on silica gel (9:1 Hexanes/EtOAc eluent) afforded **264** as a pale pink oil (1.42 g, 7.2 mmol, 90% yield), identical by <sup>1</sup>H NMR to that reported.<sup>45</sup>

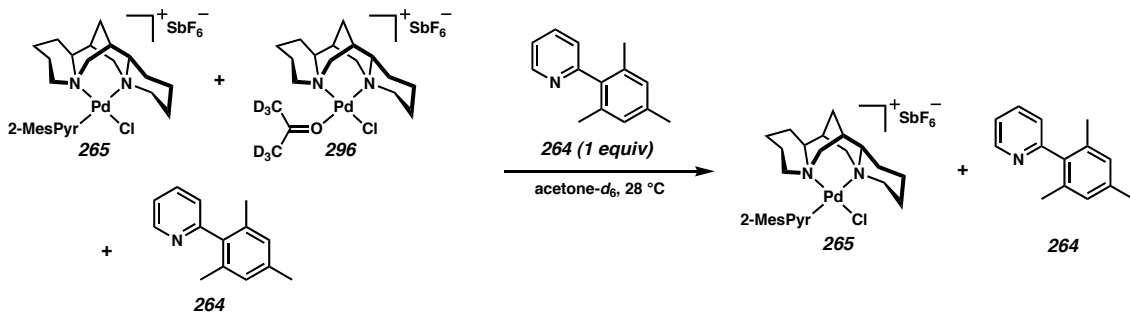


**[sparteine]Pd(2-mesitylpyridine)Cl]<sup>+</sup>SbF<sub>6</sub><sup>-</sup> (**265**).** **265** was prepared according to the method described for **257** which led to a yellow-orange solid (361 mg, 0.446 mmol, 94% yield). Crystals suitable for X-ray diffraction were grown by slow diffusion of pentane

into an acetone solution of **265**.  $^1\text{H}$  NMR (300 MHz,  $\text{CD}_2\text{Cl}_2$ )  $\delta$  8.87 (d,  $J = 5.5$  Hz, 1H), 7.94 (ddd,  $J = 1.6, 7.7, 7.7$  Hz, 1H), 7.52 (m, 1H), 7.34 (d, 7.7 Hz, 1H), 7.20 (s, 1H), 7.18 (s, 1H), 4.41 (d,  $J = 11.0$  Hz, 1H), 3.79 (d,  $J = 12.1$  Hz, 1H), 3.61 (ddd,  $J = 12.6, 2.2, 2.2$  Hz, 1H), 2.78-1.13 (comp. m, 23H), 2.42 (s, 3H), 2.21 (s, 3H), 2.08 (s, 3H);  $^{13}\text{C}$  NMR (75 MHz,  $\text{CD}_2\text{Cl}_2$ )  $\delta$  162.1, 154.9, 141.2, 139.9, 139.5, 135.5, 134.4, 130.3, 129.6, 129.4, 125.7, 70.1, 67.3, 65.3, 64.8, 64.0, 48.3, 34.8, 34.3, 28.9, 27.3, 27.0, 25.2, 24.6, 23.9, 22.2, 21.4, 21.3, 20.6; Anal. calc'd for  $\text{C}_{29}\text{H}_{41}\text{ClF}_6\text{N}_3\text{PdSb}$ : C, 43.04; H, 5.11; N, 5.19. Found: C, 43.08; H, 4.99; N, 5.02. mp 140-145 °C dec.

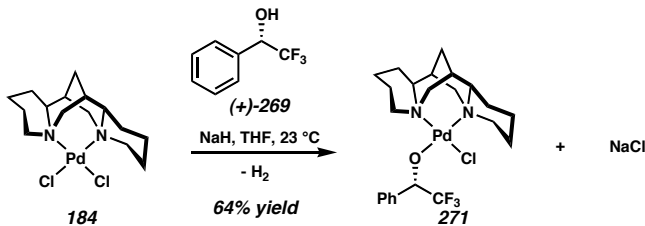


**Observation of 265 at variable temperatures.** **265** (12 mg, 0.015 mmol) was weighed into an NMR tube and dissolved in acetone- $d_6$  (0.700  $\mu\text{L}$ ). 500 MHz  $^1\text{H}$  NMR spectra were acquired from  $-60$  °C to  $+45$  °C at  $15$  °C intervals. One major complex and a minor set of peaks were observable at all temperatures. The minor set of peaks increased from 3% at  $-60$  °C to 10% at  $+45$  °C. We attribute the minor set of peaks to an acetone-ligated cation and free pyridine ligand.



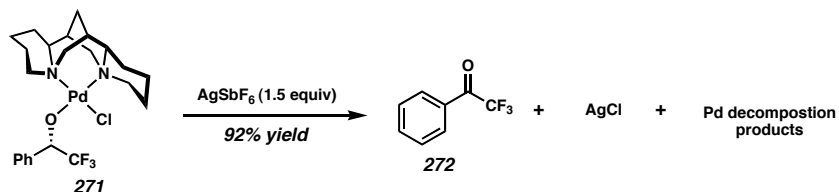
**Reaction of 265 with 2-mesitylpyridine (264).** 265 (5.2 mg, 0.0064 mmol) was weighed into a sealable NMR tube and dissolved in acetone-*d*<sub>6</sub> (0.700 mL). 2-Mesitylpyridine (264, 1.3 mg, 0.0064 mmol, 1 equiv) was added. 500 MHz <sup>1</sup>H NMR spectra were acquired at 25 °C and 28 °C.

#### 4.6.3 The preparation of palladium alkoxide complexes and the reactions thereof.



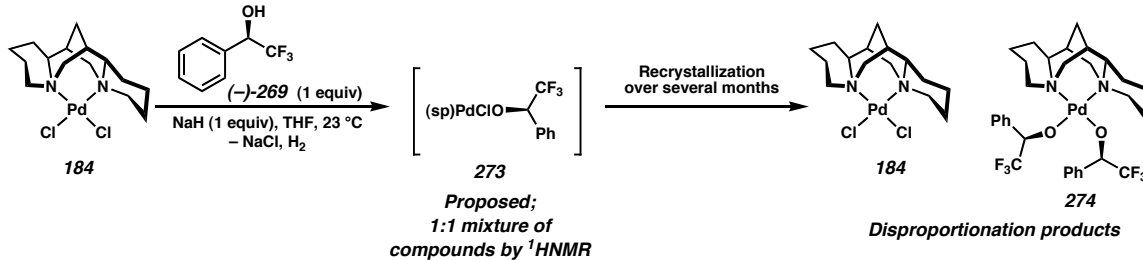
**(sparteine)Pd(OCH(CF<sub>3</sub>)C<sub>6</sub>H<sub>5</sub>)Cl (271).** (+)-*S*-α-(trifluoromethyl)benzyl alcohol ((+)-269, 97 μL, 0.713 mmol, 1.0 equiv) was treated with an excess of sodium hydride (60% dispersion in mineral oil, 57 mg, 1.43 mmol, 2.0 equiv) in THF (5 mL) under argon. After bubbling had ceased, the alkoxide was transferred to a stirring suspension of (sparteine)PdCl<sub>2</sub> (184) (294 mg, 0.713 mmol, 1.0 equiv) in THF (19 mL) under argon at 23 °C. The yellow-orange suspension gradually became an orange solution with very fine white precipitate. After stirring for 30 min, the orange solution was filtered away from the sodium chloride and the solvents removed under vacuum to afford an orange

solid (336 mg, 0.61 mmol, 84% yield) of 74% purity. **271** was obtained after recrystallization from CH<sub>2</sub>Cl<sub>2</sub> layered with hexane at -20 °C in a glove box as an unstable dark orange solid (215 mg 0.39 mmol, 64% yield from crude material). The <sup>1</sup>H NMR spectrum of the crystalline material corresponded to that of the major species in the crude product. A single crystal suitable for X-ray diffraction was grown from CH<sub>2</sub>Cl<sub>2</sub> layered with hexane at -20 °C. <sup>1</sup>H NMR (300 MHz, benzene-d<sub>6</sub>) δ 7.40 (d, *J* = 7.8 Hz, 2H), 7.26-7.16 (comp. m, 3H), 4.92 (q, *J*<sub>HF</sub> = 8.0 Hz, 1H), 4.34 (d, *J* = 11.3 Hz, 1H), 3.52-3.33 (comp. m, 3H), 2.66-2.54 (comp. m, 2H), 2.30-0.98 (comp. m, 20H); <sup>13</sup>C NMR (75 MHz, CD<sub>2</sub>Cl<sub>2</sub>) δ 129.9, 128.9, 128.8, 128.54, 128.47, 128.2, 78.5 (d, *J* = 27.7), 69.9, 65.7, 65.6, 64.3, 57.4, 49.2, 35.4, 34.9, 29.8, 28.0, 27.4, 25.3, 24.7, 24.2, 20.5; <sup>19</sup>F NMR (282 MHz, CD<sub>2</sub>Cl<sub>2</sub>) δ -76.2 (d, *J*<sub>FH</sub> = 8.6 Hz).



**Conversion of 271 to 2,2,2-trifluoroacetophenone (272).** **271** (18.8 mg, 0.034 mmol, 1.0 equiv) and bis(trimethylsilyl)benzene (4.4 mg, 0.021 mmol, 0.59 equiv) as internal standard were dissolved in CD<sub>2</sub>Cl<sub>2</sub> (700 μL) in an NMR tube in the glove box. A <sup>1</sup>H NMR spectrum was acquired and the integration of resonances corresponding to the methine proton of **6** and the methyl resonance of bis(trimethylsilyl)benzene compared. The tube was taken into the glovebox, and AgSbF<sub>6</sub> (17.5 mg, 0.051 mmol, 1.5 equiv) was added to the orange solution upon which a greenish-black suspension was produced immediately. A <sup>1</sup>H NMR spectrum was acquired which showed complete disappearance

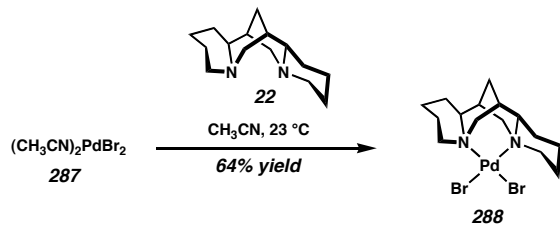
of resonances corresponding to **271** and the appearance of resonances corresponding to 2,2,2-trifluoroacetophenone (**272**, 92% yield based on integration of the *ortho*-aryl  $^1\text{H}$  resonance of 2,2,2-trifluoroacetophenone (**272**) and the methyl resonance of bis(trimethylsilyl)benzene and comparison with the first spectrum).



**(sparteine)Pd(OCH(CF<sub>3</sub>)C<sub>6</sub>H<sub>5</sub>)<sub>2</sub>** (**274**). (–)-R -  $\alpha$ -(trifluoromethyl)benzyl alcohol ((–)-**269**, 99  $\mu\text{L}$ , 0.729 mmol, 1.0 equiv) was treated with 1 equiv of sodium hydride (60% dispersion in mineral oil, 58 mg, 1.46 mmol, 1.0 equiv) in THF (5 mL) under argon. After bubbling had ceased, the alkoxide was transferred to a stirring suspension of (sparteine)PdCl<sub>2</sub> (**184**) (300 mg, 0.729 mmol, 1.0 equiv) in THF (20 mL) under argon at 23 °C. The yellow-orange suspension gradually became an orange solution with very fine white precipitate. After stirring for 30 min, the orange solution was filtered away from the sodium chloride and the solvents removed under vacuum to afford an orange solid. A  $^1\text{H}$  NMR spectrum of this material showed a 1:1 mixture of products. Recrystallization at –20 °C in a glove box from slow diffusion of hexane into a saturated solution of the material in CH<sub>2</sub>Cl<sub>2</sub> after several months provided a mixture of yellow and orange crystals. The orange crystals were identified as **184** by X-ray crystallography and  $^1\text{H}$  NMR. A solid-state structure of the unstable yellow crystals was obtained by X-ray crystallography at -20 °C identifying **274**. The  $^1\text{HNMR}$  spectrum of the crystalline

material did not correspond that of the crude material.  $^1\text{H}$  NMR (300 MHz,  $\text{CD}_2\text{Cl}_2$ )  $\delta$  7.20-6.99 (comp. m, 10H), 4.53- 4.39 (comp. m, 3H), 3.84 (ddd,  $J = 12.2, 2.3, 2.3$  Hz, 1H), 3.70-3.55 (comp. m, 2H), 3.41 (ddd,  $J = 16.7, 13.0, 3.8$  Hz, 1H), 2.92 (dd,  $J = 13.0, 3.4$  Hz, 1H), 2.79-2.70 (comp. m, 3H), 2.39 (dd,  $J = 12.5, 3.0$  Hz, 1H), 2.06-1.25 (comp. m, 16H);  $^{13}\text{C}$  NMR (125 MHz,  $\text{CD}_2\text{Cl}_2$ )  $\delta$  128.8, 128.7, 128.1, 127.8, 127.7, 127.7, 127.6, 78.3 (d,  $J_{\text{CF}} = 26.5$  Hz), 77.5 (d,  $J_{\text{CF}} = 26.5$  Hz), 70.2, 65.5, 65.4, 61.4, 58.0, 49.3, 35.6, 35.4, 30.6, 28.5, 27.2, 25.1, 24.8, 24.3, 20.4;  $^{19}\text{F}$  NMR (282 MHz,  $\text{CD}_2\text{Cl}_2$ )  $\delta$  -75.75 (d,  $J_{\text{FH}} = 9.2$  Hz), -75.90 (d,  $J_{\text{FH}} = 9.2$  Hz).

#### 4.6.4 The preparation of (*sp*) $\text{PdBr}_2$ (**288**) and the reactions thereof.



**(sp)PdBr<sub>2</sub> (288).**  $(\text{CH}_3\text{CN})_2\text{PdBr}_2$ <sup>46</sup> (**287**, 250 mg, 0.72 mmol, 1 equiv) was suspended in  $\text{CH}_3\text{CN}$  (8 mL) under argon at 23 °C. (-)-Sparteine (**22**) was added, which quickly resulted in a dark red-orange solution. After 3 h stirring, a precipitate was visible.  $\text{Et}_2\text{O}$  (10 mL) was added, the mixture triturated, and filtered to provide **288** (230 mg, 0.46 mmol, 64% yield), as a purplish-orange powder. A single crystal suitable for X-ray analysis was grown by slow diffusion of hexane into a saturated  $\text{CH}_2\text{Cl}_2$  solution of **288**.  $^1\text{H}$  NMR (300 MHz,  $\text{CDCl}_3$ )  $\delta$  4.53 (d,  $J = 11.6$  Hz, 1H), 4.20-4.15 (m, 1H), 3.97 (br.d,  $J = 12.9$  Hz, 1H), 3.52-3.39 (m, 1H), 3.24 (dd,  $J = 14.3, 1.4$  Hz, 1H), 2.90-2.77 (comp. m, 2H), 2.45 (dd,  $J = 12.7, 3.0$  Hz, 1H), 2.14-1.40 (comp. m, 18H);  $^{13}\text{C}$  NMR (125 MHz,  $\text{CDCl}_3$ )  $\delta$  70.3, 67.6, 65.5, 64.9, 62.2, 49.1, 35.0, 34.8, 30.3, 28.0, 27.5, 26.0, 24.5, 23.8,

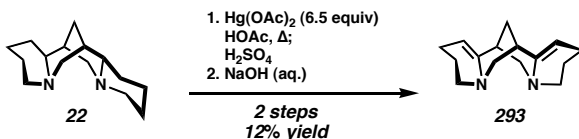
21.4; Anal. calc'd for C<sub>15</sub>H<sub>26</sub>Br<sub>2</sub>N<sub>2</sub>Pd: C, 35.99; H, 5.23; N, 5.60. Found: C, 35.62; H, 5.15; N, 5.53.

**Oxidative kinetic resolution of 1-phenylethanol (21) with 288 shown in Table 4.4.1, Conditions "A," entry 1.** A thick-walled oven-dried 10 mL (1 cm OD) tube equipped with magnetic stir bar was charged with powdered molecular sieves (MS3Å, 100 mg, 500 mg/mmol), **288** (5.0 mg, 0.01 mmol, 0.05 equiv), and tridecane (15.0 µL, 0.062 mmol, 0.31 equiv) as internal standard, followed by toluene (2.0 mL), 1-phenylethanol (**21**, 24 µL, 0.20 mmol, 1 equiv), and (–)-sparteine (**22**) (3.3 mg, 0.014 mmol, 0.07 equiv). The tube was evacuated and back-filled with O<sub>2</sub> (3 x, balloon), heated to 60 °C, and allowed to stir under O<sub>2</sub> (1 atm, balloon). To monitor the reaction, aliquots (200 µL) were removed and passed through a pipette plug of silica gel using Et<sub>2</sub>O as eluent. Conversion was analyzed by GC; the sample was then concentrated in vacuo and %ee analyzed by chiral HPLC as previously reported.<sup>4,5</sup>

**Oxidative kinetic resolution of 1-phenylethanol (21) with 288 shown in Table 4.4.1, conditions "B," entry 2.** A thick-walled oven-dried 10 mL (1 cm OD) tube equipped with magnetic stir bar was charged with powdered molecular sieves (MS3Å, 100 mg, 500 mg/mmol), **288** (5.0 mg, 0.01 mmol, 0.05 equiv), anhydrous Cs<sub>2</sub>CO<sub>3</sub> (26 mg, 0.08 mmol, 0.40 equiv) and tridecane (15.0 µL, 0.062 mmol, 0.31 equiv) as internal standard, followed by CHCl<sub>3</sub> (2.0 mL), 1-phenylethanol (**21**, 24 µL, 0.20 mmol, 1 equiv), and (–)-sparteine (**22**) (3.3 mg, 0.014 mmol, 0.07 equiv). The tube was evacuated and back-filled with O<sub>2</sub> (3 x, balloon) and allowed to stir under O<sub>2</sub> (1 atm, balloon). To monitor the

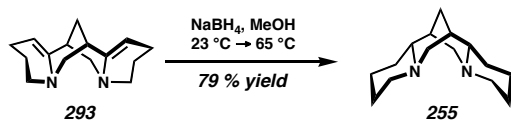
reaction, aliquots (200  $\mu$ L) were removed and passed through a pipette plug of silica gel using Et<sub>2</sub>O as eluent. Conversion was analyzed by GC; the sample was then concentrated in vacuo and %ee analyzed by chiral HPLC as previously reported.<sup>4,5</sup>

#### 4.6.5 The preparation of sparteine ligands, their metal complexes, and the reactions thereof.



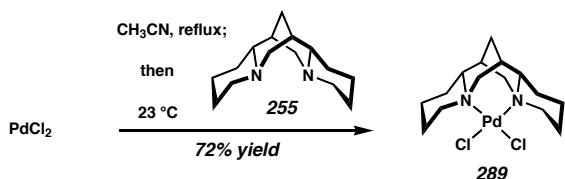
**Didehydrosparteine (293).** 293 was prepared according to the method of Leonard.<sup>30</sup> (–)-Sparteine (**22**, 5.1 g, 21.0 mmol, 1 equiv) was dissolved in a 10% aqueous solution of AcOH (70 mL). This solution was added to a stirring suspension of Hg(OAc)<sub>2</sub> (43.4 g, 136 mmol, 6.5 equiv) in H<sub>2</sub>O (60 mL). The mixture was heated to reflux under argon, during which time a pearlescent precipitate (HgOAc) formed. After 7 h, the mixture was allowed to cool to 23 °C. HgOAc was removed by filtration, and H<sub>2</sub>S gas was bubbled through the yellow filtrate for 15 min to remove excess Hg(OAc)<sub>2</sub>, during which time a fine black precipitate formed. Filtration of the mixture over Celite and a fine fritted funnel removed the black precipitate. The filtrate was acidified with aqueous H<sub>2</sub>SO<sub>4</sub>, and water was subsequently evaporated under vacuum. The resulting partially crystalline oily substance was triturated in methanol and filtered to provide the bisulfate salt as an off-white powder (3.18 g, 9.41 mmol, 45% yield). The salt (1.5 g, 4.45 mmol) was treated with 20% aqueous NaOH (50 mL) and extracted with Et<sub>2</sub>O (5 x 25 mL). The solvent was removed under reduced pressure to provide a brown residue. The crude residue was sublimed at 90-100 °C at 20 millitorr to provide the free base (**293**) as a white powder.

(282 mg, 1.18 mmol, 26.5% yield). **293** was unstable to air at 23 °C, and was thus stored in the freezer under argon. The <sup>1</sup>H NMR spectrum was identical to that reported by Okamoto and Yuki.<sup>47</sup> <sup>1</sup>H NMR (500 MHz, benzene-*d*<sub>6</sub>) δ 4.64 (br s, 2H), 3.09 (d, *J* = 9.3 Hz, 2H), 2.95 (dd, *J* = 11.3, 4.9, 3.3, 2.0 Hz, 2H), 2.81 (dd, *J* = 10.1, 3.8 Hz, 2H), 2.66 (ddd, *J* = 11.0, 11.0, 2.8 Hz, 2H), 2.36-2.35 (m, 2H), 2.26 (ddd, *J* = 16.2, 10.0, 5.7, 2.1 Hz, 2H), 2.12-2.05 (comp. m, 2H), 2.01-1.92 (comp. m, 2H), 1.70-1.64 (comp. m, 4H); <sup>13</sup>C NMR (125 MHz, benzene-*d*<sub>6</sub>) δ 147.0, 93.9, 60.4, 51.3, 37.4, 30.6, 23.1, 22.8; IR (film) 2927, 1643, 1358, 1315 cm<sup>-1</sup>.



**(–)-α-Isosparteine (255).** Didehydrosparteine (**293**) was reduced according to the procedure of Okamoto and Yuki.<sup>47</sup> A mixture of didehydrosparteine (**293**, 300 mg, 1.25 mmol, 1 equiv) and NaBH<sub>4</sub> (1.90 g, 50.1 mmol, 40 equiv) in methanol (15 mL) was allowed to stir at 23 °C for 12 h. Additional methanol (10 mL) was added, and the mixture heated to reflux for 1 h. After cooling to 23 °C, the crude reaction mixture was poured into ice water (15 mL) and basified with 20% aqueous NaOH. The solution was extracted with Et<sub>2</sub>O (5 x 75 mL), dried over K<sub>2</sub>CO<sub>3</sub>, filtered, and concentrated in vacuo to give a white hygroscopic powder. The crude product was sublimed at 65-70 °C at 20 millitorr. The sublimation apparatus was brought into a nitrogen atmosphere glovebox, and the **255** collected (239 mg, 0.982 mmol, 79% yield). The <sup>1</sup>H NMR spectrum was identical to that reported by Okamoto and Yuki.<sup>47</sup> <sup>1</sup>H NMR (500 MHz, benzene-*d*<sub>6</sub>) δ 2.99 (d, *J* = 11.2 Hz, 2H), 2.78-2.74 (m, 2H), 2.08 (dd, *J* = 11.1, 2.9 Hz, 2H), 1.89 (br. d,

$J = 10.9$  Hz, 2H), 1.82-1.64 (comp. m, 8H), 1.55-1.54 (m, 2H), 1.42-1.20 (comp. m, 8H);  $^{13}\text{C}$  NMR (125 MHz, benzene- $d_6$ )  $\delta$  66.6, 58.0, 57.3, 37.3, 36.7, 31.3, 26.6, 26.1; IR (film) 2930, 1444, 1287, 1106 cm $^{-1}$ .



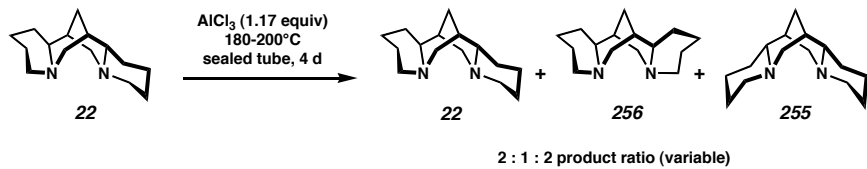
**( $\alpha$ -isosparteine) $\text{PdCl}_2$  289.**  $(\text{CH}_3\text{CN})_2\text{PdCl}_2$  (73 mg, 0.28 mmol, 1.0 equiv) and ( $-$ )- $\alpha$ -isosparteine (255, 66 mg, 0.28 mmol, 1.0 equiv) were dissolved in  $\text{CH}_3\text{CN}$  (5 mL) and allowed to stir at  $23^\circ\text{C}$  under argon for 1 h. The dark orange solution was filtered through Celite and concentrated in vacuo to afford 289 as a rust-colored microcrystalline solid (84 mg, 0.20 mmol, 72% yield). A single crystal suitable for X-ray diffraction was grown by slow evaporation from  $\text{CH}_2\text{Cl}_2$ .  $^1\text{H}$  NMR (300 MHz,  $\text{CD}_2\text{Cl}_2$ )  $\delta$  3.95 (dd,  $J = 12.4, 12.4, 12.4, 3.9$  Hz, 2H), 3.72-3.66 (m, 2H), 3.51 (d,  $J = 12.4$  Hz, 2H), 2.98-2.84 (m, 2H), 2.24-2.19 (m, 2H), 2.15-2.10 (m, 2H) 1.94-1.79 (comp. m, 10 H), 1.65-1.51 (comp. m, 4 H);  $^{13}\text{C}$  NMR (75 MHz,  $\text{CD}_2\text{Cl}_2$ )  $\delta$  72.15, 64.6, 60.7, 35.8, 35.5, 30.9, 25.5, 25.0. Anal. calc'd for  $\text{C}_{15}\text{H}_{26}\text{Cl}_2\text{N}_2\text{Pd}$ : C, 43.76; H, 6.37; N, 6.80. Found: C, 43.82; H, 6.36; N, 6.68; mp 180-182 °C.

### Oxidative kinetic resolution of 1-phenylethanol (21) with 289 or 184 shown in Table

**4.4.1.** A thick-walled oven-dried 10 mL (1 cm OD) tube equipped with magnetic stir bar was charged with powdered molecular sieves (MS3Å, 150 mg, 500 mg/mmol), 289 or 184 (6.2 mg, 0.015 mmol, 0.05 equiv), and tridecane (29.3  $\mu\text{L}$ , 0.12 mmol, 0.40 equiv) as

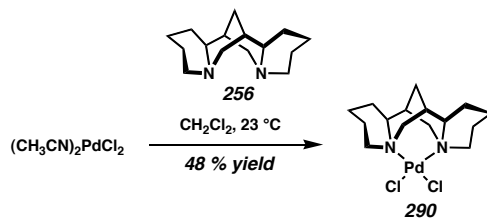
internal standard, followed by toluene (3.0 mL), 1-phenylethanol (**21**, 36  $\mu$ L, 0.30 mmol, 1 equiv), and (–)- $\alpha$ -isosparteine (**255**) or (–)-sparteine (**22**, 10.5 mg, 0.045 mmol, 0.15 equiv). The tube was evacuated and back-filled with O<sub>2</sub> (3 x, balloon), heated to 80 °C, and allowed to stir under O<sub>2</sub> (1 atm, balloon). To monitor the reaction, aliquots (200  $\mu$ L) were removed and passed through a pipette plug of silica gel using Et<sub>2</sub>O as eluent. Conversion was analyzed by GC; the sample was then concentrated in vacuo and %ee analyzed by chiral HPLC as previously reported.<sup>4,5</sup>

**Oxidative kinetic resolution of 1-phenylethanol (**21**) with **289** and **184** with Cs<sub>2</sub>CO<sub>3</sub> as the sole exogenous base shown in Table 4.4.2.** A thick-walled oven-dried 10 mL (1 cm OD) tube equipped with magnetic stir bar was charged with powdered molecular sieves (MS3Å, 150 mg, 500 mg/mmol), **289** or **184** (6.2 mg, 0.015 mmol, 0.05 equiv), and tridecane (29.3  $\mu$ L, 0.12 mmol, 0.40 equiv) as internal standard, followed by toluene (3.0 mL), 1-phenylethanol (**21**, 36  $\mu$ L, 0.30 mmol, 1 equiv), and finely ground anhydrous Cs<sub>2</sub>CO<sub>3</sub> (98 mg, 0.300 mmol, 1 equiv). The tube was evacuated and back-filled with O<sub>2</sub> (3 x, balloon), heated to 80 °C, and allowed to stir under O<sub>2</sub> (1 atm, balloon). To monitor the reaction, aliquots (100  $\mu$ L) were removed and passed through a pipette plug of silica gel using Et<sub>2</sub>O as eluent. Conversion was analyzed by GC; the sample was then concentrated in vacuo and %ee analyzed by chiral HPLC as previously reported.<sup>5</sup>



**(+)- $\beta$ -Isosparteine (256).** **256** was prepared by the method of Winterfeld.<sup>33</sup> Freshly sublimed  $\text{AlCl}_3$  (2.41 g, 18.1 mmol, 1.17 equiv) was transferred to a Schlenk flask in the glovebox. The flask was taken out of the box and distilled ( $-$ -)-sparteine (**22**) (3.96 g, 16.9 mmol, 1 equiv) added under a stream of argon, upon which a small amount of vapor and heat was produced. The flask was sealed and heated to 180–200 °C in a sand bath behind a blast shield. Additional vapor was produced which dissipated after ca. 15 min. The product mixture formed a bright red melt of low viscosity at high temperatures. After 4 d, the flask was cooled to 23 °C upon which the red liquid solidified into a hard glass. The solid was scraped out of the flask with the assistance of 3 M HCl (50 mL) which produced a yellow solution. This solution was basified with KOH and extracted with  $\text{Et}_2\text{O}$  (6 x 50 mL). The organic extracts were dried over  $\text{K}_2\text{CO}_3$ , filtered, and concentrated in vacuo to provide ca. 4.3 g of a 2:1:2 mixture of **22**, (+)- $\beta$ -isosparteine (**256**), and ( $-$ )- $\alpha$ -isosparteine (**255**). The mixture was purified by repeated column chromatography on  $\text{SiO}_2$  with mixtures of  $\text{CH}_2\text{Cl}_2$ , methanol and  $\text{NH}_4\text{OH}$  as eluent. A 100:10:1 mixture was gradually ramped up to a 85:15:1.5 eluent mixture, then to 75:25:2.5 and lastly 60:40:4  $\text{CH}_2\text{Cl}_2$ :MeOH: $\text{NH}_4\text{OH}$ . ( $-$ )-Sparteine (**22**) elutes first, followed quickly by (+)- $\beta$ -isosparteine (**256**), and, much later, ( $-$ )- $\alpha$ -isosparteine (**255**), which is isolated as its hydrate. TLC analysis by iodoplatinate staining was of some

assistance in tracking column progress. Repeated column chromatography of partially separated diastereomers (mostly **22** and **256**) yields approximately 500 mg of pure (+)- $\beta$ -isosparteine (**256**).  $^1\text{H}$  NMR (300 MHz,  $\text{CDCl}_3$ )  $\delta$  2.94 (dd,  $J = 10.7, 6.3$  Hz, 2H), 2.77 (dddd,  $J = 12.4, 4.1, 2.1, 1.9$  Hz, 2H), 2.45 (ddd,  $J = 12.4, 12.4, 2.8$  Hz, 2H), 2.31 (ddd,  $J = 11.8, 2.5, 2.5$  Hz, 2H), **2.22** (dd,  $J = 10.7, 2.8$  Hz, 2H), 1.72-1.49 (comp. m, 10H), 1.36-1.10 (comp. m, 6H);  $^{13}\text{C}$  NMR (125 MHz,  $\text{CDCl}_3$ )  $\delta$  63.3, 55.9, 55.7, 35.6, 29.4, 26.4, 23.6, 20.6; IR (film) 2925, 1447, 1357, 1129  $\text{cm}^{-1}$ ;  $[\alpha]_D^{21.1} +15.38$  ( $c$  0.142, absolute EtOH).



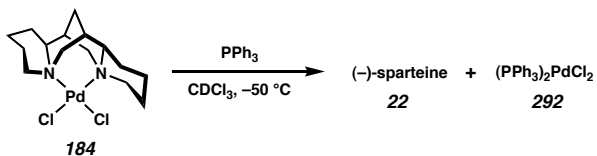
**((+)- $\beta$ -Isosparteine)PdCl<sub>2</sub> (290).** (+)- $\beta$ -Isosparteine (**256**, 48 mg, 0.21 mmol, 1 equiv) was taken up in  $\text{CH}_2\text{Cl}_2$  (4 mL) under argon. The flask was opened and  $(\text{CH}_3\text{CN})_2\text{PdCl}_2$  (53 mg, 0.21 mmol, 1 equiv) was added quickly as a solid. The resulting dark red-orange solution was allowed to stir at 23 °C for 16 h. After the solution was filtered through glass filter paper to remove a small amount of palladium black, the solvents were evaporated to give an orange powder. Trituration with pentane from  $\text{CH}_2\text{Cl}_2$  provided **290** (41 mg, 0.10 mmol, 48% yield) as a light orange powder.  $^1\text{H}$  NMR (500 MHz,  $\text{CD}_2\text{Cl}_2$ )  $\delta$  3.85-3.75 (comp. m, 4H), 3.26-3.03 (comp. m, 6H), 1.99-1.33 (comp. m, 16H);  $^{13}\text{C}$  NMR (75 MHz,  $\text{CD}_2\text{Cl}_2$ )  $\delta$  64.8, 64.5, 56.0, 35.2, 28.0, 23.9, 21.4, 20.5; Anal. calc'd for  $\text{C}_{15}\text{H}_{26}\text{Cl}_2\text{N}_2\text{Pd}$ : C, 43.76; H, 6.37; N, 6.80. Found: C, 43.97; H, 6.41; N, 6.81.

**Oxidative kinetic resolution of 1-phenylethanol (**21**) with **290** shown in Table 4.4.3.**

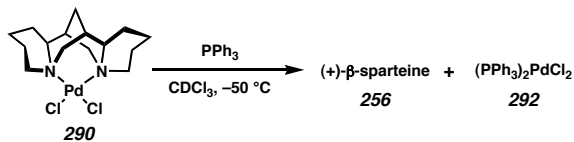
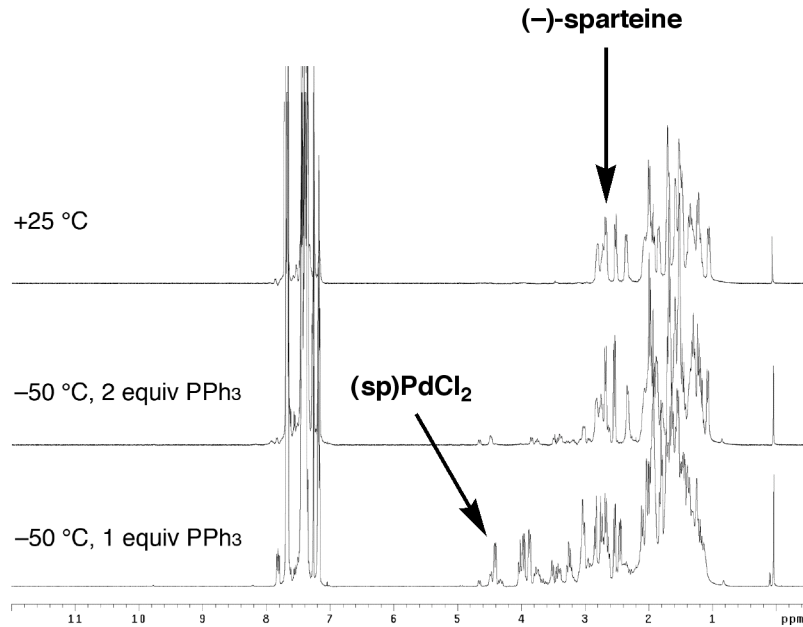
A thick-walled oven-dried 10 mL (1 cm OD) tube equipped with magnetic stir bar was charged with powdered molecular sieves (MS3Å, 100 mg, 500 mg/mmol), **290** (4.1 mg, 0.01 mmol, 0.05 equiv), and tridecane (15 µL, 0.062 mmol, 0.31 equiv) as internal standard, followed by toluene (2.0 mL), 1-phenylethanol (**21**, 24 µL, 0.20 mmol, 1 equiv), and **256** (7.0 mg, 0.03 mmol, 0.15 equiv). The tube was evacuated and back-filled with O<sub>2</sub> (3 x, balloon), heated to 80 °C, and allowed to stir under O<sub>2</sub> (1 atm, balloon). To monitor the reaction, aliquots (200 µL) were removed and passed through a pipette plug of silica gel using Et<sub>2</sub>O as eluent. Conversion was analyzed by GC; the sample was then concentrated in vacuo and %ee analyzed by chiral HPLC as previously reported.<sup>4,5</sup>

**Oxidative kinetic resolution of 1-phenylethanol (**21**) with **290** with Cs<sub>2</sub>CO<sub>3</sub> as the sole exogenous base shown in Table 4.4.3.** A thick-walled oven-dried 10 mL (1 cm OD) tube equipped with magnetic stir bar was charged with powdered molecular sieves (MS3Å, 100 mg, 500 mg/mmol), **290** (4.1 mg, 0.01 mmol, 0.05 equiv), and tridecane (15 µL, 0.062 mmol, 0.31 equiv) as internal standard, followed by toluene (2.0 mL), 1-phenylethanol (**21**, 24 µL, 0.20 mmol, 1 equiv), and finely ground anhydrous Cs<sub>2</sub>CO<sub>3</sub> (65 mg, 0.20 mmol, 1 equiv). The tube was evacuated and back-filled with O<sub>2</sub> (3 x, balloon), heated to 80 °C, and allowed to stir under O<sub>2</sub> (1 atm, balloon). To monitor the reaction, aliquots (200 µL) were removed and passed through a pipette plug of silica gel using Et<sub>2</sub>O as eluent. Conversion was analyzed by GC; the sample was then concentrated

in vacuo and %ee analyzed by chiral HPLC as previously reported.<sup>4,5</sup>



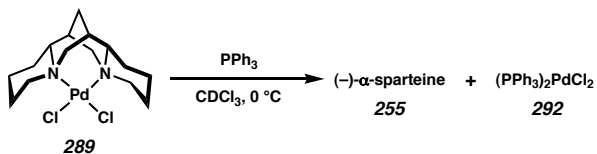
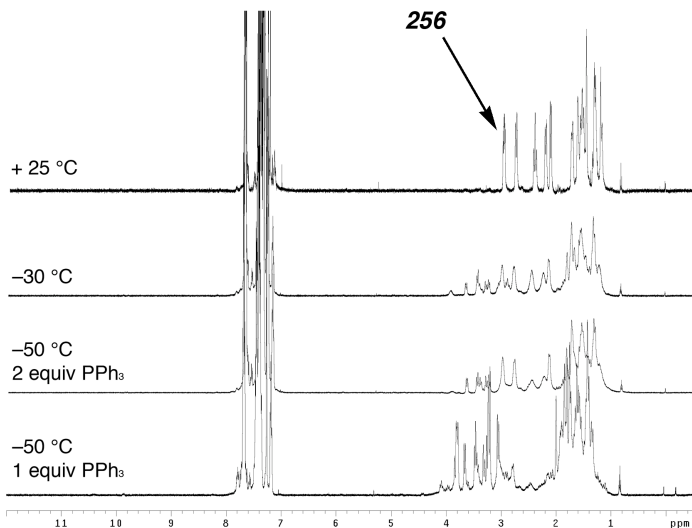
**Reaction of 184 with PPh<sub>3</sub>.** **184** (300  $\mu$ L of a 0.083M solution in CDCl<sub>3</sub>, 0.025 mmol, 1 equiv) was dissolved in CDCl<sub>3</sub> (375  $\mu$ L) in a sealable NMR tube under argon. The tube was cooled to  $-55$  °C in a CHCl<sub>3</sub>/dry ice bath. PPh<sub>3</sub> (25  $\mu$ L of a 1.0M solution in CDCl<sub>3</sub>, 0.025 mmol, 1 equiv) was added, the tube was inverted once, and inserted into a 500 MHz NMR probe at  $-50$  °C. Approximately 2.5 min elapsed before the acquisition of the first <sup>1</sup>H NMR spectrum, which showed peaks corresponding to **184**, **292**, free  $(-) -\text{sparteine}$  (**22**), and an unidentified product. The tube was ejected and a second equivalent PPh<sub>3</sub> was added (25 mL of a 1.0M solution in CDCl<sub>3</sub>, 0.025 mmol, 1 equiv). The tube was inverted once and reinserted into the NMR probe at  $-50$  °C. A <sup>1</sup>H NMR spectrum was acquired, which showed the unidentified product, **22**, but no **184**. After 5 min, another spectrum was acquired which showed no change. The tube was warmed to 25 °C, and a <sup>1</sup>H NMR spectrum was acquired, which showed primarily **22** and **(PPh<sub>3</sub>)<sub>2</sub>PdCl<sub>2</sub>** (**292**). Refer to Figure 4.6.2 for NMR spectra.

Figure 4.6.2 Reaction of **184** and  $\text{PPh}_3$  observed by  $^1\text{H}$  NMR.

**Reaction of **290** with  $\text{PPh}_3$ .** **290** (6.4 mg, 0.016 mmol, 1 equiv) was dissolved in  $\text{CDCl}_3$  (684  $\mu\text{L}$ ) in a sealable NMR tube under argon. The tube was cooled to  $-55^\circ\text{C}$  in a  $\text{CHCl}_3/\text{dry ice}$  bath.  $\text{PPh}_3$  (25  $\mu\text{L}$  of a 1.0 M solution in  $\text{CDCl}_3$ , 0.025 mmol, 1 equiv) was added, the tube was inverted once, and inserted into a 500 MHz NMR probe at  $-50^\circ\text{C}$ . Approximately 3 min elapsed before the acquisition of the first  $^1\text{H}$  spectrum, which showed peaks corresponding to **290**, **292**, free (+)- $\beta$ -isosparteine (**256**), and an unidentified product. The tube was ejected and a second equiv  $\text{PPh}_3$  was added (25 mL of a 1.0 M solution in  $\text{CDCl}_3$ , 0.025 mmol, 1 equiv). The tube was inverted once and reinserted into the NMR probe at  $-50^\circ\text{C}$ . A  $^1\text{H}$  NMR spectrum was acquired, which

showed the unidentified product, free (–)-sparteine (**22**), but no **290**. The tube was warmed to –30 °C, and a  $^1\text{H}$  NMR spectrum was acquired, which showed a complex mixture. The tube was warmed to +25 °C, and a  $^1\text{H}$  NMR spectrum was acquired, which showed only **292** and (+)- $\beta$ -isosparteine (**256**). Refer to Figure 4.6.3 for NMR spectra.

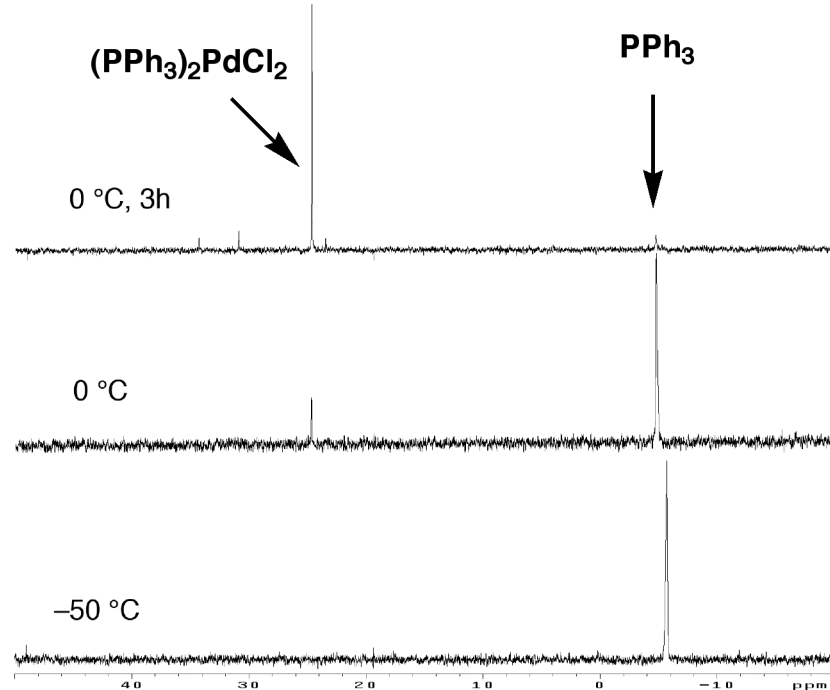
Figure 4.6.3 Reaction of **290** with  $PPh_3$  observed by  $^1H$  NMR.



**Reaction of 289 with PPh<sub>3</sub>.** ((-)- $\alpha$ -Isosparteine)PdCl<sub>2</sub> (**289**, 7.8 mg, 0.019 mmol, 1 equiv) was dissolved in CDCl<sub>3</sub> (662  $\mu$ L) in a sealable NMR tube under argon. The tube was cooled to -55 °C in a CHCl<sub>3</sub>/dry ice bath. PPh<sub>3</sub> (38  $\mu$ L of a 1.0M solution in CDCl<sub>3</sub>, 0.038 mmol, 2 equiv) was added, the tube was inverted once, and inserted into a 500 MHz NMR probe at -50 °C. A <sup>31</sup>P spectrum was acquired. No reaction was observed. The tube was gradually warmed at 10-15° intervals to 0 °C, at which temperature reaction

occurred at a reasonable rate. Reaction to free (–)- $\alpha$ -isosparteine (**255**) and  $(\text{PPh}_3)_2\text{PdCl}_2$  (**292**) was complete in approximately 3 h (Figure 4.6.4).

Figure 4.6.4 Reaction of **289** with  $\text{PPh}_3$  observed by  $^{31}\text{P}$  NMR.



## 4.7 NOTES AND REFERENCES

<sup>1</sup> Wieland, H. *Ber.* **1912**, *45*, 484-493.

<sup>2</sup> Schwartz, J.; Blackburn, T. F. *J. Chem. Soc., Chem. Commun.* **1977**, 157-158.

<sup>3</sup> For recent Pd(II) aerobic alcohol oxidations, see: (a) Peterson, K. P.; Larock, R. C. *J. Org. Chem.* **1998**, *63*, 3185-3189. (b) Nishimura, T.; Onoue, T.; Ohe, K.; Uemura, S. *J. Org. Chem.* **1999**, *64*, 6750-6755. (c) Brink, G.-J.; Arends, I. W. C. E.; Sheldon, R. A. *Science* **2000**, *287*, 1636-1639. (d) For a review, see: Muzart, J. *Tetrahedron* **2003**, *59*, 5789-5816.

<sup>4</sup> Ferreira, E. M.; Stoltz, B. M. *J. Am. Chem. Soc.* **2001**, *123*, 7725-7726.

<sup>5</sup> (a) Bagdanoff, J. T.; Ferreira, E. M.; Stoltz, B. M. *Org. Lett.* **2003**, *5*, 835-837. (b) Bagdanoff, J. T.; Stoltz, B. M. *Angew. Chem., Int. Ed.* **2004**, *43*, 353-357.

<sup>6</sup> Another group has developed a similar kinetic resolution system, see: (a) Jensen, D. R.; Pugsley, J. S.; Sigman, M. S. *J. Am. Chem. Soc.* **2001**, *123*, 7475-7476. (b) Mandal, S. K.; Jensen, D. R.; Pugsley, J. S.; Sigman, M. S. *J. Org. Chem.* **2003**, *68*, 4600-4603 and references therein. (c) Mandal, S. K.; Sigman, M. S. *J. Org. Chem.* **2003**, *68*, 7535-7537.

<sup>7</sup> (a) Caspi, D. D.; Ebner, D. C.; Bagdanoff, J. T.; Stoltz, B. M. *Adv. Synth. Catal.* **2004**, *346*, 185-189. (b) Ebner, D. C.; Stoltz, B. M. Unpublished results.

<sup>8</sup> O'Brien and coworkers have synthesized analogues of (+)-sparteine that are somewhat effective as sparteine surrogates, see: (a) Dearden, M. J.; Firkin, C. R.; Hermet, J.-P. R.; O'Brien P. *J. Am. Chem. Soc.* **2002**, *124*, 11870-11871. (b) Hermet, J.-P. R.; Porter, D. W.; Dearden, M. J.; Harrison, J. R.; Koplin, T.; O'Brien, P.; Parmene, J.; Tyurin, V.; Whitwood, A. C.; Gilday, J.; Smith, N. M. *Org. Biomol. Chem.*, **2003**, *1*, 3977-3988. (c) Dearden, M. J.; McGrath, M. J.; O'Brien, P. *J. Org. Chem.* **2004**, *69*, 5789-5792. (d) Ebner, D. C.; Stoltz, B. M. Unpublished results.

<sup>9</sup> (a) Sheldon, R. A.; Arends, I. W. C. E. in *Advances in Catalytic Activation of Dioxygen by Metal Complexes*, Simándi, L. I. 2003 Vol. 26 Ch. 3 p 123. Kluwer, Dordrecht. (b) Steinhoff, B. A.; Stahl, S. S. *Org. Lett.* **2002**, *4*, 4179-4181. (c) Stahl, S. S.; Thorman, J.

L.; Nelson, R. C.; Kozee, M. A. *J. Am. Chem. Soc.* **2001**, *123*, 7188-7189 and references therein.

<sup>10</sup> (a) Mueller, J. A.; Cowell, A.; Chandler, B. D.; Sigman, M. S. *J. Am. Chem. Soc.* **2005**, *127*, 14817-14824. (b) Mueller, J. A.; Sigman, M. S. *J. Am. Chem. Soc.* **2003**, *125*, 7005-7013. (c) Mueller, J. A.; Jensen, D. R.; Sigman, M. S. *J. Am. Chem. Soc.* **2002**, *124*, 8202-8203.

<sup>11</sup> For another example that uses similar logic, see: Li, X.; Schenkel, L. B.; Kozlowski, M. C. *Org. Lett.*, **2000**, *2*, 875-878.

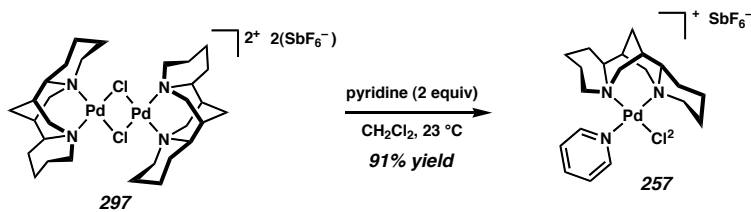
<sup>12</sup> Kagan, H. B.; Dang, T.-P. *J. Am. Chem. Soc.* **1972**, *94*, 6429-6433.

<sup>13</sup> Whitesell, J. K. *Chem. Rev.* **1989**, *89*, 1581-1590.

<sup>14</sup> X-ray quality crystals of **184** were grown by Eric Ferreira. The molecular structures are shown with 50% probability ellipsoids. The hydrogen atoms in the (-)-sparteine (**22**) backbone in the side view have been omitted for clarity.

<sup>15</sup> Leonard, N. J. in *The Alkaloids, Chemistry and Physiology*, vol. III, R. H. F. Manske and H. L. Holmes, Ed., Academic Press, New York, NY, 1953. pp. 119-199.

<sup>16</sup> The same product was observed in the reaction of chloro-bridged dimer **297** (see Appendix 4.3) with 2.0 equiv of pyridine in 91% yield.



<sup>17</sup> The molecular structures are shown with 50% probability ellipsoids. The hydrogen atoms in the (-)-sparteine (**22**) backbone in the side view and the  $\text{SbF}_6^-$  ion in both views have been omitted for clarity.

<sup>18</sup> Two molecules were found in the asymmetric unit. Molecule A is disordered as described, with the occupancies of both orientations nearly equal. The atoms of the isoquinoline in both orientations were refined isotropically (depicted in Scheme 4.2.3).

Molecule B also contains disorder in the isoquinoline, but to a much lesser extent, and can be refined anisotropically with the atoms set as rigid bodies. In molecule B, the methyl group is oriented towards quadrant IV. The bond distances and angles shown in Scheme 4.2.3 are for molecule B. See Appendix 4.5 for further details.

<sup>19</sup> For examples that possess  $\beta$ -hydrogen atoms, see Appendix 4.12.

<sup>20</sup> A racemic Pd(II) alkoxide complex of ( $\pm$ )-**269** has been reported:  $[(\text{PMe}_3)_2\text{Pd}(\text{Me})(\text{OR})]$  where R = PhCH(CF<sub>3</sub>). See: Kim, Y.-J.; Osakada, K.; Takenaka, A.; Yamamoto, A. *J. Am. Chem. Soc.* **1990**, *112*, 1096-1104.

<sup>21</sup> The molecular structures are shown with 50% probability ellipsoids. The hydrogen atoms in the (-)-sparteine (**22**) backbone in the side view have been omitted for clarity.

<sup>22</sup> Yield was determined by <sup>1</sup>H NMR using an internal standard, see Section 4.6.

<sup>23</sup> Another possibility is that the thermodynamics of solubility plays a role; one of the products could be less soluble than the other, and crystallize first, leaving the other behind in solution.

<sup>24</sup> While the structural studies we have undertaken have been almost exclusively in the solid state, the consistency of the results and the support of theoretical calculations give us confidence in our model.

<sup>25</sup> (a) Bryndza, H. E.; Tam, W. *Chem. Rev.* **1988**, *88*, 1163-1188. (b) Zhao, J.; Hesslink, H.; Hartwig, J. F. *J. Am. Chem. Soc.* **2001**, *123*, 7220-7227. (c) For an alternative with platinum see: Bryndza, H. E.; Calabrese, J. C.; Marsi, M.; Roe, D. C.; Tam, W.; Bercaw, J. E. *J. Am. Chem. Soc.* **1986**, *108*, 4805-4813.

<sup>26</sup> Thorn, D. L.; Hoffmann, R. *J. Am. Chem. Soc.* **1978**, *100*, 2079-2090.

<sup>27</sup> Nielsen, R. J.; Keith, J. M.; Stoltz, B. M.; Goddard, W. A. *J. Am. Chem. Soc.* **2004**, *126*, 7967-7974.

<sup>28</sup> For references pertaining to  $\alpha$ -isosparteine, see: (a) Winterfeld, K. *Arch. Pharm.* **1928**, *266*, 299-325. (b) Marion, L.; Turcotte, F.; Ouellet, J. *Can. J. Chem.* **1951**, *29*, 22-29. (c) Galinovsky, F.; Knoth, P.; Fischer, W. *Monatsh. Chemie* **1955**, *86*, 1014-1023. (d) Leonard, N. J.; Thomas, P. D.; Gash, V. W. *J. Am. Chem. Soc.* **1955**, *77* 1552-1558.

(e) Oinuma, H.; Dan, S.; Kakisawa, H. *J. Chem. Soc., Chem. Commun.* **1983**, 654-655.  
(f) Blakemore, P. R.; Kilner, C.; Norcross, N. R.; Astles, P. C. *Org. Lett.* **2005**, 7, 4721-4724. (g) Przybylska, M.; Barnes, W. H. *Acta Cryst.* **1953**, 6, 377-384.

<sup>29</sup> For references pertaining to  $\beta$ -isosparteine, see: (a) Greenhalgh, R.; Marion, L. *Can. J. Chem.* **1956**, 34, 456-458. (b) Carmack, M.; Douglas, B.; Martin, E. W.; Suss, H. *J. Am. Chem. Soc.* **1955**, 77, 4435. (c) Carmack, M.; Goldberg, S. I.; Martin, E. W. *J. Org. Chem.* **1967**, 32, 3045-3049. (d) Wanner, M. J.; Koomen, G.-J. *J. Org. Chem.* **1996**, 61, 5581-5586. (e) Childers, L. S.; Folting, K.; Merritt Jr., L. L.; Streib, W. E. *Acta Cryst.* **1975**, B31, 924-925.

<sup>30</sup> Leonard, N. J.; Beyler, R. E. *J. Am. Chem. Soc.* **1950**, 72, 1316-1323.

<sup>31</sup> The selectivity factor,  $s$ , or  $k_{\text{rel}}$  was determined by the following equation:  $s = k_{\text{rel}} = \ln[(1-C)(1 - ee)]/\ln[(1 - C)(1 + ee)]$  where C is conversion and ee is enantiomeric excess.

<sup>32</sup> Cesium carbonate (along with excess **22**) is a component of the "rate-accelerated" conditions for oxidative kinetic resolution.

<sup>33</sup> Winterfeld, K.; Bange, H.; Lalvani, K. S. *Justus Liebigs Ann. Chem.* **1966**, 698, 230-234.

<sup>34</sup> Although the sign of rotation is different than for  $(-)$ -sparteine (**22**) and  $(-)\alpha$ -isosparteine (**255**), it is in the same enantiomeric series.

<sup>35</sup> While the reaction also occurs in acetonitrile, complications upon isolation and purification arose that we attribute to monocoordination in the presence of a coordinating solvent.

<sup>36</sup> For a mini-review of  $C_1$  symmetric ligand in asymmetric processes, see Appendix 6.

<sup>37</sup> (a) Mikhova, B.; Duddeck, H. *Magn. Reson. Chem.* **1999**, 36, 779-796. (b) Bour, P. J. *Phys. Chem. A* **1997**, 101, 9783-9790. (c) Boczon, W. *Bull. Pol. Acad. Sci.* **1989**, 37, 9-33. (d) Sadykov, A. S.; Kamayev, F. G.; Korenevsky, V. A.; Leont'ev, V. B.; Ustynyuk, Y. A. *Org. Mag. Resonance* **1972**, 4, 837-846.

<sup>38</sup> Galasso, V.; Asaro, F.; Berti, F.; Kovac, B.; Habus, I.; Sacchetti, A. *Chem. Phys.* **2003**, 294, 155-169.

<sup>39</sup> (a) Togni, A.; Rihs, G. *Helvetica Chim. Acta* **1990**, 73, 723-732. (b) Strohmann, C.; Däschlein, C.; Auer, D. *J. Am. Chem. Soc.* **2006**, 128, 704-705. (c) Jaiewicz, B.; Sikorska, E.; Khmelinskii, I. V.; Warzajtis, B.; Rychlewska, U.; Boczon, W.; Sikorski, M. *J. Mol. Structure*, **2004**, 707, 89-96. (d) Lee, Y.-M.; Kang, S. K.; Chung, G.; Kim, Y.-K.; Won, S.-Y.; Choi, S.-N. *J. Coord. Chem.* **2003**, 56, 635-646.

<sup>40</sup> Observations in CDCl<sub>3</sub> were carried out at -50 °C.

<sup>41</sup> A similar scenario has been reported for a dineopentylmagnesium complex, see: Fraenkel, G.; Appleman, B.; Ray, J. G. *J. Am. Chem. Soc.* **1974**, 96, 5113-5119.

<sup>42</sup> In terms of the oxidative kinetic resolution, this result helps explain the empirical observation that excess ligand is required for high selectivity.

<sup>43</sup> However, no significant changes in the <sup>1</sup>H NMR spectrum of (sp)PdCl<sub>2</sub> (**184**) alone were observed at -50 °C in CDCl<sub>3</sub>.

<sup>44</sup> Another possibility is that because (-)-α-isosparteine (**255**) positions a C–H bond over the palladium atom on both sides of the square plane, approach by PPh<sub>3</sub> is hindered and therefore slower. (-)-Sparteine (**22**) positions a C–H bond over the palladium atom on only one face of the square plane, and (+)-β-isosparteine (**256**) on neither face. See Figures 4.4.1 and 4.4.2.

<sup>45</sup> Boehm, V. P. W.; Weskamp, T.; Gstoeftmayr, C. W. K.; Hermann, W. A. *Angew. Chem. Int. Ed.* **2000**, 39, 1602-1604.

<sup>46</sup> Prepared by heating PdBr<sub>2</sub> in CH<sub>3</sub>CN to reflux under nitrogen for 2 h.

<sup>47</sup> Okamoto, Y.; Suzuki, K.; Kitayama, T.; Yuki, H.; Kageyama, H.; Miki, K.; Tanaka, N.; Kasai, N. *J. Am. Chem. Soc.* **1982**, 104, 4618-4624.

## **APPENDIX 4.1**

*Spectra Relevant to Chapter 4.*

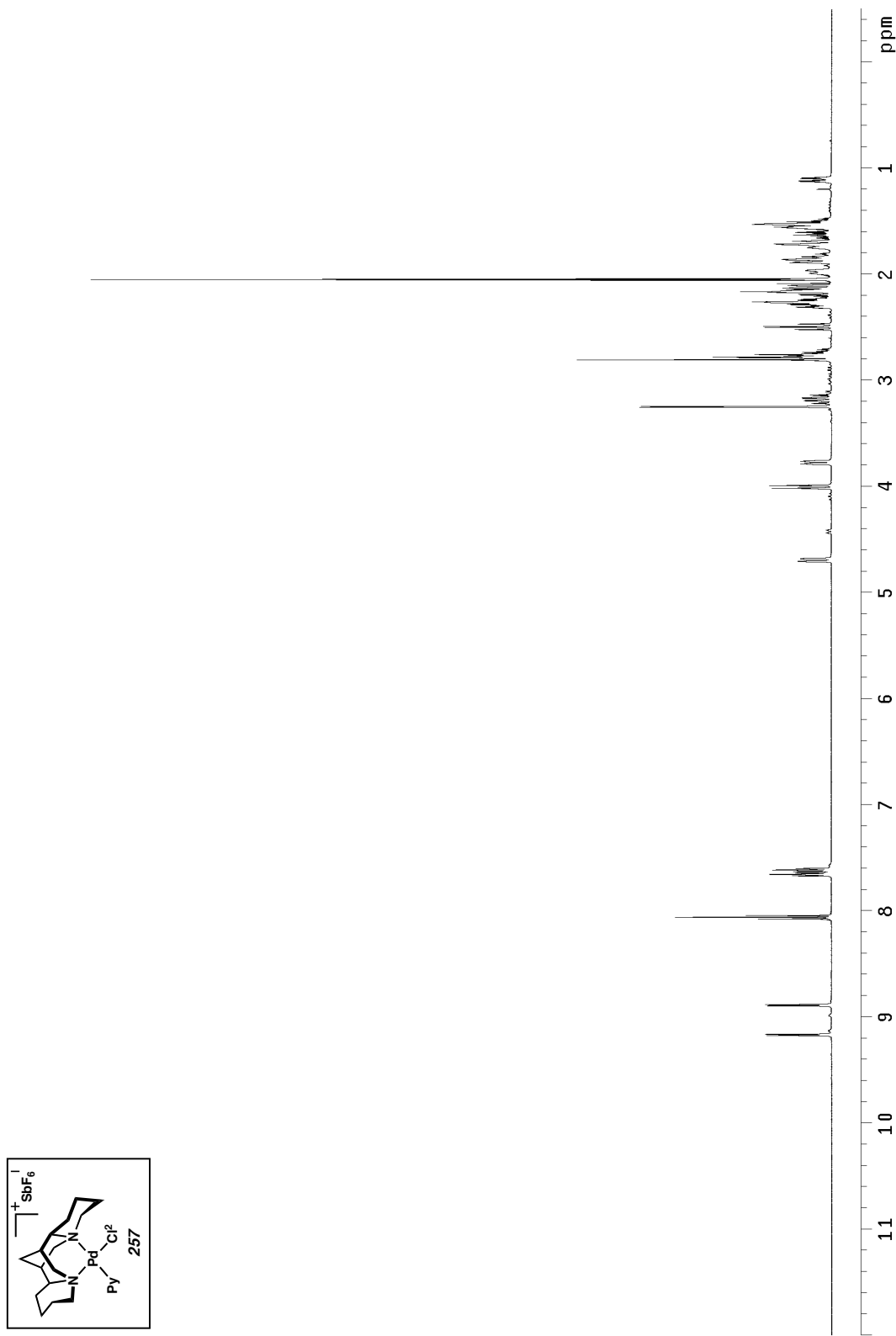


Figure A4.1.1  $^1\text{H}$  NMR spectrum (500 MHz, acetone- $d_6$ ) of **257**.

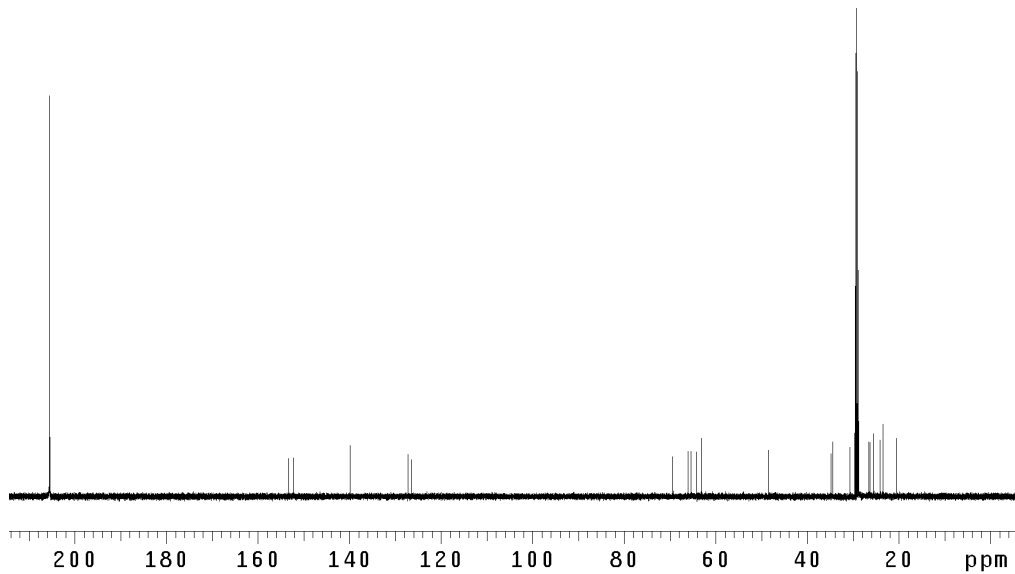


Figure A4.1.2  $^{13}\text{C}$  NMR spectrum (125 MHz, acetone- $d_6$ ) of **257**.

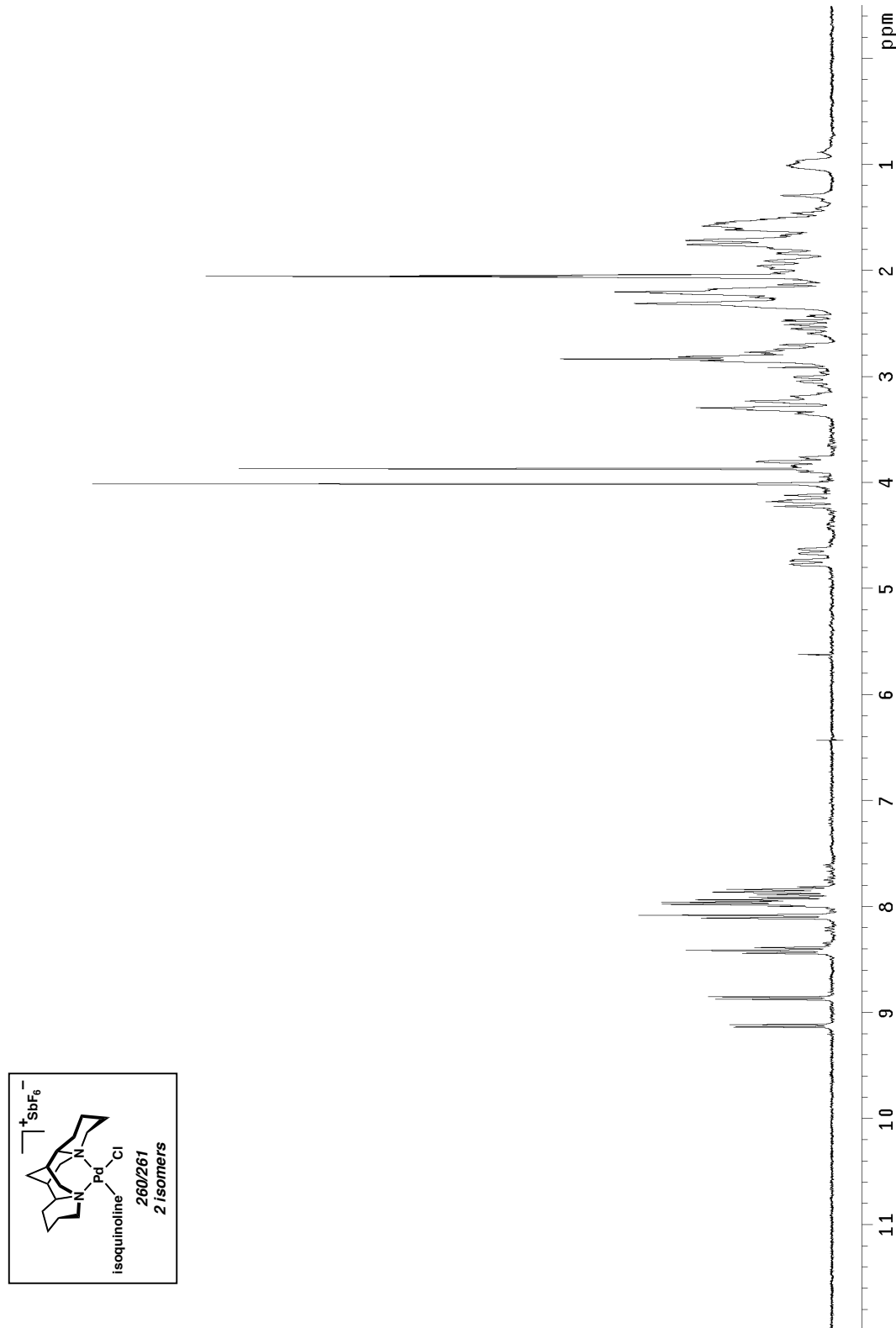


Figure A4.1.3  $^1\text{H}$  NMR spectrum (500 MHz, acetone- $d_6$ ) of **260/261**.

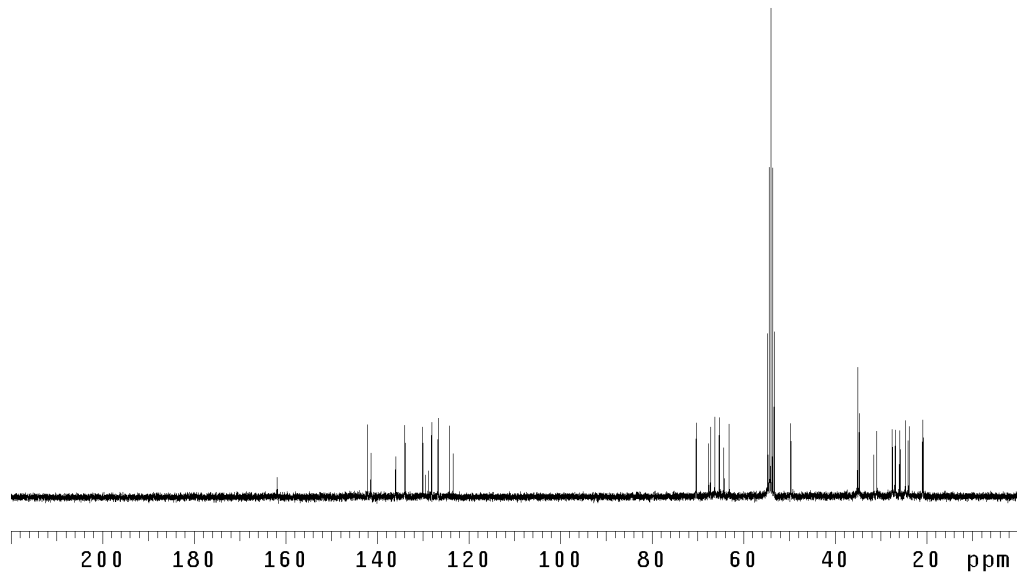


Figure A4.1.4  $^{13}\text{C}$  NMR spectrum (75 MHz,  $\text{CDCl}_3$ ) of **260/261**.

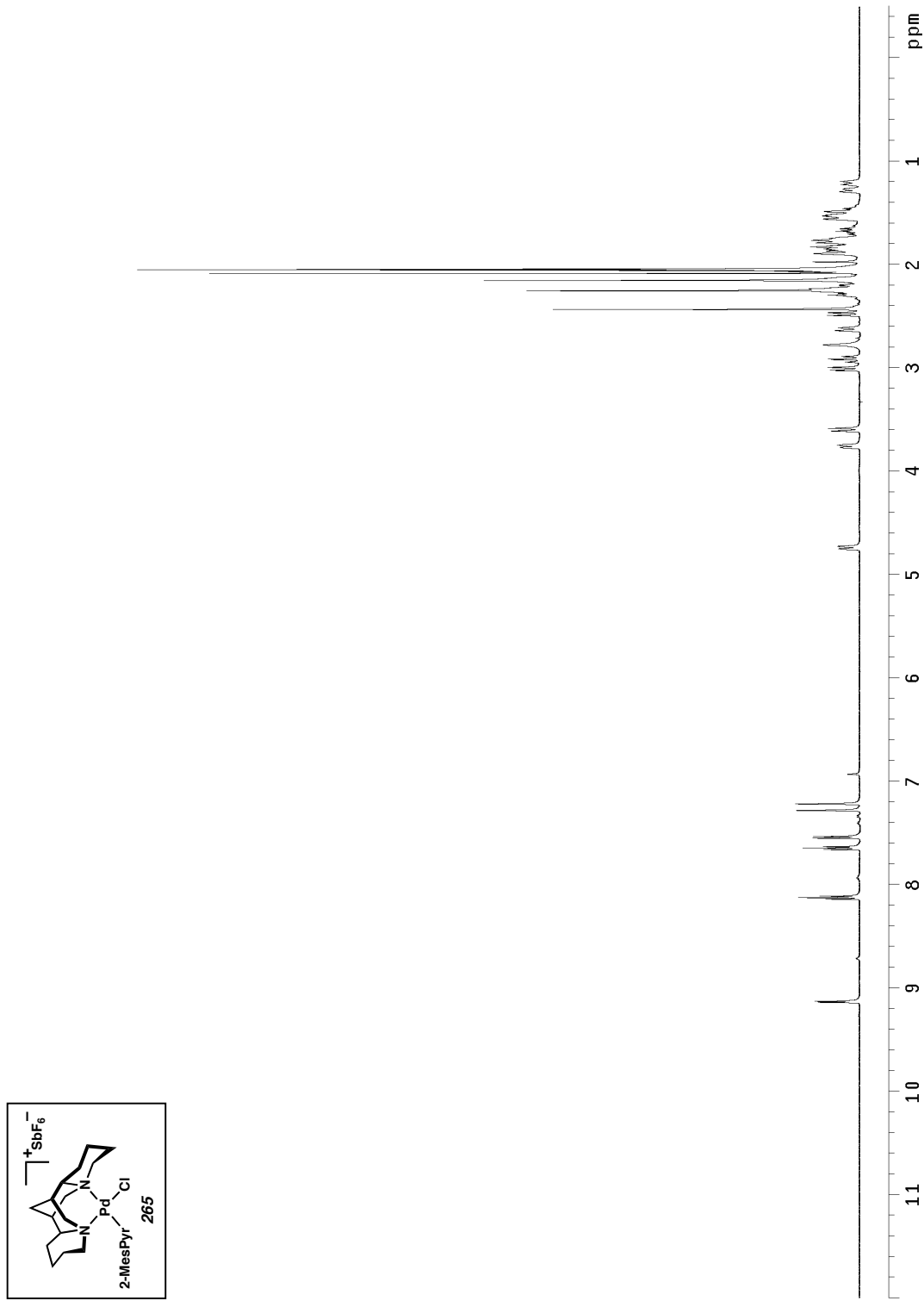


Figure A4.1.4  $^1\text{H}$  NMR spectrum (500 MHz, acetone- $d_6$ ) of **265**.

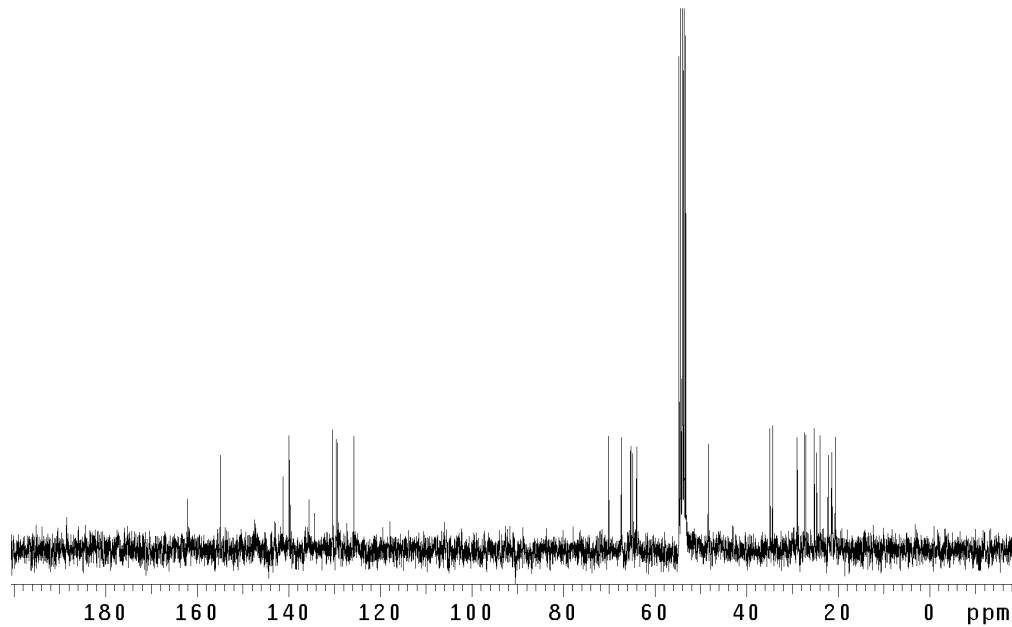


Figure A4.1.5 <sup>13</sup>C NMR spectrum (75 MHz, CDCl<sub>3</sub>) of **265**.

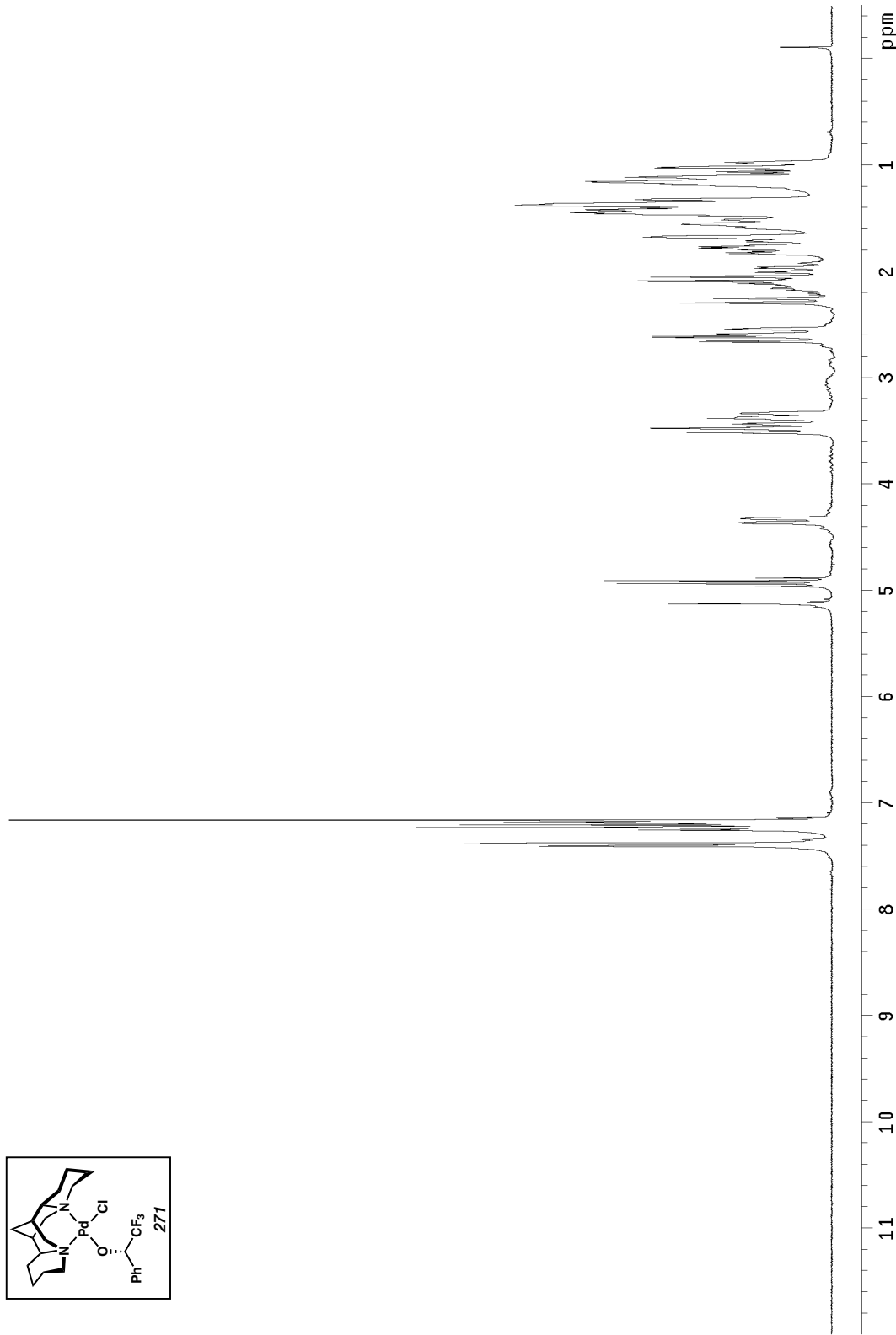


Figure A4.1.6  $^1\text{H}$  NMR spectrum (300 MHz, benzene- $d_6$ ) of **271**.

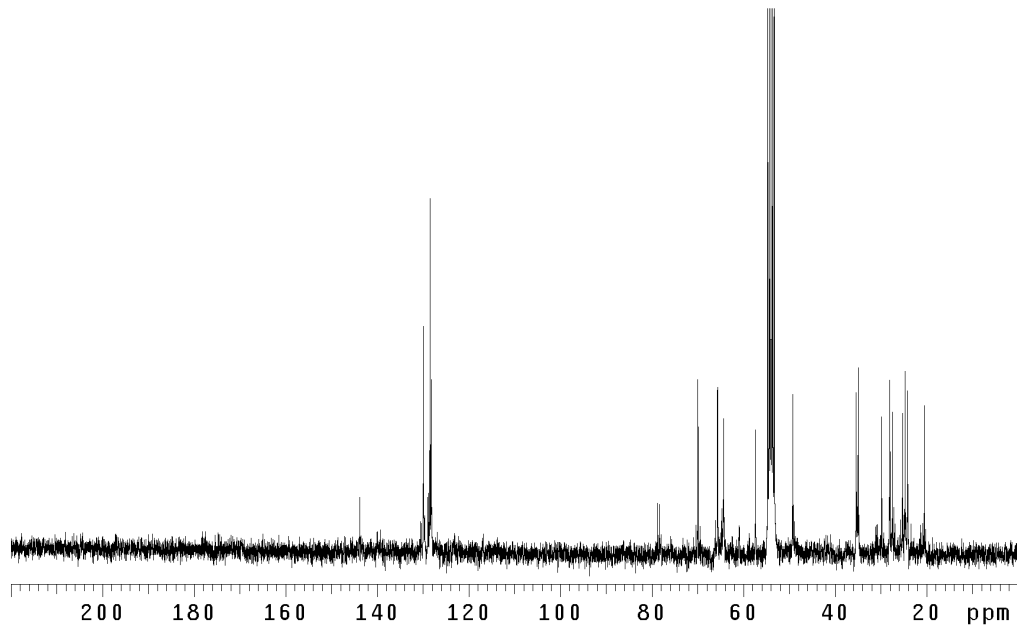


Figure A4.1.7  $^{13}\text{C}$  NMR spectrum (75 MHz,  $\text{CD}_2\text{Cl}_2$ ) of **271**.

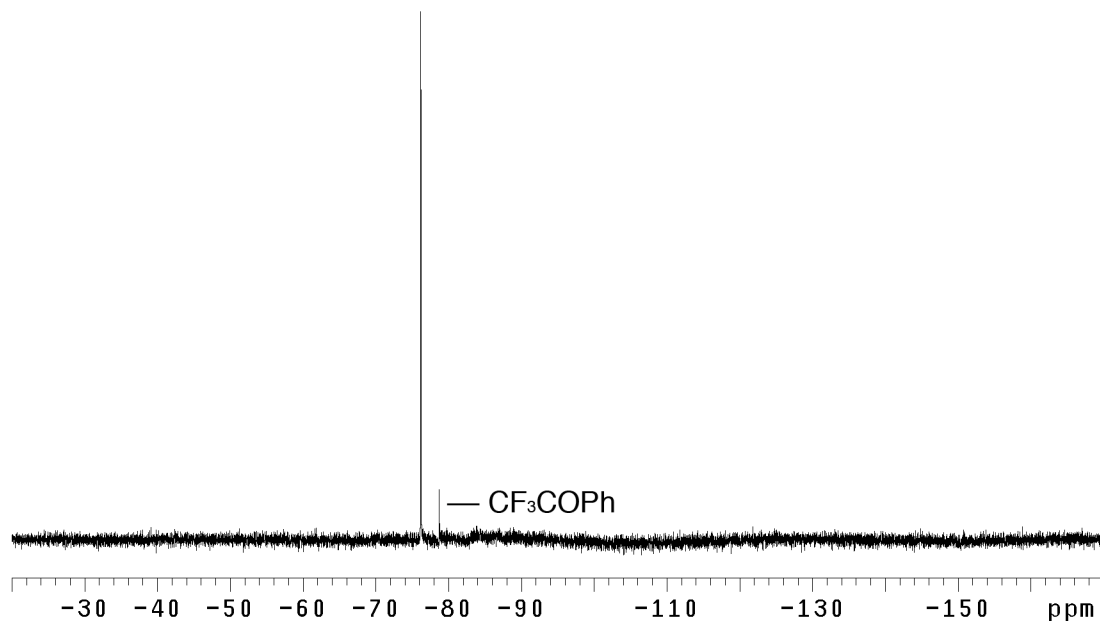


Figure A4.1.8  $^{19}\text{F}$  NMR spectrum (282 MHz,  $\text{CD}_2\text{Cl}_2$ ) of **271**.

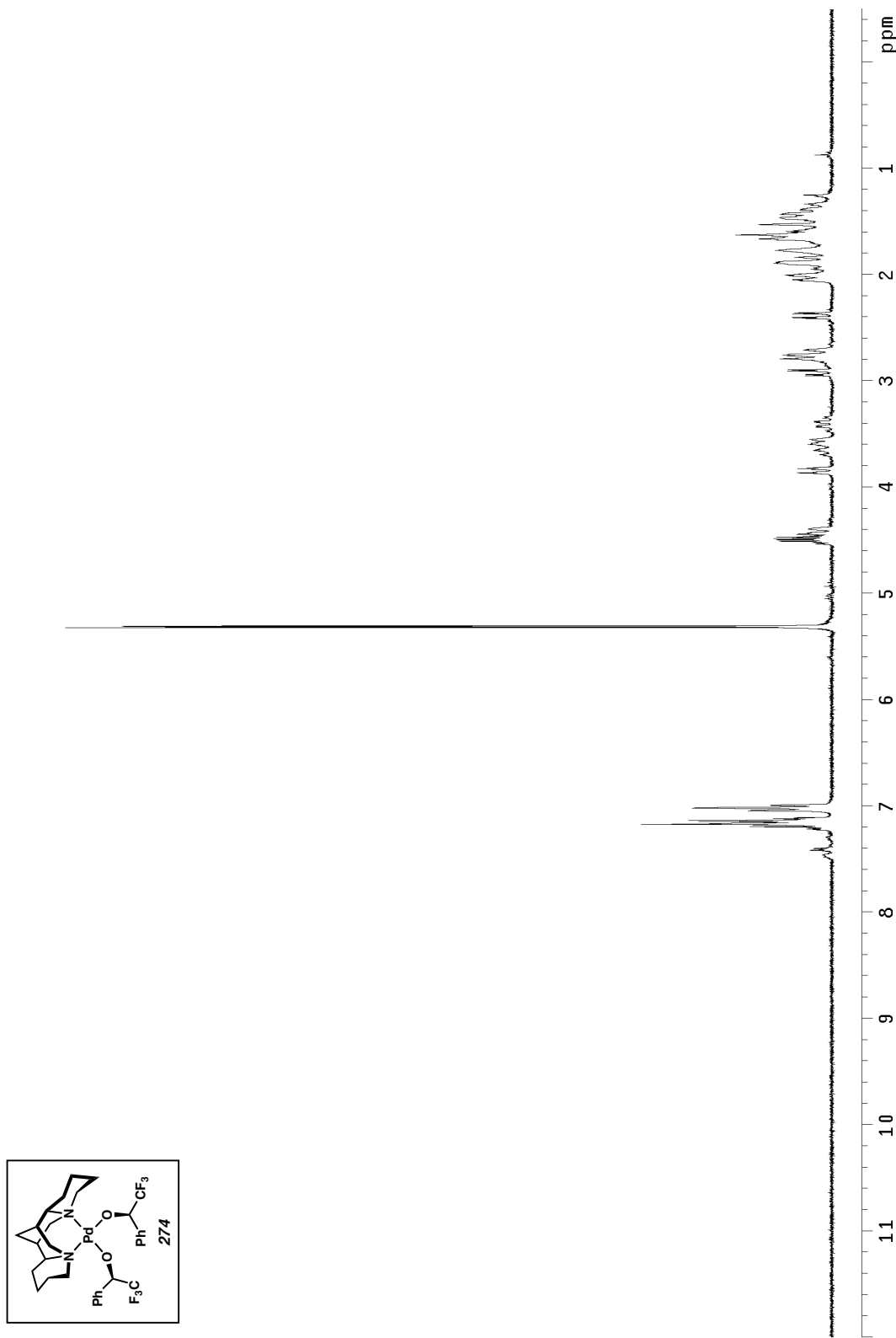


Figure A4.1.9  $^1\text{H}$  NMR spectrum (300 MHz,  $\text{CD}_2\text{Cl}_2$ ) of **274**.

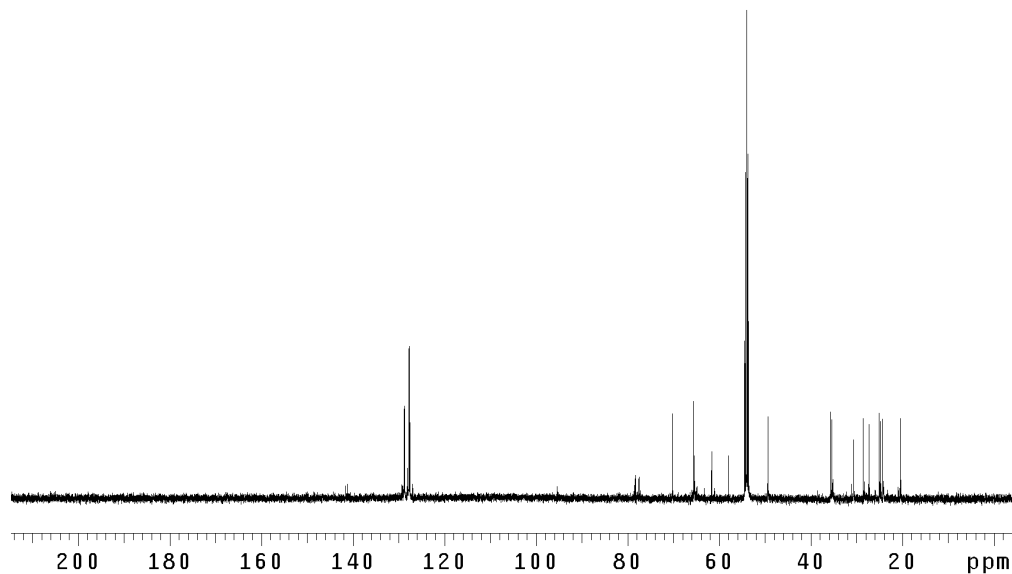


Figure A4.1.10  $^{13}\text{C}$  NMR spectrum (125 MHz,  $\text{CD}_2\text{Cl}_2$ ) of **274**.

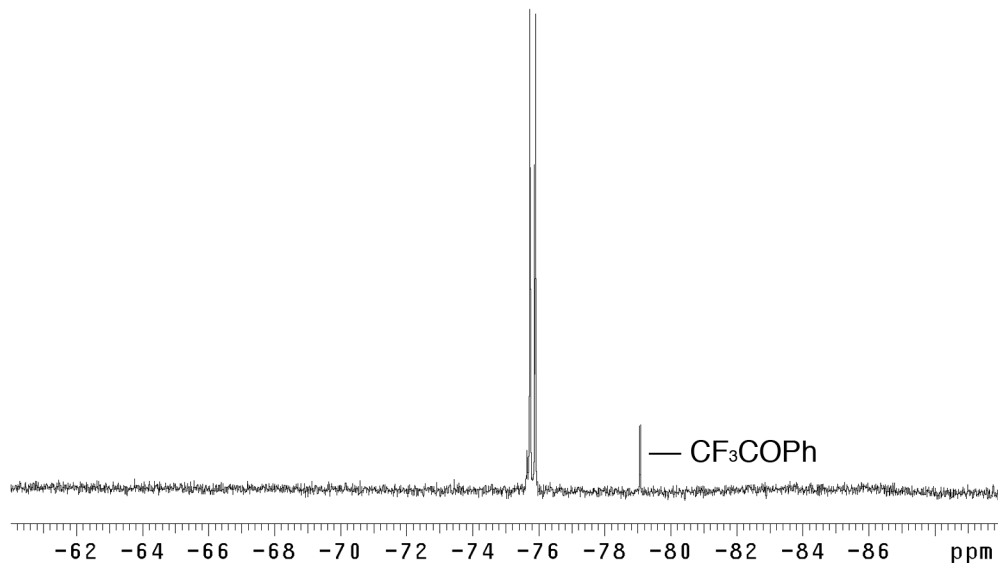


Figure A4.1.11  $^{19}\text{F}$  NMR spectrum (282 MHz,  $\text{CD}_2\text{Cl}_2$ ) of **274**.

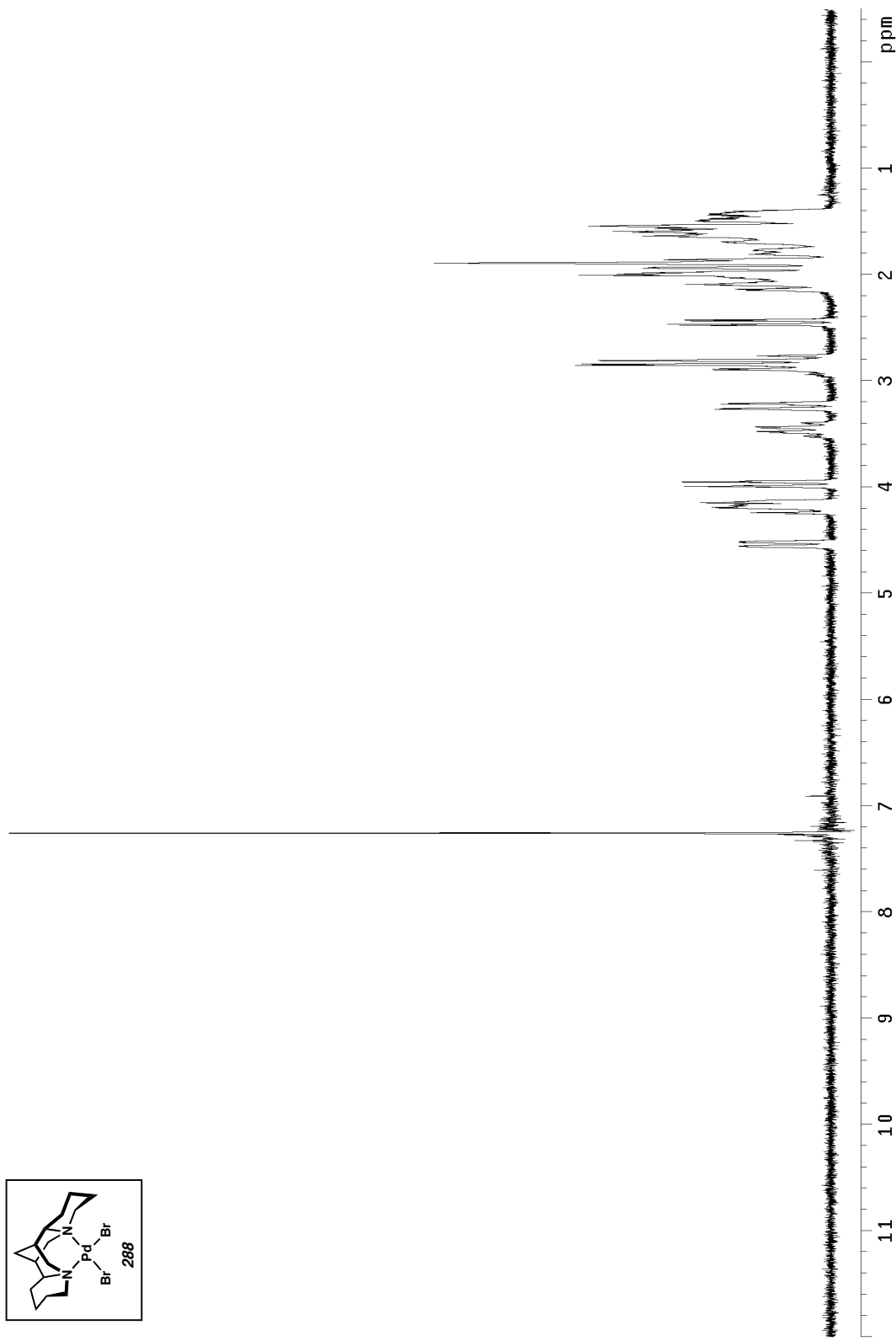


Figure A4.1.12  $^1\text{H}$  NMR spectrum (300 MHz,  $\text{CDCl}_3$ ) of **288**.

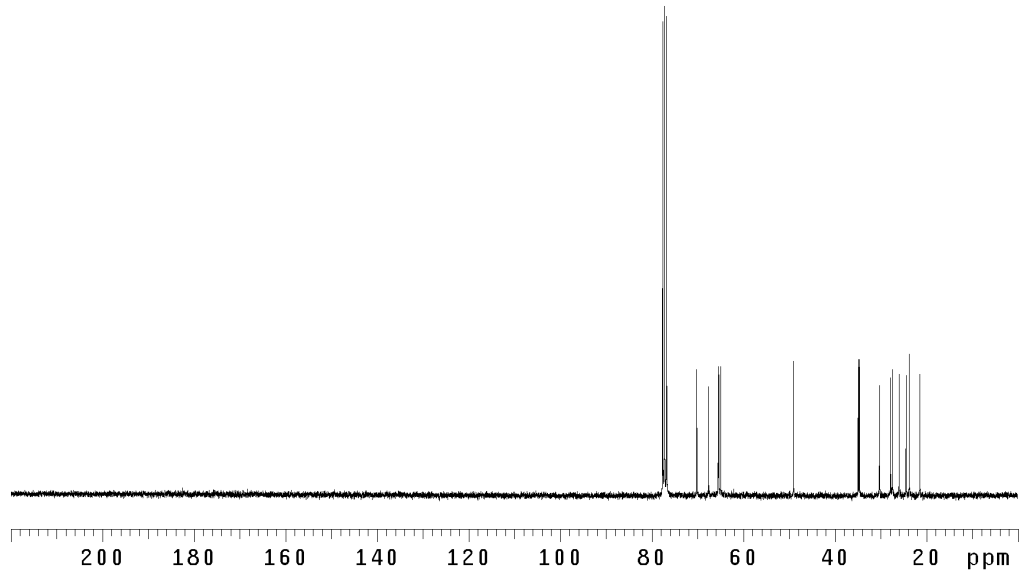


Figure A4.1.13  $^{13}\text{C}$  NMR spectrum (75 MHz,  $\text{CDCl}_3$ ) of **288**.

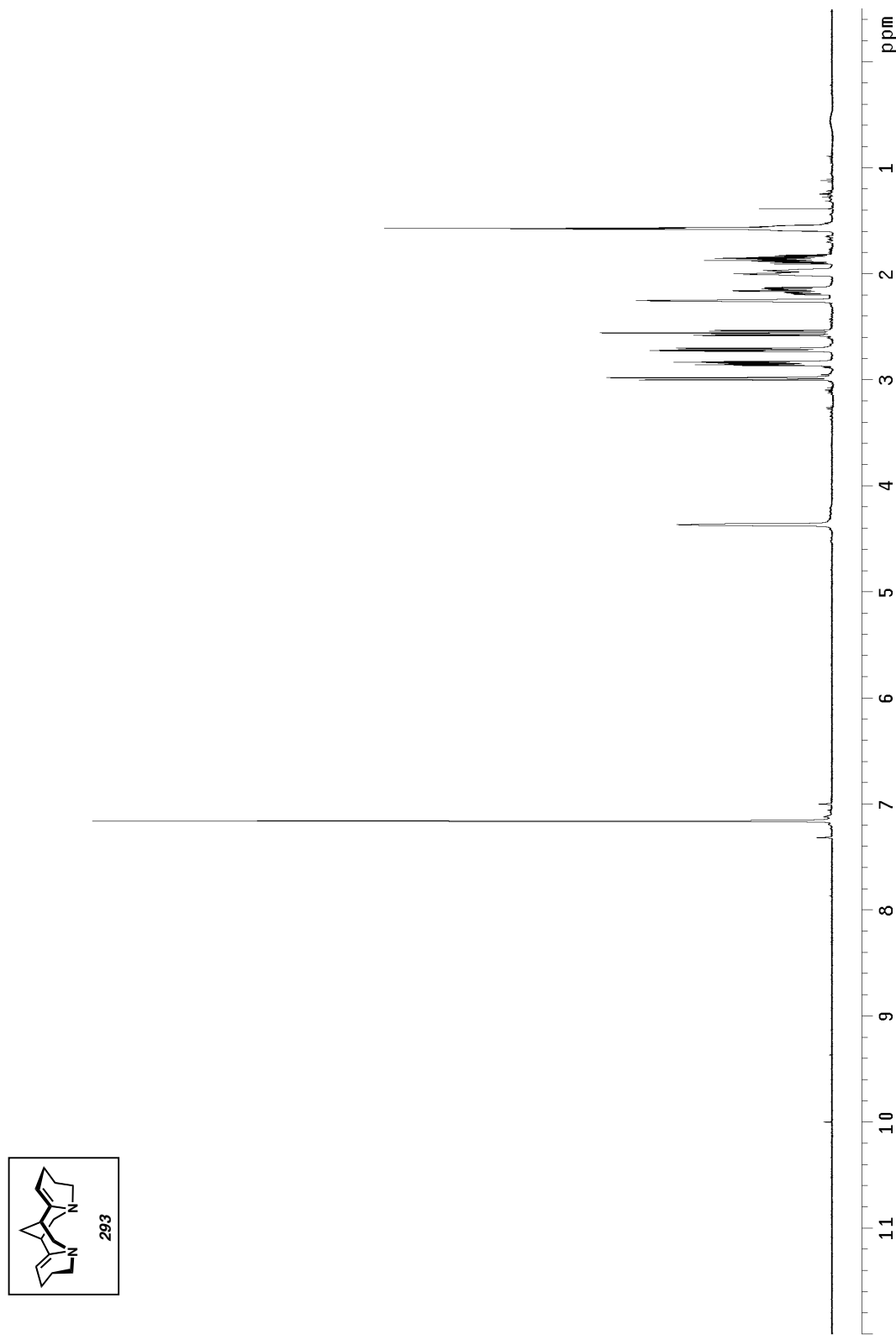


Figure A4.1.14  $^1\text{H}$  NMR spectrum (500 MHz, benzene- $d_6$ ) of **293**.

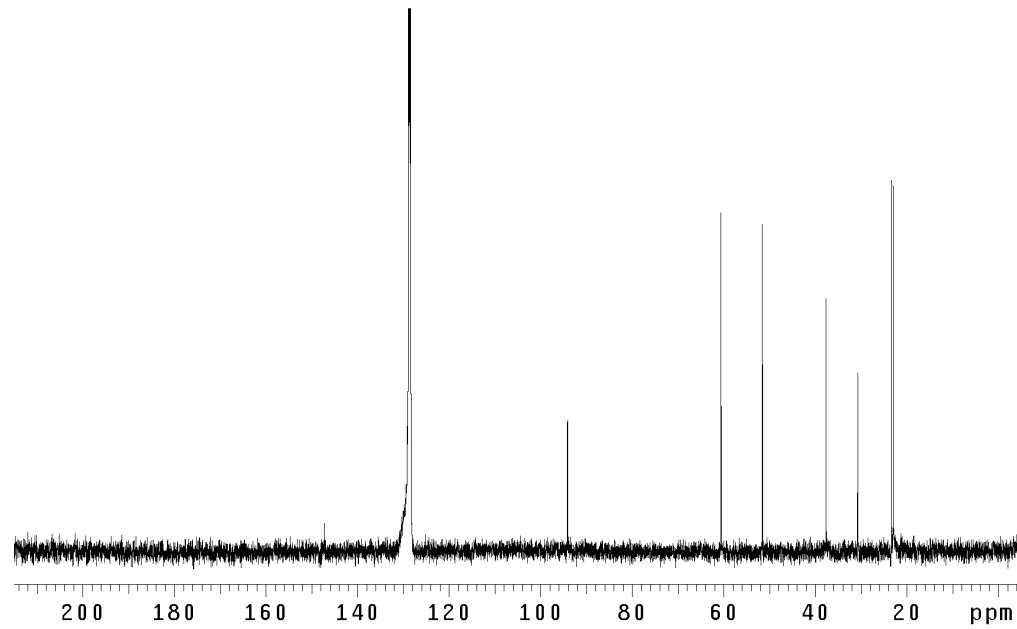


Figure A4.1.15  $^{13}\text{C}$  NMR spectrum (125 MHz,  $\text{CDCl}_3$ ) of **293**.

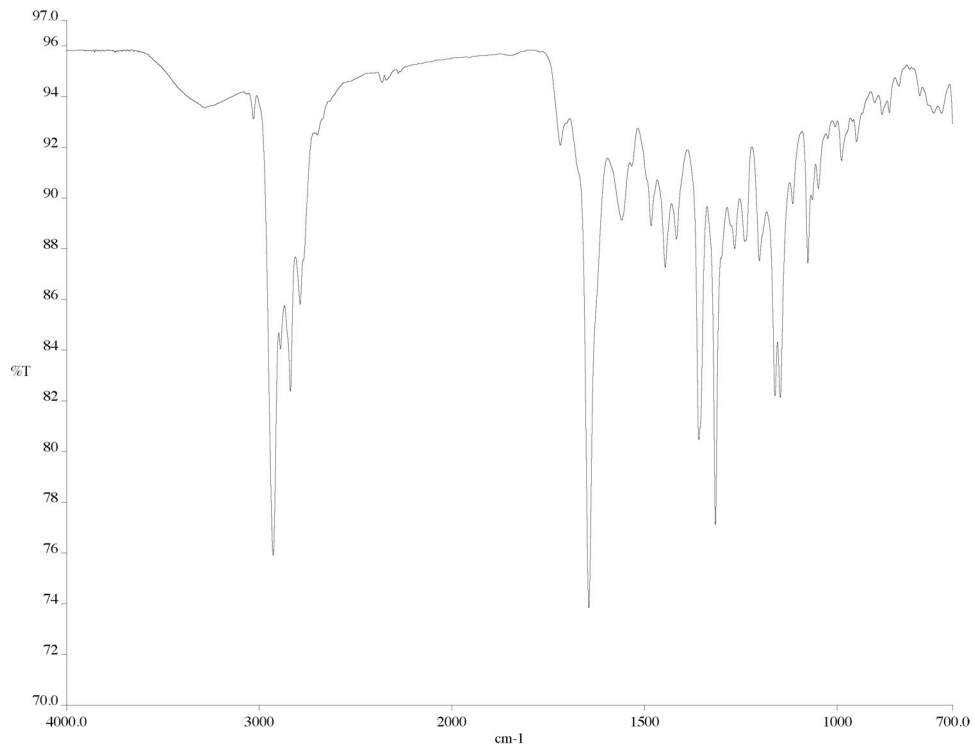


Figure A4.1.16 IR spectrum (thin film/ $\text{NaCl}$ ) of **293**.

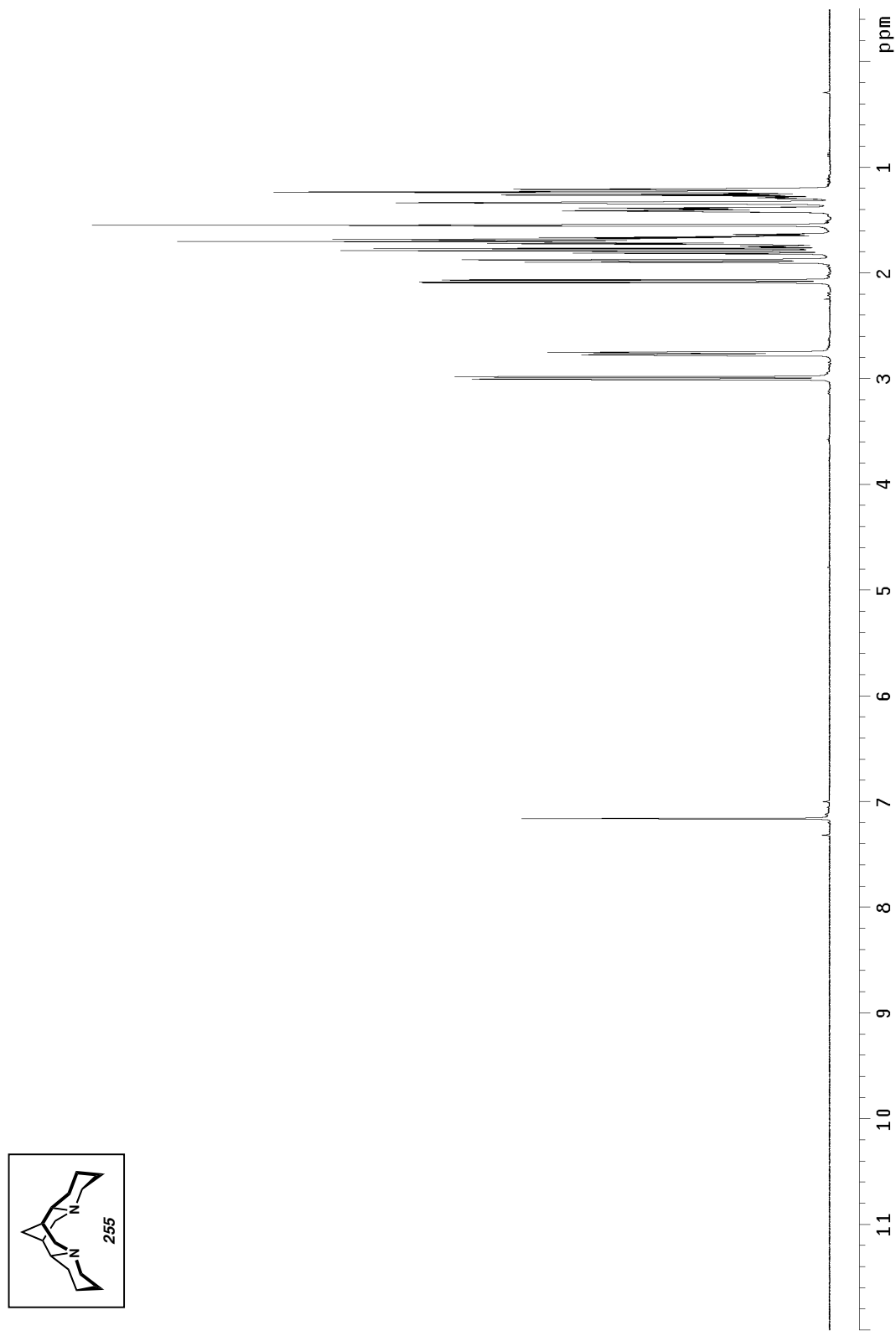


Figure A4.1.17  $^1\text{H}$  NMR spectrum (500 MHz, benzene- $d_6$ ) of **255**.

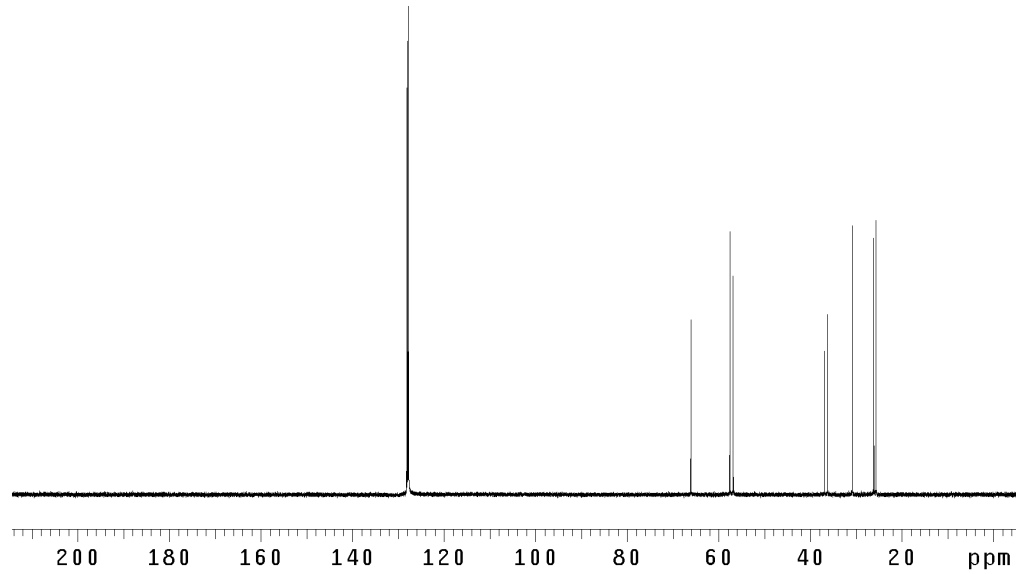


Figure A4.1.18  $^{13}\text{C}$  NMR spectrum (125 MHz, benzene- $d_6$ ) of **255**.

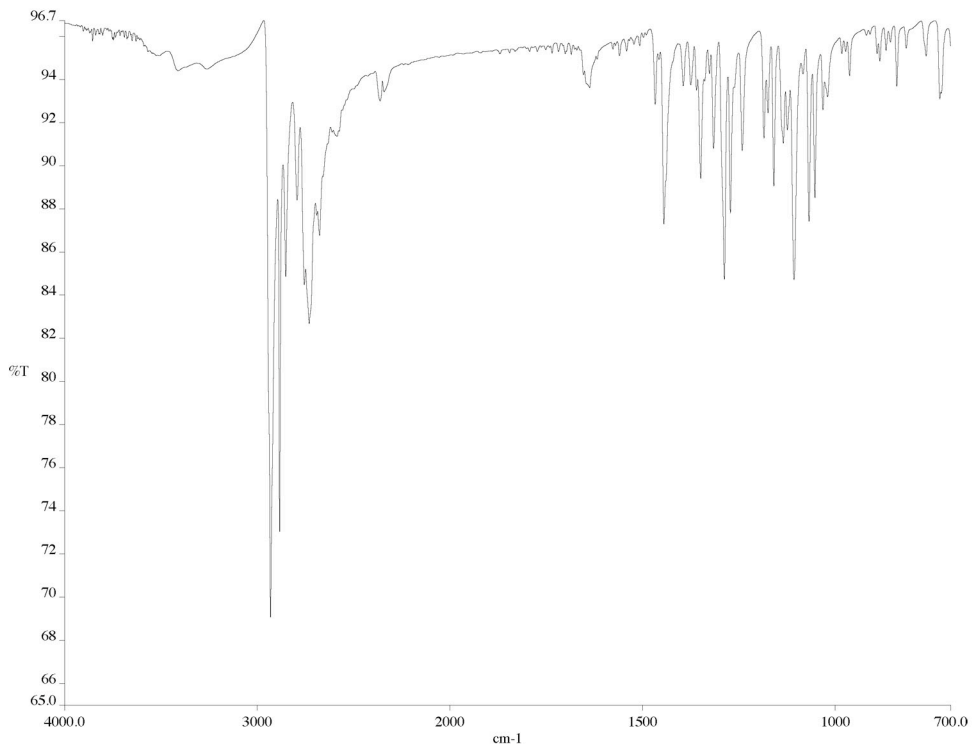


Figure A4.1.19 IR spectrum (thin film/NaCl) of **255**.

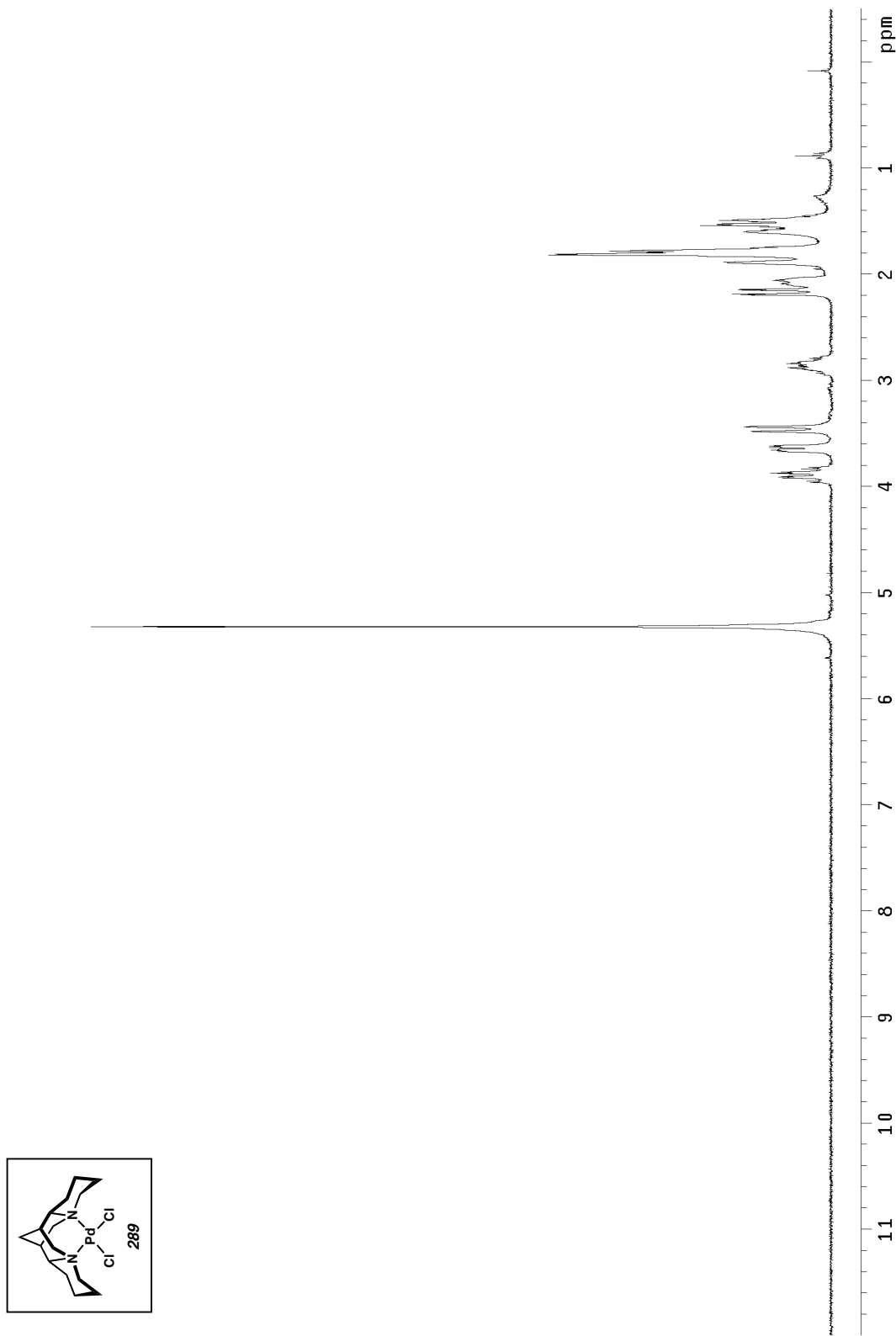


Figure A4.1.20  $^1\text{H}$  NMR spectrum (300 MHz,  $\text{CD}_2\text{Cl}_2$ ) of **289**.

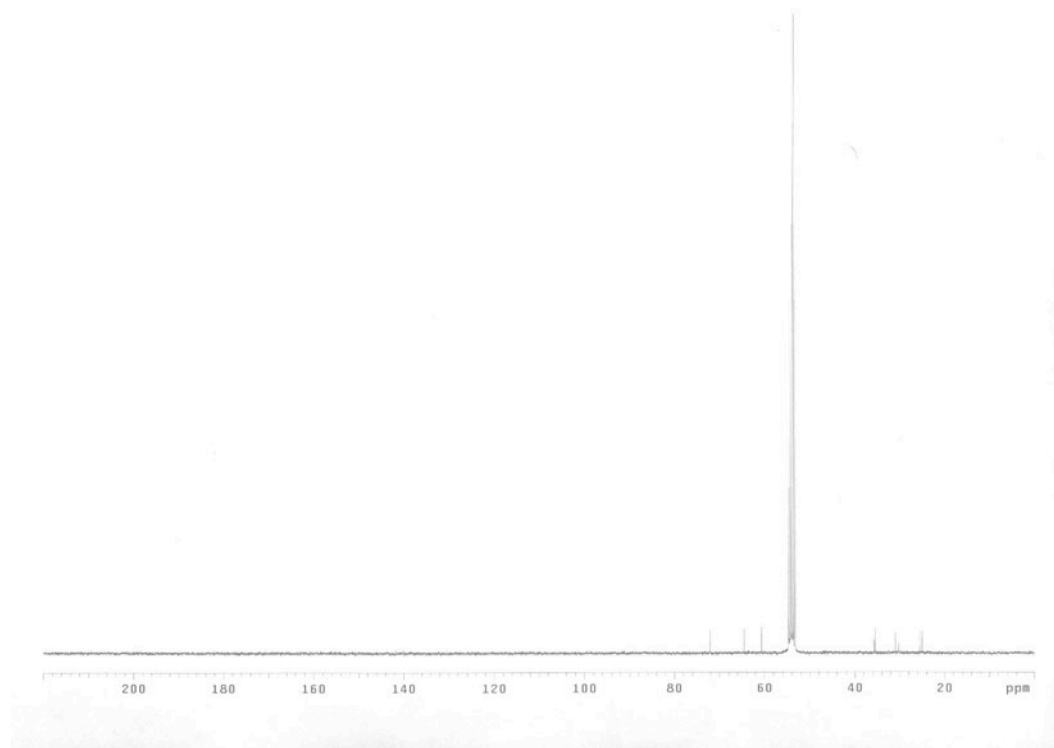


Figure A4.1.21 <sup>13</sup>C NMR spectrum (75 MHz,  $CD_2Cl_2$ ) of **289**.

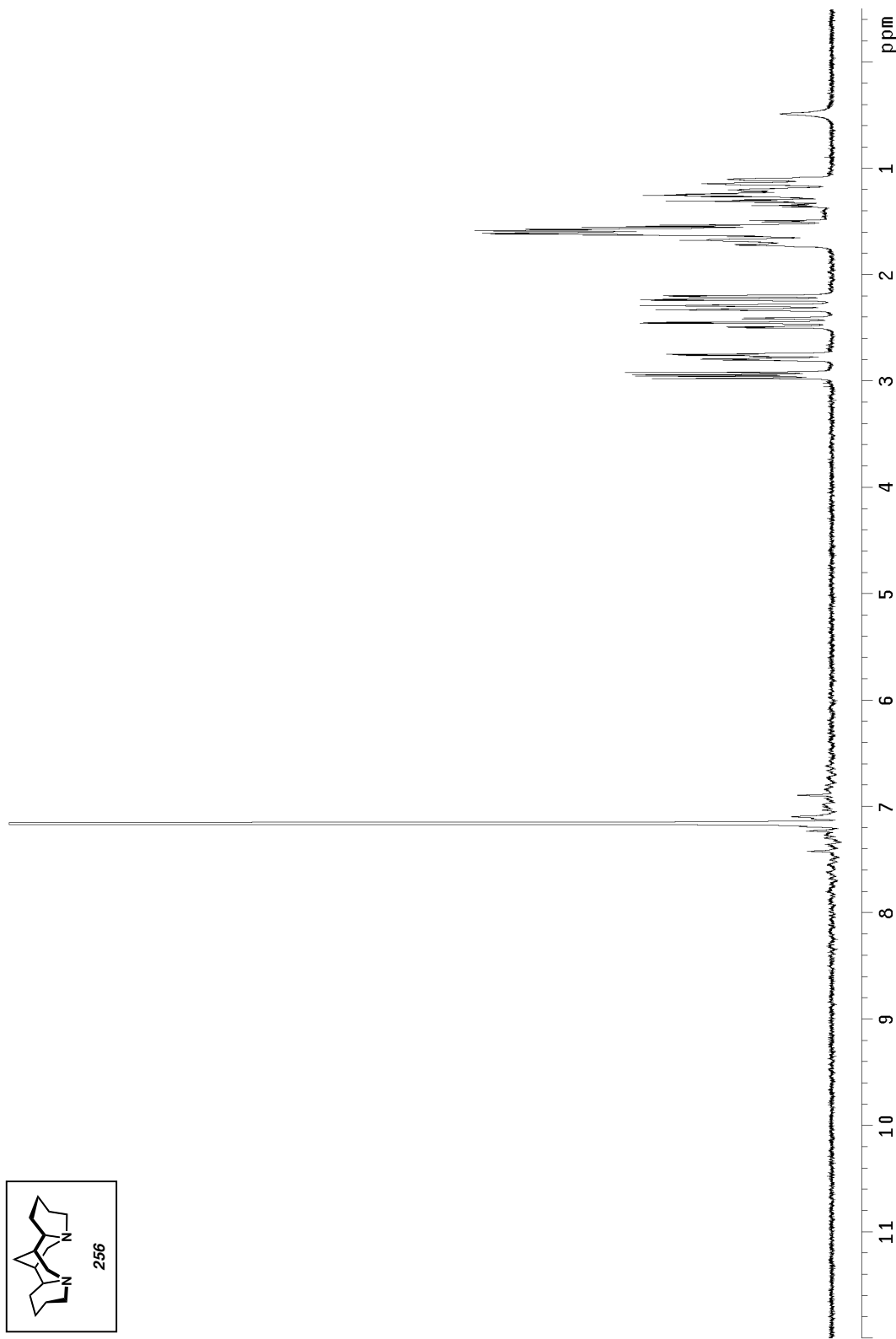


Figure A4.1.22  $^1\text{H}$  NMR spectrum (300 MHz,  $\text{CDCl}_3$ ) of **256**.

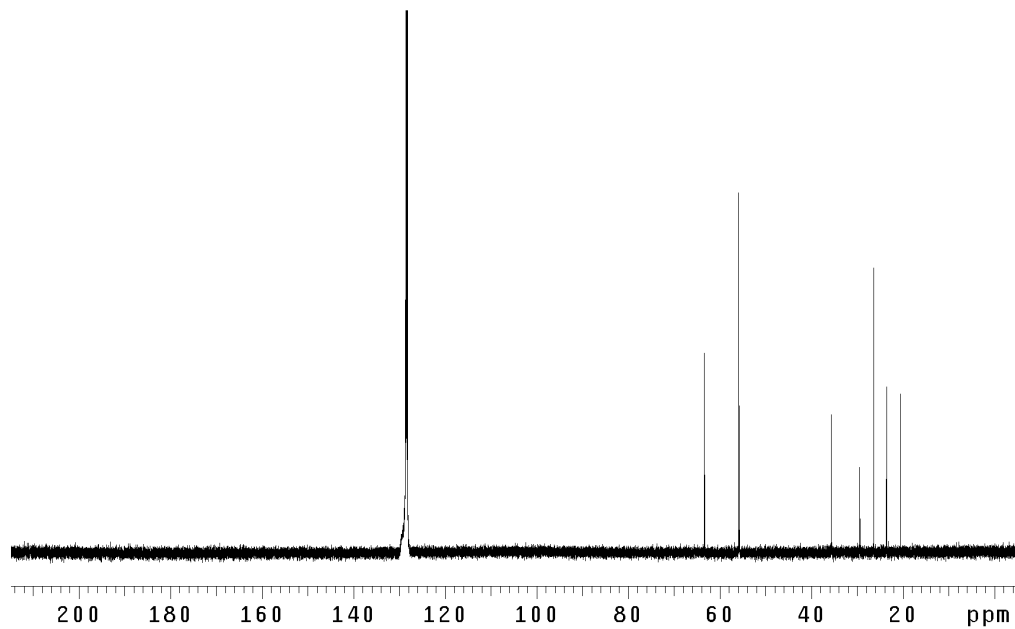


Figure A4.1.23  $^{13}\text{C}$  NMR spectrum (125 MHz,  $\text{CDCl}_3$ ) of **256**.

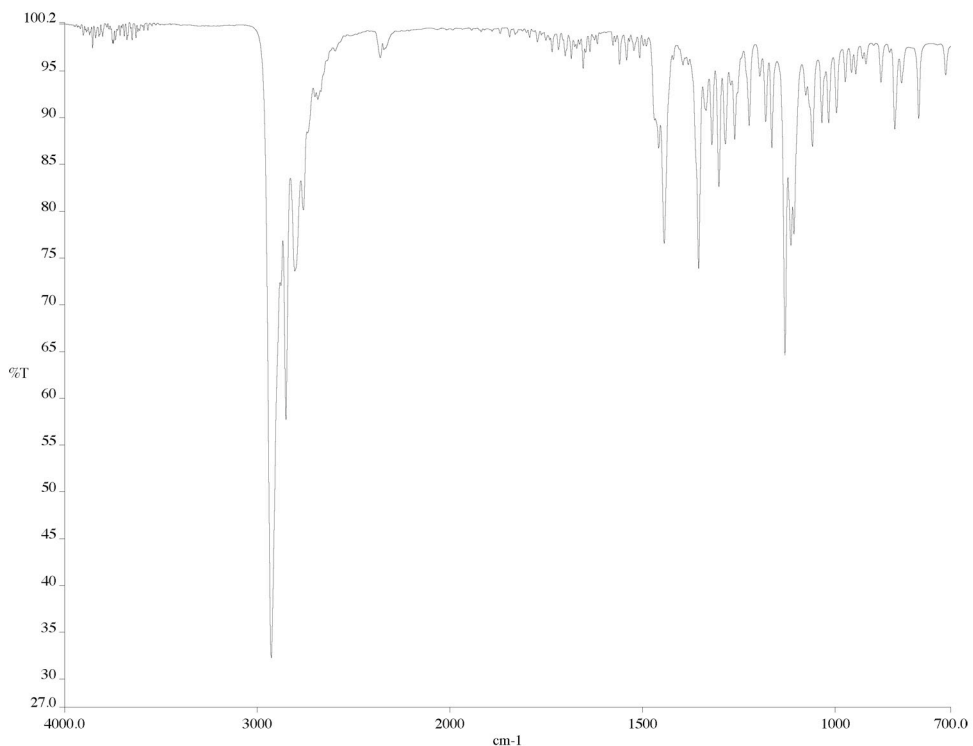


Figure A4.1.24 IR spectrum (thin film/ $\text{NaCl}$ ) of **256**.

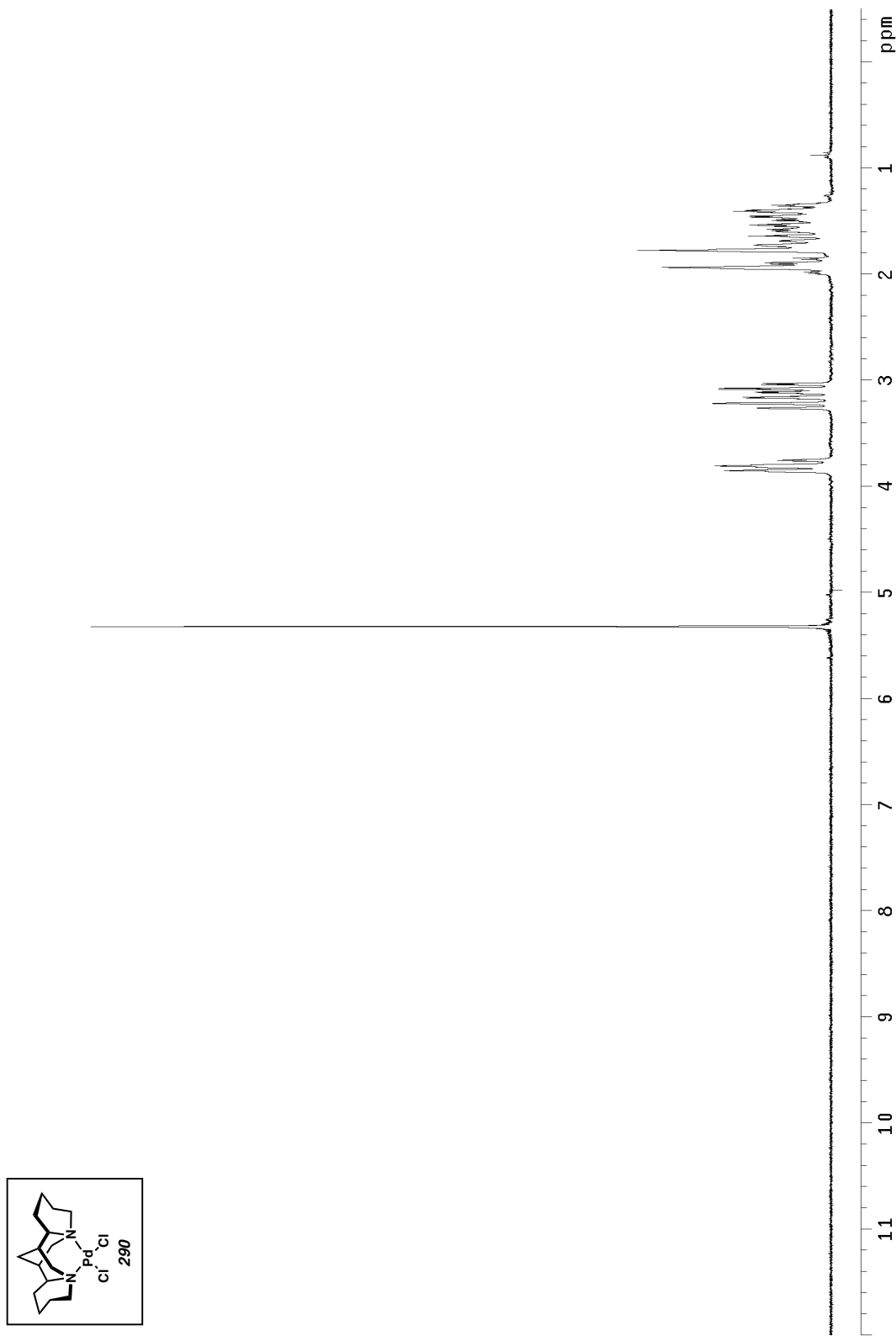


Figure A4.1.25  $^1\text{H}$  NMR spectrum (500 MHz,  $\text{CDCl}_3$ ) of **290**.

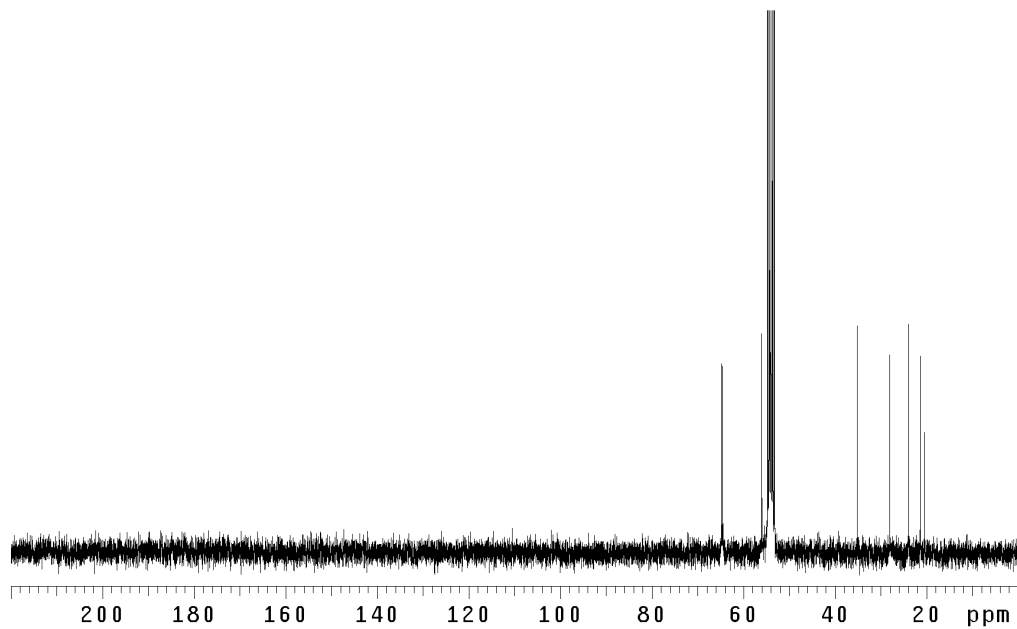
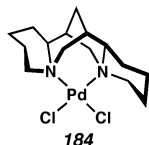


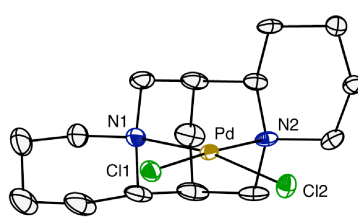
Figure A4.1.26  $^{13}\text{C}$  NMR spectrum (125 MHz,  $\text{CDCl}_3$ ) of **290**.



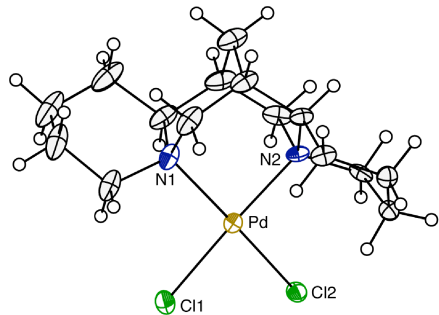
**APPENDIX 4.2***X-ray Crystallographic Data for (sp)PdCl<sub>2</sub> (**184**)*Figure A4.2.1 (sp)PdCl<sub>2</sub> (**184**).<sup>1,2</sup>

Selected bond lengths (Å) and angles (°)	
Pd–N1	2.096(3)
Pd–N2	2.127(2)
Pd–Cl1	2.3161(9)
Pd–Cl2	2.3150(8)
N1–Pd–N2	87.51(10)°
Cl1–Pd–Cl2	83.09(3)°
N2–Pd–Cl1	176.24(7)°
N1–Pd–Cl2	170.06(8)°
N1–Pd–Cl1	95.65(8)°
N2–Pd–Cl2	93.44(7)°
$\Sigma \angle$	705.94°

Side view:



Top view:



<sup>1</sup> (a) X-ray quality crystals were grown by graduate student Eric Ferreira. (b) The hydrogen atoms in the (–)-sparteine backbone are not shown.

<sup>2</sup> The crystallographic data have been deposited at the Cambridge Database (CCDC), 12 Union Road, Cambridge CB2 1EZ, UK and copies can be obtained on request, free of charge, by quoting the publication citation and the deposition number 203513.

*Crystal data and structure refinement for **184** (CCDC 203513).*

Empirical formula	C <sub>15</sub> H <sub>26</sub> Cl <sub>2</sub> N <sub>2</sub> Pd • 2CHCl <sub>3</sub>
Formula weight	650.41
Crystallization solvent	Chloroform
Crystal habit	Blade
Crystal size	0.33 x 0.15 x 0.06 mm <sup>3</sup>
Crystal color	Orange

#### *Data collection*

Preliminary photos	Rotation
Type of diffractometer	Bruker SMART 1000
Wavelength	0.71073 Å MoKα
Data collection temperature	98(2) K
θ range for 17268 reflections used in lattice determination	2.17 to 28.42°
Unit cell dimensions	a = 10.5805(7) Å b = 12.4401(8) Å c = 18.6906(12) Å 2460.1(3) Å <sup>3</sup>
Volume	4
Z	Orthorhombic
Crystal system	P2 <sub>1</sub> 2 <sub>1</sub> 2 <sub>1</sub>
Space group	1.756 Mg/m <sup>3</sup>
Density (calculated)	1304
F(000)	1.97 to 28.44°
θ range for data collection	96.7 %
Completeness to θ = 28.44°	-13 ≤ h ≤ 14, -16 ≤ k ≤ 16, -24 ≤ l ≤ 24
Index ranges	ω scans at 5 φ settings
Data collection scan type	43840
Reflections collected	5883 [R <sub>int</sub> = 0.0794]
Independent reflections	1.632 mm <sup>-1</sup>
Absorption coefficient	None
Absorption correction	0.9084 and 0.6150
Max. and min. transmission	

#### *Structure solution and refinement*

Structure solution program	SHELXS-97 (Sheldrick, 1990)
Primary solution method	Patterson method
Secondary solution method	Difference Fourier map
Hydrogen placement	Difference Fourier map
Structure refinement program	SHELXL-97 (Sheldrick, 1997)
Refinement method	Full matrix least-squares on F <sup>2</sup>
Data / restraints / parameters	5883 / 24 / 329
Treatment of hydrogen atoms	Riding
Goodness-of-fit on F <sup>2</sup>	1.367
Final R indices [I>2σ(I), 5041 reflections]	R1 = 0.0332, wR2 = 0.0526
R indices (all data)	R1 = 0.0436, wR2 = 0.0538
Type of weighting scheme used	Sigma
Weighting scheme used	w = 1/σ <sup>2</sup> (Fo <sup>2</sup> )
Max shift/error	0.002
Average shift/error	0.000
Absolute structure parameter	-0.04(2)
Largest diff. peak and hole	0.984 and -0.639 e.Å <sup>-3</sup>

*Special refinement details*

The crystals contain chloroform as a solvent of cocrystallization. Each asymmetric unit contains two molecules of disordered chloroform. The disorder was successfully modeled and all solvent atoms were refined anisotropically. However, the 1,2 and 1,3 distances within the solvents were restrained to be similar and each distance was assigned a free variable so as to not place artificial values in the geometry. All hydrogen atoms were constrained to ride on the corresponding carbon.

Refinement of  $F^2$  against ALL reflections. The weighted R-factor ( $wR$ ) and goodness of fit (S) are based on  $F^2$ , conventional R-factors (R) are based on F, with F set to zero for negative  $F^2$ . The threshold expression of  $F^2 > 2\sigma(F^2)$  is used only for calculating R-factors(gt) etc. and is not relevant to the choice of reflections for refinement. R-factors based on  $F^2$  are statistically about twice as large as those based on F, and R-factors based on ALL data will be even larger.

All esds (except the esd in the dihedral angle between two l.s. planes) are estimated using the full covariance matrix. The cell esds are taken into account individually in the estimation of esds in distances, angles and torsion angles; correlations between esds in cell parameters are only used when they are defined by crystal symmetry. An approximate (isotropic) treatment of cell esds is used for estimating esds involving l.s. planes.

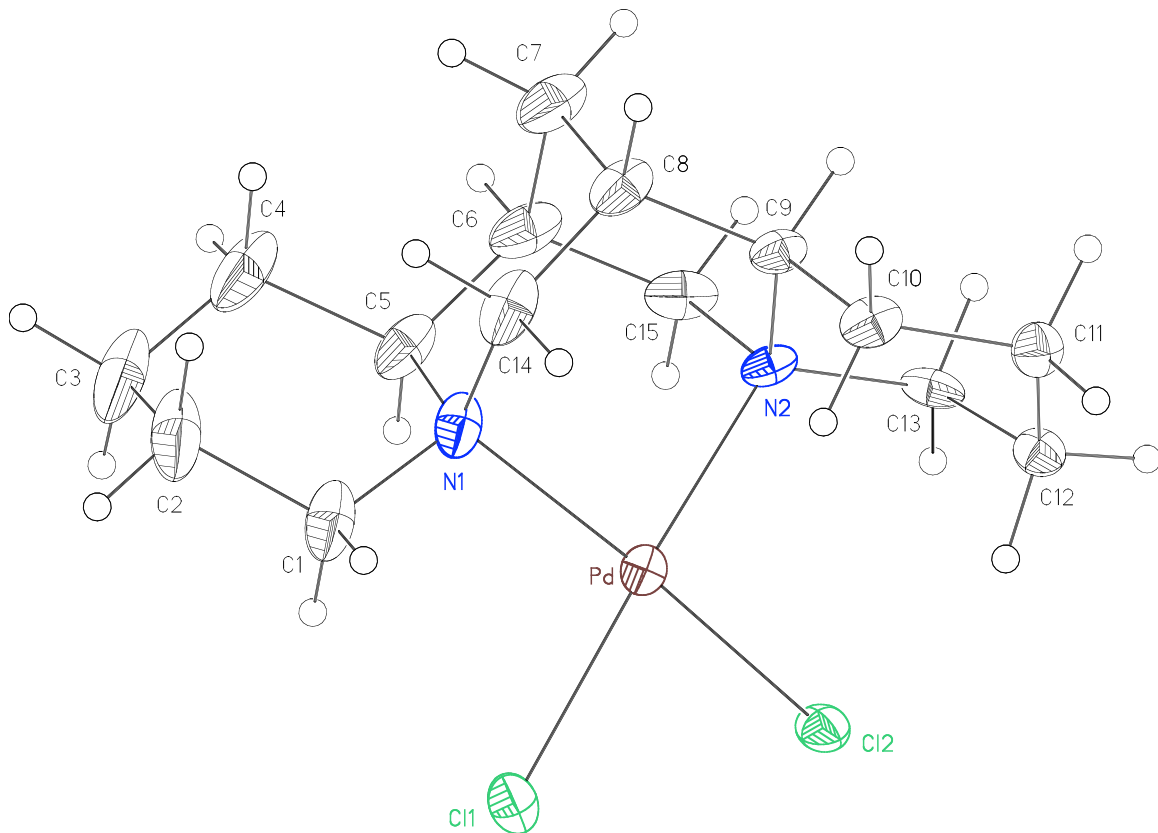


*Figure A4.2.2 Molecule **184**.*

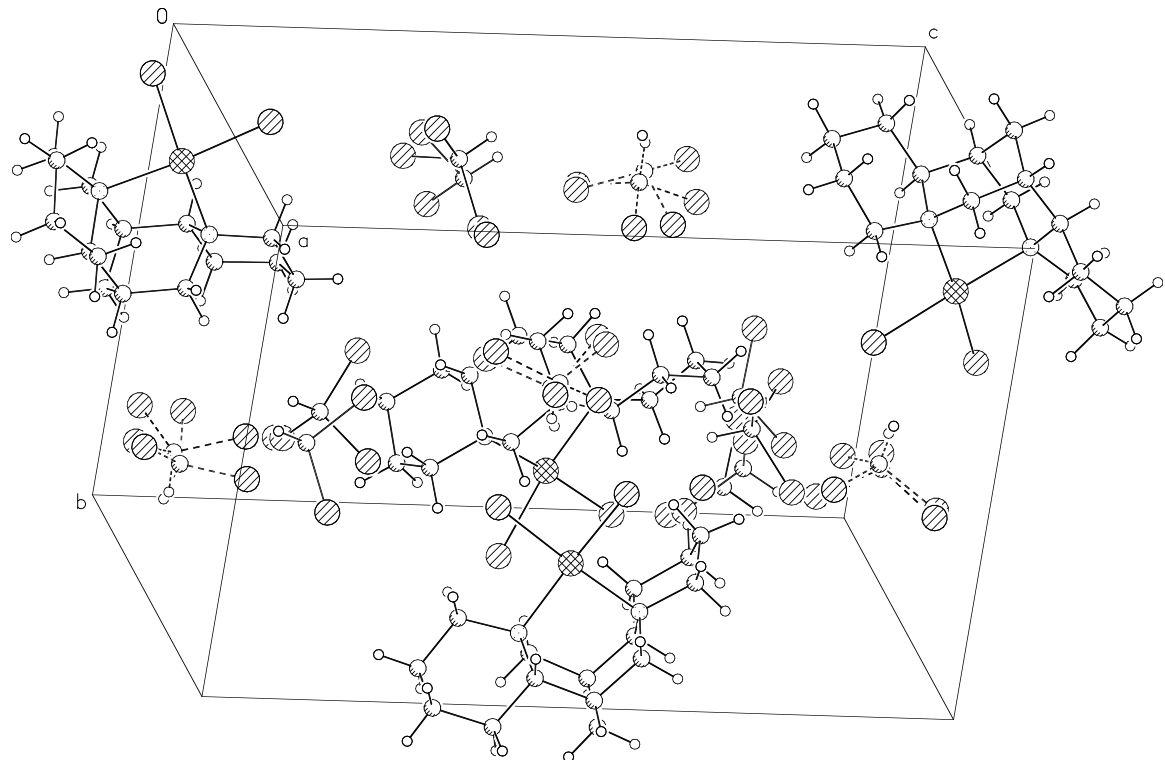


Figure A4.2.3. Unit cell contents of **184**.

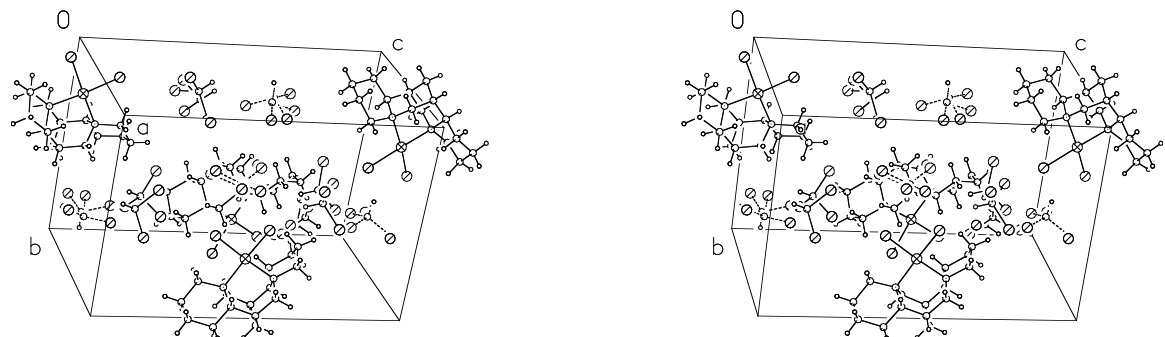


Figure A4.2.4. Stereo view of unit cell contents of **184**.

Table A4.2.1 Atomic coordinates ( $\times 10^4$ ) and equivalent isotropic displacement parameters ( $\text{\AA}^2 \times 10^3$ ) for **184** (CCDC 203513).  $U(\text{eq})$  is defined as the trace of the orthogonalized  $U^{ij}$  tensor.

	x	y	z	$U_{\text{eq}}$	Occ
Pd	6127(1)	2578(1)	9793(1)	16(1)	1
Cl(1)	6430(1)	3588(1)	8766(1)	23(1)	1
Cl(2)	5727(1)	4241(1)	10300(1)	22(1)	1
N(1)	6161(3)	1060(2)	9270(1)	23(1)	1
N(2)	5780(2)	1746(2)	10748(1)	16(1)	1
C(1)	6534(4)	1183(3)	8504(2)	33(1)	1
C(2)	6261(4)	209(3)	8033(2)	44(1)	1
C(3)	4861(4)	-33(3)	8050(2)	48(1)	1
C(4)	4454(4)	-225(3)	8811(2)	42(1)	1
C(5)	4780(3)	695(3)	9325(2)	28(1)	1
C(6)	4439(3)	404(3)	10093(2)	30(1)	1
C(7)	5283(3)	-507(3)	10358(2)	33(1)	1
C(8)	6628(3)	-48(3)	10367(2)	27(1)	1
C(9)	6689(3)	846(3)	10911(2)	19(1)	1
C(10)	8007(3)	1299(3)	11044(2)	22(1)	1
C(11)	7993(3)	2003(3)	11704(2)	22(1)	1
C(12)	7010(3)	2882(2)	11618(2)	19(1)	1
C(13)	5727(3)	2418(3)	11409(2)	20(1)	1
C(14)	7034(3)	276(3)	9620(2)	31(1)	1
C(15)	4482(3)	1304(3)	10634(2)	25(1)	1
C(16A)	516(5)	9209(5)	8232(3)	39(2)	0.669(4)
Cl(3A)	-534(4)	8190(4)	8468(3)	68(1)	0.669(4)
Cl(4A)	1767(1)	8715(2)	7721(1)	64(1)	0.669(4)
Cl(5A)	-307(2)	10180(2)	7716(1)	52(1)	0.669(4)
C(16B)	821(9)	8675(8)	8396(6)	36(4)	0.331(4)
Cl(3B)	-688(5)	8128(5)	8540(5)	31(2)	0.331(4)
Cl(4B)	1883(3)	7660(4)	8165(2)	80(2)	0.331(4)
Cl(5B)	763(7)	9641(4)	7725(2)	114(4)	0.331(4)
C(17A)	6072(7)	6401(10)	9225(4)	27(3)	0.523(5)
Cl(6A)	6365(4)	6902(2)	8365(1)	55(1)	0.523(5)
Cl(7A)	4516(2)	6717(2)	9484(2)	38(1)	0.523(5)
Cl(8A)	7155(6)	6948(9)	9833(3)	32(1)	0.523(5)
C(17B)	6234(7)	6229(12)	9150(4)	27(4)	0.477(5)
Cl(6B)	4728(3)	6713(2)	8939(3)	64(1)	0.477(5)
Cl(7B)	7253(4)	6374(4)	8420(1)	64(1)	0.477(5)
Cl(8B)	6842(6)	6923(10)	9897(4)	42(2)	0.477(5)

C(1)-N(1)-Pd	110.8(2)	C(14)-C(8)-C(7)	110.7(3)
C(14)-N(1)-Pd	112.87(19)	C(9)-C(8)-H(8)	107.6
C(5)-N(1)-Pd	102.44(19)	C(14)-C(8)-H(8)	107.6
C(13)-N(2)-C(15)	106.9(2)	C(7)-C(8)-H(8)	107.6
C(13)-N(2)-C(9)	105.8(2)	N(2)-C(9)-C(8)	112.6(3)
C(15)-N(2)-C(9)	110.0(2)	N(2)-C(9)-C(10)	110.0(3)
C(13)-N(2)-Pd	115.78(18)	C(8)-C(9)-C(10)	115.0(3)
C(15)-N(2)-Pd	102.76(19)	N(2)-C(9)-H(9)	106.2
C(9)-N(2)-Pd	115.25(18)	C(8)-C(9)-H(9)	106.2
N(1)-C(1)-C(2)	115.0(3)	C(10)-C(9)-H(9)	106.2
N(1)-C(1)-H(1A)	108.5	C(11)-C(10)-C(9)	109.7(3)
C(2)-C(1)-H(1A)	108.5	C(11)-C(10)-H(10A)	109.7
N(1)-C(1)-H(1B)	108.5	C(9)-C(10)-H(10A)	109.7
C(2)-C(1)-H(1B)	108.5	C(11)-C(10)-H(10B)	109.7
H(1A)-C(1)-H(1B)	107.5	C(9)-C(10)-H(10B)	109.7
C(3)-C(2)-C(1)	109.4(3)	H(10A)-C(10)-H(10B)	108.2
C(3)-C(2)-H(2A)	109.8	C(10)-C(11)-C(12)	109.8(3)
C(1)-C(2)-H(2A)	109.8	C(10)-C(11)-H(11A)	109.7
C(3)-C(2)-H(2B)	109.8	C(12)-C(11)-H(11A)	109.7
C(1)-C(2)-H(2B)	109.8	C(10)-C(11)-H(11B)	109.7
H(2A)-C(2)-H(2B)	108.2	C(12)-C(11)-H(11B)	109.7
C(4)-C(3)-C(2)	109.4(3)	H(11A)-C(11)-H(11B)	108.2
C(4)-C(3)-H(3A)	109.8	C(11)-C(12)-C(13)	111.3(3)
C(2)-C(3)-H(3A)	109.8	C(11)-C(12)-H(12A)	109.4
C(4)-C(3)-H(3B)	109.8	C(13)-C(12)-H(12A)	109.4
C(2)-C(3)-H(3B)	109.8	C(11)-C(12)-H(12B)	109.4
H(3A)-C(3)-H(3B)	108.2	C(13)-C(12)-H(12B)	109.4
C(3)-C(4)-C(5)	114.1(3)	H(12A)-C(12)-H(12B)	108.0
C(3)-C(4)-H(4A)	108.7	N(2)-C(13)-C(12)	113.0(2)
C(5)-C(4)-H(4A)	108.7	N(2)-C(13)-H(13A)	109.0
C(3)-C(4)-H(4B)	108.7	C(12)-C(13)-H(13A)	109.0
C(5)-C(4)-H(4B)	108.7	N(2)-C(13)-H(13B)	109.0
H(4A)-C(4)-H(4B)	107.6	C(12)-C(13)-H(13B)	109.0
C(6)-C(5)-C(4)	111.1(3)	H(13A)-C(13)-H(13B)	107.8
C(6)-C(5)-N(1)	111.1(3)	N(1)-C(14)-C(8)	113.7(3)
C(4)-C(5)-N(1)	113.1(3)	N(1)-C(14)-H(14A)	108.8
C(6)-C(5)-H(5)	107.0	C(8)-C(14)-H(14A)	108.8
C(4)-C(5)-H(5)	107.0	N(1)-C(14)-H(14B)	108.8
N(1)-C(5)-H(5)	107.0	C(8)-C(14)-H(14B)	108.8
C(15)-C(6)-C(5)	116.6(3)	H(14A)-C(14)-H(14B)	107.7
C(15)-C(6)-C(7)	108.4(3)	N(2)-C(15)-C(6)	113.4(3)
C(5)-C(6)-C(7)	110.1(3)	N(2)-C(15)-H(15A)	108.9
C(15)-C(6)-H(6)	107.1	C(6)-C(15)-H(15A)	108.9
C(5)-C(6)-H(6)	107.1	N(2)-C(15)-H(15B)	108.9
C(7)-C(6)-H(6)	107.1	C(6)-C(15)-H(15B)	108.9
C(6)-C(7)-C(8)	105.7(3)	H(15A)-C(15)-H(15B)	107.7
C(6)-C(7)-H(7A)	110.6	Cl(3A)-C(16A)-Cl(4A)	111.5(4)
C(8)-C(7)-H(7A)	110.6	Cl(3A)-C(16A)-Cl(5A)	108.7(3)
C(6)-C(7)-H(7B)	110.6	Cl(4A)-C(16A)-Cl(5A)	108.4(3)
C(8)-C(7)-H(7B)	110.6	Cl(3A)-C(16A)-H(16A)	109.4
H(7A)-C(7)-H(7B)	108.7	Cl(4A)-C(16A)-H(16A)	109.4
C(9)-C(8)-C(14)	114.3(3)	Cl(5A)-C(16A)-H(16A)	109.4
C(9)-C(8)-C(7)	108.7(3)	Cl(5B)-C(16B)-Cl(4B)	110.1(6)

Cl(5B)-C(16B)-Cl(3B)	110.2(6)	Cl(6A)-C(17A)-H(17A)	108.9
Cl(4B)-C(16B)-Cl(3B)	110.1(6)	Cl(7A)-C(17A)-H(17A)	108.9
Cl(5B)-C(16B)-H(16B)	108.8	Cl(7B)-C(17B)-Cl(6B)	110.5(5)
Cl(4B)-C(16B)-H(16B)	108.8	Cl(7B)-C(17B)-Cl(8B)	110.0(6)
Cl(3B)-C(16B)-H(16B)	108.8	Cl(6B)-C(17B)-Cl(8B)	110.0(6)
Cl(8A)-C(17A)-Cl(6A)	110.0(6)	Cl(7B)-C(17B)-H(17B)	108.7
Cl(8A)-C(17A)-Cl(7A)	110.3(5)	Cl(6B)-C(17B)-H(17B)	108.7
Cl(6A)-C(17A)-Cl(7A)	109.7(5)	Cl(8B)-C(17B)-H(17B)	108.7
Cl(8A)-C(17A)-H(17A)	108.9		

Table A4.2.2 Selected bond lengths [ $\text{\AA}$ ] and angles [ $^\circ$ ] for **184** (CCDC 203513).

Pd-N(2)	2.096(3)	N(2)-Pd-N(1)	87.51(10)
Pd-N(1)	2.127(2)	N(2)-Pd-Cl(2)	93.44(7)
Pd-Cl(2)	2.3150(8)	N(1)-Pd-Cl(2)	170.06(8)
Pd-Cl(1)	2.3161(9)	N(2)-Pd-Cl(1)	176.24(7)
		N(1)-Pd-Cl(1)	95.65(8)
		Cl(2)-Pd-Cl(1)	83.09(3)

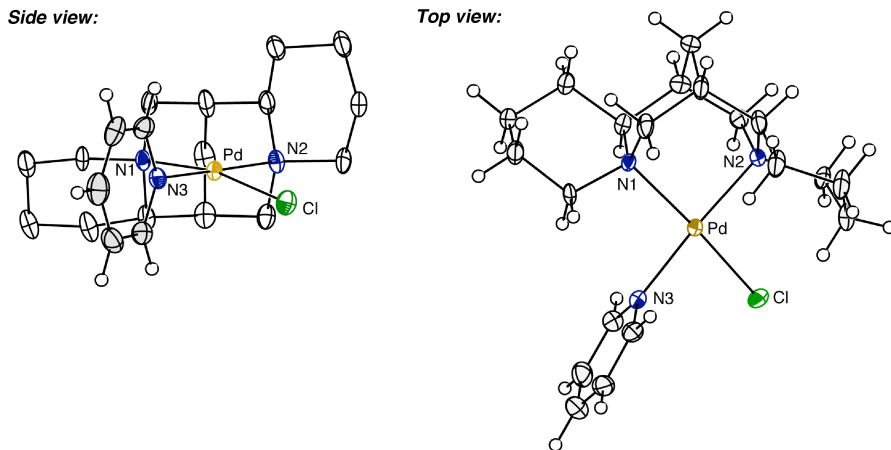
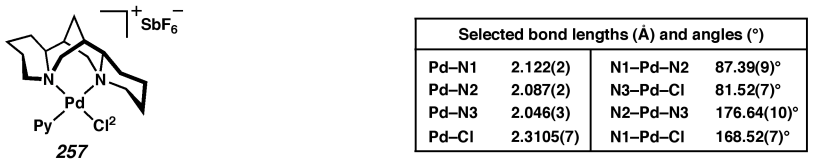
Table A4.2.3 Bond lengths [ $\text{\AA}$ ] and angles [ $^\circ$ ] for **184** (CCDC 203513).

Pd-N(2)	2.096(3)	C(11)-C(12)	1.517(4)
Pd-N(1)	2.127(2)	C(11)-H(11A)	0.9900
Pd-Cl(2)	2.3150(8)	C(11)-H(11B)	0.9900
Pd-Cl(1)	2.3161(9)	C(12)-C(13)	1.526(4)
N(1)-C(1)	1.492(4)	C(12)-H(12A)	0.9900
N(1)-C(14)	1.494(4)	C(12)-H(12B)	0.9900
N(1)-C(5)	1.534(4)	C(13)-H(13A)	0.9900
N(2)-C(13)	1.493(4)	C(13)-H(13B)	0.9900
N(2)-C(15)	1.495(4)	C(14)-H(14A)	0.9900
N(2)-C(9)	1.507(4)	C(14)-H(14B)	0.9900
C(1)-C(2)	1.524(5)	C(15)-H(15A)	0.9900
C(1)-H(1A)	0.9900	C(15)-H(15B)	0.9900
C(1)-H(1B)	0.9900	C(16A)-Cl(3A)	1.742(6)
C(2)-C(3)	1.512(6)	C(16A)-Cl(4A)	1.743(6)
C(2)-H(2A)	0.9900	C(16A)-Cl(5A)	1.773(6)
C(2)-H(2B)	0.9900	C(16A)-H(16A)	1.0000
C(3)-C(4)	1.506(6)	C(16B)-Cl(5B)	1.739(8)
C(3)-H(3A)	0.9900	C(16B)-Cl(4B)	1.744(9)
C(3)-H(3B)	0.9900	C(16B)-Cl(3B)	1.756(8)
C(4)-C(5)	1.534(5)	C(16B)-H(16B)	1.0000
C(4)-H(4A)	0.9900	C(17A)-Cl(8A)	1.751(8)
C(4)-H(4B)	0.9900	C(17A)-Cl(6A)	1.752(8)
C(5)-C(6)	1.523(5)	C(17A)-Cl(7A)	1.761(8)
C(5)-H(5)	1.0000	C(17A)-H(17A)	1.0000
C(6)-C(15)	1.508(5)	C(17B)-Cl(7B)	1.747(8)
C(6)-C(7)	1.526(4)	C(17B)-Cl(6B)	1.749(8)
C(6)-H(6)	1.0000	C(17B)-Cl(8B)	1.763(8)
C(7)-C(8)	1.533(4)	C(17B)-H(17B)	1.0000
C(7)-H(7A)	0.9900		
C(7)-H(7B)	0.9900	N(2)-Pd-N(1)	87.51(10)
C(8)-C(9)	1.509(5)	N(2)-Pd-Cl(2)	93.44(7)
C(8)-C(14)	1.515(5)	N(1)-Pd-Cl(2)	170.06(8)
C(8)-H(8)	1.0000	N(2)-Pd-Cl(1)	176.24(7)
C(9)-C(10)	1.525(4)	N(1)-Pd-Cl(1)	95.65(8)
C(9)-H(9)	1.0000	Cl(2)-Pd-Cl(1)	83.09(3)
C(10)-C(11)	1.513(4)	C(1)-N(1)-C(14)	108.9(3)
C(10)-H(10A)	0.9900	C(1)-N(1)-C(5)	110.3(3)
C(10)-H(10B)	0.9900	C(14)-N(1)-C(5)	111.4(3)

## APPENDIX 4.3

*X-ray Crystallographic data for (sp)Pd(pyr)Cl<sup>+</sup>SbF<sub>6</sub><sup>-</sup> (257)*

Figure A4.3.1 (sp)Pd(pyr)Cl<sup>+</sup>SbF<sub>6</sub><sup>-</sup> (257).<sup>1,2</sup>



<sup>1</sup> (a) The numbering in Figure A4.3.1 differs from that in the crystallographic report. (b) The SbF<sub>6</sub> anion in both views and the hydrogens in the (–)-sparteine backbone in the side view are not shown.

<sup>2</sup> The crystallographic data have been deposited at the Cambridge Database (CCDC), 12 Union Road, Cambridge CB2 1EZ, UK and copies can be obtained on request, free of charge, by quoting the publication citation and the deposition number 213927.

*Crystal data and structure refinement for 257 (CCDC213927).*

Empirical formula	[C <sub>20</sub> H <sub>31</sub> ClN <sub>3</sub> Pd] <sup>+</sup> [SbF <sub>6</sub> ] <sup>-</sup>
Formula weight	691.08
Crystallization solvent	Acetone/pentane
Crystal habit	Block
Crystal size	0.23 x 0.20 x 0.19 mm <sup>3</sup>
Crystal color	Yellow

#### *Data collection*

Preliminary photos	Rotation
Type of diffractometer	Bruker SMART 1000
Wavelength	0.71073 Å MoKα
Data collection temperature	100(2) K
θ range for 54240 reflections used in lattice determination	2.19 to 39.64°
Unit cell dimensions	a = 10.3598(2) Å b = 22.2422(3) Å c = 10.8117(2) Å 2414.07(7) Å <sup>3</sup> β = 104.3020(10)°
Volume	2414.07(7) Å <sup>3</sup>
Z	4
Crystal system	Monoclinic
Space group	P2 <sub>1</sub>
Density (calculated)	1.901 Mg/m <sup>3</sup>
F(000)	1360
Data collection program	Bruker SMART v5.054
θ range for data collection	1.83 to 40.92°
Completeness to θ = 40.92°	97.6 %
Index ranges	-18 ≤ h ≤ 18, -40 ≤ k ≤ 40, -19 ≤ l ≤ 19
Data collection scan type	ω scans at 7 φ and 2 2θ settings
Data reduction program	Bruker SAINT v6.022
Reflections collected	110239
Independent reflections	29947 [R <sub>int</sub> = 0.0717]
Absorption coefficient	2.034 mm <sup>-1</sup>
Absorption correction	Calculated, NOT applied
Max. and min. transmission	0.6986 and 0.6520

#### *Structure solution and refinement*

Structure solution program	SHELXS-97 (Sheldrick, 1990)
Primary solution method	Patterson method
Secondary solution method	Difference Fourier map
Hydrogen placement	Geometric positions
Structure refinement program	SHELXL-97 (Sheldrick, 1997)
Refinement method	Full matrix least-squares on F <sup>2</sup>
Data / restraints / parameters	29947 / 1 / 577
Treatment of hydrogen atoms	Constrained
Goodness-of-fit on F <sup>2</sup>	1.664
Final R indices [I>2σ(I), 22793 reflections]	R1 = 0.0503, wR2 = 0.0842
R indices (all data)	R1 = 0.0709, wR2 = 0.0864
Type of weighting scheme used	Sigma
Weighting scheme used	w = 1/σ <sup>2</sup> (Fo <sup>2</sup> )
Max shift/error	0.001
Average shift/error	0.000

Absolute structure parameter	-0.018(12)
Largest diff. peak and hole	5.743 and -4.948 e. $\text{\AA}^{-3}$

*Special refinement details*

Refinement of  $F^2$  against ALL reflections. The weighted R-factor ( $wR$ ) and goodness of fit (S) are based on  $F^2$ , conventional R-factors (R) are based on F, with F set to zero for negative  $F^2$ . The threshold expression of  $F^2 > 2\sigma(F^2)$  is used only for calculating R-factors(gt) etc. and is not relevant to the choice of reflections for refinement. R-factors based on  $F^2$  are statistically about twice as large as those based on F, and R-factors based on ALL data will be even larger.

All esds (except the esd in the dihedral angle between two l.s. planes) are estimated using the full covariance matrix. The cell esds are taken into account individually in the estimation of esds in distances, angles and torsion angles; correlations between esds in cell parameters are only used when they are defined by crystal symmetry. An approximate (isotropic) treatment of cell esds is used for estimating esds involving l.s. planes.

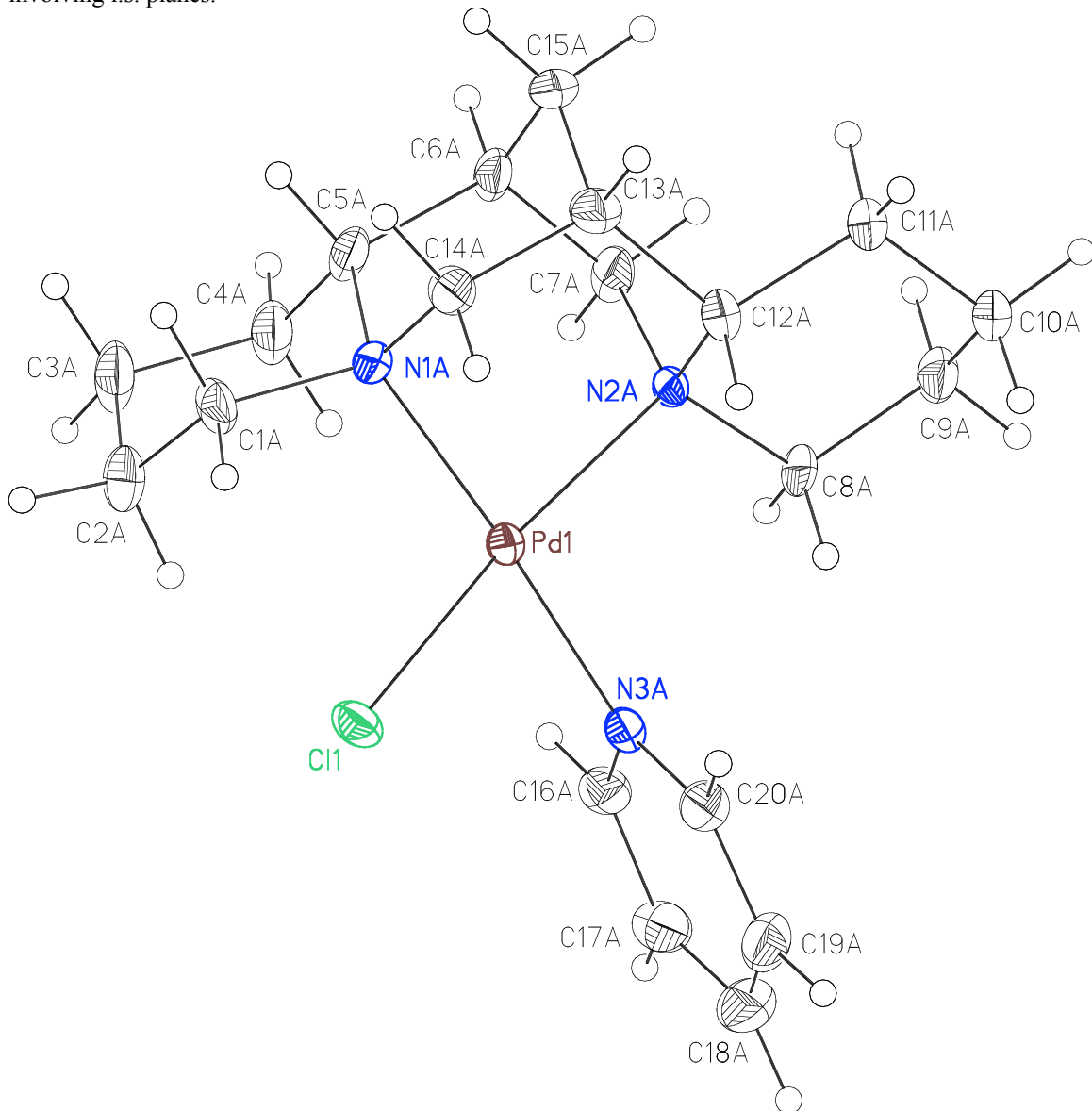


Figure A4.3.2 Molecule A of 257.

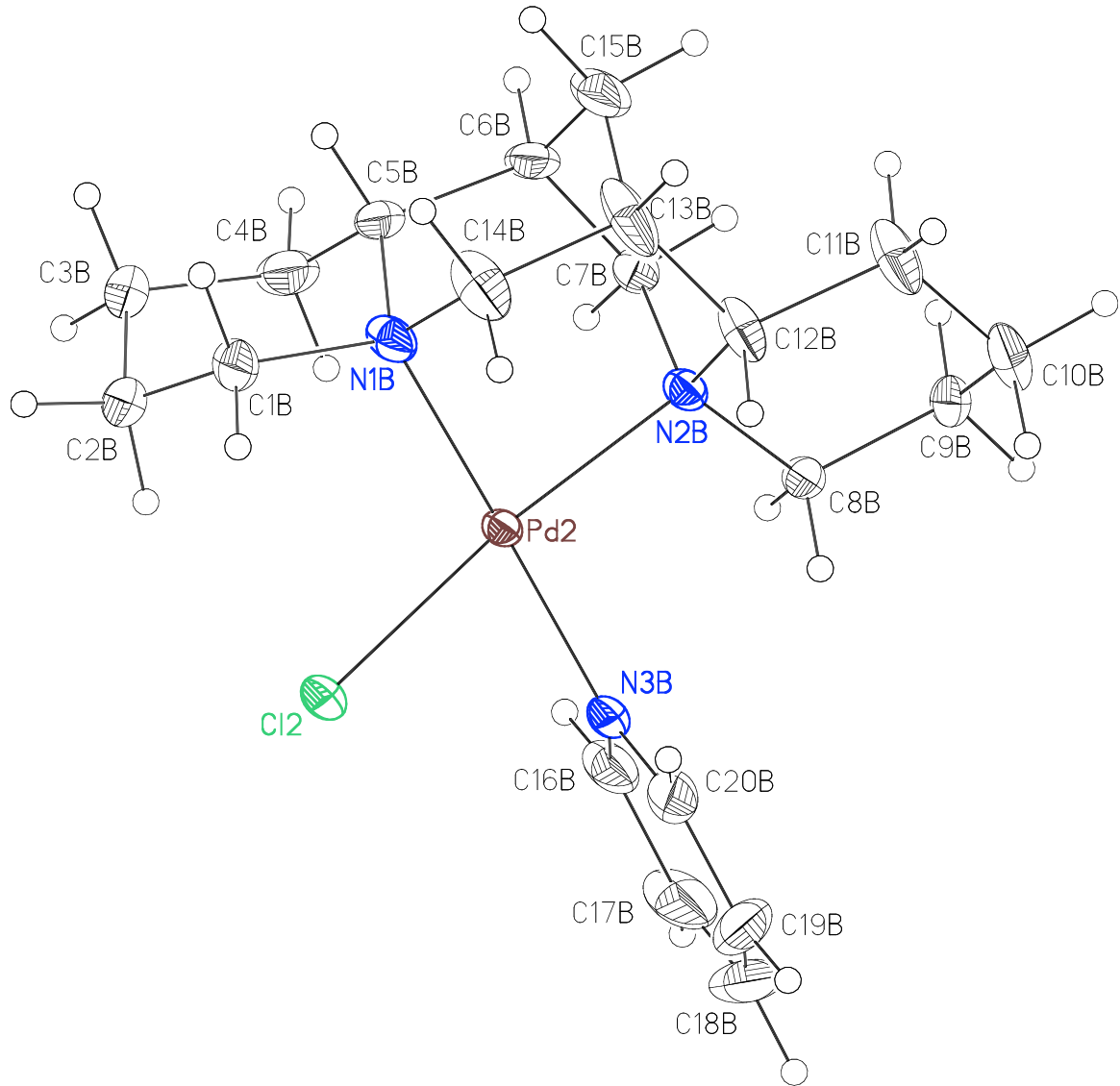


Figure A4.3.3 Molecule B of 257.

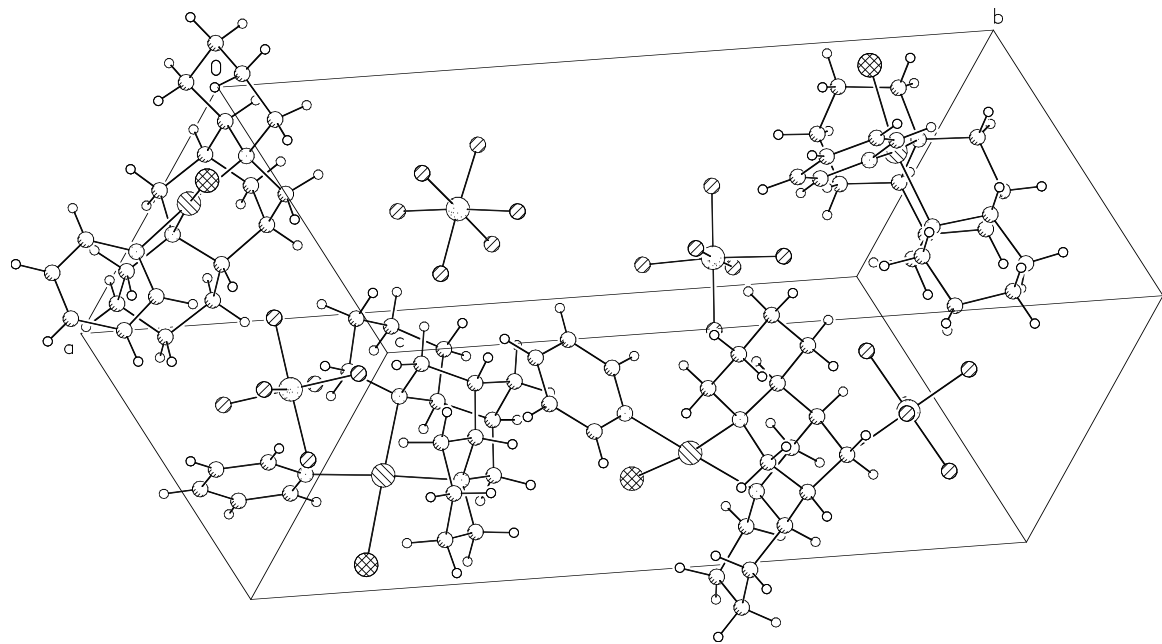


Figure A4.3.4 Unit cell contents of **257**.

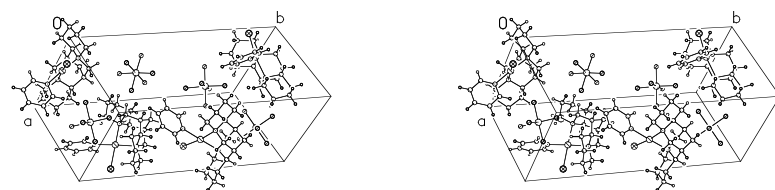


Figure A.4.3.4. Stereo view of unit cell contents of **257**.

Table A4.3.1 Atomic coordinates ( $\times 10^4$ ) and equivalent isotropic displacement parameters ( $\text{\AA}^2 \times 10^3$ ) for 257 (CCDC 213927).  $U(\text{eq})$  is defined as the trace of the orthogonalized  $U^{ij}$  tensor.

	x	y	z	$U_{\text{eq}}$
Pd(1)	10320(1)	2723(1)	5621(1)	14(1)
Cl(1)	12080(1)	2448(1)	7292(1)	22(1)
N(1A)	9566(2)	3377(1)	6637(2)	18(1)
N(2A)	9001(2)	3065(1)	3945(2)	15(1)
N(3A)	11093(2)	2054(1)	4722(2)	17(1)
C(1A)	10112(3)	3338(2)	8078(3)	23(1)
C(2A)	9698(3)	2751(2)	8630(3)	26(1)
C(3A)	8180(3)	2674(2)	8277(3)	31(1)
C(4A)	7680(3)	2736(2)	6840(3)	27(1)
C(5A)	8067(3)	3341(2)	6411(3)	23(1)
C(6A)	7375(3)	3512(2)	5054(3)	26(1)
C(7A)	7584(3)	3077(2)	4038(3)	24(1)
C(8A)	9095(3)	2672(2)	2831(2)	20(1)
C(9A)	8413(3)	2933(2)	1536(3)	26(1)
C(10A)	9048(4)	3532(2)	1363(3)	26(1)
C(11A)	8921(4)	3954(2)	2440(3)	28(1)
C(12A)	9527(3)	3683(2)	3778(3)	22(1)
C(13A)	9256(3)	4118(2)	4823(3)	24(1)
C(14A)	9992(3)	3962(2)	6193(3)	22(1)
C(15A)	7760(4)	4151(2)	4766(3)	30(1)
C(16A)	10559(3)	1497(2)	4646(3)	22(1)
C(17A)	11158(3)	1014(2)	4253(3)	28(1)
C(18A)	12354(4)	1099(2)	3895(3)	34(1)
C(19A)	12886(3)	1669(2)	3974(3)	29(1)
C(20A)	12237(3)	2131(2)	4392(3)	22(1)
Pd(2)	3905(1)	147(1)	783(1)	13(1)
Cl(2)	2076(1)	-111(1)	1564(1)	21(1)
N(1B)	3125(2)	946(1)	-112(3)	22(1)
N(2B)	5730(2)	363(1)	299(2)	17(1)
N(3B)	4640(3)	-612(1)	1749(3)	24(1)
C(1B)	1684(3)	1064(2)	-122(3)	26(1)
C(2B)	696(3)	661(2)	-1013(3)	27(1)
C(3B)	907(3)	650(2)	-2361(4)	33(1)
C(4B)	2384(4)	514(2)	-2287(4)	32(1)
C(5B)	3216(3)	991(2)	-1490(3)	32(1)
C(6B)	4667(3)	1007(2)	-1585(4)	31(1)
C(7B)	5481(3)	459(2)	-1104(3)	22(1)
C(8B)	6705(3)	-140(1)	674(3)	20(1)
C(9B)	8115(3)	-3(2)	620(3)	22(1)
C(10B)	8636(3)	520(2)	1497(3)	30(1)
C(11B)	7722(3)	1059(2)	1087(4)	33(1)
C(12B)	6250(3)	920(2)	1058(3)	25(1)
C(13B)	5362(3)	1466(2)	515(5)	39(1)
C(14B)	3935(3)	1423(2)	675(4)	34(1)
C(15B)	5302(4)	1558(2)	-890(5)	44(1)

C(16B)	4655(4)	-1135(2)	1170(5)	35(1)
C(17B)	5123(4)	-1642(2)	1878(6)	62(2)
C(18B)	5569(5)	-1610(3)	3196(7)	87(3)
C(19B)	5540(4)	-1057(3)	3785(5)	63(2)
C(20B)	5068(3)	-567(2)	3054(4)	38(1)
Sb(1)	6705(1)	950(1)	5357(1)	40(1)
F(1A)	5882(5)	325(2)	5990(4)	102(2)
F(2A)	7934(4)	1054(3)	6895(4)	136(2)
F(3A)	7451(4)	1562(2)	4591(4)	84(1)
F(4A)	5439(2)	852(2)	3818(2)	61(1)
F(5A)	5618(2)	1517(1)	5894(2)	48(1)
F(6A)	7826(3)	406(2)	4785(3)	65(1)
Sb(2)	3555(1)	3287(1)	1991(1)	27(1)
F(1B)	2277(2)	2665(1)	1700(2)	48(1)
F(2B)	4500(3)	2908(2)	3474(3)	98(2)
F(3B)	4846(2)	3897(1)	2246(3)	52(1)
F(4B)	2567(3)	3679(1)	579(3)	69(1)
F(5B)	4555(3)	2890(2)	1067(4)	83(1)
F(6B)	2601(3)	3656(2)	3051(4)	98(2)

Table A4.3.2 Bond lengths [Å] and angles [°] for 257 (CCDC 213927).

Pd(1)-N(3A)	2.046(3)	C(13A)-C(15A)	1.537(5)
Pd(1)-N(1A)	2.087(2)	C(16A)-C(17A)	1.360(5)
Pd(1)-N(2A)	2.122(2)	C(17A)-C(18A)	1.399(5)
Pd(1)-Cl(1)	2.3105(7)	C(18A)-C(19A)	1.376(6)
N(1A)-C(14A)	1.492(4)	C(19A)-C(20A)	1.365(5)
N(1A)-C(5A)	1.513(4)		
N(1A)-C(1A)	1.523(3)	Pd(2)-N(3B)	2.031(3)
N(2A)-C(7A)	1.496(4)	Pd(2)-N(1B)	2.087(3)
N(2A)-C(12A)	1.507(4)	Pd(2)-N(2B)	2.136(2)
N(2A)-C(8A)	1.510(4)	Pd(2)-Cl(2)	2.3294(7)
N(3A)-C(20A)	1.331(4)	N(1B)-C(14B)	1.484(4)
N(3A)-C(16A)	1.351(4)	N(1B)-C(1B)	1.514(4)
C(1A)-C(2A)	1.539(5)	N(1B)-C(5B)	1.519(4)
C(2A)-C(3A)	1.534(5)	N(2B)-C(7B)	1.491(4)
C(3A)-C(4A)	1.518(4)	N(2B)-C(8B)	1.494(4)
C(4A)-C(5A)	1.510(5)	N(2B)-C(12B)	1.511(4)
C(5A)-C(6A)	1.514(4)	N(3B)-C(16B)	1.324(5)
C(6A)-C(7A)	1.518(4)	N(3B)-C(20B)	1.374(5)
C(6A)-C(15A)	1.530(5)	C(1B)-C(2B)	1.513(5)
C(8A)-C(9A)	1.521(4)	C(2B)-C(3B)	1.526(5)
C(9A)-C(10A)	1.517(5)	C(3B)-C(4B)	1.543(5)
C(10A)-C(11A)	1.526(5)	C(4B)-C(5B)	1.498(6)
C(11A)-C(12A)	1.550(4)	C(5B)-C(6B)	1.532(4)
C(12A)-C(13A)	1.563(4)	C(6B)-C(15B)	1.501(6)
C(13A)-C(14A)	1.529(4)	C(6B)-C(7B)	1.501(5)

C(8B)-C(9B)	1.507(4)	C(4A)-C(5A)-N(1A)	109.7(3)
C(9B)-C(10B)	1.514(5)	C(4A)-C(5A)-C(6A)	115.1(3)
C(10B)-C(11B)	1.523(5)	N(1A)-C(5A)-C(6A)	111.4(2)
C(11B)-C(12B)	1.548(4)	C(5A)-C(6A)-C(7A)	115.0(3)
C(12B)-C(13B)	1.549(5)	C(5A)-C(6A)-C(15A)	110.3(3)
C(13B)-C(15B)	1.519(7)	C(7A)-C(6A)-C(15A)	110.7(3)
C(13B)-C(14B)	1.533(5)	N(2A)-C(7A)-C(6A)	112.2(3)
C(16B)-C(17B)	1.381(6)	N(2A)-C(8A)-C(9A)	113.9(3)
C(17B)-C(18B)	1.388(9)	C(10A)-C(9A)-C(8A)	109.4(3)
C(18B)-C(19B)	1.390(10)	C(9A)-C(10A)-C(11A)	108.9(3)
C(19B)-C(20B)	1.363(6)	C(10A)-C(11A)-C(12A)	112.5(3)
		N(2A)-C(12A)-C(11A)	113.0(3)
Sb(1)-F(2A)	1.842(3)	N(2A)-C(12A)-C(13A)	110.1(2)
Sb(1)-F(1A)	1.848(4)	C(11A)-C(12A)-C(13A)	109.3(3)
Sb(1)-F(3A)	1.858(3)	C(14A)-C(13A)-C(15A)	107.8(3)
Sb(1)-F(4A)	1.860(2)	C(14A)-C(13A)-C(12A)	115.1(3)
Sb(1)-F(5A)	1.876(3)	C(15A)-C(13A)-C(12A)	111.1(3)
Sb(1)-F(6A)	1.883(3)	N(1A)-C(14A)-C(13A)	113.1(3)
		C(6A)-C(15A)-C(13A)	104.9(3)
Sb(2)-F(5B)	1.834(3)	N(3A)-C(16A)-C(17A)	122.1(3)
Sb(2)-F(4B)	1.835(2)	C(16A)-C(17A)-C(18A)	119.0(3)
Sb(2)-F(2B)	1.861(3)	C(19A)-C(18A)-C(17A)	118.3(3)
Sb(2)-F(6B)	1.878(3)	C(20A)-C(19A)-C(18A)	119.5(3)
Sb(2)-F(3B)	1.879(3)	N(3A)-C(20A)-C(19A)	122.4(3)
Sb(2)-F(1B)	1.886(2)		
		N(3B)-Pd(2)-N(1B)	176.62(12)
		N(3B)-Pd(2)-N(2B)	94.05(10)
		N(1B)-Pd(2)-N(2B)	87.73(10)
N(3A)-Pd(1)-N(1A)	176.64(10)	N(3B)-Pd(2)-Cl(2)	80.99(7)
N(3A)-Pd(1)-N(2A)	95.73(9)	N(1B)-Pd(2)-Cl(2)	96.98(7)
N(1A)-Pd(1)-N(2A)	87.39(9)	N(2B)-Pd(2)-Cl(2)	172.89(7)
N(3A)-Pd(1)-Cl(1)	81.52(7)	C(14B)-N(1B)-C(1B)	107.3(3)
N(1A)-Pd(1)-Cl(1)	95.67(7)	C(14B)-N(1B)-C(5B)	110.6(3)
N(2A)-Pd(1)-Cl(1)	168.52(7)	C(1B)-N(1B)-C(5B)	106.4(3)
C(14A)-N(1A)-C(5A)	111.5(2)	C(14B)-N(1B)-Pd(2)	104.1(2)
C(14A)-N(1A)-C(1A)	108.3(2)	C(1B)-N(1B)-Pd(2)	114.8(2)
C(5A)-N(1A)-C(1A)	105.6(2)	C(5B)-N(1B)-Pd(2)	113.6(2)
C(14A)-N(1A)-Pd(1)	105.07(18)	C(7B)-N(2B)-C(8B)	108.6(2)
C(5A)-N(1A)-Pd(1)	112.38(19)	C(7B)-N(2B)-C(12B)	112.6(3)
C(1A)-N(1A)-Pd(1)	113.98(19)	C(8B)-N(2B)-C(12B)	109.9(2)
C(7A)-N(2A)-C(12A)	112.3(3)	C(7B)-N(2B)-Pd(2)	109.87(18)
C(7A)-N(2A)-C(8A)	108.8(2)	C(8B)-N(2B)-Pd(2)	110.24(18)
C(12A)-N(2A)-C(8A)	109.7(2)	C(12B)-N(2B)-Pd(2)	105.69(17)
C(7A)-N(2A)-Pd(1)	112.62(18)	C(16B)-N(3B)-C(20B)	120.6(4)
C(12A)-N(2A)-Pd(1)	104.67(17)	C(16B)-N(3B)-Pd(2)	122.3(3)
C(8A)-N(2A)-Pd(1)	108.57(17)	C(20B)-N(3B)-Pd(2)	117.0(3)
C(20A)-N(3A)-C(16A)	118.7(3)	C(2B)-C(1B)-N(1B)	114.4(3)
C(20A)-N(3A)-Pd(1)	120.9(2)	C(1B)-C(2B)-C(3B)	112.6(3)
C(16A)-N(3A)-Pd(1)	119.5(2)	C(2B)-C(3B)-C(4B)	109.1(3)
N(1A)-C(1A)-C(2A)	112.1(3)	C(5B)-C(4B)-C(3B)	108.2(3)
C(3A)-C(2A)-C(1A)	111.4(3)	C(4B)-C(5B)-N(1B)	110.6(3)
C(4A)-C(3A)-C(2A)	108.3(3)	C(4B)-C(5B)-C(6B)	114.4(3)
C(5A)-C(4A)-C(3A)	110.3(3)	N(1B)-C(5B)-C(6B)	111.6(3)

C(15B)-C(6B)-C(7B)	110.5(3)	F(3A)-Sb(1)-F(4A)	88.07(17)
C(15B)-C(6B)-C(5B)	107.6(3)	F(2A)-Sb(1)-F(5A)	88.28(14)
C(7B)-C(6B)-C(5B)	115.7(3)	F(1A)-Sb(1)-F(5A)	91.38(15)
N(2B)-C(7B)-C(6B)	114.2(3)	F(3A)-Sb(1)-F(5A)	89.58(13)
N(2B)-C(8B)-C(9B)	115.9(3)	F(4A)-Sb(1)-F(5A)	90.62(11)
C(8B)-C(9B)-C(10B)	109.2(3)	F(2A)-Sb(1)-F(6A)	91.87(15)
C(9B)-C(10B)-C(11B)	108.8(3)	F(1A)-Sb(1)-F(6A)	90.95(17)
C(10B)-C(11B)-C(12B)	112.8(3)	F(3A)-Sb(1)-F(6A)	88.09(14)
N(2B)-C(12B)-C(11B)	113.0(3)	F(4A)-Sb(1)-F(6A)	89.24(13)
N(2B)-C(12B)-C(13B)	109.8(3)	F(5A)-Sb(1)-F(6A)	177.66(15)
C(11B)-C(12B)-C(13B)	110.0(3)		
C(15B)-C(13B)-C(14B)	108.6(4)	F(5B)-Sb(2)-F(4B)	92.88(19)
C(15B)-C(13B)-C(12B)	110.9(3)	F(5B)-Sb(2)-F(2B)	90.2(2)
C(14B)-C(13B)-C(12B)	114.0(3)	F(4B)-Sb(2)-F(2B)	176.9(2)
N(1B)-C(14B)-C(13B)	113.8(3)	F(5B)-Sb(2)-F(6B)	175.4(2)
C(6B)-C(15B)-C(13B)	107.2(3)	F(4B)-Sb(2)-F(6B)	91.73(19)
N(3B)-C(16B)-C(17B)	120.0(5)	F(2B)-Sb(2)-F(6B)	85.2(2)
C(16B)-C(17B)-C(18B)	120.7(5)	F(5B)-Sb(2)-F(3B)	87.13(13)
C(17B)-C(18B)-C(19B)	118.4(4)	F(4B)-Sb(2)-F(3B)	90.50(11)
C(20B)-C(19B)-C(18B)	119.1(5)	F(2B)-Sb(2)-F(3B)	89.79(13)
C(19B)-C(20B)-N(3B)	121.1(5)	F(6B)-Sb(2)-F(3B)	93.28(15)
		F(5B)-Sb(2)-F(1B)	91.39(13)
F(2A)-Sb(1)-F(1A)	92.3(3)	F(4B)-Sb(2)-F(1B)	89.18(11)
F(2A)-Sb(1)-F(3A)	92.3(2)	F(2B)-Sb(2)-F(1B)	90.60(12)
F(1A)-Sb(1)-F(3A)	175.40(19)	F(6B)-Sb(2)-F(1B)	88.23(15)
F(2A)-Sb(1)-F(4A)	178.85(15)	F(3B)-Sb(2)-F(1B)	178.47(13)
F(1A)-Sb(1)-F(4A)	87.42(18)		



## APPENDIX 4.4

*X-ray Crystallographic Data for  $((sp)PdCl)_2^{2+}2SbF_6^-$  (297)*

*Scheme A4.4.1.*

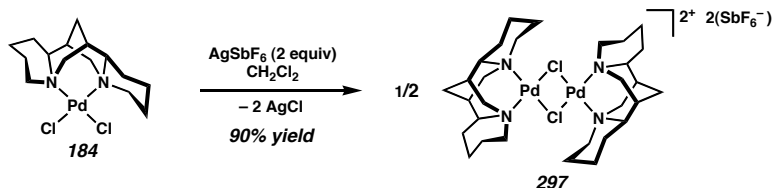
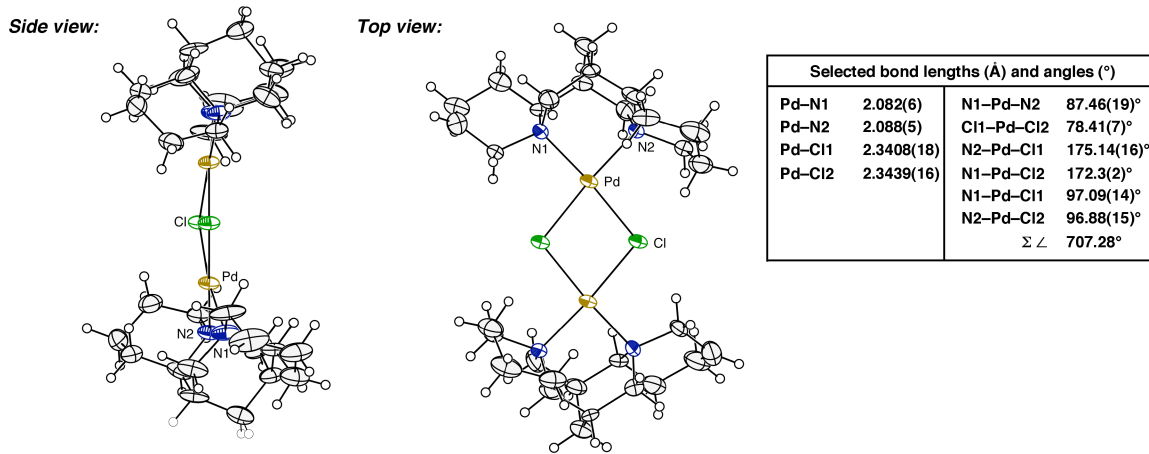


*Figure A4.4.1  $((sp)PdCl)_2^{2+}2SbF_6^-$  (297).*<sup>1,2</sup>



<sup>1</sup> (a) The  $SbF_6^-$  anions are not shown. (b) The molecular structures are shown with 50% probability ellipsoids.

<sup>2</sup> The crystallographic data have been deposited at the Cambridge Database (CCDC), 12 Union Road, Cambridge CB2 1EZ, UK and copies can be obtained on request, free of charge, by quoting the publication citation and the deposition number 214435.

Crystal data and structure refinement for 297 (CCDC 214435).

Empirical formula	$[C_{15}H_{26}ClN_2Pd]^+ [SbF_6]^-$
Formula weight	611.98
Crystallization solvent	Dichloromethane/hexanes
Crystal habit	Blade
Crystal size	0.33 x 0.29 x 0.03 mm <sup>3</sup>
Crystal color	Orange
<i>Data collection</i>	
Preliminary photos	Rotation
Type of diffractometer	Bruker SMART 1000
Wavelength	0.71073 Å MoKα
Data collection temperature	100(2) K
θ range for 7630 reflections used in lattice determination	2.35 to 27.88°
Unit cell dimensions	$a = 13.373(3)$ Å $b = 11.904(2)$ Å $c = 13.744(3)$ Å $2052.9(7)$ Å <sup>3</sup>
Volume	
Z	4
Crystal system	Monoclinic
Space group	C2
Density (calculated)	1.980 Mg/m <sup>3</sup>
F(000)	1192
Data collection program	Bruker SMART v5.054
θ range for data collection	1.58 to 28.26°
Completeness to θ = 28.26°	94.2 %
Index ranges	-17 ≤ h ≤ 17, -15 ≤ k ≤ 15, -17 ≤ l ≤ 18
Data collection scan type	ω scans at 5 φ settings
Data reduction program	Bruker SAINT v6.022
Reflections collected	14714
Independent reflections	4651 [ $R_{int} = 0.0539$ ]
Absorption coefficient	2.376 mm <sup>-1</sup>
Absorption correction	Analytical
Max. and min. transmission	0.9321 and 0.5077

#### Structure solution and refinement

Structure solution program	SHELXS-97 (Sheldrick, 1990)
Primary solution method	Patterson method
Secondary solution method	Difference Fourier map
Hydrogen placement	Geometric positions
Structure refinement program	SHELXL-97 (Sheldrick, 1997)
Refinement method	Full matrix least-squares on F <sup>2</sup>
Data / restraints / parameters	4651 / 1 / 235
Treatment of hydrogen atoms	Constrained
Goodness-of-fit on F <sup>2</sup>	2.099
Final R indices [I>2σ(I), 3634 reflections]	R1 = 0.0507, wR2 = 0.0816
R indices (all data)	R1 = 0.0873, wR2 = 0.0879
Type of weighting scheme used	Sigma
Weighting scheme used	w=1/σ <sup>2</sup> (Fo <sup>2</sup> )
Max shift/error	0.001

Average shift/error	0.000
Absolute structure parameter	-0.01(4)
Largest diff. peak and hole	3.062 and -1.438 e. $\text{\AA}^{-3}$

#### Special refinement details

Refinement of  $F^2$  against ALL reflections. The weighted R-factor ( $wR$ ) and goodness of fit (S) are based on  $F^2$ , conventional R-factors (R) are based on F, with F set to zero for negative  $F^2$ . The threshold expression of  $F^2 > 2\sigma(F^2)$  is used only for calculating R-factors(gt) etc. and is not relevant to the choice of reflections for refinement. R-factors based on  $F^2$  are statistically about twice as large as those based on F, and R-factors based on ALL data will be even larger.

All esds (except the esd in the dihedral angle between two l.s. planes) are estimated using the full covariance matrix. The cell esds are taken into account individually in the estimation of esds in distances, angles and torsion angles; correlations between esds in cell parameters are only used when they are defined by crystal symmetry. An approximate (isotropic) treatment of cell esds is used for estimating esds involving l.s. planes.

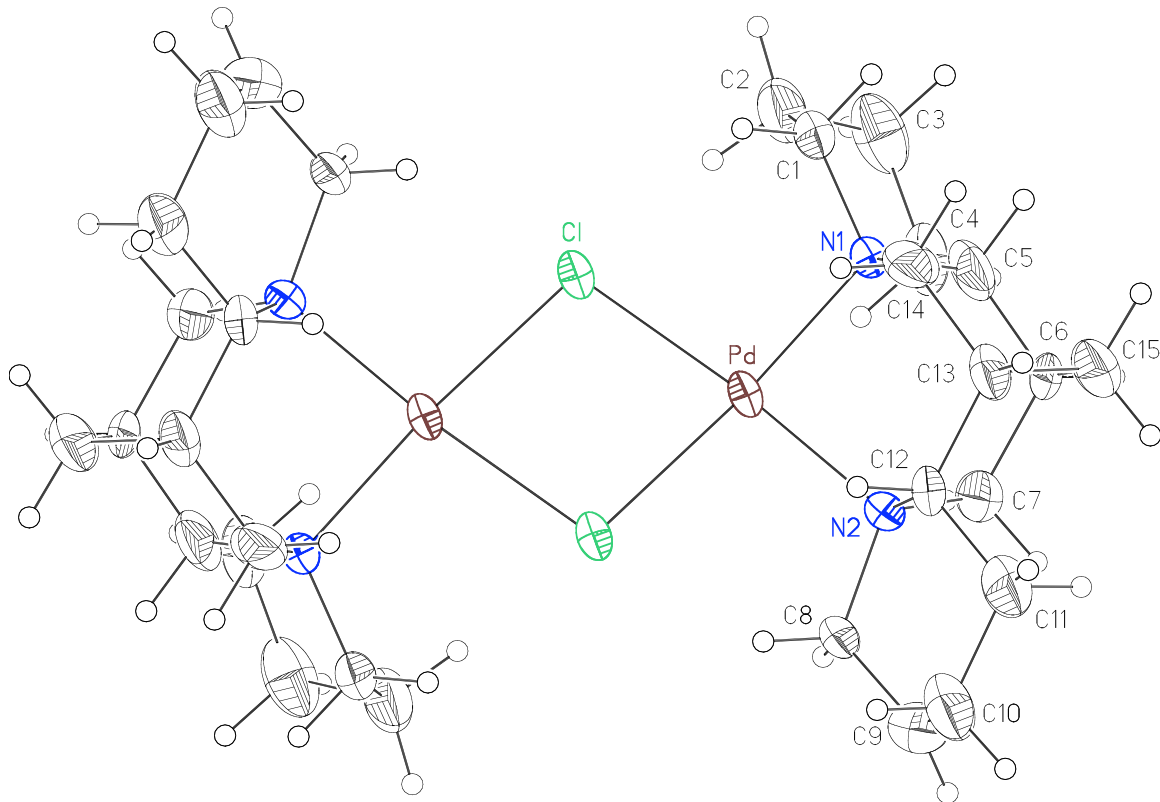


Figure A4.4.2 Molecule of 297.

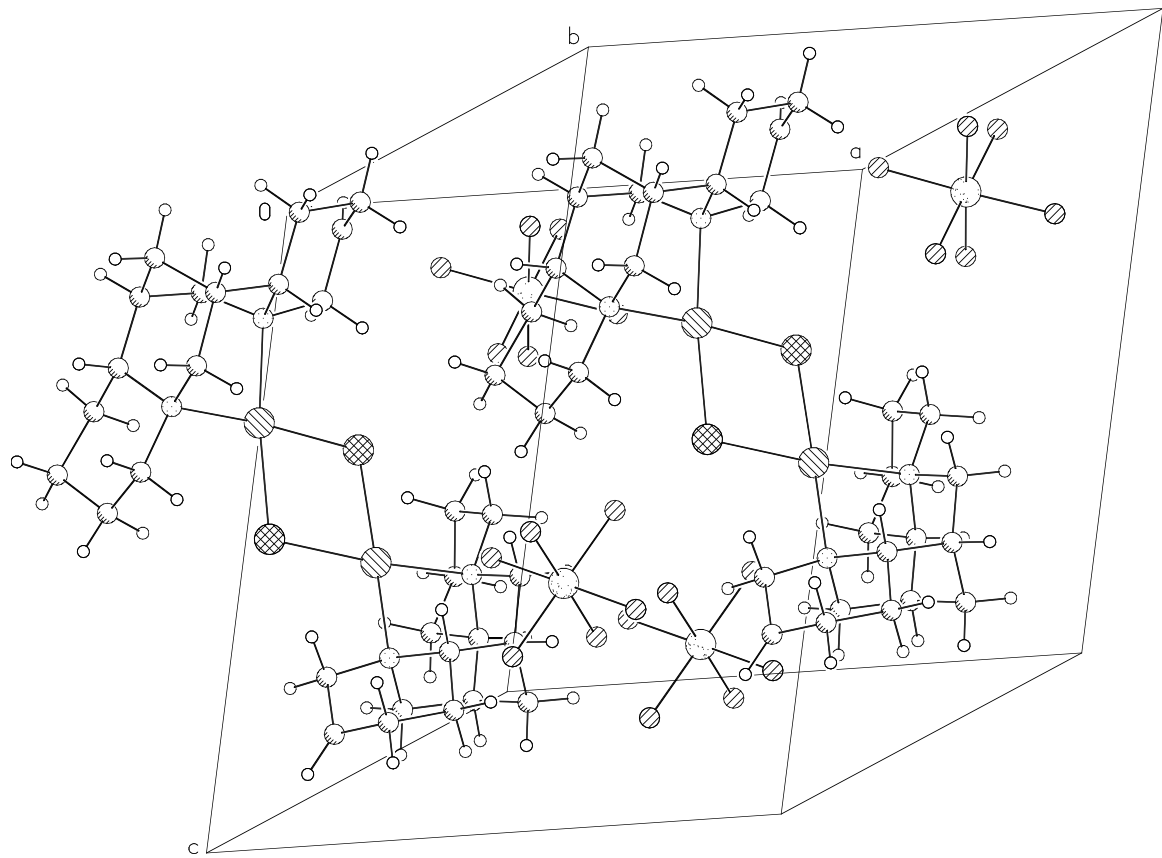


Figure A4.4.3. Unit cell contents of **297**.

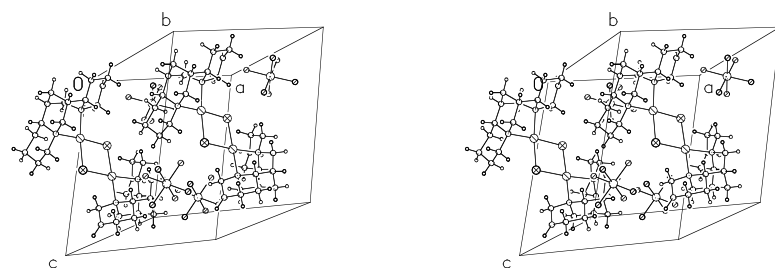


Figure A4.4.4. Stereo view of unit cell contents of **297**.

Table A4.4.1 Atomic coordinates ( $\times 10^4$ ) and equivalent isotropic displacement parameters ( $\text{\AA}^2 \times 10^3$ ) for **297** (CCDC 214435).  $U(\text{eq})$  is defined as the trace of the orthogonalized  $U^{ij}$  tensor.

	x	y	z	$U_{\text{eq}}$	Occ
Pd	6179(1)	7343(1)	6155(1)	28(1)	
Cl	5681(1)	7224(2)	4349(1)	31(1)	
N(1)	7818(4)	7480(7)	6472(4)	32(2)	
N(2)	6484(4)	7634(8)	7725(4)	39(2)	
C(1)	8132(5)	7310(8)	5516(5)	34(2)	
C(2)	8048(6)	6134(8)	5165(7)	48(3)	
C(3)	8597(7)	5292(8)	6003(8)	56(3)	
C(4)	8202(7)	5511(8)	6908(7)	47(3)	
C(5)	8460(6)	6706(8)	7303(7)	45(2)	
C(6)	8372(6)	6972(9)	8333(6)	40(3)	
C(7)	7227(6)	6824(9)	8368(7)	50(3)	
C(8)	5453(5)	7578(12)	7947(6)	58(3)	
C(9)	5490(7)	8033(13)	8947(8)	79(4)	
C(10)	5822(7)	9232(11)	9086(9)	66(3)	
C(11)	6906(7)	9304(10)	8978(7)	56(3)	
C(12)	6906(6)	8886(7)	7964(6)	36(2)	
C(13)	8009(6)	8922(8)	7897(7)	40(2)	
C(14)	8070(7)	8696(9)	6818(8)	47(3)	
C(15)	8768(6)	8132(8)	8674(7)	49(3)	
Sb	6903(1)	2663(1)	7849(1)	47(1)	
F(1)	6327(4)	2337(7)	8870(4)	78(2)	
F(2)	8045(4)	1755(5)	8522(7)	100(3)	
F(3)	7621(5)	3890(5)	8603(4)	65(2)	
F(4)	7470(5)	3009(6)	6839(5)	103(3)	
F(5)	6171(5)	1457(6)	7107(5)	82(2)	
F(6)	5751(5)	3590(6)	7211(6)	92(2)	

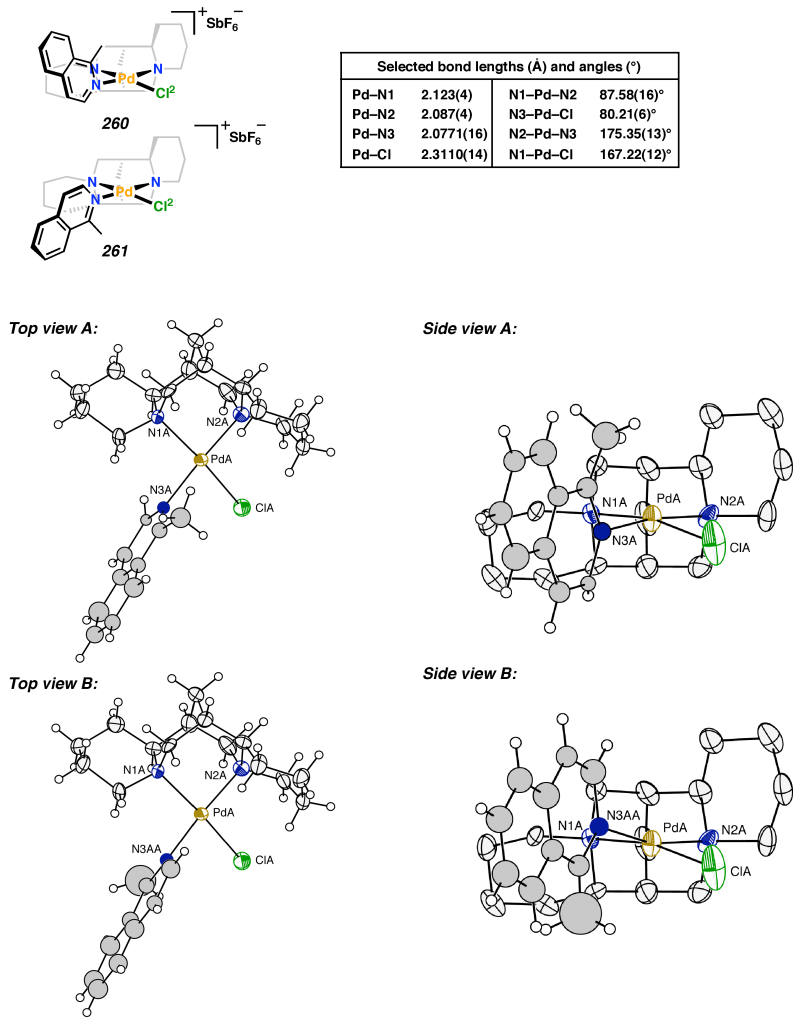
Table A4.4.2 Bond lengths [ $\text{\AA}$ ] and angles [ $^\circ$ ] for **297** (CCDC 214435).

Pd-N(2)	2.082(6)	C(4)-C(5)	1.519(13)
Pd-N(1)	2.088(5)	C(5)-C(6)	1.495(13)
Pd-Cl	2.3408(18)	C(6)-C(15)	1.495(13)
Pd-Cl#1	2.3439(16)	C(6)-C(7)	1.558(10)
Cl-Pd#1	2.3439(16)	C(8)-C(9)	1.462(12)
N(1)-C(5)	1.488(10)	C(9)-C(10)	1.488(16)
N(1)-C(1)	1.525(8)	C(10)-C(11)	1.510(12)
N(1)-C(14)	1.525(13)	C(11)-C(12)	1.479(12)
N(2)-C(7)	1.447(11)	C(12)-C(13)	1.511(10)
N(2)-C(8)	1.512(8)	C(13)-C(14)	1.536(13)
N(2)-C(12)	1.588(12)	C(13)-C(15)	1.518(11)
C(1)-C(2)	1.472(13)	Sb-F(6)	1.851(6)
C(2)-C(3)	1.512(13)	Sb-F(2)	1.838(6)
C(3)-C(4)	1.532(13)	Sb-F(5)	1.835(6)

Sb-F(4)	1.844(5)	C(15)-C(6)-C(7)	109.9(8)
Sb-F(1)	1.860(5)	C(5)-C(6)-C(7)	113.9(7)
Sb-F(3)	1.856(6)	N(2)-C(7)-C(6)	112.4(7)
		N(2)-C(8)-C(9)	115.9(7)
N(2)-Pd-N(1)	87.46(19)	C(10)-C(9)-C(8)	112.8(11)
N(2)-Pd-Cl	172.3(2)	C(9)-C(10)-C(11)	107.2(9)
N(1)-Pd-Cl	96.88(15)	C(12)-C(11)-C(10)	112.7(8)
N(2)-Pd-Cl#1	97.09(14)	C(11)-C(12)-C(13)	111.5(7)
N(1)-Pd-Cl#1	175.14(16)	C(11)-C(12)-N(2)	113.3(7)
Cl-Pd-Cl#1	78.41(7)	C(13)-C(12)-N(2)	107.4(6)
Pd-Cl-Pd#1	101.16(7)	C(14)-C(13)-C(15)	109.0(7)
C(5)-N(1)-C(1)	108.8(6)	C(14)-C(13)-C(12)	115.7(7)
C(5)-N(1)-C(14)	110.0(7)	C(15)-C(13)-C(12)	111.6(7)
C(1)-N(1)-C(14)	107.3(6)	C(13)-C(14)-N(1)	112.8(8)
C(5)-N(1)-Pd	113.5(5)	C(6)-C(15)-C(13)	105.9(6)
C(1)-N(1)-Pd	113.1(4)	F(6)-Sb-F(2)	178.2(4)
C(14)-N(1)-Pd	104.0(5)	F(6)-Sb-F(5)	90.4(3)
C(7)-N(2)-C(8)	109.2(7)	F(2)-Sb-F(5)	90.6(3)
C(7)-N(2)-C(12)	112.2(6)	F(6)-Sb-F(4)	90.1(3)
C(8)-N(2)-C(12)	106.4(7)	F(2)-Sb-F(4)	91.4(4)
C(7)-N(2)-Pd	111.7(6)	F(5)-Sb-F(4)	92.1(3)
C(8)-N(2)-Pd	109.7(4)	F(6)-Sb-F(1)	89.3(3)
C(12)-N(2)-Pd	107.4(5)	F(2)-Sb-F(1)	89.2(3)
C(2)-C(1)-N(1)	113.3(7)	F(5)-Sb-F(1)	88.6(3)
C(1)-C(2)-C(3)	114.8(7)	F(4)-Sb-F(1)	179.1(4)
C(2)-C(3)-C(4)	107.0(7)	F(6)-Sb-F(3)	88.9(3)
C(5)-C(4)-C(3)	110.5(8)	F(2)-Sb-F(3)	90.1(3)
N(1)-C(5)-C(4)	107.8(7)	F(5)-Sb-F(3)	179.0(3)
N(1)-C(5)-C(6)	112.5(7)	F(4)-Sb-F(3)	88.6(3)
C(4)-C(5)-C(6)	117.1(8)	F(1)-Sb-F(3)	90.7(3)
C(15)-C(6)-C(5)	110.9(8)		

Symmetry transformations used to generate equivalent atoms:

#1 -x+1,y,-z+1

**APPENDIX 4.5***X-ray Crystallographic Data for (sp)Pd(2-methylisoquinoline)Cl<sup>+</sup>SbF<sub>6</sub><sup>-</sup> (260/261)*Figure A4.5.1 (sp)Pd(2-methylisoquinoline)Cl<sup>+</sup>SbF<sub>6</sub><sup>-</sup> (260/261).<sup>1,2</sup>

<sup>1</sup> (a) The numbering shown in Figure A4.5.1 does not match that in the crystallographic report. (b) A and B in Figure A4.5.1 refer to the same molecule, but with the disorder in the isoquinoline modeled in two different orientations (i.e., 260 and 261). (c) The SbF<sub>6</sub> anion in both views and the hydrogen atoms of the (-)-sparteine backbone of the side view are not shown.

<sup>2</sup> The crystallographic data have been deposited at the Cambridge Database (CCDC), 12 Union Road, Cambridge CB2 1EZ, UK and copies can be obtained on request, free of charge, by quoting the publication citation and the deposition number 217276.

*Crystal data and structure refinement for 260/261 (CCDC 217276).*

Empirical formula	[C <sub>25</sub> H <sub>35</sub> N <sub>3</sub> ClPd] <sup>+</sup> [SbF <sub>6</sub> ] <sup>-</sup>
Formula weight	755.16
Crystallization Solvent	Dichloromethane
Crystal Habit	Block
Crystal size	0.30 x 0.28 x 0.27 mm <sup>3</sup>
Crystal color	Orange

#### *Data collection*

Preliminary photos	Rotation
Type of diffractometer	Bruker SMART 1000
Wavelength	0.71073 Å MoKα
Data collection temperature	100(2) K
θ range for 29306 reflections used in lattice determination	2.25 to 28.19°
Unit cell dimensions	a = 9.7500(5) Å b = 21.3471(10) Å c = 13.1934(6) Å 2745.1(2) Å <sup>3</sup>
Volume	
Z	4
Crystal system	Monoclinic
Space group	P2 <sub>1</sub>
Density (calculated)	1.827 Mg/m <sup>3</sup>
F(000)	1496
θ range for data collection	1.54 to 28.41°
Completeness to θ = 28.41°	93.1 %
Index ranges	-12 ≤ h ≤ 12, -28 ≤ k ≤ 27, -17 ≤ l ≤ 17
Data collection scan type	ω scans at 4 φ settings and 1 φ scan
Reflections collected	47919
Independent reflections	12521 [R <sub>int</sub> = 0.0494]
Absorption coefficient	1.797 mm <sup>-1</sup>
Absorption correction	None
Max. and min. transmission (predicted)	0.6425 and 0.6146

#### *Structure solution and refinement*

Structure solution program	SHELXS-97 (Sheldrick, 1990)
Primary solution method	Patterson method
Secondary solution method	Difference Fourier map
Hydrogen placement	Geometric positions
Structure refinement program	SHELXL-97 (Sheldrick, 1997)
Refinement method	Full matrix least-squares on F <sup>2</sup>
Data / restraints / parameters	12521 / 1 / 542
Treatment of hydrogen atoms	Riding
Goodness-of-fit on F <sup>2</sup>	2.140
Final R indices [I>2σ(I), 11419 reflections]	R1 = 0.0440, wR2 = 0.0763
R indices (all data)	R1 = 0.0505, wR2 = 0.0772
Type of weighting scheme used	Sigma
Weighting scheme used	w=1/σ <sup>2</sup> (Fo <sup>2</sup> )
Max shift/error	0.001
Average shift/error	0.000
Absolute structure parameter	-0.028(18)

Largest diff. peak and hole                            2.187 and -1.798 e. $\text{\AA}^{-3}$

*Special refinement details*

Disorder is observed in the crystals. One of the two molecules in the asymmetric unit is disordered in that both isomers with respect to the orientation of the isoquinoline ligand occupy the site. Molecule A has two orientations of the isoquinoline related by a rotation of 180° around the Pd-N bond. The atoms of both orientations were refined isotropically with riding hydrogen atoms. The occupancies of both orientations are nearly equal, see Table A4.5.1. The final difference Fourier map suggests similar disorder in the isoquinoline ligand of Molecule B but to a much lesser extent. Because the evidence was so weak no attempt was made to model it, anisotropic displacement parameters were used for nonhydrogen atoms. The isoquinoline ligands were refined with the ring systems set as rigid bodies (distances = 1.39 $\text{\AA}$ ). No restraints were placed on the methyl group.

The largest peak in the final difference Fourier map is within 0.8 $\text{\AA}$  of Sb(2). All other peaks greater than 1.0e $\text{/}\text{\AA}^3$  (four of them ranging from 1.41-1.06 e $\text{/}\text{\AA}^3$ ) evidence unmodeled disorder.

Refinement of  $F^2$  against ALL reflections. The weighted R-factor ( $wR$ ) and goodness of fit (S) are based on  $F^2$ , conventional R-factors (R) are based on F, with F set to zero for negative  $F^2$ . The threshold expression of  $F^2 > 2\sigma(F^2)$  is used only for calculating R-factors(gt) etc. and is not relevant to the choice of reflections for refinement. R-factors based on  $F^2$  are statistically about twice as large as those based on F, and R-factors based on ALL data will be even larger.

All esds (except the esd in the dihedral angle between two l.s. planes) are estimated using the full covariance matrix. The cell esds are taken into account individually in the estimation of esds in distances, angles and torsion angles; correlations between esds in cell parameters are only used when they are defined by crystal symmetry. An approximate (isotropic) treatment of cell esds is used for estimating esds involving l.s. planes.

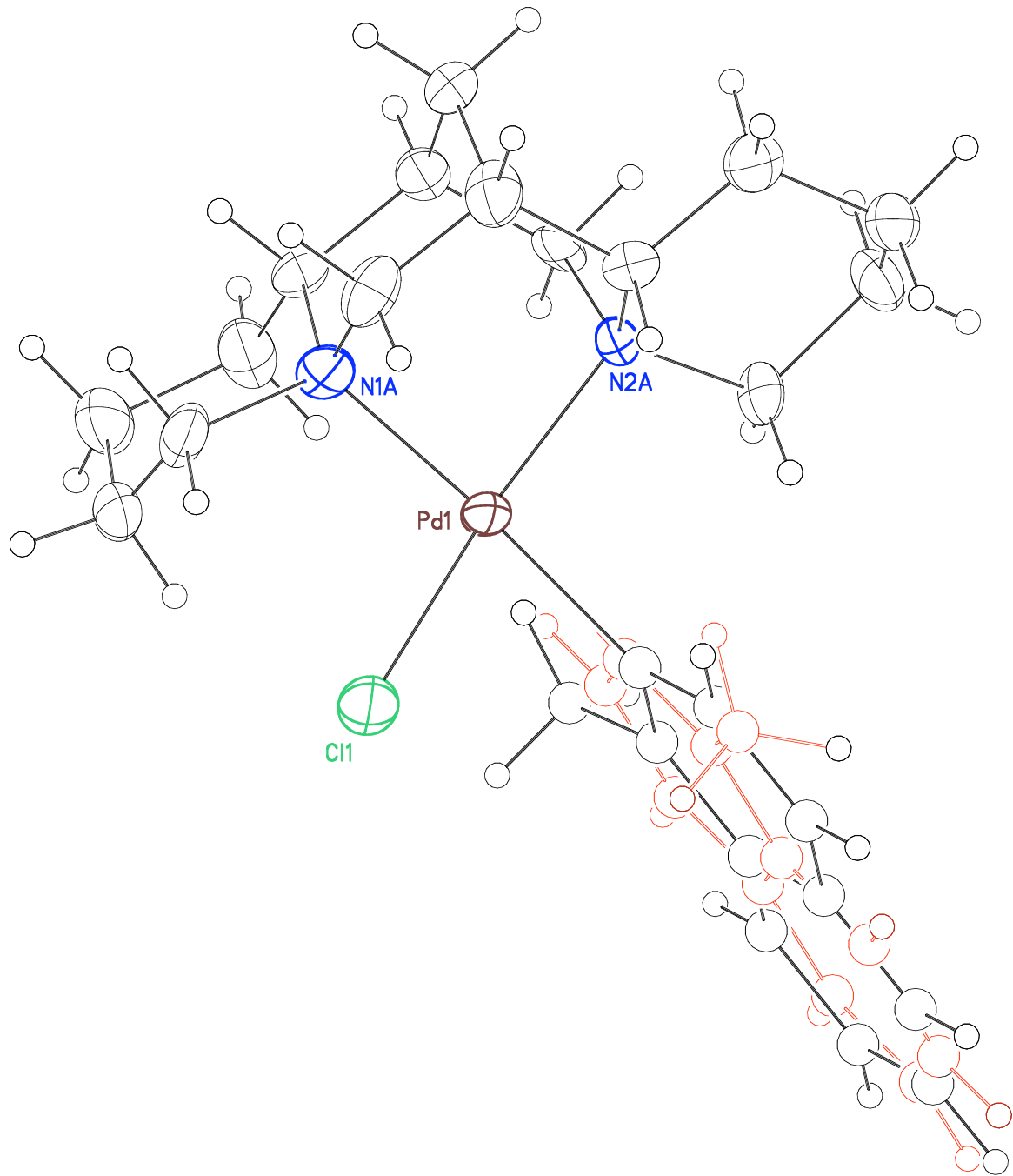


Figure A4.5.2 Molecule A of **260/261** showing the disorder in the isoquinoline ligand.

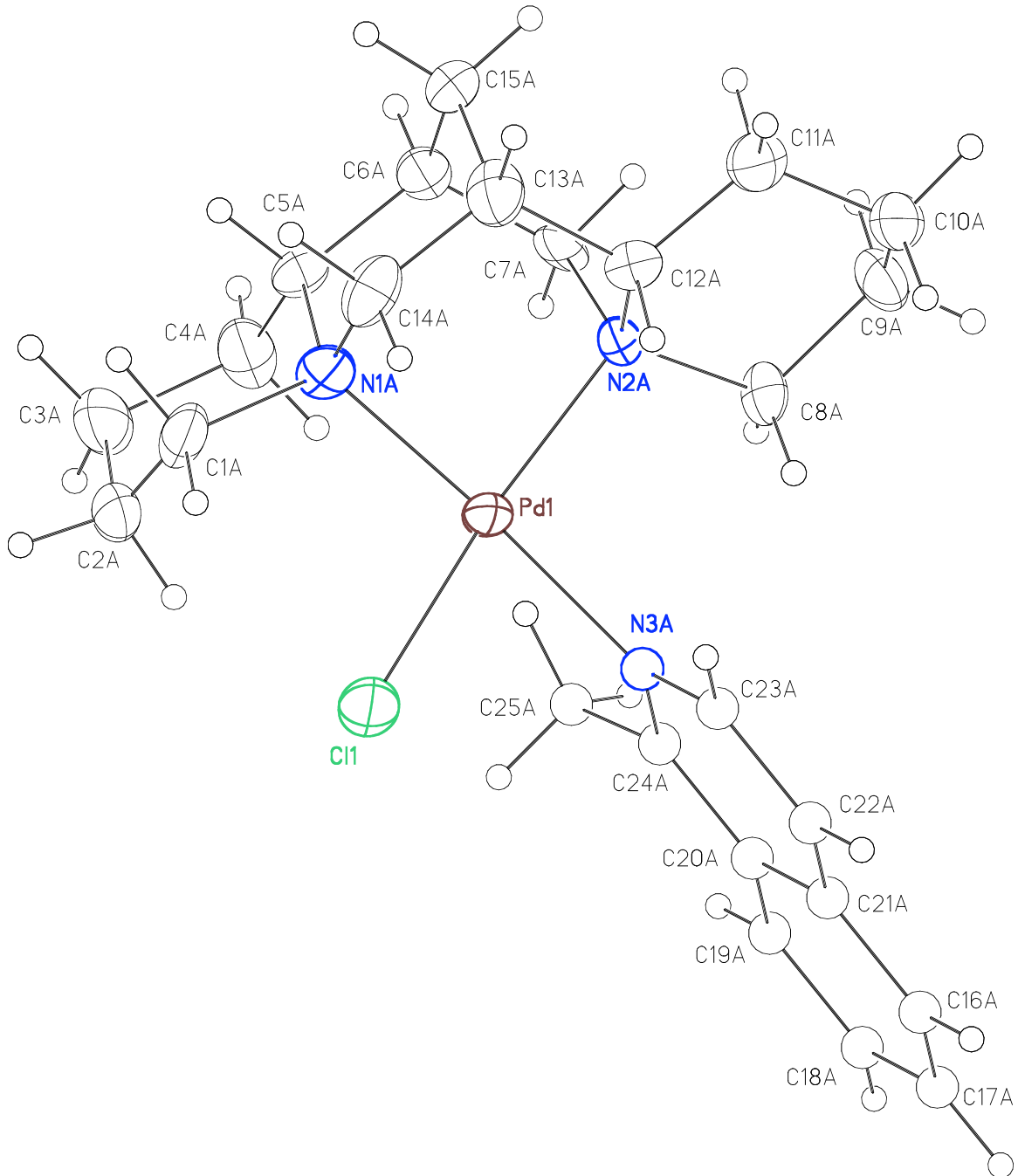


Figure A4.5.3 Molecule A of **260/261** showing the disorder modeled isotropically in one orientation of the isoquinoline ligand.

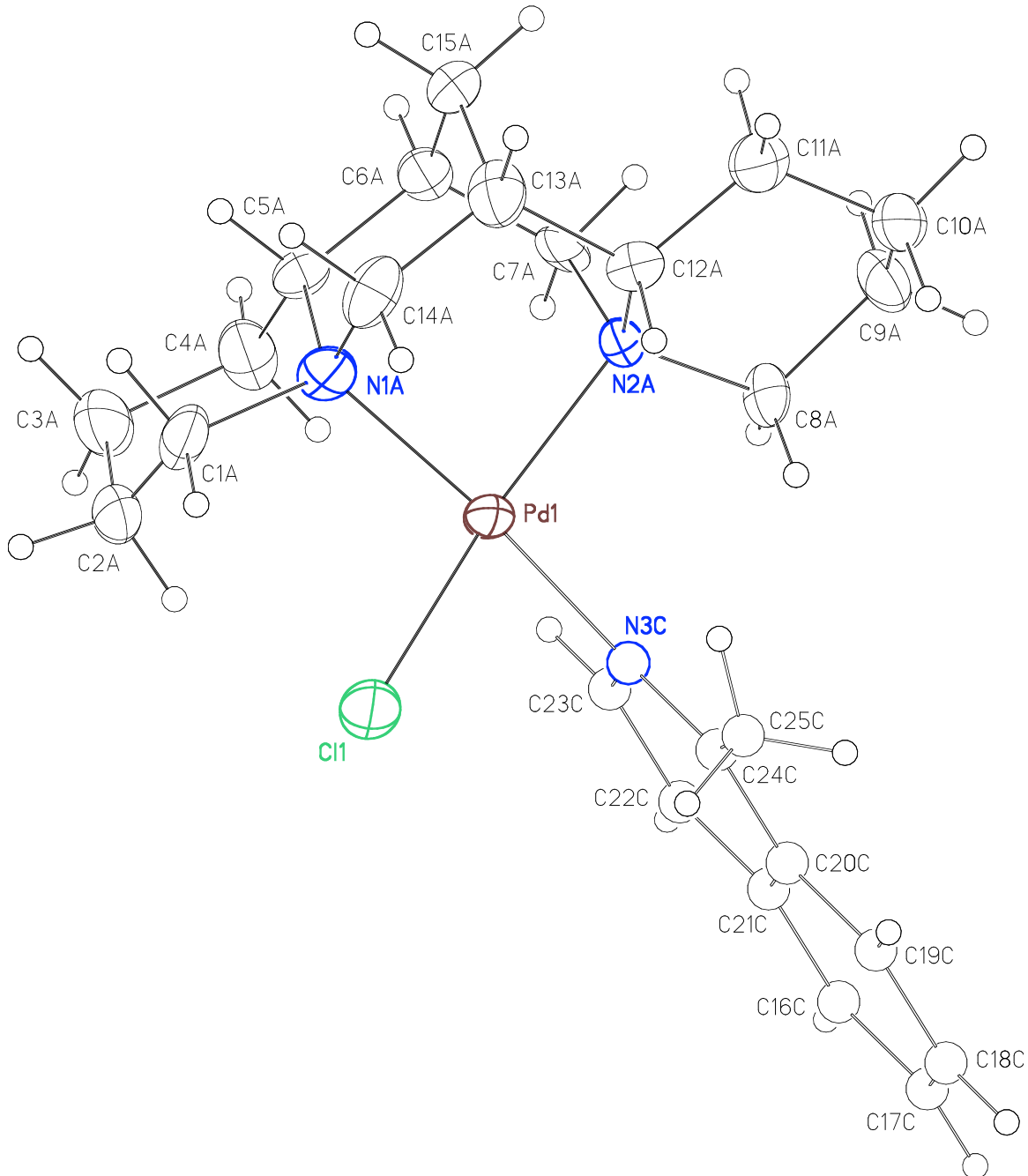
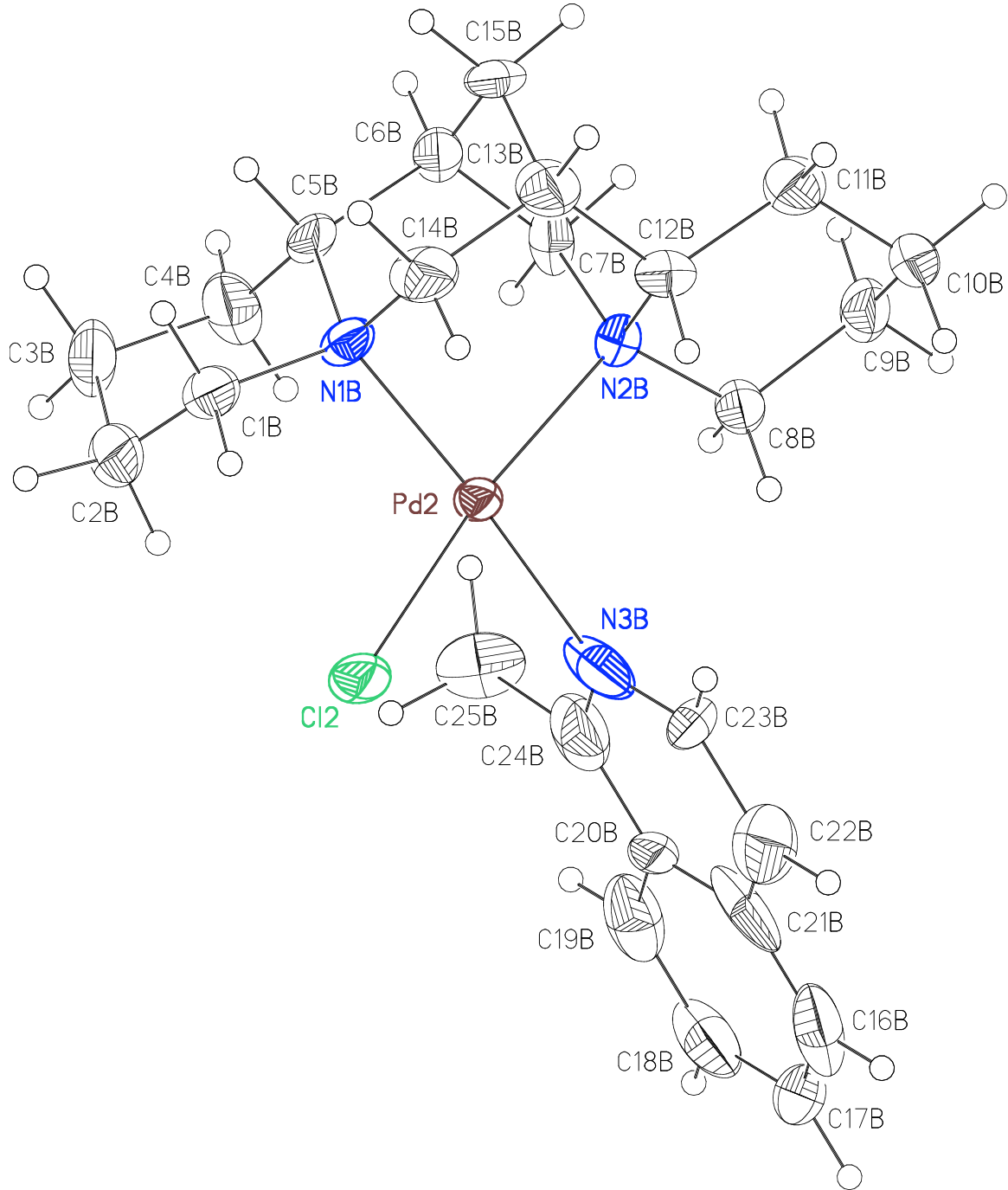


Figure A4.5.4 Molecule A of **260/261** showing the disorder modeled isotropically in another orientation of the isoquinoline ligand, related to the first by 180°.

Figure A4.5.5 Molecule B of **260/261**.

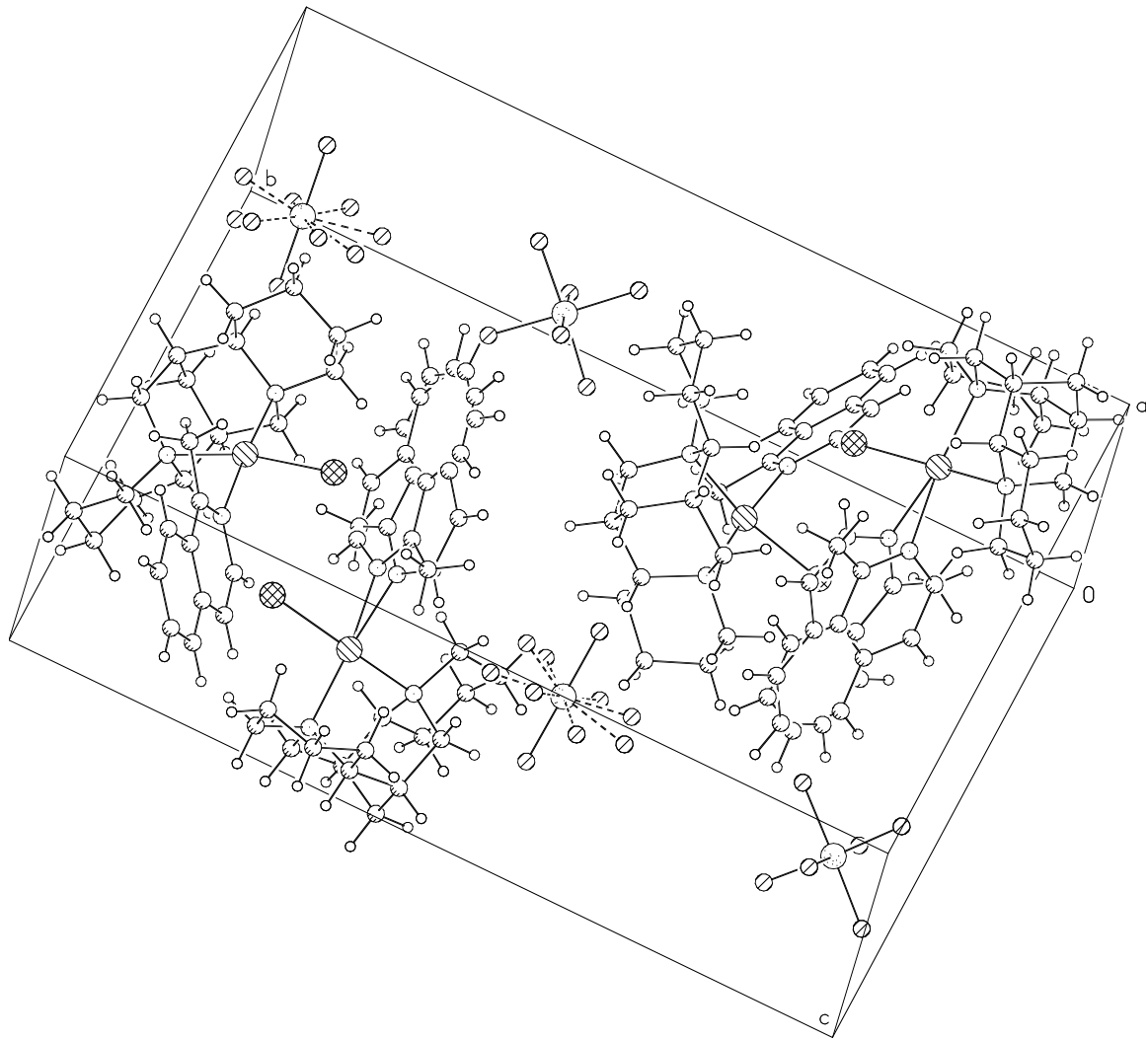


Figure A4.5.6 Unit cell contents of **260/261**.

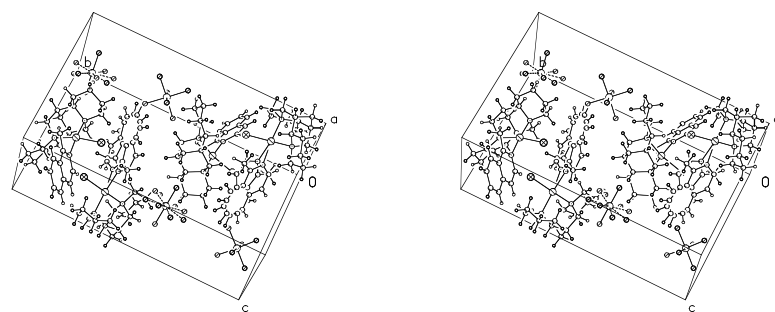


Figure A4.5.7 Stereo view of unit cell contents of **260/261**.

Table A4.5.1 Atomic coordinates ( $\times 10^4$ ) and equivalent isotropic displacement parameters ( $\text{\AA}^2 \times 10^3$ ) for **260/261** (CCDC 217276).  $U(\text{eq})$  is defined as the trace of the orthogonalized  $U^{ij}$  tensor.

	x	y	z	$U_{\text{eq}}$	Occ
Pd(1)	1832(1)	6593(1)	7944(1)	28(1)	1
Cl(1)	2816(2)	7575(1)	8009(1)	67(1)	1
N(1A)	1233(5)	6599(2)	9440(3)	29(1)	1
N(2A)	597(4)	5795(2)	7721(3)	22(1)	1
C(1A)	1873(7)	7099(3)	10106(4)	41(2)	1
C(2A)	3401(7)	7002(3)	10287(4)	41(2)	1
C(3A)	3765(7)	6355(3)	10705(5)	48(2)	1
C(4A)	3042(6)	5864(3)	10044(4)	42(2)	1
C(5A)	1523(6)	5979(3)	9966(4)	32(1)	1
C(6A)	666(6)	5445(3)	9536(4)	34(1)	1
C(7A)	971(6)	5280(2)	8428(4)	26(1)	1
C(8A)	742(5)	5559(2)	6642(4)	27(1)	1
C(9A)	-382(6)	5091(3)	6300(4)	36(1)	1
C(10A)	-1781(6)	5395(3)	6376(4)	38(2)	1
C(11A)	-1956(6)	5592(3)	7449(4)	35(1)	1
C(12A)	-856(5)	6033(2)	7867(4)	24(1)	1
C(13A)	-1094(6)	6183(3)	8973(4)	37(1)	1
C(14A)	-269(6)	6729(3)	9405(4)	37(2)	1
C(15A)	-833(7)	5597(3)	9629(4)	44(2)	1
C(16A)	3596(6)	7149(3)	3531(3)	47(4)	0.471(7)
C(17A)	4830(7)	6914(4)	3189(4)	34(3)	0.471(7)
C(18A)	5641(5)	6537(3)	3819(4)	29(3)	0.471(7)
C(19A)	5218(5)	6395(3)	4791(4)	45(4)	0.471(7)
C(20A)	3984(4)	6631(2)	5133(3)	26(3)	0.471(7)
C(21A)	3173(4)	7008(2)	4503(3)	31(3)	0.471(7)
C(22A)	1938(5)	7244(3)	4844(4)	28(3)	0.471(7)
C(23A)	1515(4)	7102(3)	5816(4)	14(3)	0.471(7)
N(3A)	2326(5)	6725(3)	6447(3)	20(2)	0.471(7)
C(24A)	3561(5)	6490(2)	6105(3)	27(3)	0.471(7)
C(25A)	4390(7)	6146(4)	6816(4)	47(4)	0.471(7)
C(16C)	5473(5)	6425(3)	4151(4)	40(3)	0.529(7)
C(17C)	5178(6)	6774(3)	3284(3)	45(3)	0.529(7)
C(18C)	4002(7)	7142(3)	3229(3)	45(3)	0.529(7)
C(19C)	3122(6)	7161(3)	4041(3)	44(3)	0.529(7)
C(20C)	3418(4)	6812(2)	4909(3)	31(3)	0.529(7)
C(21C)	4594(4)	6444(2)	4964(3)	44(3)	0.529(7)
C(22C)	4889(5)	6095(3)	5831(4)	28(3)	0.529(7)
C(23C)	4010(6)	6114(3)	6644(3)	40(3)	0.529(7)
N(3C)	2834(5)	6482(3)	6589(3)	23(2)	0.529(7)
C(24C)	2538(4)	6831(2)	5721(3)	28(3)	0.529(7)
C(25C)	1549(5)	7149(3)	5583(5)	112(8)	0.529(7)
Pd(2)	6747(1)	8406(1)	7215(1)	23(1)	1
Cl(2)	7697(2)	7416(1)	7135(1)	51(1)	1
N(1B)	6206(4)	8452(2)	5677(3)	27(1)	1
N(2B)	5497(4)	9208(2)	7426(3)	20(1)	1

C(1B)	6883(7)	7967(3)	5029(4)	42(2)	1
C(2B)	8430(7)	8066(3)	4952(5)	47(2)	1
C(3B)	8785(8)	8716(3)	4605(5)	57(2)	1
C(4B)	8070(7)	9192(3)	5273(5)	51(2)	1
C(5B)	6561(7)	9087(3)	5225(4)	41(2)	1
C(6B)	5701(7)	9618(3)	5659(5)	47(2)	1
C(7B)	5940(6)	9742(2)	6787(4)	33(1)	1
C(8B)	5593(5)	9397(3)	8517(4)	27(1)	1
C(9B)	4488(6)	9860(3)	8837(4)	36(1)	1
C(10B)	3080(6)	9571(3)	8661(4)	34(1)	1
C(11B)	2935(6)	9410(3)	7544(4)	39(2)	1
C(12B)	4044(5)	8979(2)	7174(4)	26(1)	1
C(13B)	3866(6)	8874(3)	6036(4)	39(2)	1
C(14B)	4710(6)	8328(3)	5623(4)	41(2)	1
C(15B)	4209(8)	9464(3)	5442(5)	58(2)	1
C(16B)	8608(2)	7857(1)	11686(1)	56(2)	1
C(17B)	9843(2)	8092(1)	12074(1)	58(2)	1
C(18B)	10653(2)	8471(1)	11475(1)	56(2)	1
C(19B)	10228(2)	8614(1)	10488(1)	53(2)	1
C(20B)	8993(2)	8378(1)	10101(1)	47(2)	1
C(21B)	8183(2)	8000(1)	10700(1)	55(2)	1
C(22B)	6949(2)	7764(1)	10312(1)	60(2)	1
C(23B)	6524(2)	7908(1)	9326(1)	39(2)	1
N(3B)	7334(2)	8286(1)	8727(1)	51(2)	1
C(24B)	8568(2)	8522(1)	9114(1)	57(2)	1
C(25B)	9321(2)	8901(1)	8419(1)	48(2)	1
Sb(1)	4944(1)	4157(1)	8114(1)	33(1)	1
F(1A)	6312(1)	4087(1)	7164(1)	71(1)	1
F(2A)	3580(1)	4233(1)	9068(1)	50(1)	1
F(3A)	5543(1)	4958(1)	8534(1)	101(3)	0.855(6)
F(4A)	6017(1)	3788(1)	9070(1)	95(3)	0.855(6)
F(5A)	4243(1)	3421(1)	7628(1)	63(2)	0.855(6)
F(6A)	3832(1)	4574(1)	7165(1)	84(2)	0.855(6)
F(3AB)	4921(1)	4787(1)	7476(1)	92(12)	0.145(6)
F(4AB)	6618(1)	4393(1)	8911(1)	21(5)	0.145(6)
F(5AB)	5340(1)	3303(1)	8584(1)	32(6)	0.145(6)
F(6AB)	3638(1)	3841(1)	7381(1)	60(9)	0.145(6)
Sb(2)	123(1)	925(1)	6831(1)	41(1)	1
F(1B)	-897(1)	1504(1)	7510(1)	73(1)	1
F(2B)	-506(1)	304(1)	7640(1)	95(2)	1
F(3B)	1205(1)	377(1)	6126(1)	154(3)	1
F(4B)	788(1)	1575(1)	6043(1)	129(3)	1
F(5B)	1567(1)	1043(1)	7771(1)	67(1)	1
F(6B)	-1317(1)	792(1)	5887(1)	59(1)	1

Table A4.5.2 Bond lengths [ $\text{\AA}$ ] and angles [ $^\circ$ ] for **260/261** (CCDC 217276).

Pd(1)-N(3C)	2.072(4)	Pd(2)-N(3B)	2.0771(16)
Pd(1)-N(3A)	2.064(4)	Pd(2)-N(1B)	2.087(4)
Pd(1)-N(1A)	2.072(4)	Pd(2)-N(2B)	2.123(4)
Pd(1)-N(2A)	2.103(4)	Pd(2)-Cl(2)	2.3110(14)
Pd(1)-Cl(1)	2.3056(16)	N(1B)-C(14B)	1.482(7)
N(1A)-C(14A)	1.490(7)	N(1B)-C(1B)	1.506(7)
N(1A)-C(1A)	1.507(7)	N(1B)-C(5B)	1.524(7)
N(1A)-C(5A)	1.518(7)	N(2B)-C(7B)	1.488(6)
N(2A)-C(7A)	1.483(6)	N(2B)-C(8B)	1.496(6)
N(2A)-C(12A)	1.522(6)	N(2B)-C(12B)	1.527(6)
N(2A)-C(8A)	1.520(6)	C(1B)-C(2B)	1.529(9)
C(1A)-C(2A)	1.517(9)	C(2B)-C(3B)	1.504(9)
C(2A)-C(3A)	1.527(8)	C(3B)-C(4B)	1.525(8)
C(3A)-C(4A)	1.524(8)	C(4B)-C(5B)	1.488(9)
C(4A)-C(5A)	1.502(8)	C(5B)-C(6B)	1.530(7)
C(5A)-C(6A)	1.517(8)	C(6B)-C(15B)	1.511(10)
C(6A)-C(15A)	1.505(9)	C(6B)-C(7B)	1.524(8)
C(6A)-C(7A)	1.539(7)	C(8B)-C(9B)	1.529(7)
C(8A)-C(9A)	1.542(7)	C(9B)-C(10B)	1.518(8)
C(9A)-C(10A)	1.516(8)	C(10B)-C(11B)	1.516(8)
C(10A)-C(11A)	1.491(8)	C(11B)-C(12B)	1.509(8)
C(11A)-C(12A)	1.520(7)	C(12B)-C(13B)	1.524(7)
C(12A)-C(13A)	1.517(7)	C(13B)-C(15B)	1.524(9)
C(13A)-C(14A)	1.518(8)	C(13B)-C(14B)	1.534(8)
C(13A)-C(15A)	1.539(8)	C(16B)-C(17B)	1.3900
C(16A)-C(17A)	1.3900	C(16B)-C(21B)	1.3900
C(16A)-C(21A)	1.3900	C(17B)-C(18B)	1.3900
C(17A)-C(18A)	1.3900	C(18B)-C(19B)	1.3900
C(18A)-C(19A)	1.3900	C(19B)-C(20B)	1.3900
C(19A)-C(20A)	1.3900	C(20B)-C(21B)	1.3900
C(20A)-C(21A)	1.3900	C(20B)-C(24B)	1.3900
C(20A)-C(24A)	1.3900	C(21B)-C(22B)	1.3900
C(21A)-C(22A)	1.3900	C(22B)-C(23B)	1.3900
C(22A)-C(23A)	1.3900	C(23B)-N(3B)	1.3900
C(23A)-N(3A)	1.3900	N(3B)-C(24B)	1.3900
N(3A)-C(24A)	1.3900	C(24B)-C(25B)	1.4388
C(24A)-C(25A)	1.4263	Sb(1)-F(3AB)	1.5859
C(16C)-C(17C)	1.3900	Sb(1)-F(6AB)	1.7176
C(16C)-C(21C)	1.3900	Sb(1)-F(4A)	1.8007
C(17C)-C(18C)	1.3900	Sb(1)-F(5A)	1.8233
C(18C)-C(19C)	1.3900	Sb(1)-F(1A)	1.8592
C(19C)-C(20C)	1.3900	Sb(1)-F(2A)	1.8610
C(20C)-C(21C)	1.3900	Sb(1)-F(6A)	1.8622
C(20C)-C(24C)	1.3900	Sb(1)-F(3A)	1.8852
C(21C)-C(22C)	1.3900	Sb(1)-F(5AB)	1.9618
C(22C)-C(23C)	1.3900	Sb(1)-F(4AB)	1.9850
C(23C)-N(3C)	1.3900	Sb(2)-F(2B)	1.8187
N(3C)-C(24C)	1.3900	Sb(2)-F(1B)	1.8327
C(24C)-C(25C)	1.1893	Sb(2)-F(3B)	1.8431

Sb(2)-F(4B)	1.8601	C(19A)-C(20A)-C(21A)	120.0
Sb(2)-F(5B)	1.8697	C(19A)-C(20A)-C(24A)	120.0
Sb(2)-F(6B)	1.8748	C(21A)-C(20A)-C(24A)	120.0
		C(22A)-C(21A)-C(20A)	120.0
N(3C)-Pd(1)-N(3A)	20.57(18)	C(22A)-C(21A)-C(16A)	120.0
N(3C)-Pd(1)-N(1A)	166.55(19)	C(20A)-C(21A)-C(16A)	120.0
N(3A)-Pd(1)-N(1A)	171.34(19)	C(21A)-C(22A)-C(23A)	120.0
N(3C)-Pd(1)-N(2A)	93.84(19)	N(3A)-C(23A)-C(22A)	120.0
N(3A)-Pd(1)-N(2A)	97.07(19)	C(23A)-N(3A)-C(24A)	120.0
N(1A)-Pd(1)-N(2A)	87.97(16)	C(23A)-N(3A)-Pd(1)	120.6(2)
N(3C)-Pd(1)-Cl(1)	86.08(16)	C(24A)-N(3A)-Pd(1)	119.1(2)
N(3A)-Pd(1)-Cl(1)	78.75(16)	N(3A)-C(24A)-C(20A)	120.0
N(1A)-Pd(1)-Cl(1)	94.91(13)	N(3A)-C(24A)-C(25A)	117.0
N(2A)-Pd(1)-Cl(1)	167.96(13)	C(20A)-C(24A)-C(25A)	122.8
C(14A)-N(1A)-C(1A)	106.2(4)	C(17C)-C(16C)-C(21C)	120.0
C(14A)-N(1A)-C(5A)	110.4(4)	C(18C)-C(17C)-C(16C)	120.0
C(1A)-N(1A)-C(5A)	106.3(4)	C(17C)-C(18C)-C(19C)	120.0
C(14A)-N(1A)-Pd(1)	105.8(3)	C(18C)-C(19C)-C(20C)	120.0
C(1A)-N(1A)-Pd(1)	115.9(3)	C(19C)-C(20C)-C(21C)	120.0
C(5A)-N(1A)-Pd(1)	112.1(3)	C(19C)-C(20C)-C(24C)	120.0
C(7A)-N(2A)-C(12A)	112.5(4)	C(21C)-C(20C)-C(24C)	120.0
C(7A)-N(2A)-C(8A)	108.4(4)	C(22C)-C(21C)-C(20C)	120.0
C(12A)-N(2A)-C(8A)	109.8(4)	C(22C)-C(21C)-C(16C)	120.0
C(7A)-N(2A)-Pd(1)	112.5(3)	C(20C)-C(21C)-C(16C)	120.0
C(12A)-N(2A)-Pd(1)	104.1(3)	C(23C)-C(22C)-C(21C)	120.0
C(8A)-N(2A)-Pd(1)	109.5(3)	C(22C)-C(23C)-N(3C)	120.0
N(1A)-C(1A)-C(2A)	112.7(5)	C(24C)-N(3C)-C(23C)	120.0
C(3A)-C(2A)-C(1A)	113.5(5)	C(24C)-N(3C)-Pd(1)	123.8(2)
C(2A)-C(3A)-C(4A)	108.4(5)	C(23C)-N(3C)-Pd(1)	115.2(2)
C(5A)-C(4A)-C(3A)	111.6(5)	C(25C)-C(24C)-N(3C)	125.6
C(4A)-C(5A)-N(1A)	110.3(4)	C(25C)-C(24C)-C(20C)	114.3
C(4A)-C(5A)-C(6A)	115.8(5)	N(3C)-C(24C)-C(20C)	120.0
N(1A)-C(5A)-C(6A)	113.0(4)	N(3B)-Pd(2)-N(1B)	175.35(13)
C(15A)-C(6A)-C(5A)	109.5(5)	N(3B)-Pd(2)-N(2B)	96.85(11)
C(15A)-C(6A)-C(7A)	109.8(5)	N(1B)-Pd(2)-N(2B)	87.58(16)
C(5A)-C(6A)-C(7A)	114.2(5)	N(3B)-Pd(2)-Cl(2)	80.21(6)
N(2A)-C(7A)-C(6A)	112.2(4)	N(1B)-Pd(2)-Cl(2)	95.16(13)
N(2A)-C(8A)-C(9A)	114.0(4)	N(2B)-Pd(2)-Cl(2)	167.22(12)
C(10A)-C(9A)-C(8A)	109.7(5)	C(14B)-N(1B)-C(1B)	107.2(4)
C(11A)-C(10A)-C(9A)	107.9(5)	C(14B)-N(1B)-C(5B)	111.9(4)
C(10A)-C(11A)-C(12A)	115.0(5)	C(1B)-N(1B)-C(5B)	106.4(4)
C(13A)-C(12A)-C(11A)	110.9(4)	C(14B)-N(1B)-Pd(2)	105.2(3)
C(13A)-C(12A)-N(2A)	111.0(4)	C(1B)-N(1B)-Pd(2)	114.6(3)
C(11A)-C(12A)-N(2A)	113.5(4)	C(5B)-N(1B)-Pd(2)	111.6(3)
C(14A)-C(13A)-C(12A)	115.5(5)	C(7B)-N(2B)-C(8B)	109.0(4)
C(14A)-C(13A)-C(15A)	109.5(5)	C(7B)-N(2B)-C(12B)	113.8(4)
C(12A)-C(13A)-C(15A)	110.0(5)	C(8B)-N(2B)-C(12B)	109.3(4)
N(1A)-C(14A)-C(13A)	112.3(5)	C(7B)-N(2B)-Pd(2)	111.6(3)
C(6A)-C(15A)-C(13A)	106.1(5)	C(8B)-N(2B)-Pd(2)	108.7(3)
C(17A)-C(16A)-C(21A)	120.0	C(12B)-N(2B)-Pd(2)	104.2(3)
C(18A)-C(17A)-C(16A)	120.0	N(1B)-C(1B)-C(2B)	112.9(5)
C(17A)-C(18A)-C(19A)	120.0	C(3B)-C(2B)-C(1B)	112.5(5)
C(20A)-C(19A)-C(18A)	120.0	C(2B)-C(3B)-C(4B)	109.0(5)

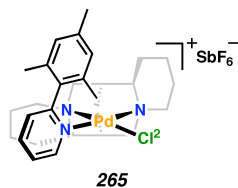
C(5B)-C(4B)-C(3B)	110.0(6)	F(6AB)-Sb(1)-F(2A)	83.3
C(4B)-C(5B)-N(1B)	110.6(4)	F(4A)-Sb(1)-F(2A)	88.7
C(4B)-C(5B)-C(6B)	115.1(6)	F(5A)-Sb(1)-F(2A)	92.6
N(1B)-C(5B)-C(6B)	112.4(4)	F(1A)-Sb(1)-F(2A)	179.5
C(15B)-C(6B)-C(7B)	110.3(5)	F(3AB)-Sb(1)-F(6A)	40.4
C(15B)-C(6B)-C(5B)	107.6(6)	F(6AB)-Sb(1)-F(6A)	53.0
C(7B)-C(6B)-C(5B)	115.0(5)	F(4A)-Sb(1)-F(6A)	177.2
N(2B)-C(7B)-C(6B)	112.3(4)	F(5A)-Sb(1)-F(6A)	88.2
N(2B)-C(8B)-C(9B)	114.4(4)	F(1A)-Sb(1)-F(6A)	90.0
C(10B)-C(9B)-C(8B)	109.6(5)	F(2A)-Sb(1)-F(6A)	90.0
C(11B)-C(10B)-C(9B)	107.6(4)	F(3AB)-Sb(1)-F(3A)	52.2
C(12B)-C(11B)-C(10B)	113.7(5)	F(6AB)-Sb(1)-F(3A)	137.9
C(11B)-C(12B)-N(2B)	113.8(4)	F(4A)-Sb(1)-F(3A)	91.2
C(11B)-C(12B)-C(13B)	110.1(4)	F(5A)-Sb(1)-F(3A)	174.5
N(2B)-C(12B)-C(13B)	110.1(4)	F(1A)-Sb(1)-F(3A)	92.8
C(15B)-C(13B)-C(12B)	111.3(5)	F(2A)-Sb(1)-F(3A)	86.8
C(15B)-C(13B)-C(14B)	108.5(5)	F(6A)-Sb(1)-F(3A)	86.3
C(12B)-C(13B)-C(14B)	114.4(5)	F(3AB)-Sb(1)-F(5AB)	162.9
N(1B)-C(14B)-C(13B)	112.6(5)	F(6AB)-Sb(1)-F(5AB)	87.2
C(6B)-C(15B)-C(13B)	107.8(5)	F(4A)-Sb(1)-F(5AB)	42.7
C(17B)-C(16B)-C(21B)	120.0	F(5A)-Sb(1)-F(5AB)	51.6
C(18B)-C(17B)-C(16B)	120.0	F(1A)-Sb(1)-F(5AB)	90.0
C(17B)-C(18B)-C(19B)	120.0	F(2A)-Sb(1)-F(5AB)	90.3
C(18B)-C(19B)-C(20B)	120.0	F(6A)-Sb(1)-F(5AB)	139.8
C(21B)-C(20B)-C(19B)	120.0	F(3A)-Sb(1)-F(5AB)	133.8
C(21B)-C(20B)-C(24B)	120.0	F(3AB)-Sb(1)-F(4AB)	93.8
C(19B)-C(20B)-C(24B)	120.0	F(6AB)-Sb(1)-F(4AB)	170.5
C(22B)-C(21B)-C(20B)	120.0	F(4A)-Sb(1)-F(4AB)	44.3
C(22B)-C(21B)-C(16B)	120.0	F(5A)-Sb(1)-F(4AB)	134.5
C(20B)-C(21B)-C(16B)	120.0	F(1A)-Sb(1)-F(4AB)	77.5
C(21B)-C(22B)-C(23B)	120.0	F(2A)-Sb(1)-F(4AB)	102.2
N(3B)-C(23B)-C(22B)	120.0	F(6A)-Sb(1)-F(4AB)	133.9
C(24B)-N(3B)-C(23B)	120.0	F(3A)-Sb(1)-F(4AB)	50.9
C(24B)-N(3B)-Pd(2)	121.60(5)	F(5AB)-Sb(1)-F(4AB)	85.1
C(23B)-N(3B)-Pd(2)	118.1	F(2B)-Sb(2)-F(1B)	90.6
N(3B)-C(24B)-C(20B)	120.0	F(2B)-Sb(2)-F(3B)	92.2
N(3B)-C(24B)-C(25B)	114.8	F(1B)-Sb(2)-F(3B)	177.0
C(20B)-C(24B)-C(25B)	125.2	F(2B)-Sb(2)-F(4B)	178.1
F(3AB)-Sb(1)-F(6AB)	92.0	F(1B)-Sb(2)-F(4B)	88.4
F(3AB)-Sb(1)-F(4A)	138.0	F(3B)-Sb(2)-F(4B)	88.8
F(6AB)-Sb(1)-F(4A)	129.2	F(2B)-Sb(2)-F(5B)	88.2
F(3AB)-Sb(1)-F(5A)	122.9	F(1B)-Sb(2)-F(5B)	89.7
F(6AB)-Sb(1)-F(5A)	36.6	F(3B)-Sb(2)-F(5B)	89.3
F(4A)-Sb(1)-F(5A)	94.3	F(4B)-Sb(2)-F(5B)	90.2
F(3AB)-Sb(1)-F(1A)	73.2	F(2B)-Sb(2)-F(6B)	91.2
F(6AB)-Sb(1)-F(1A)	97.1	F(1B)-Sb(2)-F(6B)	91.2
F(4A)-Sb(1)-F(1A)	91.3	F(3B)-Sb(2)-F(6B)	89.8
F(5A)-Sb(1)-F(1A)	87.9	F(4B)-Sb(2)-F(6B)	90.4
F(3AB)-Sb(1)-F(2A)	106.5	F(5B)-Sb(2)-F(6B)	179.0



**APPENDIX 4.6**

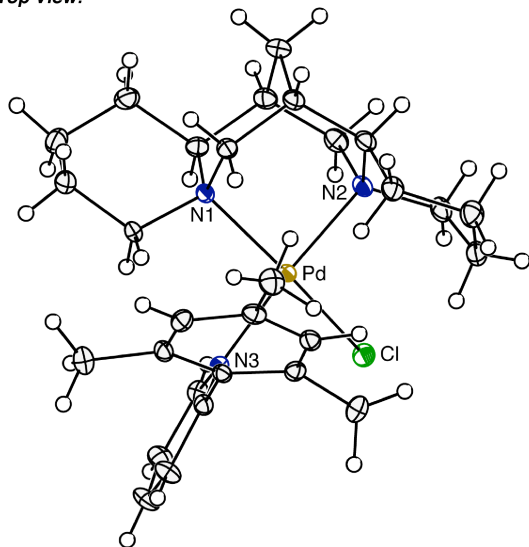
*X-ray Crystallographic Data for (sp)Pd(2-mesitylpyridine)Cl<sup>+</sup>SbF<sub>6</sub><sup>-</sup> (265)*

Figure A4.6.1 (sp)Pd(2-mesitylpyridine)Cl<sup>+</sup>SbF<sub>6</sub><sup>-</sup> (265).<sup>1,2</sup>

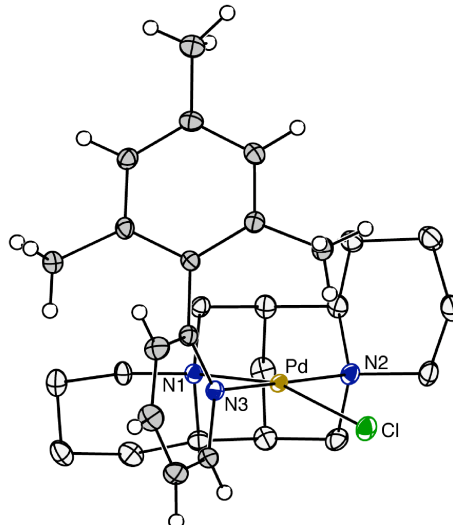


Selected bond lengths (Å) and angles (°)	
Pd–N1	2.1326(14)
Pd–N2	2.0914(14)
Pd–N3	2.0809(13)
Pd–Cl	2.3345(4)
N1–Pd–N2	87.48(5)°
N3–Pd–Cl	82.53(4)°
N2–Pd–N3	175.42(5)°
N1–Pd–Cl	163.51(4)°

Top View:



Side View:



<sup>1</sup> (a) The numbering shown in Figure A4.6.1 does not match that in the crystallographic report. (b) The SbF<sub>6</sub> anion in both views and the hydrogen atoms of the sparteine backbone of the side view are not shown.

<sup>2</sup> The crystallographic data have been deposited at the Cambridge Database (CCDC), 12 Union Road, Cambridge CB2 1EZ, UK and copies can be obtained on request, free of charge, by quoting the publication citation and the deposition number 215758.

*Crystal data and structure refinement for 265 (CCDC 217276).*

Empirical formula	[C <sub>29</sub> H <sub>41</sub> N <sub>3</sub> ClPd] <sup>+</sup> [SbF <sub>6</sub> ] <sup>-</sup>
Formula weight	809.25
Crystallization solvent	Acetone/pentane
Crystal Habit	Block
Crystal size	0.30 x 0.30 x 0.26 mm <sup>3</sup>
Crystal color	Clear

#### *Data collection*

Preliminary photos	Rotation
Type of diffractometer	Bruker SMART 1000
Wavelength	0.71073 Å MoKα
Data collection temperature	100(2) K
θ range for 41762 reflections used in lattice determination	2.27 to 40.10°
Unit cell dimensions	a = 12.3773(2) Å b = 13.1425(2) Å c = 18.7060(3) Å
Volume	3042.88(8) Å <sup>3</sup>
Z	4
Crystal system	Orthorhombic
Space group	P2 <sub>1</sub> 2 <sub>1</sub> 2 <sub>1</sub>
Density (calculated)	1.766 Mg/m <sup>3</sup>
F(000)	1616
Data collection program	Bruker SMART v5.054
θ range for data collection	1.89 to 40.43°
Completeness to θ = 40.43°	96.5 %
Index ranges	-22 ≤ h ≤ 22, -22 ≤ k ≤ 23, -33 ≤ l ≤ 32
Data collection scan type	ω scans at 3 φ settings each for two 2θ settings
Data reduction program	Bruker SAINT v6.022
Reflections collected	77220
Independent reflections	18496 [R <sub>int</sub> = 0.0639]
Absorption coefficient	1.628 mm <sup>-1</sup>
Absorption correction	None
Max. and min. transmission (predicted)	0.6769 and 0.6409

#### *Structure solution and refinement*

Structure solution program	SHELXS-97 (Sheldrick, 1990)
Primary solution method	Direct methods
Secondary solution method	Difference Fourier map
Hydrogen placement	Difference Fourier map
Structure refinement program	SHELXL-97 (Sheldrick, 1997)
Refinement method	Full matrix least-squares on F <sup>2</sup>
Data / restraints / parameters	18496 / 0 / 534
Treatment of hydrogen atoms	Unrestrained
Goodness-of-fit on F <sup>2</sup>	1.165
Final R indices [I>2σ(I), 15330 reflections]	R1 = 0.0313, wR2 = 0.0489
R indices (all data)	R1 = 0.0450, wR2 = 0.0507
Type of weighting scheme used	Sigma
Weighting scheme used	w=1/σ <sup>2</sup> (Fo <sup>2</sup> )
Max shift/error	0.003

Average shift/error	0.000
Absolute structure parameter	-0.036(8)
Largest diff. peak and hole	2.104 and -0.833 e. $\text{\AA}^{-3}$

*Special refinement details*

All peaks in the final difference Fourier map greater than  $1\text{e}/\text{\AA}^3$  are within  $1\text{\AA}$  of either Pd or Sb.

Refinement of  $F^2$  against ALL reflections. The weighted R-factor ( $wR$ ) and goodness of fit (S) are based on  $F^2$ , conventional R-factors (R) are based on F, with F set to zero for negative  $F^2$ . The threshold expression of  $F^2 > 2\sigma(F^2)$  is used only for calculating R-factors(gt) etc. and is not relevant to the choice of reflections for refinement. R-factors based on  $F^2$  are statistically about twice as large as those based on F, and R-factors based on ALL data will be even larger.

All esds (except the esd in the dihedral angle between two l.s. planes) are estimated using the full covariance matrix. The cell esds are taken into account individually in the estimation of esds in distances, angles and torsion angles; correlations between esds in cell parameters are only used when they are defined by crystal symmetry. An approximate (isotropic) treatment of cell esds is used for estimating esds involving l.s. planes.

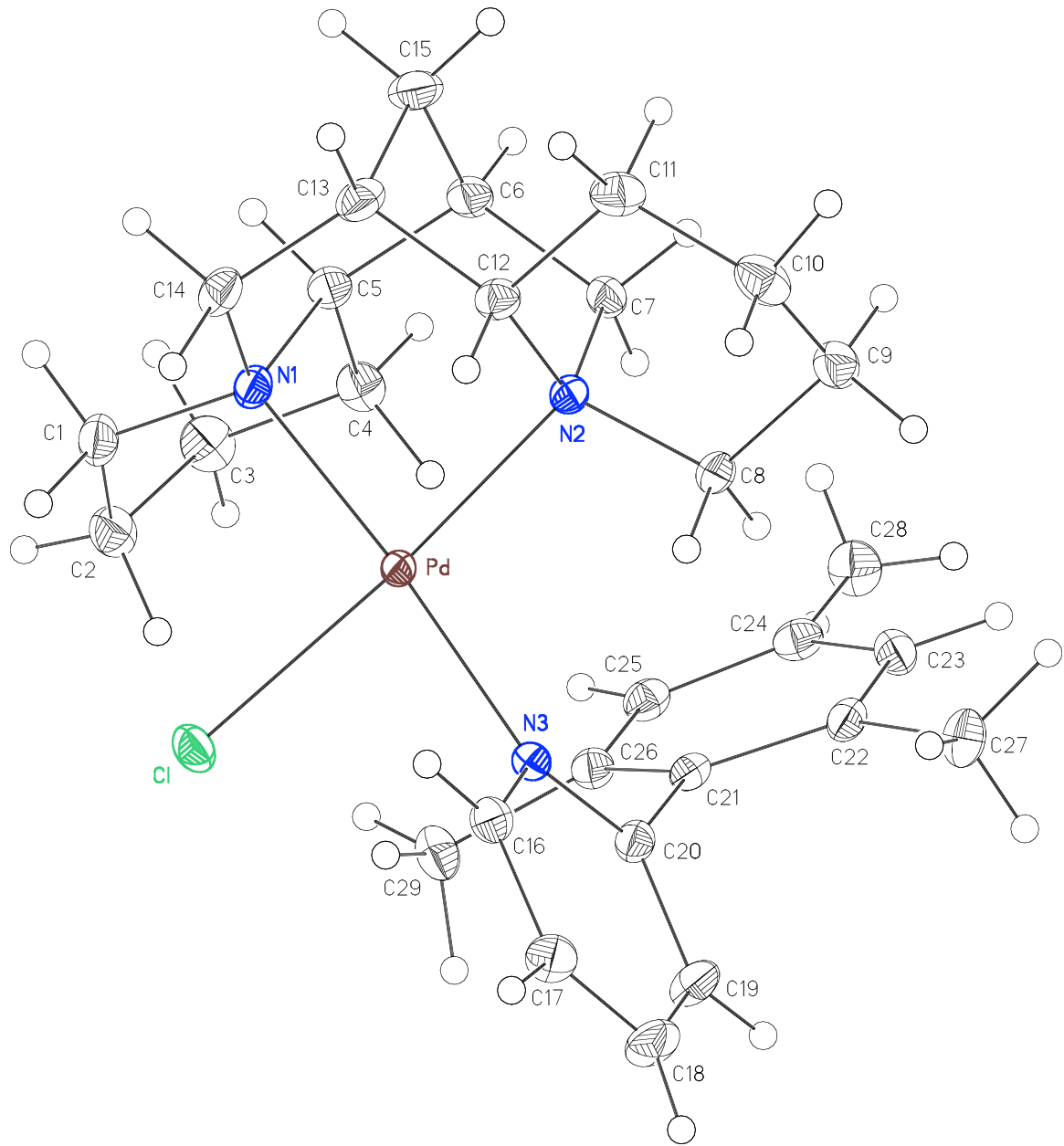


Figure A4.6.2 Molecule of **265**.

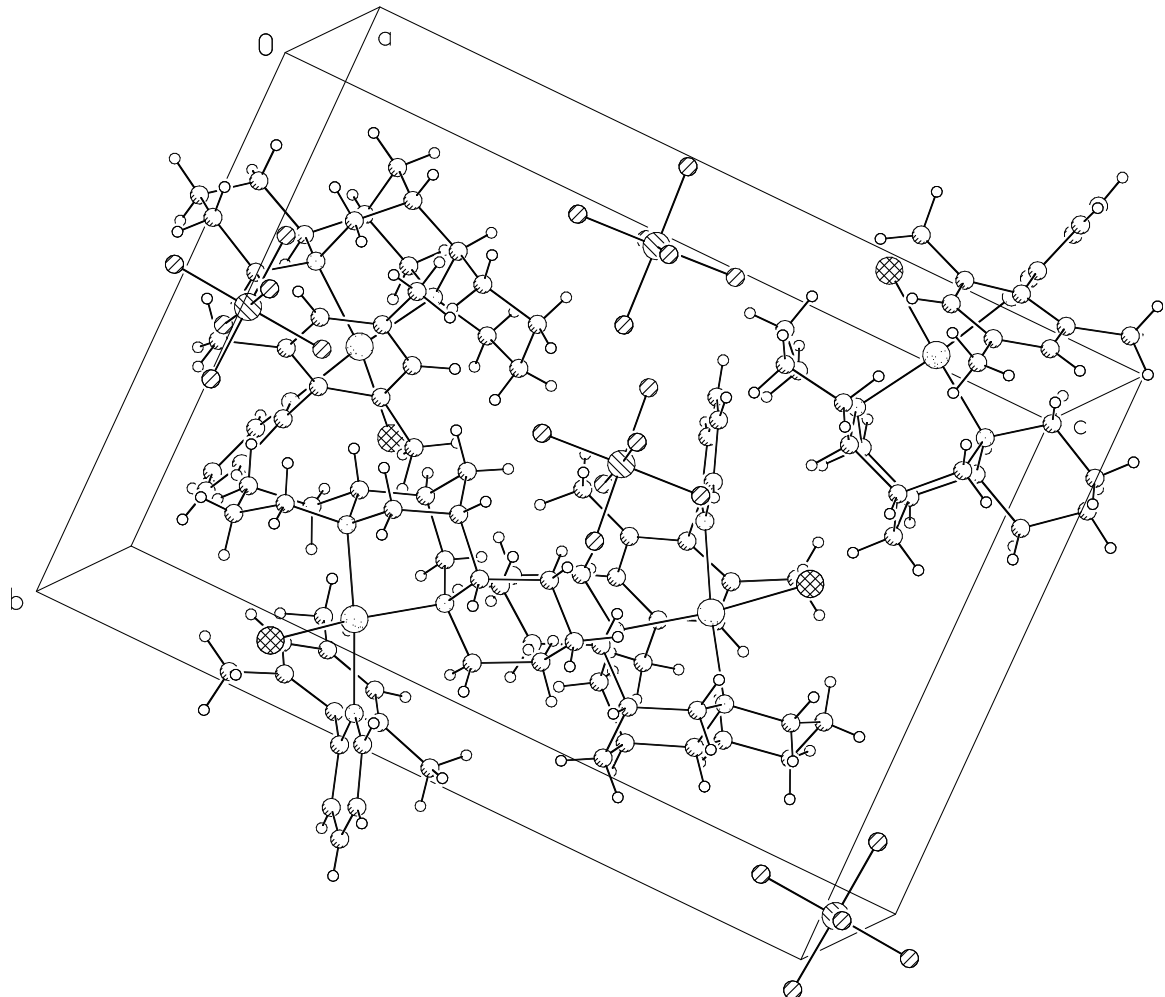


Figure A4.6.3 Unit cell contents of **265**.

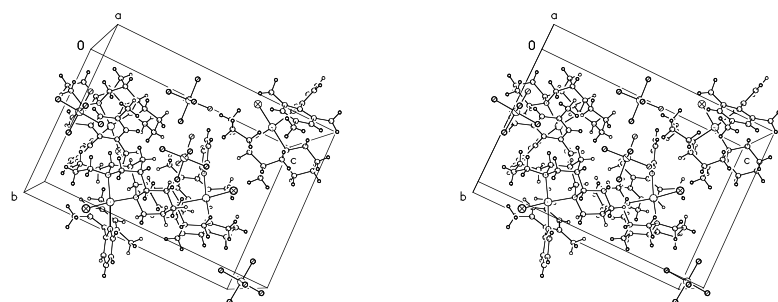


Figure A4.6.4 Stereo view of unit cell contents of **265**.

Table A4.6.1 Atomic coordinates ( $\times 10^4$ ) and equivalent isotropic displacement parameters ( $\text{\AA}^2 \times 10^3$ ) for **265** (CCDC 215758).  $U(\text{eq})$  is defined as the trace of the orthogonalized  $U^{ij}$  tensor.

	x	y	z	$U_{\text{eq}}$	Occ
Pd		7977(1)	9200(1)	2910(1)	10(1)
Cl		8780(1)	10248(1)	2054(1)	18(1)
N(1)		8300(1)	7866(1)	2338(1)	14(1)
N(2)		7698(1)	8262(1)	3822(1)	12(1)
N(3)		7646(1)	10586(1)	3401(1)	12(1)
C(1)		8532(2)	8028(2)	1554(1)	19(1)
C(2)		7571(2)	8421(2)	1130(1)	20(1)
C(3)		6574(2)	7756(2)	1229(1)	22(1)
C(4)		6378(1)	7573(1)	2025(1)	18(1)
C(5)		7371(1)	7116(1)	2374(1)	16(1)
C(6)		7197(1)	6700(1)	3124(1)	16(1)
C(7)		6853(1)	7483(1)	3677(1)	14(1)
C(8)		7347(1)	8917(1)	4438(1)	14(1)
C(9)		7344(1)	8399(1)	5168(1)	19(1)
C(10)		8471(2)	8001(2)	5335(1)	21(1)
C(11)		8835(2)	7301(1)	4739(1)	20(1)
C(12)		8785(1)	7789(1)	3989(1)	15(1)
C(13)		9104(1)	7003(1)	3420(1)	17(1)
C(14)		9294(1)	7433(1)	2678(1)	18(1)
C(15)		8234(2)	6168(1)	3368(1)	20(1)
C(16)		8539(1)	11119(1)	3575(1)	15(1)
C(17)		8500(2)	12106(1)	3823(1)	19(1)
C(18)		7512(2)	12579(2)	3875(1)	21(1)
C(19)		6591(2)	12036(1)	3703(1)	19(1)
C(20)		6668(1)	11035(1)	3475(1)	14(1)
C(21)		5660(1)	10427(1)	3337(1)	12(1)
C(22)		4994(1)	10172(1)	3923(1)	14(1)
C(23)		4067(1)	9586(1)	3788(1)	16(1)
C(24)		3775(1)	9282(1)	3107(1)	16(1)
C(25)		4421(1)	9595(1)	2536(1)	15(1)
C(26)		5344(1)	10178(1)	2639(1)	14(1)
C(27)		5200(1)	10522(2)	4674(1)	19(1)
C(28)		2766(1)	8665(2)	2979(1)	21(1)
C(29)		5902(1)	10624(2)	1993(1)	19(1)
Sb		6064(1)	4630(1)	5153(1)	16(1)
F(1)		4576(1)	4858(1)	5179(1)	35(1)
F(2)		6099(1)	4534(1)	6155(1)	25(1)
F(3)		7550(1)	4388(1)	5096(1)	30(1)
F(4)		6037(1)	4736(1)	4153(1)	31(1)
F(5)		5796(1)	3231(1)	5090(1)	24(1)
F(6)		6316(1)	6030(1)	5228(1)	40(1)

*Table A4.6.2 Selected bond lengths [ $\text{\AA}$ ] and angles [ $^\circ$ ] for **265** (CCDC 215758).*

Pd-N(3)	2.0809(13)	N(3)-Pd-N(1)	175.42(5)
Pd-N(1)	2.0914(14)	N(3)-Pd-N(2)	96.95(5)
Pd-N(2)	2.1326(14)	N(1)-Pd-N(2)	87.48(5)
Pd-Cl	2.3345(4)	N(3)-Pd-Cl	82.53(4)
		N(1)-Pd-Cl	93.56(4)
		N(2)-Pd-Cl	163.51(4)

*Table A4.6.3 Bond lengths [ $\text{\AA}$ ] and angles [ $^\circ$ ] for **265** (CCDC 215758).*

Pd-N(3)	2.0809(13)	C(9)-H(9B)	0.92(2)
Pd-N(1)	2.0914(14)	C(10)-C(11)	1.515(3)
Pd-N(2)	2.1326(14)	C(10)-H(10A)	0.82(2)
Pd-Cl	2.3345(4)	C(10)-H(10B)	0.96(2)
N(1)-C(14)	1.497(2)	C(11)-C(12)	1.544(2)
N(1)-C(1)	1.509(2)	C(11)-H(11A)	1.00(2)
N(1)-C(5)	1.517(2)	C(11)-H(11B)	0.98(2)
N(2)-C(7)	1.488(2)	C(12)-C(13)	1.535(2)
N(2)-C(8)	1.503(2)	C(12)-H(12)	0.92(2)
N(2)-C(12)	1.515(2)	C(13)-C(14)	1.516(3)
N(3)-C(16)	1.348(2)	C(13)-C(15)	1.540(3)
N(3)-C(20)	1.355(2)	C(13)-H(13)	0.956(18)
C(1)-C(2)	1.519(3)	C(14)-H(14A)	1.00(2)
C(1)-H(1A)	0.92(2)	C(14)-H(14B)	0.97(2)
C(1)-H(1B)	1.01(2)	C(15)-H(15A)	0.93(2)
C(2)-C(3)	1.524(3)	C(15)-H(15B)	0.96(2)
C(2)-H(2A)	0.94(2)	C(16)-C(17)	1.379(2)
C(2)-H(2B)	0.85(2)	C(16)-H(16)	0.877(19)
C(3)-C(4)	1.528(3)	C(17)-C(18)	1.375(3)
C(3)-H(3A)	0.92(2)	C(17)-H(17)	0.93(3)
C(3)-H(3B)	0.95(2)	C(18)-C(19)	1.383(3)
C(4)-C(5)	1.515(2)	C(18)-H(18)	0.83(2)
C(4)-H(4A)	0.97(2)	C(19)-C(20)	1.385(2)
C(4)-H(4B)	0.91(2)	C(19)-H(19)	0.89(2)
C(5)-C(6)	1.522(2)	C(20)-C(21)	1.503(2)
C(5)-H(5)	0.95(2)	C(21)-C(26)	1.401(2)
C(6)-C(7)	1.518(2)	C(21)-C(22)	1.413(2)
C(6)-C(15)	1.531(2)	C(22)-C(23)	1.404(2)
C(6)-H(6)	0.99(2)	C(22)-C(27)	1.499(2)
C(7)-H(7A)	0.85(2)	C(23)-C(24)	1.384(2)
C(7)-H(7B)	0.891(19)	C(23)-H(23)	0.94(2)
C(8)-C(9)	1.526(3)	C(24)-C(25)	1.396(2)
C(8)-H(8A)	0.937(18)	C(24)-C(28)	1.508(2)
C(8)-H(8B)	0.93(2)	C(25)-C(26)	1.389(2)
C(9)-C(10)	1.522(3)	C(25)-H(25)	0.95(2)
C(9)-H(9A)	0.89(2)	C(26)-C(29)	1.511(2)

C(27)-H(27A)	0.91(2)	C(4)-C(3)-H(3B)	111.7(14)
C(27)-H(27B)	1.03(3)	H(3A)-C(3)-H(3B)	113.6(19)
C(27)-H(27C)	0.94(3)	C(5)-C(4)-C(3)	110.71(15)
C(28)-H(28A)	0.85(2)	C(5)-C(4)-H(4A)	113.7(12)
C(28)-H(28B)	1.02(3)	C(3)-C(4)-H(4A)	110.0(12)
C(28)-H(28C)	0.85(3)	C(5)-C(4)-H(4B)	106.8(13)
C(29)-H(29A)	0.94(2)	C(3)-C(4)-H(4B)	113.5(15)
C(29)-H(29B)	0.85(2)	H(4A)-C(4)-H(4B)	101.8(18)
C(29)-H(29C)	1.01(3)	N(1)-C(5)-C(4)	109.80(14)
Sb-F(1)	1.8662(11)	N(1)-C(5)-C(6)	112.37(14)
Sb-F(3)	1.8697(10)	C(4)-C(5)-C(6)	115.16(14)
Sb-F(5)	1.8716(11)	N(1)-C(5)-H(5)	104.1(12)
Sb-F(6)	1.8720(12)	C(4)-C(5)-H(5)	108.3(12)
Sb-F(4)	1.8753(10)	C(6)-C(5)-H(5)	106.3(13)
Sb-F(2)	1.8794(10)	C(7)-C(6)-C(5)	115.08(14)
		C(7)-C(6)-C(15)	110.01(14)
N(3)-Pd-N(1)	175.42(5)	C(5)-C(6)-C(15)	108.66(14)
N(3)-Pd-N(2)	96.95(5)	C(7)-C(6)-H(6)	103.4(13)
N(1)-Pd-N(2)	87.48(5)	C(5)-C(6)-H(6)	105.0(14)
N(3)-Pd-Cl	82.53(4)	C(15)-C(6)-H(6)	114.7(13)
N(1)-Pd-Cl	93.56(4)	N(2)-C(7)-C(6)	113.19(13)
N(2)-Pd-Cl	163.51(4)	N(2)-C(7)-H(7A)	104.5(13)
C(14)-N(1)-C(1)	108.07(13)	C(6)-C(7)-H(7A)	112.2(14)
C(14)-N(1)-C(5)	110.91(13)	N(2)-C(7)-H(7B)	112.7(12)
C(1)-N(1)-C(5)	106.14(13)	C(6)-C(7)-H(7B)	107.3(12)
C(14)-N(1)-Pd	105.02(10)	H(7A)-C(7)-H(7B)	106.9(17)
C(1)-N(1)-Pd	114.53(11)	N(2)-C(8)-C(9)	115.59(14)
C(5)-N(1)-Pd	112.17(10)	N(2)-C(8)-H(8A)	105.7(12)
C(7)-N(2)-C(8)	109.35(12)	C(9)-C(8)-H(8A)	112.1(11)
C(7)-N(2)-C(12)	112.26(13)	N(2)-C(8)-H(8B)	107.6(13)
C(8)-N(2)-C(12)	109.49(12)	C(9)-C(8)-H(8B)	109.3(13)
C(7)-N(2)-Pd	111.44(10)	H(8A)-C(8)-H(8B)	106.0(17)
C(8)-N(2)-Pd	109.25(10)	C(10)-C(9)-C(8)	109.59(15)
C(12)-N(2)-Pd	104.94(9)	C(10)-C(9)-H(9A)	111.0(15)
C(16)-N(3)-C(20)	118.76(14)	C(8)-C(9)-H(9A)	116.2(16)
C(16)-N(3)-Pd	113.61(11)	C(10)-C(9)-H(9B)	108.7(13)
C(20)-N(3)-Pd	127.09(11)	C(8)-C(9)-H(9B)	105.6(14)
N(1)-C(1)-C(2)	113.97(14)	H(9A)-C(9)-H(9B)	105(2)
N(1)-C(1)-H(1A)	108.7(14)	C(11)-C(10)-C(9)	109.29(15)
C(2)-C(1)-H(1A)	110.3(14)	C(11)-C(10)-H(10A)	109.7(16)
N(1)-C(1)-H(1B)	110.8(12)	C(9)-C(10)-H(10A)	110.8(15)
C(2)-C(1)-H(1B)	109.5(11)	C(11)-C(10)-H(10B)	106.5(12)
H(1A)-C(1)-H(1B)	103.0(17)	C(9)-C(10)-H(10B)	115.7(11)
C(1)-C(2)-C(3)	112.13(16)	H(10A)-C(10)-H(10B)	104.6(19)
C(1)-C(2)-H(2A)	112.8(14)	C(10)-C(11)-C(12)	113.93(15)
C(3)-C(2)-H(2A)	109.0(13)	C(10)-C(11)-H(11A)	104.6(14)
C(1)-C(2)-H(2B)	111.1(14)	C(12)-C(11)-H(11A)	110.5(14)
C(3)-C(2)-H(2B)	107.0(15)	C(10)-C(11)-H(11B)	111.5(13)
H(2A)-C(2)-H(2B)	104(2)	C(12)-C(11)-H(11B)	106.4(13)
C(2)-C(3)-C(4)	109.62(15)	H(11A)-C(11)-H(11B)	110.0(17)
C(2)-C(3)-H(3A)	110.2(14)	N(2)-C(12)-C(13)	111.18(13)
C(4)-C(3)-H(3A)	104.5(14)	N(2)-C(12)-C(11)	113.15(14)
C(2)-C(3)-H(3B)	107.3(14)	C(13)-C(12)-C(11)	109.96(14)

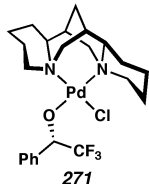
N(2)-C(12)-H(12)	106.5(12)	C(22)-C(23)-H(23)	116.8(14)
C(13)-C(12)-H(12)	111.6(13)	C(23)-C(24)-C(25)	118.05(15)
C(11)-C(12)-H(12)	104.2(13)	C(23)-C(24)-C(28)	121.12(16)
C(14)-C(13)-C(12)	115.11(15)	C(25)-C(24)-C(28)	120.79(16)
C(14)-C(13)-C(15)	108.42(15)	C(26)-C(25)-C(24)	121.77(15)
C(12)-C(13)-C(15)	110.11(14)	C(26)-C(25)-H(25)	121.5(12)
C(14)-C(13)-H(13)	109.8(11)	C(24)-C(25)-H(25)	116.7(12)
C(12)-C(13)-H(13)	104.7(11)	C(25)-C(26)-C(21)	119.29(15)
C(15)-C(13)-H(13)	108.4(11)	C(25)-C(26)-C(29)	118.55(15)
N(1)-C(14)-C(13)	113.76(13)	C(21)-C(26)-C(29)	121.77(15)
N(1)-C(14)-H(14A)	105.3(12)	C(22)-C(27)-H(27A)	118.7(16)
C(13)-C(14)-H(14A)	116.2(12)	C(22)-C(27)-H(27B)	109.5(13)
N(1)-C(14)-H(14B)	105.3(11)	H(27A)-C(27)-H(27B)	111(2)
C(13)-C(14)-H(14B)	110.3(11)	C(22)-C(27)-H(27C)	112.9(16)
H(14A)-C(14)-H(14B)	105.2(16)	H(27A)-C(27)-H(27C)	102(2)
C(6)-C(15)-C(13)	106.20(14)	H(27B)-C(27)-H(27C)	100.9(19)
C(6)-C(15)-H(15A)	115.2(13)	C(24)-C(28)-H(28A)	115.3(15)
C(13)-C(15)-H(15A)	109.7(13)	C(24)-C(28)-H(28B)	113.5(17)
C(6)-C(15)-H(15B)	110.4(11)	H(28A)-C(28)-H(28B)	99(2)
C(13)-C(15)-H(15B)	111.2(11)	C(24)-C(28)-H(28C)	113.1(16)
H(15A)-C(15)-H(15B)	104.1(17)	H(28A)-C(28)-H(28C)	104(2)
N(3)-C(16)-C(17)	122.84(16)	H(28B)-C(28)-H(28C)	111(2)
N(3)-C(16)-H(16)	116.9(13)	C(26)-C(29)-H(29A)	114.8(13)
C(17)-C(16)-H(16)	120.2(13)	C(26)-C(29)-H(29B)	116.7(15)
C(18)-C(17)-C(16)	118.69(16)	H(29A)-C(29)-H(29B)	105.0(18)
C(18)-C(17)-H(17)	125.7(16)	C(26)-C(29)-H(29C)	110.5(17)
C(16)-C(17)-H(17)	115.4(16)	H(29A)-C(29)-H(29C)	111(2)
C(17)-C(18)-C(19)	118.84(17)	H(29B)-C(29)-H(29C)	97(2)
C(17)-C(18)-H(18)	118.2(15)	F(1)-Sb-F(3)	178.15(6)
C(19)-C(18)-H(18)	122.9(15)	F(1)-Sb-F(5)	89.11(5)
C(18)-C(19)-C(20)	120.36(17)	F(3)-Sb-F(5)	90.21(5)
C(18)-C(19)-H(19)	119.2(13)	F(1)-Sb-F(6)	90.27(6)
C(20)-C(19)-H(19)	120.4(14)	F(3)-Sb-F(6)	90.43(6)
N(3)-C(20)-C(19)	120.44(15)	F(5)-Sb-F(6)	179.07(6)
N(3)-C(20)-C(21)	119.50(14)	F(1)-Sb-F(4)	89.79(5)
C(19)-C(20)-C(21)	120.02(15)	F(3)-Sb-F(4)	88.49(5)
C(26)-C(21)-C(22)	120.24(14)	F(5)-Sb-F(4)	90.41(5)
C(26)-C(21)-C(20)	121.10(14)	F(6)-Sb-F(4)	90.28(6)
C(22)-C(21)-C(20)	118.51(14)	F(1)-Sb-F(2)	90.41(5)
C(23)-C(22)-C(21)	117.88(14)	F(3)-Sb-F(2)	91.32(5)
C(23)-C(22)-C(27)	118.47(14)	F(5)-Sb-F(2)	90.05(5)
C(21)-C(22)-C(27)	123.62(15)	F(6)-Sb-F(2)	89.27(5)
C(24)-C(23)-C(22)	122.49(15)	F(4)-Sb-F(2)	179.50(5)
C(24)-C(23)-H(23)	120.7(14)		



## APPENDIX 4.7

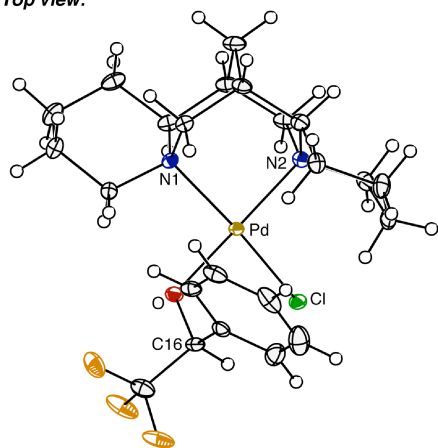
### *X-ray Crystallographic Data for (sp)Pd(OCCF<sub>3</sub>Ph)Cl (271)*

*Figure A4.7.1 (sp)Pd(OCCF<sub>3</sub>Ph)Cl (271).<sup>1,2</sup>*

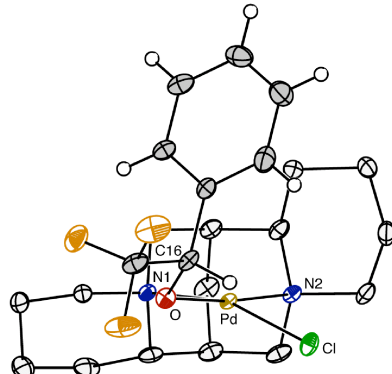


Selected bond lengths (Å) and angles (°)		
Pd–N1	2.1234(17)	N1–Pd–N2 88.07(6)°
Pd–N2	2.0925(16)	O–Pd–Cl 87.71(4)°
Pd–N3	2.0012(14)	N2–Pd–O 176.27(6)°
Pd–Cl	2.3316(5)	N1–Pd–Cl 164.59(5)°

*Top view:*



*Side view:*



<sup>1</sup> The hydrogen atoms of the sparteine backbone of the side view are not shown.

<sup>2</sup> The crystallographic data have been deposited at the Cambridge Database (CCDC), 12 Union Road, Cambridge CB2 1EZ, UK and copies can be obtained on request, free of charge, by quoting the publication citation and the deposition number 222289.

*Crystal data and structure refinement for 271 (CCDC 222289).*

Empirical formula	C <sub>23</sub> H <sub>32</sub> ClF <sub>3</sub> N <sub>2</sub> OPd · 2CH <sub>2</sub> Cl <sub>2</sub>
Formula weight	721.21
Crystallization solvent	Dichloromethane/hexane
Crystal habit	Block
Crystal size	0.33 x 0.33 x 0.26 mm <sup>3</sup>
Crystal color	Orange

*Data collection*

Preliminary photos	Rotation
Type of diffractometer	Bruker SMART 1000
Wavelength	0.71073 Å MoKα
Data collection temperature	100(2) K
θ range for 30297 reflections used in lattice determination	2.35 to 38.68°
Unit cell dimensions	a = 14.8633(3) Å b = 13.4427(3) Å c = 15.0189(3) Å 2967.54(11) Å <sup>3</sup>
Volume	4
Z	Monoclinic
Crystal system	P2 <sub>1</sub>
Space group	1.614 Mg/m <sup>3</sup>
Density (calculated)	1464
F(000)	Bruker SMART v5.054
Data collection program	1.80 to 40.44°
θ range for data collection	93.7 %
Completeness to θ = 40.44°	-26 ≤ h ≤ 26, -24 ≤ k ≤ 24, -27 ≤ l ≤ 27
Index ranges	ω scans at 7 φ settings
Data collection scan type	Bruker SAINT v6.022
Data reduction program	79009
Reflections collected	33021 [R <sub>int</sub> = 0.0654]
Independent reflections	1.117 mm <sup>-1</sup>
Absorption coefficient	None
Absorption correction	0.7600 and 0.7094
Max. and min. transmission (predicted)	

*Structure solution and refinement*

Structure solution program	SHELXS-97 (Sheldrick, 1990)
Primary solution method	Direct methods
Secondary solution method	Difference Fourier map
Hydrogen placement	Geometric positions
Structure refinement program	SHELXL-97 (Sheldrick, 1997)
Refinement method	Full matrix least-squares on F <sup>2</sup>
Data / restraints / parameters	33021 / 1 / 667
Treatment of hydrogen atoms	Riding
Goodness-of-fit on F <sup>2</sup>	0.987
Final R indices [I>2σ(I), 21505 reflections]	R1 = 0.0401, wR2 = 0.0608
R indices (all data)	R1 = 0.0826, wR2 = 0.0669
Type of weighting scheme used	Sigma
Weighting scheme used	w = 1/σ <sup>2</sup> (Fo <sup>2</sup> )
Max shift/error	0.003

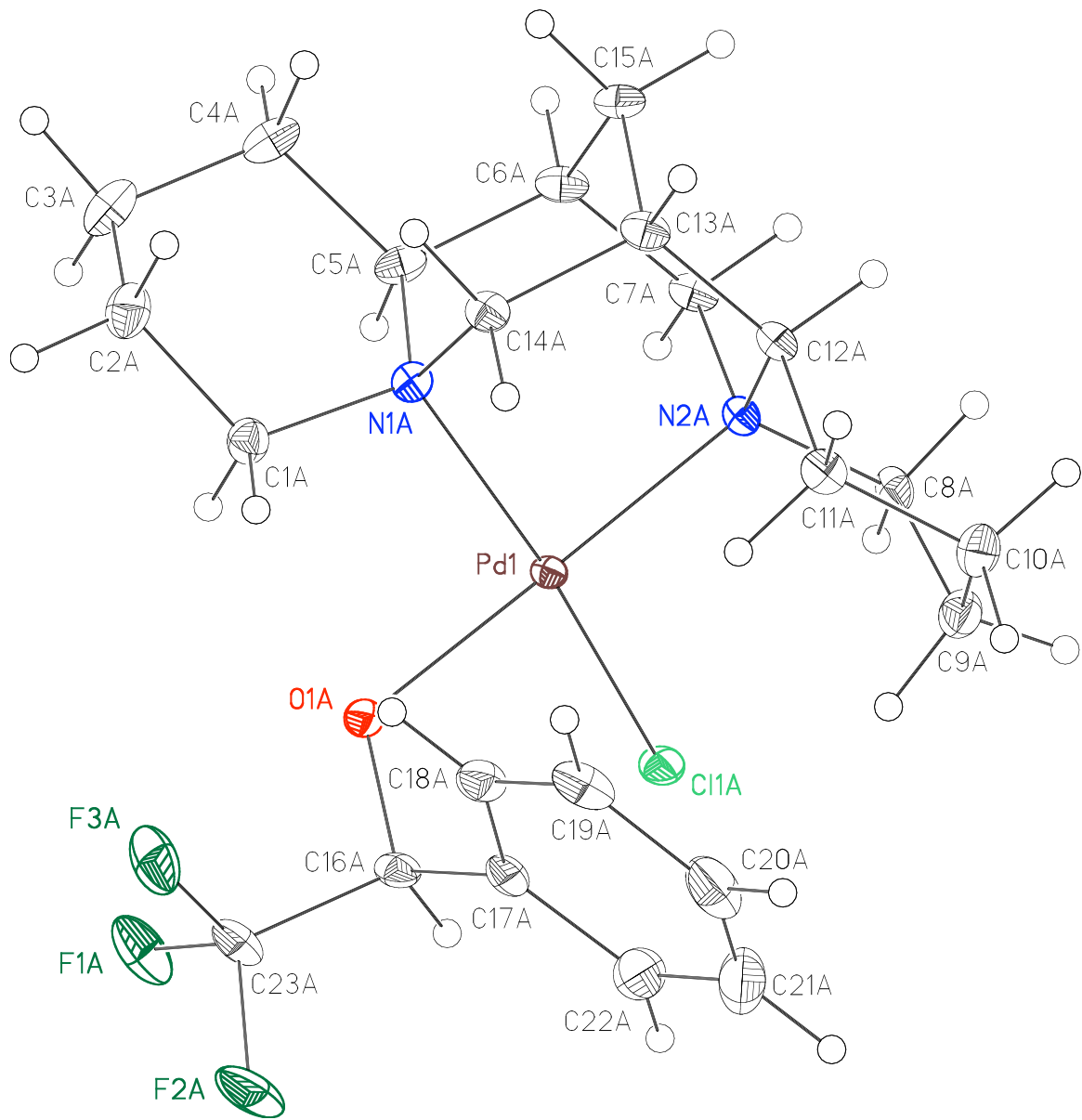
Average shift/error	0.000
Absolute structure parameter	-0.036(10)
Largest diff. peak and hole	2.072 and -1.257 e. $\text{\AA}^{-3}$

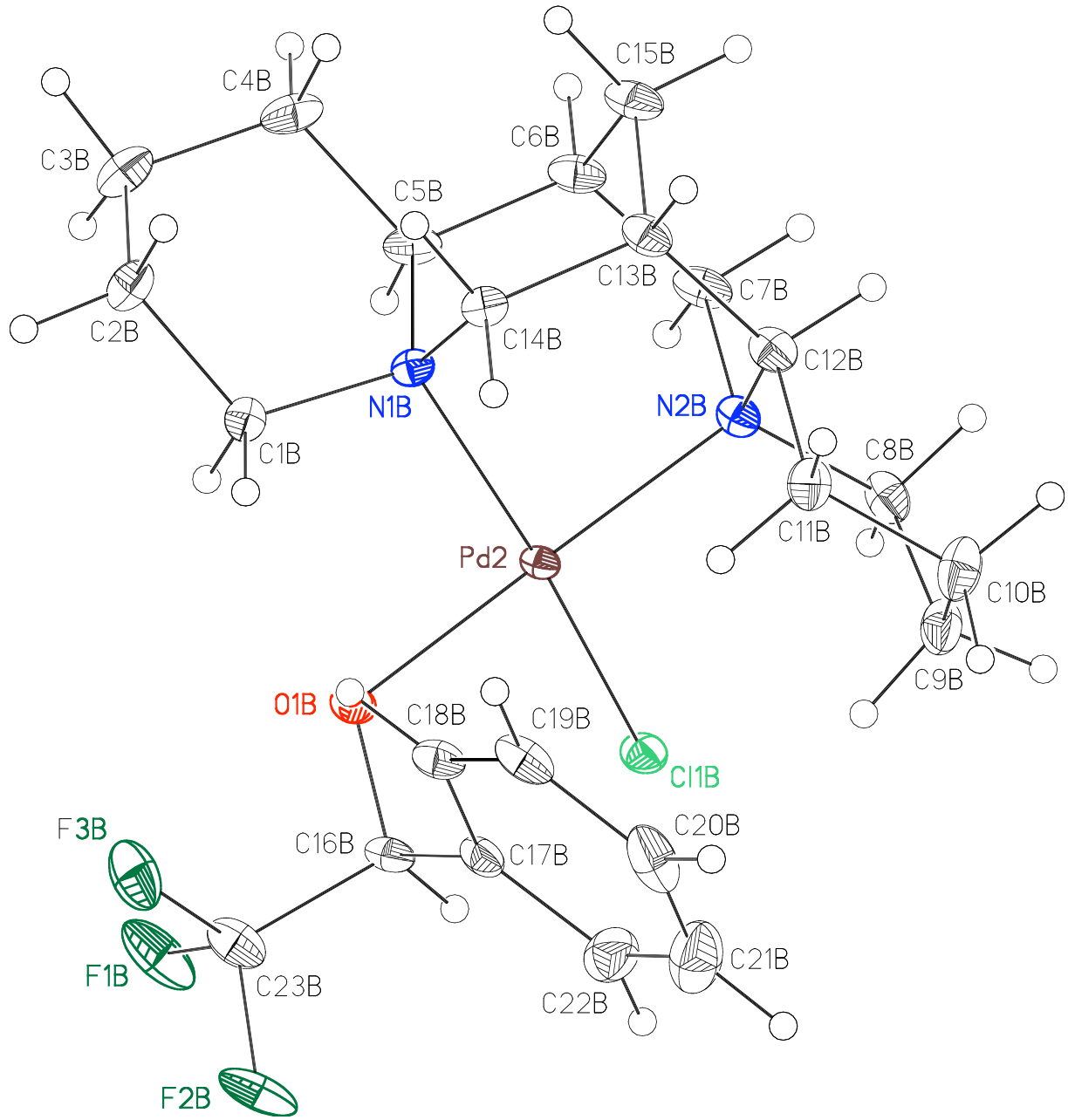
*Special refinement details*

Peaks in the difference Fourier larger than  $1\text{e}^{-3}\text{\AA}^3$  lie near metal centers or near solvent molecules.

Refinement of  $F^2$  against ALL reflections. The weighted R-factor ( $wR$ ) and goodness of fit (S) are based on  $F^2$ , conventional R-factors (R) are based on F, with F set to zero for negative  $F^2$ . The threshold expression of  $F^2 > 2\sigma(F^2)$  is used only for calculating R-factors(gt) etc. and is not relevant to the choice of reflections for refinement. R-factors based on  $F^2$  are statistically about twice as large as those based on F, and R-factors based on ALL data will be even larger.

All esds (except the esd in the dihedral angle between two l.s. planes) are estimated using the full covariance matrix. The cell esds are taken into account individually in the estimation of esds in distances, angles and torsion angles; correlations between esds in cell parameters are only used when they are defined by crystal symmetry. An approximate (isotropic) treatment of cell esds is used for estimating esds involving l.s. planes.

Figure A4.7.2 Molecule A of **271**.

Figure A4.7.3 Molecule B of **271**.

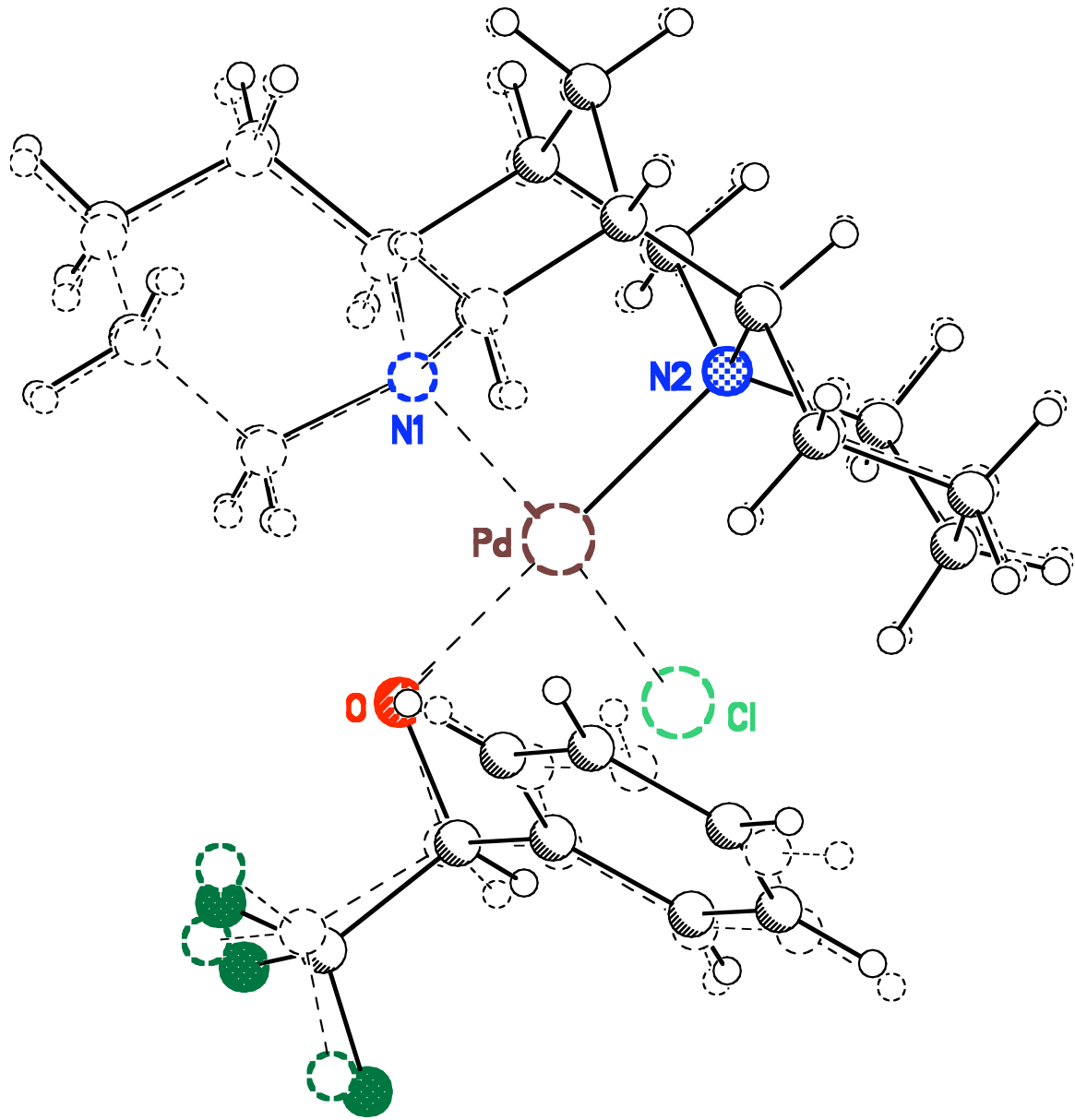


Figure A4.7.4 Overlay of molecules A and B of **271**.

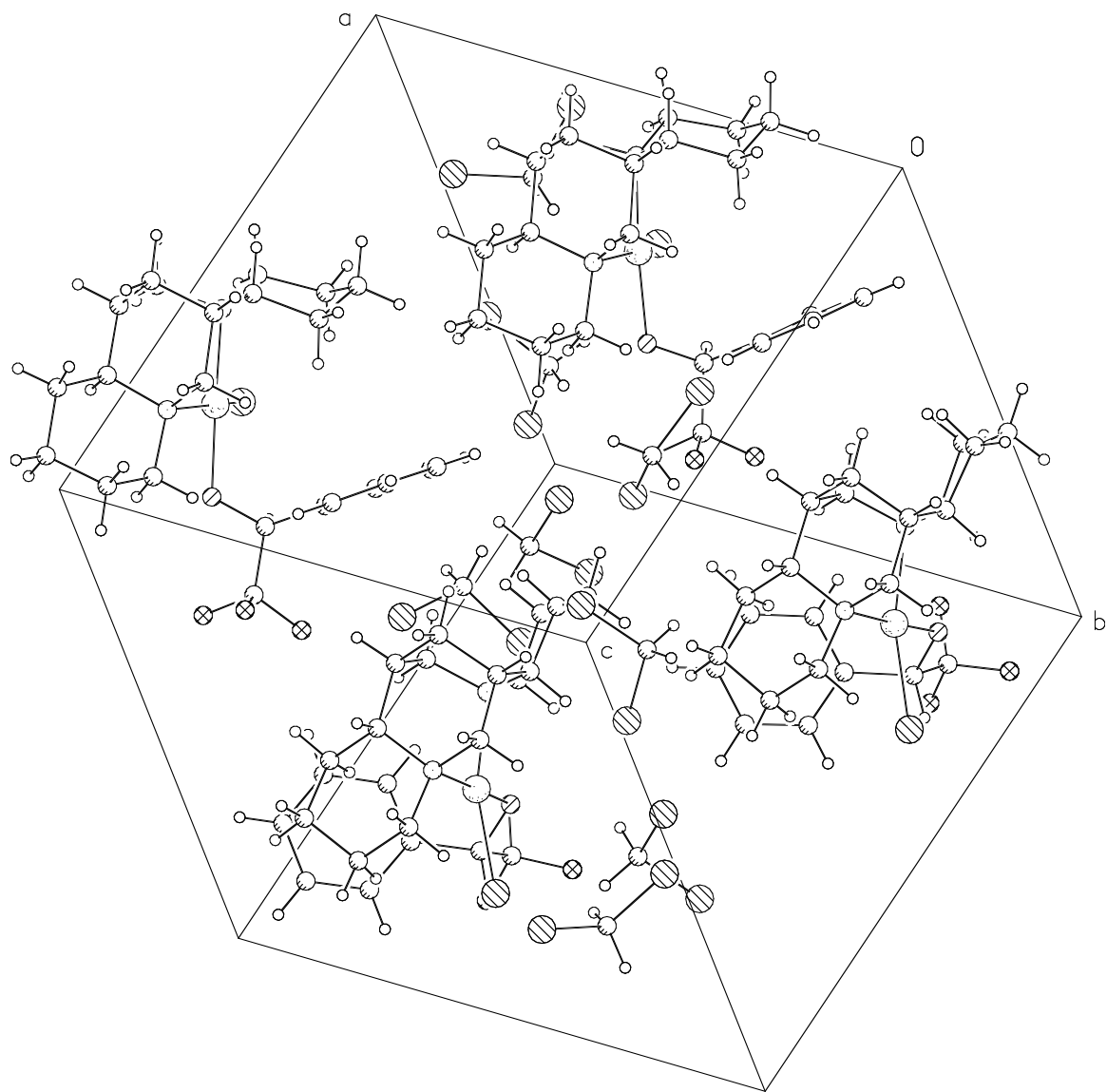


Figure A4.7.5 Unit cell contents of **271**.

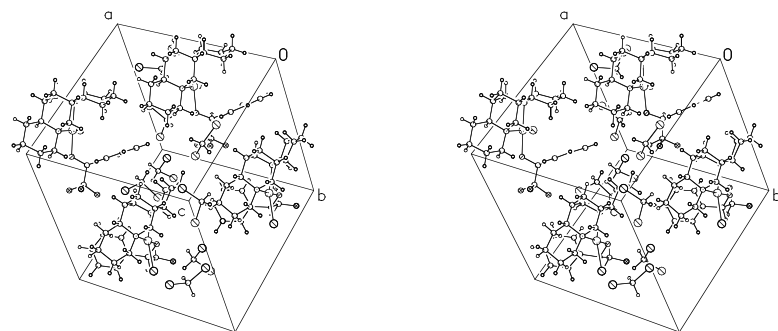


Figure A4.7.6 Stereo view of unit cell contents of **271**.

Table A4.7.1 Atomic coordinates ( $\times 10^4$ ) and equivalent isotropic displacement parameters ( $\text{\AA}^2 \times 10^3$ ) for 271 (CCDC 222289).  $U(\text{eq})$  is defined as the trace of the orthogonalized  $U^{ij}$  tensor.

	x	y	z	$U_{\text{eq}}$	Occ
Pd(1)		9658(1)	1631(1)	6561(1)	9(1)
Cl(1A)		10145(1)	2782(1)	5574(1)	15(1)
F(1A)		9805(1)	4511(1)	8328(1)	27(1)
F(2A)		8480(1)	5031(1)	7720(1)	29(1)
F(3A)		8599(1)	3725(1)	8568(1)	25(1)
O(1A)		9590(1)	2755(1)	7422(1)	13(1)
N(1A)		9586(1)	600(1)	7620(1)	10(1)
N(2A)		9650(1)	419(1)	5686(1)	10(1)
C(1A)		9524(1)	1159(2)	8481(1)	15(1)
C(2A)		9673(2)	521(2)	9325(1)	19(1)
C(3A)		10620(2)	66(2)	9425(2)	22(1)
C(4A)		10706(2)	-538(2)	8589(1)	19(1)
C(5A)		10482(1)	41(2)	7711(1)	14(1)
C(6A)		10505(1)	-655(1)	6901(1)	14(1)
C(7A)		10509(1)	-141(1)	5999(1)	13(1)
C(8A)		9648(1)	690(2)	4709(1)	13(1)
C(9A)		8793(1)	1235(2)	4292(1)	17(1)
C(10A)		7926(1)	666(2)	4410(1)	17(1)
C(11A)		7963(1)	370(2)	5397(1)	14(1)
C(12A)		8824(1)	-232(1)	5714(1)	12(1)
C(13A)		8843(1)	-756(2)	6615(1)	14(1)
C(14A)		8780(1)	-70(1)	7411(1)	13(1)
C(15A)		9707(1)	-1382(1)	6810(1)	14(1)
C(16A)		9043(1)	3566(1)	7101(1)	13(1)
C(17A)		8105(1)	3301(1)	6612(1)	14(1)
C(18A)		7536(1)	2645(1)	6981(2)	16(1)
C(19A)		6681(2)	2399(2)	6525(2)	22(1)
C(20A)		6387(2)	2824(2)	5686(2)	28(1)
C(21A)		6944(2)	3467(2)	5305(2)	29(1)
C(22A)		7795(2)	3698(2)	5770(2)	22(1)
C(23A)		8981(2)	4202(2)	7923(2)	18(1)
Pd(2)		5335(1)	6767(1)	8409(1)	9(1)
Cl(1B)		4743(1)	7843(1)	9400(1)	15(1)
F(1B)		5357(1)	9923(1)	7127(1)	32(1)
F(2B)		6682(1)	10294(1)	7854(1)	31(1)
F(3B)		6559(1)	9240(1)	6755(1)	27(1)
O(1B)		5545(1)	7965(1)	7666(1)	14(1)
N(1B)		5470(1)	5806(1)	7313(1)	11(1)
N(2B)		5260(1)	5492(1)	9195(1)	12(1)
C(1B)		5580(1)	6435(1)	6501(1)	14(1)
C(2B)		5487(1)	5866(2)	5610(1)	18(1)
C(3B)		4556(2)	5373(2)	5418(2)	22(1)
C(4B)		4431(2)	4708(2)	6215(2)	20(1)
C(5B)		4574(1)	5242(2)	7128(1)	16(1)
C(6B)		4490(1)	4491(2)	7883(2)	17(1)

C(7B)	4422(1)	4946(2)	8799(2)	17(1)
C(8B)	5199(1)	5700(2)	10174(1)	17(1)
C(9B)	6035(2)	6214(2)	10670(1)	20(1)
C(10B)	6910(2)	5644(2)	10592(1)	21(1)
C(11B)	6950(1)	5421(2)	9600(1)	17(1)
C(12B)	6099(1)	4845(2)	9190(1)	15(1)
C(13B)	6149(2)	4388(2)	8271(2)	15(1)
C(14B)	6264(1)	5127(1)	7525(1)	13(1)
C(15B)	5293(1)	3763(2)	7987(2)	19(1)
C(16B)	6090(1)	8699(1)	8131(2)	14(1)
C(17B)	7021(1)	8338(1)	8570(1)	14(1)
C(18B)	7542(1)	7725(1)	8102(2)	16(1)
C(19B)	8389(2)	7381(2)	8508(2)	20(1)
C(20B)	8727(2)	7661(2)	9384(2)	26(1)
C(21B)	8221(2)	8277(2)	9851(2)	31(1)
C(22B)	7369(2)	8607(2)	9446(2)	24(1)
C(23B)	6174(2)	9530(2)	7470(2)	20(1)
Cl(1)	2364(1)	2484(1)	7629(1)	42(1)
Cl(2)	2011(1)	4589(1)	7957(1)	28(1)
C(1)	1617(2)	3498(2)	7362(2)	25(1)
Cl(3)	2857(1)	7766(1)	7195(1)	35(1)
Cl(4)	3021(1)	9919(1)	6994(1)	27(1)
C(2)	3595(2)	8794(2)	7351(2)	27(1)
Cl(5)	8073(1)	6412(1)	6004(1)	29(1)
Cl(6)	7021(1)	7850(1)	4830(1)	38(1)
C(3)	7710(2)	6783(2)	4890(2)	25(1)
Cl(7)	8491(1)	1853(1)	1115(1)	50(1)
Cl(8)	7230(1)	1720(1)	-585(1)	54(1)
C(4)	7657(2)	2468(2)	337(2)	43(1)

C(11B)-C(12B)	1.532(3)	C(11A)-C(10A)-C(9A)	109.49(17)
C(12B)-C(13B)	1.522(3)	C(10A)-C(11A)-C(12A)	110.33(16)
C(13B)-C(14B)	1.526(3)	N(2A)-C(12A)-C(13A)	112.53(16)
C(13B)-C(15B)	1.532(3)	N(2A)-C(12A)-C(11A)	109.26(15)
C(16B)-C(23B)	1.512(3)	C(13A)-C(12A)-C(11A)	115.21(16)
C(16B)-C(17B)	1.523(3)	C(14A)-C(13A)-C(12A)	115.02(16)
C(17B)-C(22B)	1.388(3)	C(14A)-C(13A)-C(15A)	109.37(17)
C(17B)-C(18B)	1.391(3)	C(12A)-C(13A)-C(15A)	109.23(16)
C(18B)-C(19B)	1.394(3)	N(1A)-C(14A)-C(13A)	112.92(16)
C(19B)-C(20B)	1.388(3)	C(13A)-C(15A)-C(6A)	106.51(15)
C(20B)-C(21B)	1.379(3)	O(1A)-C(16A)-C(23A)	105.17(16)
C(21B)-C(22B)	1.392(3)	O(1A)-C(16A)-C(17A)	115.29(16)
Cl(1)-C(1)	1.766(2)	C(23A)-C(16A)-C(17A)	111.31(17)
Cl(2)-C(1)	1.771(2)	C(22A)-C(17A)-C(18A)	117.9(2)
Cl(3)-C(2)	1.758(2)	C(22A)-C(17A)-C(16A)	120.47(19)
Cl(4)-C(2)	1.780(2)	C(18A)-C(17A)-C(16A)	121.62(19)
Cl(5)-C(3)	1.752(2)	C(19A)-C(18A)-C(17A)	121.2(2)
Cl(6)-C(3)	1.756(2)	C(18A)-C(19A)-C(20A)	119.3(2)
Cl(7)-C(4)	1.776(3)	C(21A)-C(20A)-C(19A)	120.3(2)
Cl(8)-C(4)	1.752(3)	C(20A)-C(21A)-C(22A)	119.4(2)
		C(21A)-C(22A)-C(17A)	121.8(2)
O(1A)-Pd(1)-N(2A)	176.27(6)	F(2A)-C(23A)-F(1A)	106.42(17)
O(1A)-Pd(1)-N(1A)	89.78(6)	F(2A)-C(23A)-F(3A)	106.08(17)
N(2A)-Pd(1)-N(1A)	88.07(6)	F(1A)-C(23A)-F(3A)	105.72(18)
O(1A)-Pd(1)-Cl(1A)	87.71(4)	F(2A)-C(23A)-C(16A)	112.35(18)
N(2A)-Pd(1)-Cl(1A)	95.16(4)	F(1A)-C(23A)-C(16A)	112.28(17)
N(1A)-Pd(1)-Cl(1A)	164.59(5)	F(3A)-C(23A)-C(16A)	113.43(17)
C(16A)-O(1A)-Pd(1)	116.60(12)	O(1B)-Pd(2)-N(2B)	174.13(6)
C(14A)-N(1A)-C(1A)	109.38(15)	O(1B)-Pd(2)-N(1B)	90.94(6)
C(14A)-N(1A)-C(5A)	112.71(15)	N(2B)-Pd(2)-N(1B)	87.58(6)
C(1A)-N(1A)-C(5A)	109.47(15)	O(1B)-Pd(2)-Cl(1B)	87.82(4)
C(14A)-N(1A)-Pd(1)	111.32(12)	N(2B)-Pd(2)-Cl(1B)	95.24(5)
C(1A)-N(1A)-Pd(1)	109.42(12)	N(1B)-Pd(2)-Cl(1B)	163.00(5)
C(5A)-N(1A)-Pd(1)	104.43(11)	C(16B)-O(1B)-Pd(2)	114.46(12)
C(7A)-N(2A)-C(8A)	107.75(14)	C(14B)-N(1B)-C(1B)	109.72(15)
C(7A)-N(2A)-C(12A)	111.01(14)	C(14B)-N(1B)-C(5B)	112.21(15)
C(8A)-N(2A)-C(12A)	106.35(15)	C(1B)-N(1B)-C(5B)	109.15(15)
C(7A)-N(2A)-Pd(1)	105.65(11)	C(14B)-N(1B)-Pd(2)	111.73(12)
C(8A)-N(2A)-Pd(1)	114.91(11)	C(1B)-N(1B)-Pd(2)	108.59(12)
C(12A)-N(2A)-Pd(1)	111.18(11)	C(5B)-N(1B)-Pd(2)	105.29(11)
N(1A)-C(1A)-C(2A)	114.37(17)	C(7B)-N(2B)-C(8B)	108.17(15)
C(1A)-C(2A)-C(3A)	109.16(17)	C(7B)-N(2B)-C(12B)	110.69(15)
C(4A)-C(3A)-C(2A)	108.86(18)	C(8B)-N(2B)-C(12B)	106.13(16)
C(3A)-C(4A)-C(5A)	114.05(18)	C(7B)-N(2B)-Pd(2)	106.80(12)
N(1A)-C(5A)-C(4A)	114.01(16)	C(8B)-N(2B)-Pd(2)	114.37(12)
N(1A)-C(5A)-C(6A)	110.60(16)	C(12B)-N(2B)-Pd(2)	110.70(12)
C(4A)-C(5A)-C(6A)	110.21(16)	N(1B)-C(1B)-C(2B)	114.80(16)
C(7A)-C(6A)-C(15A)	108.46(17)	C(3B)-C(2B)-C(1B)	110.19(17)
C(7A)-C(6A)-C(5A)	115.59(16)	C(2B)-C(3B)-C(4B)	108.64(18)
C(15A)-C(6A)-C(5A)	110.57(16)	C(3B)-C(4B)-C(5B)	114.21(17)
N(2A)-C(7A)-C(6A)	113.05(16)	N(1B)-C(5B)-C(4B)	113.38(16)
N(2A)-C(8A)-C(9A)	113.46(16)	N(1B)-C(5B)-C(6B)	110.94(17)
C(8A)-C(9A)-C(10A)	112.24(17)	C(4B)-C(5B)-C(6B)	109.68(17)

C(7B)-C(6B)-C(15B)	108.63(18)	C(22B)-C(17B)-C(18B)	118.5(2)
C(7B)-C(6B)-C(5B)	115.20(17)	C(22B)-C(17B)-C(16B)	120.97(19)
C(15B)-C(6B)-C(5B)	110.31(17)	C(18B)-C(17B)-C(16B)	120.55(19)
N(2B)-C(7B)-C(6B)	113.25(16)	C(17B)-C(18B)-C(19B)	120.6(2)
N(2B)-C(8B)-C(9B)	113.50(16)	C(20B)-C(19B)-C(18B)	120.0(2)
C(8B)-C(9B)-C(10B)	112.23(18)	C(21B)-C(20B)-C(19B)	119.8(2)
C(9B)-C(10B)-C(11B)	109.21(18)	C(20B)-C(21B)-C(22B)	119.9(2)
C(10B)-C(11B)-C(12B)	109.94(17)	C(17B)-C(22B)-C(21B)	121.1(2)
N(2B)-C(12B)-C(13B)	112.69(17)	F(3B)-C(23B)-F(2B)	106.45(17)
N(2B)-C(12B)-C(11B)	109.69(16)	F(3B)-C(23B)-F(1B)	105.80(19)
C(13B)-C(12B)-C(11B)	114.75(17)	F(2B)-C(23B)-F(1B)	106.22(17)
C(12B)-C(13B)-C(14B)	115.49(17)	F(3B)-C(23B)-C(16B)	113.32(17)
C(12B)-C(13B)-C(15B)	108.85(17)	F(2B)-C(23B)-C(16B)	112.11(19)
C(14B)-C(13B)-C(15B)	109.29(18)	F(1B)-C(23B)-C(16B)	112.42(17)
N(1B)-C(14B)-C(13B)	112.61(16)	Cl(1)-C(1)-Cl(2)	112.06(13)
C(13B)-C(15B)-C(6B)	106.30(16)	Cl(3)-C(2)-Cl(4)	111.44(13)
O(1B)-C(16B)-C(23B)	106.98(18)	Cl(5)-C(3)-Cl(6)	112.04(12)
O(1B)-C(16B)-C(17B)	114.46(16)	Cl(8)-C(4)-Cl(7)	112.80(15)
C(23B)-C(16B)-C(17B)	111.21(17)		

---

Table A4.7.2 Selected bond lengths [ $\text{\AA}$ ] and angles [ $^\circ$ ] for **271** (CCDC 222289).

Pd(1)-O(1A)	2.0012(14)	O(1A)-Pd(1)-N(2A)	176.27(6)
Pd(1)-N(2A)	2.0925(16)	O(1A)-Pd(1)-N(1A)	89.78(6)
Pd(1)-N(1A)	2.1243(17)	N(2A)-Pd(1)-N(1A)	88.07(6)
Pd(1)-Cl(1A)	2.3316(5)	O(1A)-Pd(1)-Cl(1A)	87.71(4)
Pd(2)-O(1B)	2.0101(14)	N(2A)-Pd(1)-Cl(1A)	95.16(4)
Pd(2)-N(2B)	2.0936(16)	N(1A)-Pd(1)-Cl(1A)	164.59(5)
Pd(2)-N(1B)	2.1260(16)	O(1B)-Pd(2)-N(2B)	174.13(6)
Pd(2)-Cl(1B)	2.3384(5)	O(1B)-Pd(2)-N(1B)	90.94(6)
		N(2B)-Pd(2)-N(1B)	87.58(6)
		O(1B)-Pd(2)-Cl(1B)	87.82(4)
		N(2B)-Pd(2)-Cl(1B)	95.24(5)
		N(1B)-Pd(2)-Cl(1B)	163.00(5)

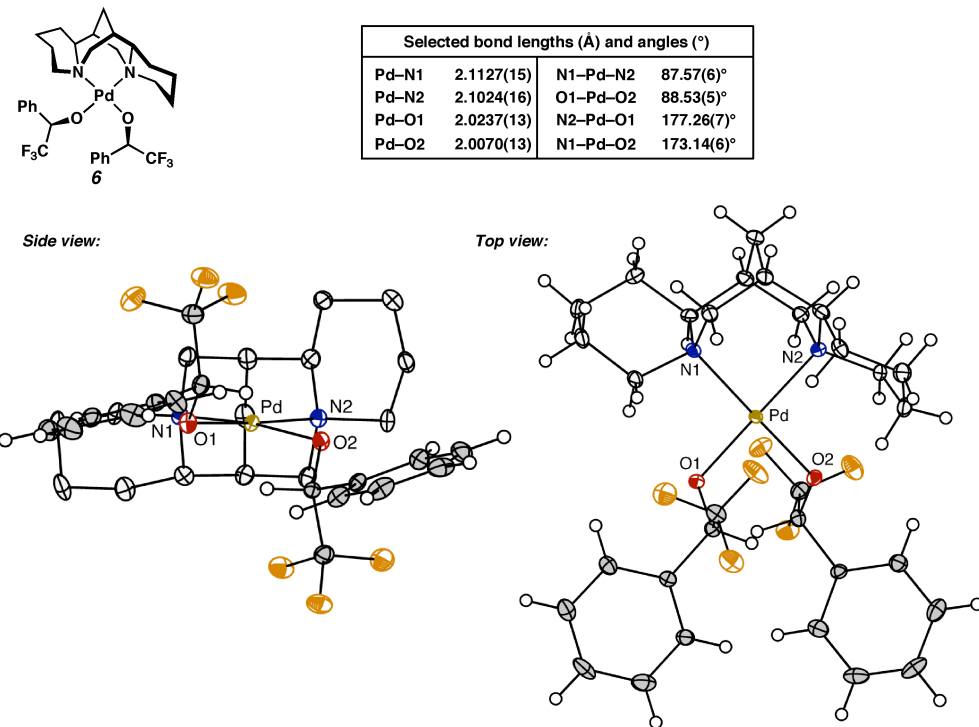
Table A4.7.3 Bond lengths [ $\text{\AA}$ ] and angles [ $^\circ$ ] for **271** (CCDC 222289).

Pd(1)-O(1A)	2.0012(14)	C(17A)-C(22A)	1.387(3)
Pd(1)-N(2A)	2.0925(16)	C(17A)-C(18A)	1.393(3)
Pd(1)-N(1A)	2.1243(17)	C(18A)-C(19A)	1.390(3)
Pd(1)-Cl(1A)	2.3316(5)	C(19A)-C(20A)	1.393(3)
F(1A)-C(23A)	1.350(2)	C(20A)-C(21A)	1.379(4)
F(2A)-C(23A)	1.349(2)	C(21A)-C(22A)	1.385(3)
F(3A)-C(23A)	1.355(2)	Pd(2)-O(1B)	2.0101(14)
O(1A)-C(16A)	1.402(2)	Pd(2)-N(2B)	2.0936(16)
N(1A)-C(14A)	1.494(2)	Pd(2)-N(1B)	2.1260(16)
N(1A)-C(1A)	1.510(2)	Pd(2)-Cl(1B)	2.3384(5)
N(1A)-C(5A)	1.518(2)	F(1B)-C(23B)	1.353(2)
N(2A)-C(7A)	1.496(2)	F(2B)-C(23B)	1.352(2)
N(2A)-C(8A)	1.511(2)	F(3B)-C(23B)	1.348(2)
N(2A)-C(12A)	1.515(2)	O(1B)-C(16B)	1.396(2)
C(1A)-C(2A)	1.519(3)	N(1B)-C(14B)	1.488(2)
C(2A)-C(3A)	1.521(3)	N(1B)-C(1B)	1.513(2)
C(3A)-C(4A)	1.517(3)	N(1B)-C(5B)	1.522(2)
C(4A)-C(5A)	1.525(3)	N(2B)-C(7B)	1.492(3)
C(5A)-C(6A)	1.539(3)	N(2B)-C(8B)	1.512(3)
C(6A)-C(7A)	1.522(3)	N(2B)-C(12B)	1.521(2)
C(6A)-C(15A)	1.527(3)	C(1B)-C(2B)	1.528(3)
C(8A)-C(9A)	1.519(3)	C(2B)-C(3B)	1.522(3)
C(9A)-C(10A)	1.531(3)	C(3B)-C(4B)	1.527(3)
C(10A)-C(11A)	1.527(3)	C(4B)-C(5B)	1.534(3)
C(11A)-C(12A)	1.529(3)	C(5B)-C(6B)	1.536(3)
C(12A)-C(13A)	1.523(3)	C(6B)-C(7B)	1.523(3)
C(13A)-C(14A)	1.522(3)	C(6B)-C(15B)	1.533(3)
C(13A)-C(15A)	1.527(3)	C(8B)-C(9B)	1.517(3)
C(16A)-C(23A)	1.515(3)	C(9B)-C(10B)	1.528(3)
C(16A)-C(17A)	1.519(3)	C(10B)-C(11B)	1.531(3)

**APPENDIX 4.8**

*X-ray Crystallographic Data for  
(sp)Pd(OCCF<sub>3</sub>Ph)<sub>2</sub> (274)*

Figure A4.8.1 (sp)Pd(OCCF<sub>3</sub>Ph)<sub>2</sub> (274).<sup>1,2</sup>



<sup>1</sup> The hydrogen atoms of the (–)-sparteine backbone of the side view are not shown.

<sup>2</sup> The crystallographic data have been deposited at the Cambridge Database (CCDC), 12 Union Road, Cambridge CB2 1EZ, UK and copies can be obtained on request, free of charge, by quoting the publication citation and the deposition number 260858.

*Crystal data and structure refinement for 274 (CCDC 260858).*

Empirical formula	C <sub>31</sub> H <sub>38</sub> F <sub>6</sub> N <sub>2</sub> O <sub>2</sub> Pd • CH <sub>2</sub> Cl <sub>2</sub>
Formula weight	775.96
Crystallization solvent	Dichloromethane/hexane
Crystal habit	Prism
Crystal size	0.44 x 0.29 x 0.09 mm <sup>3</sup>
Crystal color	Yellow
<i>Data collection</i>	
Type of diffractometer	Bruker SMART 1000
Wavelength	0.71073 Å MoKα
Data collection temperature	100(2) K
θ range for 17094 reflections used in lattice determination	2.30 to 41.38°
Unit cell dimensions	a = 10.7694(4) Å b = 13.1518(5) Å c = 11.4564(4) Å V = 1562.25(10) Å <sup>3</sup> β = 105.6820(10)°
Volume	1562.25(10) Å <sup>3</sup>
Z	2
Crystal system	Monoclinic
Space group	P2 <sub>1</sub>
Density (calculated)	1.650 Mg/m <sup>3</sup>
F(000)	792
Data collection program	Bruker SMART v5.630
θ range for data collection	1.85 to 42.67°
Completeness to θ = 42.67°	91.7 %
Index ranges	-18 ≤ h ≤ 20, -24 ≤ k ≤ 24, -20 ≤ l ≤ 21
Data collection scan type	ω scans at 5 φ settings
Data reduction program	Bruker SAINT v6.45A
Reflections collected	31764
Independent reflections	17119 [R <sub>int</sub> = 0.0618]
Absorption coefficient	0.835 mm <sup>-1</sup>
Absorption correction	None
Max. and min. transmission	0.9286 and 0.7102
<i>Structure solution and refinement</i>	
Structure solution program	Bruker XS v6.12
Primary solution method	Direct methods
Secondary solution method	Difference Fourier map
Hydrogen placement	Difference Fourier map
Structure refinement program	Bruker XL v6.12
Refinement method	Full matrix least-squares on F <sup>2</sup>
Data / restraints / parameters	17119 / 1 / 566
Treatment of hydrogen atoms	Unrestrained
Goodness-of-fit on F <sup>2</sup>	1.067
Final R indices [I>2σ(I), 14299 reflections]	R1 = 0.0375, wR2 = 0.0708
R indices (all data)	R1 = 0.0489, wR2 = 0.0733
Type of weighting scheme used	Sigma
Weighting scheme used	w = 1/σ <sup>2</sup> (F <sub>o</sub> <sup>2</sup> )
Max shift/error	0.002
Average shift/error	0.000
Absolute structure parameter	-0.049(12)

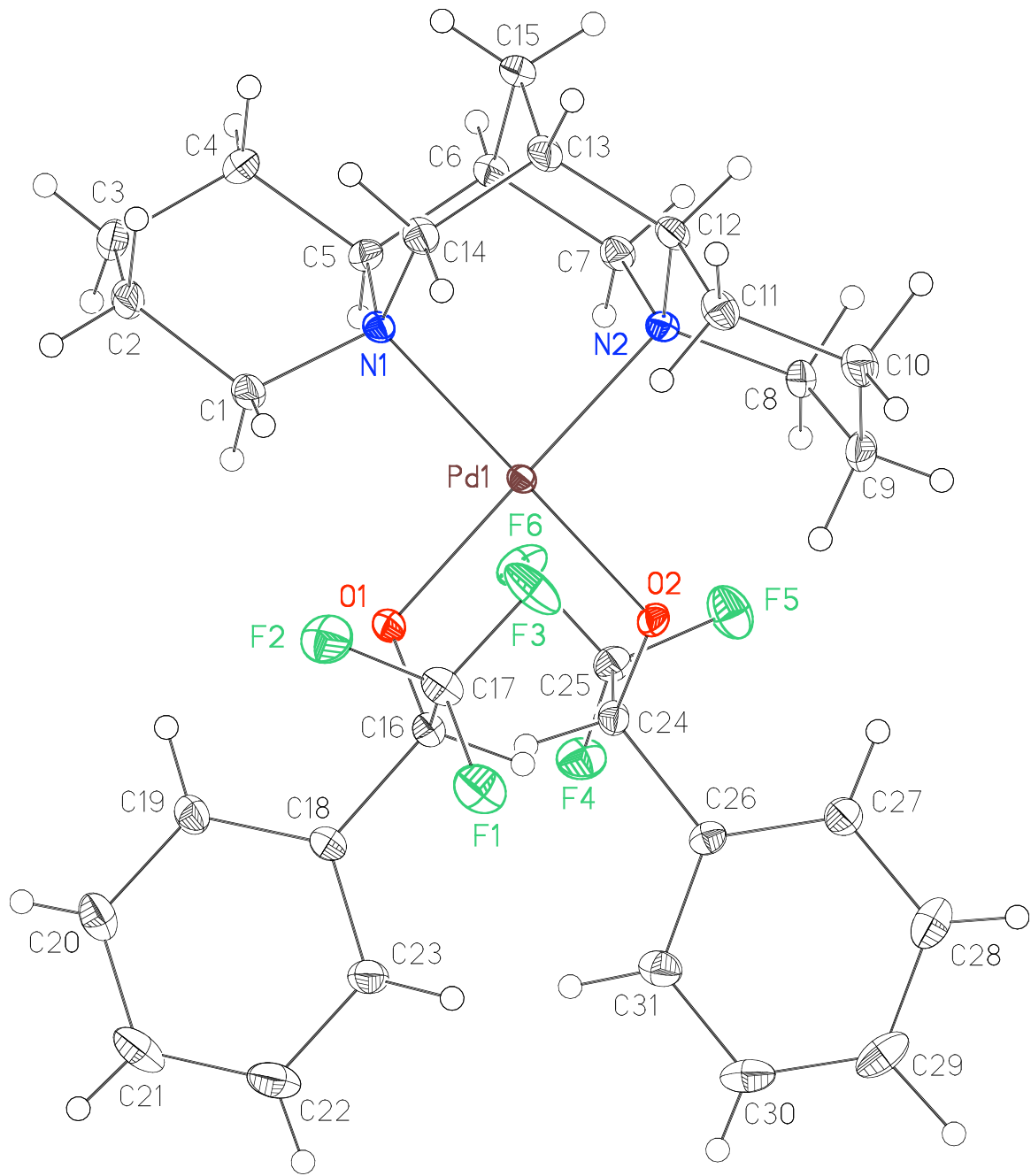
Largest diff. peak and hole                            2.146 and -1.876 e. $\text{\AA}^{-3}$

*Special refinement details*

All difference Fourier peaks larger than  $1\text{e}/\text{\AA}^3$  lie with  $1\text{\AA}$  of Pd.

Refinement of  $F^2$  against ALL reflections. The weighted R-factor ( $wR$ ) and goodness of fit ( $S$ ) are based on  $F^2$ , conventional R-factors ( $R$ ) are based on  $F$ , with  $F$  set to zero for negative  $F^2$ . The threshold expression of  $F^2 > 2\sigma(F^2)$  is used only for calculating R-factors(gt) etc. and is not relevant to the choice of reflections for refinement. R-factors based on  $F^2$  are statistically about twice as large as those based on  $F$ , and R-factors based on ALL data will be even larger.

All esds (except the esd in the dihedral angle between two l.s. planes) are estimated using the full covariance matrix. The cell esds are taken into account individually in the estimation of esds in distances, angles and torsion angles; correlations between esds in cell parameters are only used when they are defined by crystal symmetry. An approximate (isotropic) treatment of cell esds is used for estimating esds involving l.s. planes.

Figure A4.8.2 Molecule of **274**.

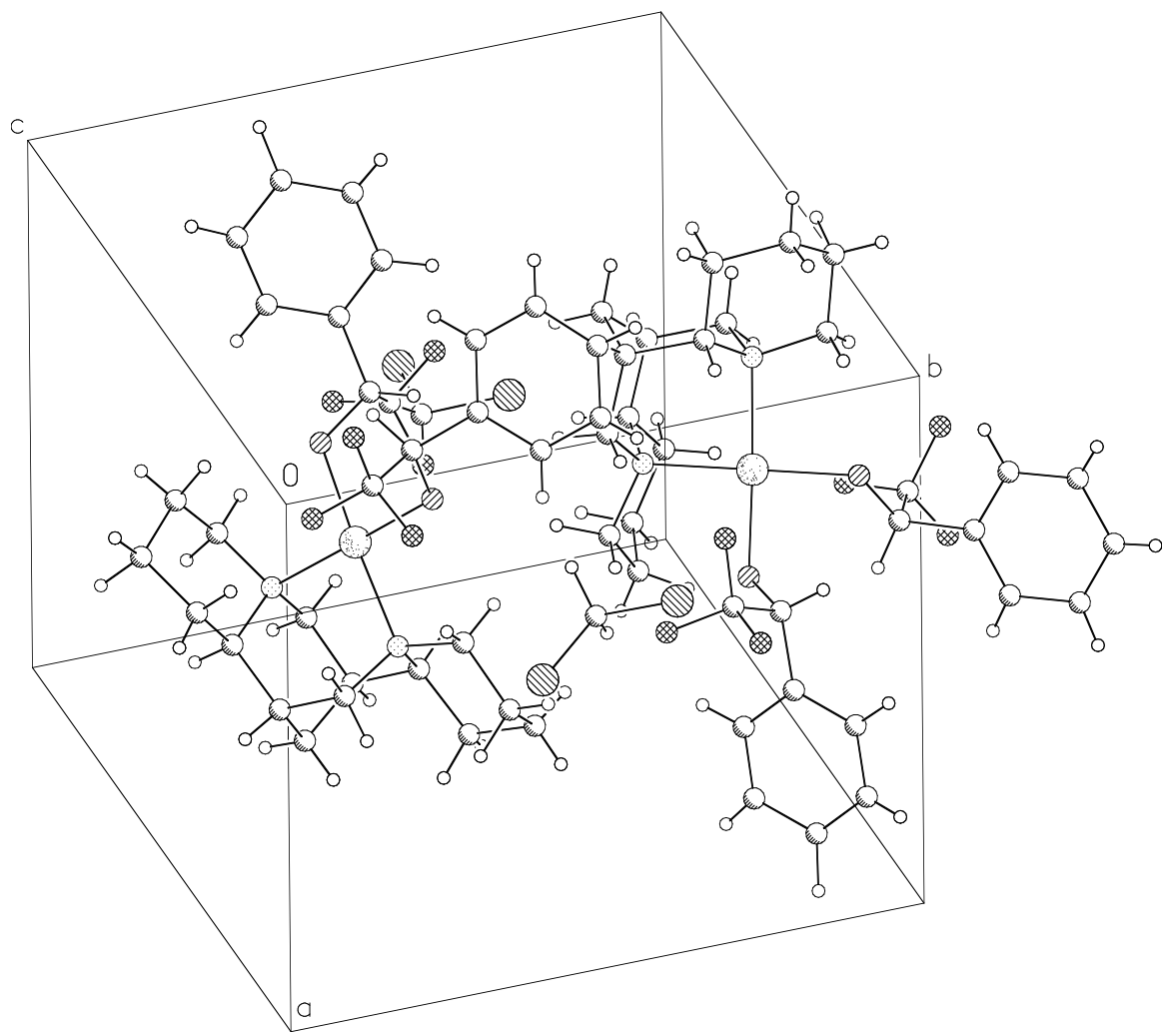


Figure A4.8.3 Unit cell contents of **274**.

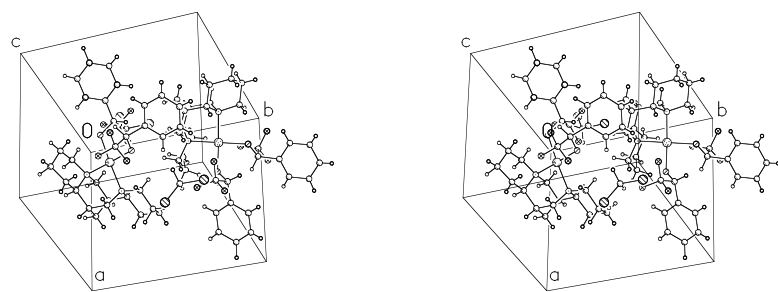


Figure A4.8.4 Stereo view of unit cell contents of **274**.

Table A4.8.1 Atomic coordinates ( $\times 10^4$ ) and equivalent isotropic displacement parameters ( $\text{\AA}^2 \times 10^3$ ) for **274** (CCDC 259858).  $U(\text{eq})$  is defined as the trace of the orthogonalized  $U^{ij}$  tensor.

	x	y	z	$U_{\text{eq}}$	Occ
Pd(1)		6173(1)	3730(1)	6585(1)	9(1)
F(1)		7204(2)	5258(1)	10414(1)	24(1)
F(2)		8293(1)	5661(1)	9148(1)	24(1)
F(3)		7651(2)	4119(1)	9227(1)	27(1)
F(4)		1711(1)	4422(1)	5130(1)	20(1)
F(5)		2404(2)	2875(1)	5293(1)	24(1)
F(6)		3481(1)	4050(1)	4690(1)	22(1)
O(1)		6101(1)	5181(1)	7153(1)	13(1)
O(2)		4605(1)	3427(1)	7153(1)	13(1)
N(1)		7672(2)	4063(1)	5776(2)	11(1)
N(2)		6308(2)	2206(1)	6075(2)	11(1)
C(1)		8007(2)	5173(1)	5972(2)	15(1)
C(2)		8859(2)	5592(2)	5215(2)	19(1)
C(3)		8199(2)	5445(2)	3872(2)	19(1)
C(4)		7924(2)	4314(2)	3639(2)	18(1)
C(5)		7123(2)	3853(2)	4436(2)	13(1)
C(6)		6947(2)	2701(1)	4187(2)	14(1)
C(7)		5941(2)	2200(2)	4720(2)	13(1)
C(8)		5382(2)	1510(1)	6469(2)	15(1)
C(9)		5682(2)	1410(2)	7839(2)	17(1)
C(10)		7073(2)	1092(2)	8415(2)	17(1)
C(11)		7990(2)	1783(2)	7968(2)	16(1)
C(12)		7645(2)	1781(1)	6585(2)	14(1)
C(13)		8628(2)	2300(2)	6045(2)	16(1)
C(14)		8841(2)	3437(1)	6327(2)	15(1)
C(15)		8235(2)	2142(2)	4679(2)	17(1)
C(16)		6021(2)	5339(1)	8326(2)	13(1)
C(17)		7287(2)	5093(2)	9274(2)	17(1)
C(18)		5683(2)	6447(1)	8494(2)	13(1)
C(19)		6216(2)	7219(2)	7942(2)	15(1)
C(20)		5973(2)	8235(2)	8129(2)	20(1)
C(21)		5186(3)	8495(2)	8870(2)	24(1)
C(22)		4620(2)	7737(2)	9398(2)	23(1)
C(23)		4873(2)	6713(2)	9209(2)	17(1)
C(24)		3556(2)	4067(1)	6804(2)	12(1)
C(25)		2789(2)	3851(2)	5487(2)	14(1)
C(26)		2669(2)	3929(1)	7636(2)	12(1)
C(27)		2502(2)	2962(2)	8065(2)	16(1)
C(28)		1707(2)	2810(2)	8821(2)	21(1)
C(29)		1073(2)	3651(3)	9166(2)	22(1)
C(30)		1255(2)	4611(2)	8757(2)	20(1)
C(31)		2045(2)	4754(2)	7991(2)	17(1)
Cl(1)		396(1)	4352(1)	2045(1)	38(1)
Cl(2)		-966(1)	2414(1)	1556(1)	41(1)
C(41)		524(4)	3018(3)	2170(4)	37(1)

Table A4.8.2 Selected bond lengths [ $\text{\AA}$ ] and angles [ $^\circ$ ] for 274 (CCDC 259858).

Pd(1)-O(2)	2.0070(13)	O(2)-Pd(1)-O(1)	88.53(5)
Pd(1)-O(1)	2.0237(13)	O(2)-Pd(1)-N(2)	91.57(6)
Pd(1)-N(2)	2.1042(16)	O(1)-Pd(1)-N(2)	177.26(7)
Pd(1)-N(1)	2.1127(15)	O(2)-Pd(1)-N(1)	173.14(6)
		O(1)-Pd(1)-N(1)	92.65(6)
		N(2)-Pd(1)-N(1)	87.57(6)

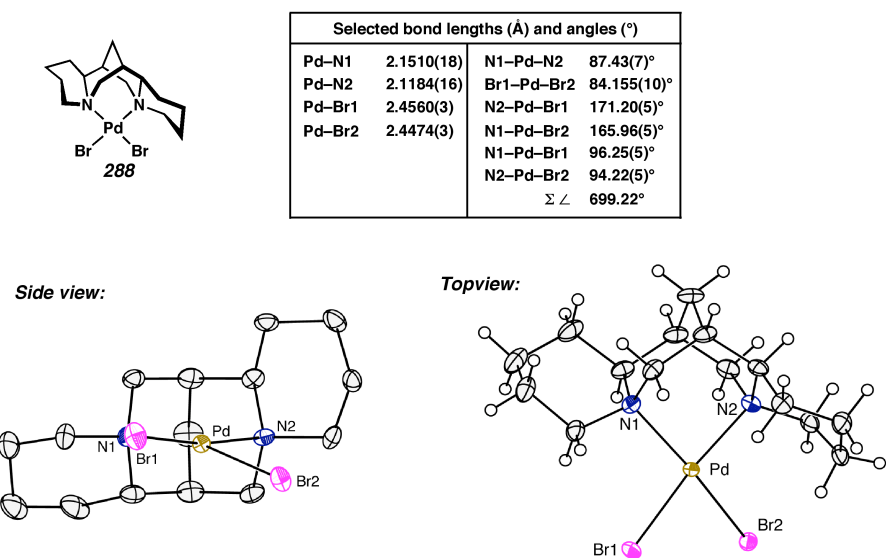
Table A4.8.3 Bond lengths [ $\text{\AA}$ ] and angles [ $^\circ$ ] for 274 (CCDC 259858).

Pd(1)-O(2)	2.0070(13)	C(7)-H(7B)	0.92(3)
Pd(1)-O(1)	2.0237(13)	C(8)-C(9)	1.521(3)
Pd(1)-N(2)	2.1042(16)	C(8)-H(8A)	1.01(3)
Pd(1)-N(1)	2.1127(15)	C(8)-H(8B)	1.00(3)
F(1)-C(17)	1.351(2)	C(9)-C(10)	1.523(3)
F(2)-C(17)	1.356(3)	C(9)-H(9A)	0.86(4)
F(3)-C(17)	1.345(2)	C(9)-H(9B)	0.99(3)
F(4)-C(25)	1.349(2)	C(10)-C(11)	1.529(3)
F(5)-C(25)	1.348(3)	C(10)-H(10A)	1.02(3)
F(6)-C(25)	1.351(2)	C(10)-H(10B)	0.97(3)
O(1)-C(16)	1.385(2)	C(11)-C(12)	1.526(3)
O(2)-C(24)	1.379(2)	C(11)-H(11A)	0.95(3)
N(1)-C(14)	1.494(2)	C(11)-H(11B)	0.84(3)
N(1)-C(1)	1.506(2)	C(12)-C(13)	1.525(3)
N(1)-C(5)	1.514(2)	C(12)-H(12)	0.96(3)
N(2)-C(7)	1.495(3)	C(13)-C(15)	1.521(3)
N(2)-C(12)	1.507(3)	C(13)-C(14)	1.533(3)
N(2)-C(8)	1.510(2)	C(13)-H(13)	0.96(4)
C(1)-C(2)	1.526(3)	C(14)-H(14A)	0.94(2)
C(1)-H(1A)	0.82(2)	C(14)-H(14B)	0.96(2)
C(1)-H(1B)	1.00(3)	C(15)-H(15A)	0.92(4)
C(2)-C(3)	1.522(4)	C(15)-H(15B)	0.91(3)
C(2)-H(2A)	0.93(3)	C(16)-C(18)	1.526(3)
C(2)-H(2B)	1.10(3)	C(16)-C(17)	1.531(3)
C(3)-C(4)	1.526(3)	C(16)-H(16)	1.01(2)
C(3)-H(3A)	0.87(3)	C(18)-C(23)	1.393(3)
C(3)-H(3B)	0.89(3)	C(18)-C(19)	1.399(3)
C(4)-C(5)	1.540(3)	C(19)-C(20)	1.390(3)
C(4)-H(4A)	0.98(2)	C(19)-H(19)	0.91(3)
C(4)-H(4B)	0.91(3)	C(20)-C(21)	1.395(4)
C(5)-C(6)	1.544(3)	C(20)-H(20)	0.78(3)
C(5)-H(5)	0.97(3)	C(21)-C(22)	1.390(4)
C(6)-C(7)	1.529(3)	C(21)-H(21)	0.85(3)
C(6)-C(15)	1.537(3)	C(22)-C(23)	1.403(3)
C(6)-H(6)	1.04(2)	C(22)-H(22)	0.87(3)
C(7)-H(7A)	0.99(3)	C(23)-H(23)	0.89(3)

C(24)-C(26)	1.532(2)	C(4)-C(3)-H(3A)	110(2)
C(24)-C(25)	1.539(3)	C(2)-C(3)-H(3B)	112.2(19)
C(24)-H(24)	0.93(3)	C(4)-C(3)-H(3B)	112(2)
C(26)-C(27)	1.393(3)	H(3A)-C(3)-H(3B)	102(3)
C(26)-C(31)	1.394(3)	C(3)-C(4)-C(5)	113.16(17)
C(27)-C(28)	1.388(3)	C(3)-C(4)-H(4A)	108.8(13)
C(27)-H(27)	0.92(3)	C(5)-C(4)-H(4A)	111.1(13)
C(28)-C(29)	1.410(4)	C(3)-C(4)-H(4B)	111.8(17)
C(28)-H(28)	0.88(3)	C(5)-C(4)-H(4B)	111.4(18)
C(29)-C(30)	1.379(4)	H(4A)-C(4)-H(4B)	100(2)
C(29)-H(29)	1.08(2)	N(1)-C(5)-C(4)	113.66(16)
C(30)-C(31)	1.390(3)	N(1)-C(5)-C(6)	111.23(15)
C(30)-H(30)	0.82(4)	C(4)-C(5)-C(6)	109.65(15)
C(31)-H(31)	0.95(3)	N(1)-C(5)-H(5)	111.7(19)
Cl(1)-C(41)	1.762(4)	C(4)-C(5)-H(5)	105.3(18)
Cl(2)-C(41)	1.757(4)	C(6)-C(5)-H(5)	104.7(18)
C(41)-H(41A)	1.02(4)	C(7)-C(6)-C(15)	108.29(16)
C(41)-H(41B)	1.02(3)	C(7)-C(6)-C(5)	114.43(15)
		C(15)-C(6)-C(5)	110.38(16)
O(2)-Pd(1)-O(1)	88.53(5)	C(7)-C(6)-H(6)	104.2(14)
O(2)-Pd(1)-N(2)	91.57(6)	C(15)-C(6)-H(6)	111.0(14)
O(1)-Pd(1)-N(2)	177.26(7)	C(5)-C(6)-H(6)	108.3(13)
O(2)-Pd(1)-N(1)	173.14(6)	N(2)-C(7)-C(6)	113.30(16)
O(1)-Pd(1)-N(1)	92.65(6)	N(2)-C(7)-H(7A)	111.0(14)
N(2)-Pd(1)-N(1)	87.57(6)	C(6)-C(7)-H(7A)	109.6(14)
C(16)-O(1)-Pd(1)	118.15(11)	N(2)-C(7)-H(7B)	111.4(18)
C(24)-O(2)-Pd(1)	118.66(11)	C(6)-C(7)-H(7B)	107.8(17)
C(14)-N(1)-C(1)	109.32(15)	H(7A)-C(7)-H(7B)	103(2)
C(14)-N(1)-C(5)	112.41(15)	N(2)-C(8)-C(9)	112.77(16)
C(1)-N(1)-C(5)	109.92(15)	N(2)-C(8)-H(8A)	104.1(15)
C(14)-N(1)-Pd(1)	110.89(12)	C(9)-C(8)-H(8A)	114.1(15)
C(1)-N(1)-Pd(1)	108.44(11)	N(2)-C(8)-H(8B)	110.5(15)
C(5)-N(1)-Pd(1)	105.74(10)	C(9)-C(8)-H(8B)	110.9(15)
C(7)-N(2)-C(12)	110.92(14)	H(8A)-C(8)-H(8B)	104(2)
C(7)-N(2)-C(8)	107.21(15)	C(8)-C(9)-C(10)	112.38(17)
C(12)-N(2)-C(8)	107.35(14)	C(8)-C(9)-H(9A)	121(3)
C(7)-N(2)-Pd(1)	105.93(11)	C(10)-C(9)-H(9A)	103(3)
C(12)-N(2)-Pd(1)	112.12(11)	C(8)-C(9)-H(9B)	113.2(15)
C(8)-N(2)-Pd(1)	113.23(11)	C(10)-C(9)-H(9B)	110.4(16)
N(1)-C(1)-C(2)	114.95(16)	H(9A)-C(9)-H(9B)	95(3)
N(1)-C(1)-H(1A)	103.4(16)	C(9)-C(10)-C(11)	109.95(17)
C(2)-C(1)-H(1A)	114.7(17)	C(9)-C(10)-H(10A)	114.8(17)
N(1)-C(1)-H(1B)	105.1(15)	C(11)-C(10)-H(10A)	105.0(16)
C(2)-C(1)-H(1B)	105.1(15)	C(9)-C(10)-H(10B)	114.8(19)
H(1A)-C(1)-H(1B)	113(2)	C(11)-C(10)-H(10B)	112.5(19)
C(3)-C(2)-C(1)	109.91(18)	H(10A)-C(10)-H(10B)	99(2)
C(3)-C(2)-H(2A)	111.8(18)	C(12)-C(11)-C(10)	110.37(17)
C(1)-C(2)-H(2A)	110.1(18)	C(12)-C(11)-H(11A)	112.9(19)
C(3)-C(2)-H(2B)	110.4(16)	C(10)-C(11)-H(11A)	109.5(19)
C(1)-C(2)-H(2B)	111.3(16)	C(12)-C(11)-H(11B)	104.9(19)
H(2A)-C(2)-H(2B)	103(2)	C(10)-C(11)-H(11B)	113.5(19)
C(2)-C(3)-C(4)	108.44(18)	H(11A)-C(11)-H(11B)	106(3)
C(2)-C(3)-H(3A)	111(2)	N(2)-C(12)-C(13)	111.80(16)

N(2)-C(12)-C(11)	109.93(15)	C(22)-C(21)-H(21)	123(2)
C(13)-C(12)-C(11)	114.81(17)	C(20)-C(21)-H(21)	117(2)
N(2)-C(12)-H(12)	107.5(17)	C(21)-C(22)-C(23)	119.7(2)
C(13)-C(12)-H(12)	105.2(17)	C(21)-C(22)-H(22)	122.1(19)
C(11)-C(12)-H(12)	107.2(16)	C(23)-C(22)-H(22)	117.7(19)
C(15)-C(13)-C(12)	109.04(17)	C(18)-C(23)-C(22)	120.7(2)
C(15)-C(13)-C(14)	109.53(17)	C(18)-C(23)-H(23)	121(2)
C(12)-C(13)-C(14)	115.59(16)	C(22)-C(23)-H(23)	117(2)
C(15)-C(13)-H(13)	113(2)	O(2)-C(24)-C(26)	110.30(15)
C(12)-C(13)-H(13)	99(2)	O(2)-C(24)-C(25)	110.57(16)
C(14)-C(13)-H(13)	110(2)	C(26)-C(24)-C(25)	109.17(15)
N(1)-C(14)-C(13)	112.81(16)	O(2)-C(24)-H(24)	113.6(16)
N(1)-C(14)-H(14A)	106.3(15)	C(26)-C(24)-H(24)	110.0(15)
C(13)-C(14)-H(14A)	108.2(14)	C(25)-C(24)-H(24)	103.0(16)
N(1)-C(14)-H(14B)	109.4(16)	F(5)-C(25)-F(4)	106.17(17)
C(13)-C(14)-H(14B)	107.6(18)	F(5)-C(25)-F(6)	105.99(16)
H(14A)-C(14)-H(14B)	113(2)	F(4)-C(25)-F(6)	105.85(16)
C(13)-C(15)-C(6)	106.53(16)	F(5)-C(25)-C(24)	113.42(16)
C(13)-C(15)-H(15A)	108(2)	F(4)-C(25)-C(24)	112.59(17)
C(6)-C(15)-H(15A)	109(2)	F(6)-C(25)-C(24)	112.23(16)
C(13)-C(15)-H(15B)	113(2)	C(27)-C(26)-C(31)	119.33(17)
C(6)-C(15)-H(15B)	106(2)	C(27)-C(26)-C(24)	119.33(16)
H(15A)-C(15)-H(15B)	115(3)	C(31)-C(26)-C(24)	121.33(16)
O(1)-C(16)-C(18)	110.21(16)	C(28)-C(27)-C(26)	120.76(19)
O(1)-C(16)-C(17)	112.30(16)	C(28)-C(27)-H(27)	117.8(19)
C(18)-C(16)-C(17)	108.03(16)	C(26)-C(27)-H(27)	121.5(19)
O(1)-C(16)-H(16)	117.8(13)	C(27)-C(28)-C(29)	119.3(2)
C(18)-C(16)-H(16)	111.1(13)	C(27)-C(28)-H(28)	125(2)
C(17)-C(16)-H(16)	96.3(14)	C(29)-C(28)-H(28)	115(2)
F(3)-C(17)-F(1)	106.73(17)	C(30)-C(29)-C(28)	119.91(19)
F(3)-C(17)-F(2)	105.74(17)	C(30)-C(29)-H(29)	121.6(13)
F(1)-C(17)-F(2)	106.15(17)	C(28)-C(29)-H(29)	117.5(13)
F(3)-C(17)-C(16)	112.75(17)	C(29)-C(30)-C(31)	120.4(2)
F(1)-C(17)-C(16)	111.89(17)	C(29)-C(30)-H(30)	122(3)
F(2)-C(17)-C(16)	113.07(17)	C(31)-C(30)-H(30)	117(3)
C(23)-C(18)-C(19)	118.84(18)	C(30)-C(31)-C(26)	120.3(2)
C(23)-C(18)-C(16)	121.50(17)	C(30)-C(31)-H(31)	118.0(15)
C(19)-C(18)-C(16)	119.65(17)	C(26)-C(31)-H(31)	121.4(15)
C(20)-C(19)-C(18)	120.72(19)	Cl(2)-C(41)-Cl(1)	112.0(2)
C(20)-C(19)-H(19)	120.8(16)	Cl(2)-C(41)-H(41A)	109(2)
C(18)-C(19)-H(19)	118.5(16)	Cl(1)-C(41)-H(41A)	109(2)
C(19)-C(20)-C(21)	120.0(2)	Cl(2)-C(41)-H(41B)	108.8(19)
C(19)-C(20)-H(20)	121(2)	Cl(1)-C(41)-H(41B)	102(2)
C(21)-C(20)-H(20)	118(2)	H(41A)-C(41)-H(41B)	115(3)
C(22)-C(21)-C(20)	119.9(2)		



**APPENDIX 4.9****X-ray Crystallographic Data for (*sp*)PdBr<sub>2</sub> (288)**Figure A.4.9.1 (*sp*)PdBr<sub>2</sub> (288).<sup>1,2</sup>

<sup>1</sup> (a) The numbering shown in Figure 4.9.1 differs from that in the crystallographic report. (b) The protons of the (–)-sparteine backbone in the side view are not shown.

<sup>2</sup> The crystallographic data have been deposited at the Cambridge Database (CCDC), 12 Union Road, Cambridge CB2 1EZ, UK and copies can be obtained on request, free of charge, by quoting the publication citation and the deposition number 298214.

*Crystal data and structure refinement for 288 (CCDC 298214).*

Empirical formula	C <sub>15</sub> H <sub>26</sub> N <sub>2</sub> Br <sub>2</sub> Pd • CH <sub>2</sub> Cl <sub>2</sub>
Formula weight	585.52
Crystallization solvent	Dichloromethane/pentane
Crystal habit	Blade
Crystal size	0.31 x 0.18 x 0.10 mm <sup>3</sup>
Crystal color	Dark red

#### *Data collection*

Type of diffractometer	Bruker SMART 1000
Wavelength	0.71073 Å MoKα
Data collection temperature	100(2) K
θ range for 19178 reflections used in lattice determination	2.64 to 37.85°
Unit cell dimensions	a = 8.8518(3) Å b = 14.7348(4) Å c = 15.4442(4) Å
Volume	2014.38(10) Å <sup>3</sup>
Z	4
Crystal system	Orthorhombic
Space group	P2 <sub>1</sub> 2 <sub>1</sub> 2 <sub>1</sub>
Density (calculated)	1.931 Mg/m <sup>3</sup>
F(000)	1152
Data collection program	Bruker SMART v5.630
θ range for data collection	1.91 to 38.18°
Completeness to θ = 38.18°	98.0 %
Index ranges	-15 ≤ h ≤ 15, -25 ≤ k ≤ 25, -26 ≤ l ≤ 26
Data collection scan type	ω scans at 7 φ settings
Data reduction program	Bruker SAINT v6.45A
Reflections collected	52177
Independent reflections	10756 [R <sub>int</sub> = 0.0625]
Absorption coefficient	5.154 mm <sup>-1</sup>
Absorption correction	SADABS
Max. and min. transmission	1.000000 and 0.647147

#### *Structure solution and refinement*

Structure solution program	Bruker XS v6.12
Primary solution method	Direct methods
Secondary solution method	Difference Fourier map
Hydrogen placement	Geometric positions
Structure refinement program	Bruker XL v6.12
Refinement method	Full matrix least-squares on F <sup>2</sup>
Data / restraints / parameters	10756 / 0 / 208
Treatment of hydrogen atoms	Riding
Goodness-of-fit on F <sup>2</sup>	1.046
Final R indices [I>2σ(I), 8371 reflections]	R1 = 0.0341, wR2 = 0.0526
R indices (all data)	R1 = 0.0565, wR2 = 0.0574
Type of weighting scheme used	Sigma
Weighting scheme used	w = 1/σ <sup>2</sup> (Fo <sup>2</sup> )
Max shift/error	0.002
Average shift/error	0.000
Absolute structure determination	Anomalous dispersion

Absolute structure parameter	0.011(4)
Largest diff. peak and hole	1.149 and -0.876 e. $\text{\AA}^{-3}$

*Special refinement details*

Refinement of  $F^2$  against ALL reflections. The weighted R-factor ( $wR$ ) and goodness of fit (S) are based on  $F^2$ , conventional R-factors (R) are based on F, with F set to zero for negative  $F^2$ . The threshold expression of  $F^2 > 2\sigma(F^2)$  is used only for calculating R-factors(gt) etc. and is not relevant to the choice of reflections for refinement. R-factors based on  $F^2$  are statistically about twice as large as those based on F, and R-factors based on ALL data will be even larger.

All esds (except the esd in the dihedral angle between two l.s. planes) are estimated using the full covariance matrix. The cell esds are taken into account individually in the estimation of esds in distances, angles and torsion angles; correlations between esds in cell parameters are only used when they are defined by crystal symmetry. An approximate (isotropic) treatment of cell esds is used for estimating esds involving l.s. planes.

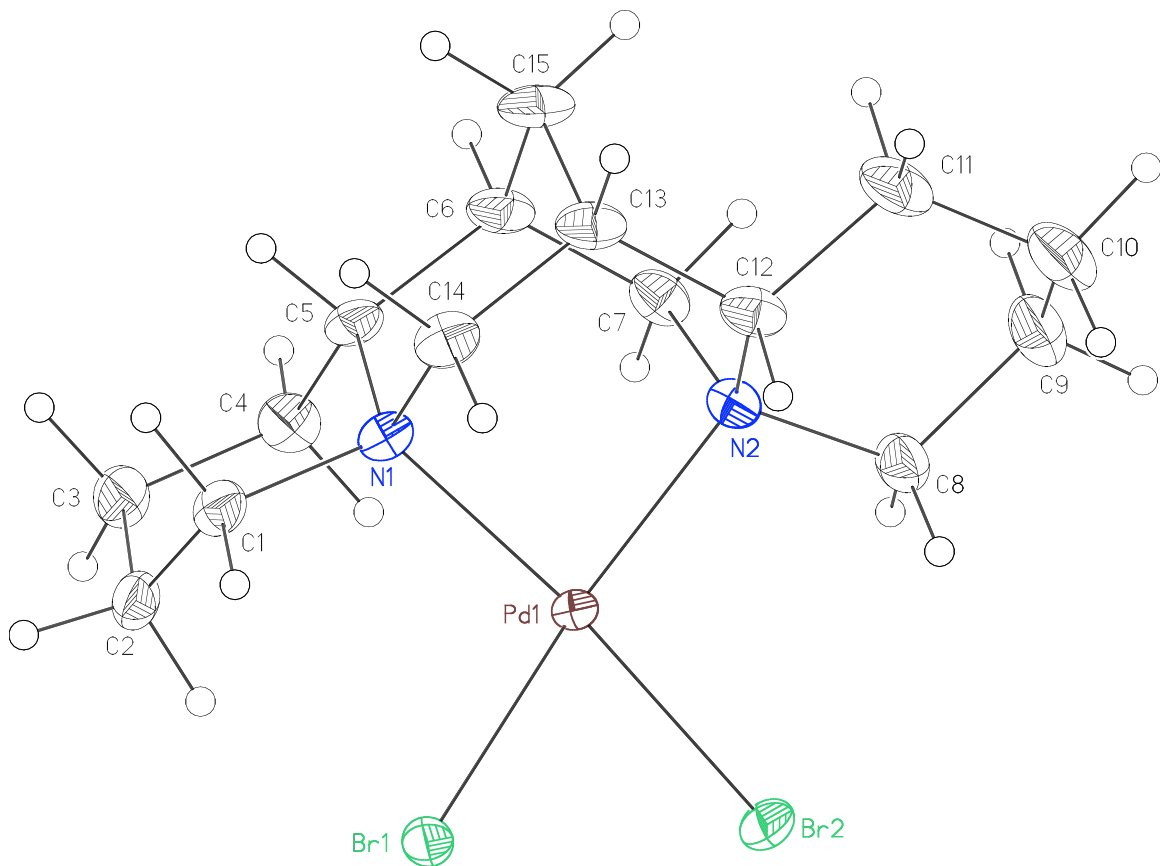


Figure A4.9.2 Molecule of **288**.

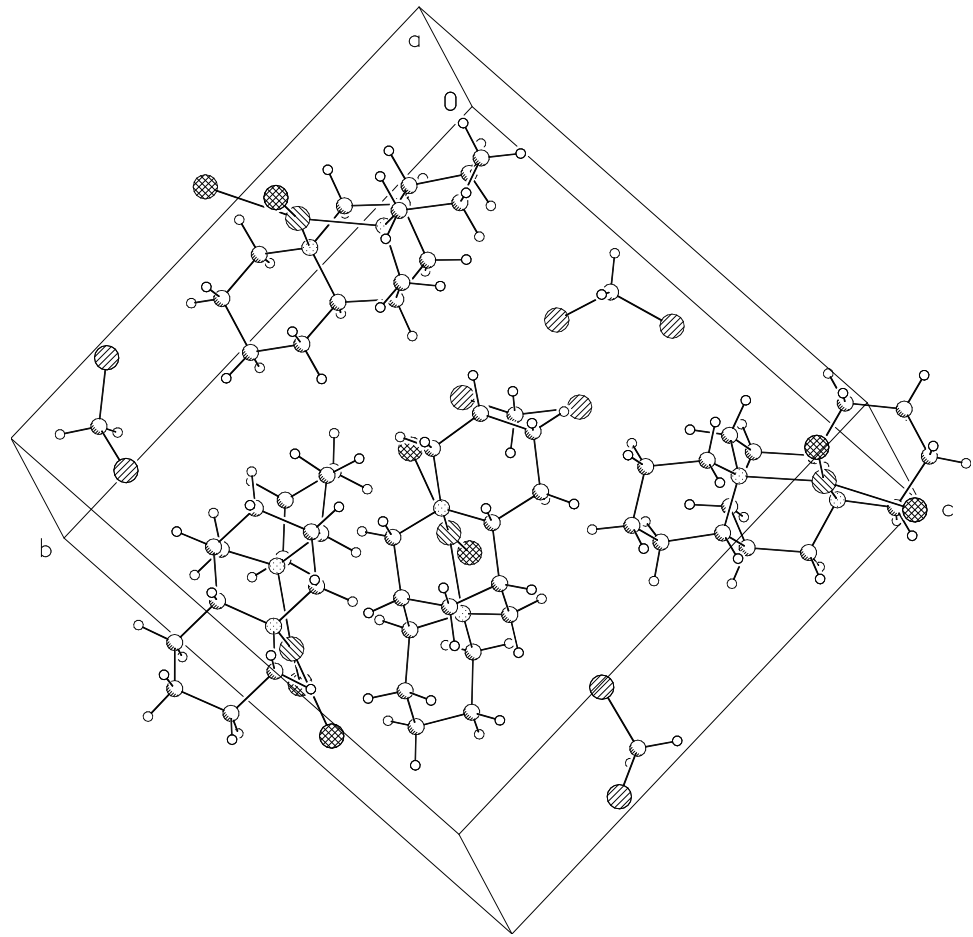


Figure A4.9.3 Unit cell contents of **288**.

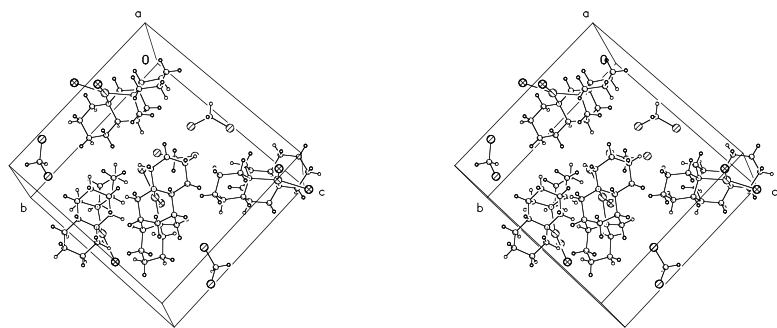


Figure A.4.9.4 Stereo view of unit cell contents of **288**.

Table A4.9.1 Atomic coordinates ( $\times 10^4$ ) and equivalent isotropic displacement parameters ( $\text{\AA}^2 \times 10^3$ ) for **288** (CCDC 298214).  $U(\text{eq})$  is defined as the trace of the orthogonalized  $U^{ij}$  tensor.

	x	y	z	$U_{\text{eq}}$	Occ
Pd(1)		3767(1)	1058(1)	9264(1)	13(1)
Br(1)		3925(1)	416(1)	10723(1)	23(1)
Br(2)		6528(1)	893(1)	9277(1)	24(1)
N(1)		1379(2)	984(1)	9210(1)	16(1)
N(2)		3661(2)	1931(1)	8150(1)	18(1)
C(1)		644(3)	382(2)	9876(2)	21(1)
C(2)		1012(3)	-618(2)	9760(2)	22(1)
C(3)		669(3)	-955(2)	8852(2)	26(1)
C(4)		1390(3)	-325(2)	8194(2)	23(1)
C(5)		844(3)	641(2)	8333(1)	20(1)
C(6)		1191(3)	1302(2)	7603(2)	23(1)
C(7)		2865(3)	1470(2)	7423(2)	21(1)
C(8)		5230(3)	2193(2)	7861(2)	24(1)
C(9)		5307(3)	2964(2)	7200(2)	32(1)
C(10)		4599(4)	3813(2)	7582(2)	35(1)
C(11)		2979(3)	3591(2)	7839(2)	32(1)
C(12)		2831(3)	2778(2)	8455(2)	22(1)
C(13)		1155(3)	2579(2)	8624(2)	24(1)
C(14)		831(2)	1933(2)	9368(2)	22(1)
C(15)		410(3)	2204(2)	7805(2)	28(1)
C(20)		8408(3)	1359(2)	5322(2)	36(1)
Cl(1)		7393(1)	2244(1)	4808(1)	38(1)
Cl(2)	7559(1)	1047(1)	6310(1)	36(1)	

Table A4.9.2 Selected bond lengths [ $\text{\AA}$ ] and angles [ $^\circ$ ] for **288** (CCDC 298214).

Pd(1)-N(1)	2.1184(16)	N(1)-Pd(1)-N(2)	87.43(7)
Pd(1)-N(2)	2.1510(18)	N(1)-Pd(1)-Br(1)	94.22(5)
Pd(1)-Br(1)	2.4474(3)	N(2)-Pd(1)-Br(1)	165.96(5)
Pd(1)-Br(2)	2.4560(3)	N(1)-Pd(1)-Br(2)	171.20(5)
		N(2)-Pd(1)-Br(2)	96.25(5)
		Br(1)-Pd(1)-Br(2)	84.155(10)

Table A4.9.3 Bond lengths [ $\text{\AA}$ ] and angles [ $^\circ$ ] for **288** (CCDC 298214).

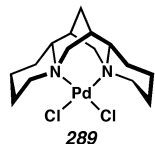
Pd(1)-N(1)	2.1184(16)	N(1)-C(14)	1.501(3)
Pd(1)-N(2)	2.1510(18)	N(1)-C(1)	1.506(3)
Pd(1)-Br(1)	2.4474(3)	N(1)-C(5)	1.520(3)
Pd(1)-Br(2)	2.4560(3)	N(2)-C(7)	1.490(3)

N(2)-C(8)	1.509(3)	C(7)-N(2)-C(8)	109.20(18)
N(2)-C(12)	1.522(3)	C(7)-N(2)-C(12)	112.30(18)
C(1)-C(2)	1.519(4)	C(8)-N(2)-C(12)	109.03(18)
C(2)-C(3)	1.518(3)	C(7)-N(2)-Pd(1)	110.53(14)
C(3)-C(4)	1.517(4)	C(8)-N(2)-Pd(1)	110.43(14)
C(4)-C(5)	1.518(3)	C(12)-N(2)-Pd(1)	105.30(14)
C(5)-C(6)	1.522(3)	N(1)-C(1)-C(2)	113.45(19)
C(6)-C(7)	1.528(4)	C(1)-C(2)-C(3)	112.5(2)
C(6)-C(15)	1.531(3)	C(4)-C(3)-C(2)	109.52(19)
C(8)-C(9)	1.529(4)	C(3)-C(4)-C(5)	110.2(2)
C(9)-C(10)	1.518(4)	C(6)-C(5)-N(1)	112.60(18)
C(10)-C(11)	1.524(4)	C(6)-C(5)-C(4)	115.5(2)
C(11)-C(12)	1.536(4)	N(1)-C(5)-C(4)	109.79(18)
C(12)-C(13)	1.535(4)	C(5)-C(6)-C(7)	115.74(19)
C(13)-C(14)	1.519(4)	C(5)-C(6)-C(15)	108.3(2)
C(13)-C(15)	1.530(4)	C(7)-C(6)-C(15)	109.6(2)
C(20)-Cl(2)	1.761(3)	N(2)-C(7)-C(6)	113.26(19)
C(20)-Cl(1)	1.771(3)	N(2)-C(8)-C(9)	115.4(2)
		C(10)-C(9)-C(8)	109.5(2)
N(1)-Pd(1)-N(2)	87.43(7)	C(9)-C(10)-C(11)	108.2(2)
N(1)-Pd(1)-Br(1)	94.22(5)	C(10)-C(11)-C(12)	114.1(2)
N(2)-Pd(1)-Br(1)	165.96(5)	N(2)-C(12)-C(11)	114.0(2)
N(1)-Pd(1)-Br(2)	171.20(5)	N(2)-C(12)-C(13)	111.27(19)
N(2)-Pd(1)-Br(2)	96.25(5)	C(11)-C(12)-C(13)	109.6(2)
Br(1)-Pd(1)-Br(2)	84.155(10)	C(14)-C(13)-C(15)	108.6(2)
C(14)-N(1)-C(1)	107.33(18)	C(14)-C(13)-C(12)	115.46(19)
C(14)-N(1)-C(5)	110.77(18)	C(15)-C(13)-C(12)	110.2(2)
C(1)-N(1)-C(5)	106.14(17)	N(1)-C(14)-C(13)	113.54(19)
C(14)-N(1)-Pd(1)	105.53(13)	C(13)-C(15)-C(6)	106.70(19)
C(1)-N(1)-Pd(1)	115.73(13)	Cl(2)-C(20)-Cl(1)	111.38(16)
C(5)-N(1)-Pd(1)	111.30(13)		

**APPENDIX 4.10**

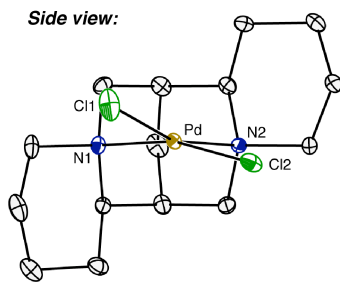
*X-ray Crystallographic Data for  
( $\alpha$ -isosp)PdCl<sub>2</sub> (**289**)*

Figure A4.10.1 ( $\alpha$ -isosp)PdCl<sub>2</sub> (**289**).<sup>1,2</sup>

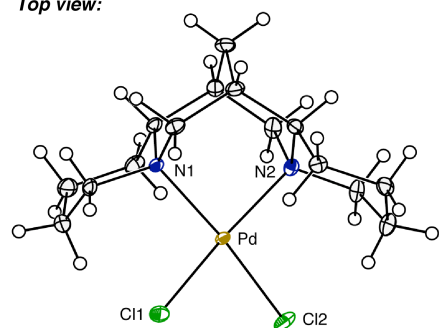


Selected bond lengths (Å) and angles (°)	
Pd–N1	2.1091(11)
Pd–N2	2.1271(12)
Pd–Cl1	2.3275(4)
Pd–Cl2	2.3140(3)
N1–Pd–N2	87.23(4)°
C11–Pd–Cl2	82.205(15)°
N1–Pd–Cl2	166.25(4)°
N2–Pd–Cl1	163.54(3)°

Side view:



Top view:



<sup>1</sup> The protons of the (–)- $\alpha$ -sparteine backbone in the side view are not shown.

<sup>2</sup> The crystallographic data have been deposited at the Cambridge Database (CCDC), 12 Union Road, Cambridge CB2 1EZ, UK and copies can be obtained on request, free of charge, by quoting the publication citation and the deposition number 223628.

*Crystal data and structure refinement for 289 (CCDC 223628).*

Empirical formula	C <sub>15</sub> H <sub>26</sub> Cl <sub>2</sub> N <sub>2</sub> Pd
Formula weight	411.68
Crystallization solvent	Dichloromethane
Crystal habit	Fragment
Crystal size	0.39 x 0.24 x 0.22 mm <sup>3</sup>
Crystal color	Maroon

#### *Data collection*

Preliminary photos	Rotation
Type of diffractometer	Bruker SMART 1000
Wavelength	0.71073 Å MoKα
Data collection temperature	100(2) K
θ range for 24049 reflections used in lattice determination	2.22 to 44.96°
Unit cell dimensions	a = 9.2815(3) Å b = 11.4873(4) Å c = 15.1073(5) Å 1610.73(9) Å <sup>3</sup>
Volume	4
Z	Orthorhombic
Crystal system	P2 <sub>1</sub> 2 <sub>1</sub> 2 <sub>1</sub>
Space group	1.698 Mg/m <sup>3</sup>
Density (calculated)	840
F(000)	Bruker SMART v5.054
Data collection program	2.23 to 44.97°
θ range for data collection	94.4 %
Completeness to θ = 44.97°	-17 ≤ h ≤ 16, -22 ≤ k ≤ 20, -28 ≤ l ≤ 29
Index ranges	ω scans at 7 φ settings
Data collection scan type	Bruker SAINT v6.45
Data reduction program	44470
Reflections collected	11830 [R <sub>int</sub> = 0.0673]
Independent reflections	1.476 mm <sup>-1</sup>
Absorption coefficient	None
Absorption correction	0.7372 and 0.5968
Max. and min. transmission (predicted)	

#### *Structure solution and refinement*

Structure solution program	SHELXS-97 (Sheldrick, 1990)
Primary solution method	Direct methods
Secondary solution method	Difference Fourier map
Hydrogen placement	Difference Fourier map
Structure refinement program	SHELXL-97 (Sheldrick, 1997)
Refinement method	Full-matrix least-squares on F <sup>2</sup>
Data / restraints / parameters	11830 / 0 / 285
Treatment of hydrogen atoms	Unrestrained
Goodness-of-fit on F <sup>2</sup>	1.139
Final R indices [I>2σ(I), 9732 reflections]	R1 = 0.0317, wR2 = 0.0525
R indices (all data)	R1 = 0.0452, wR2 = 0.0542
Type of weighting scheme used	Sigma
Weighting scheme used	w = 1/σ <sup>2</sup> (Fo <sup>2</sup> )
Max shift/error	0.004
Average shift/error	0.000

Absolute structure parameter	-0.042(13)
Largest diff. peak and hole	1.557 and -1.497 e. $\text{\AA}^{-3}$

*Special refinement details*

Refinement of  $F^2$  against ALL reflections. The weighted R-factor ( $wR$ ) and goodness of fit (S) are based on  $F^2$ , conventional R-factors (R) are based on F, with F set to zero for negative  $F^2$ . The threshold expression of  $F^2 > 2\sigma(F^2)$  is used only for calculating R-factors(gt) etc. and is not relevant to the choice of reflections for refinement. R-factors based on  $F^2$  are statistically about twice as large as those based on F, and R-factors based on ALL data will be even larger.

All esds (except the esd in the dihedral angle between two l.s. planes) are estimated using the full covariance matrix. The cell esds are taken into account individually in the estimation of esds in distances, angles and torsion angles; correlations between esds in cell parameters are only used when they are defined by crystal symmetry. An approximate (isotropic) treatment of cell esds is used for estimating esds involving l.s. planes.

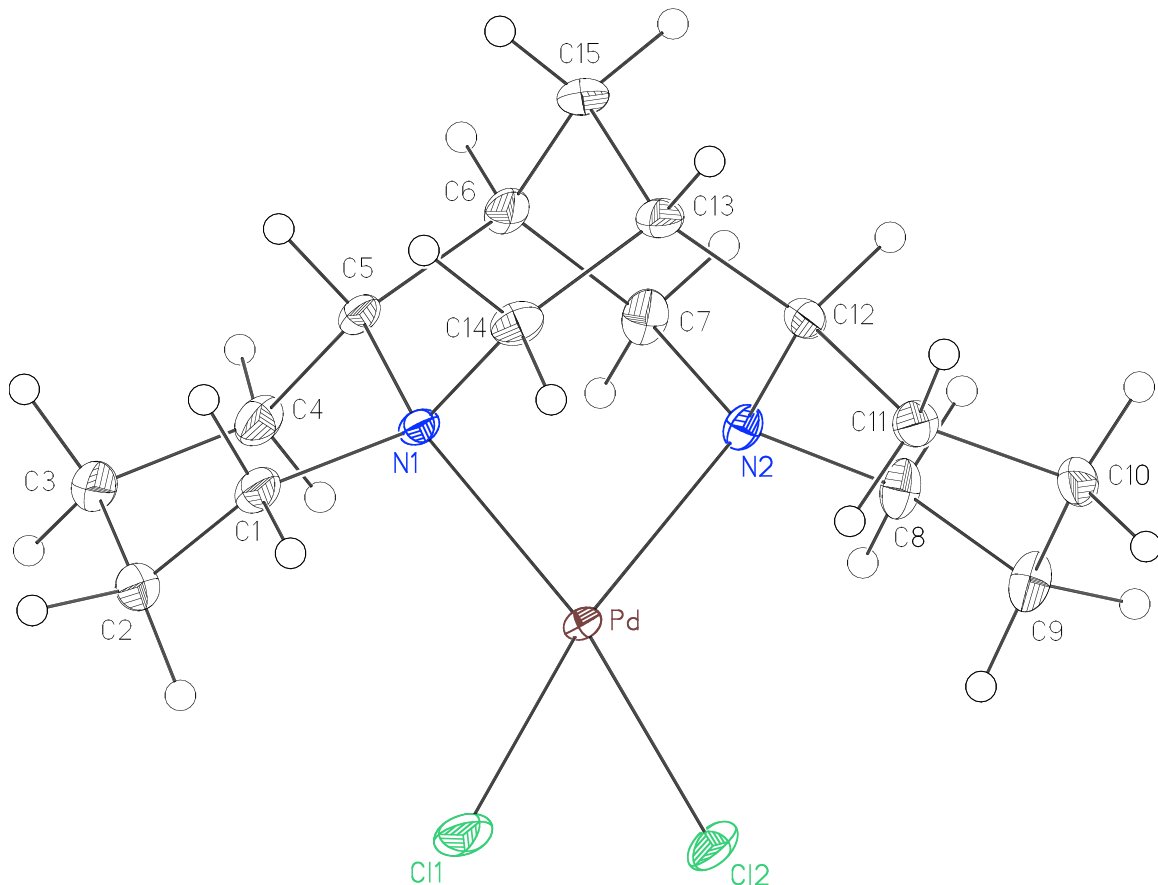


Figure A4.10.2 Molecule of **289**.

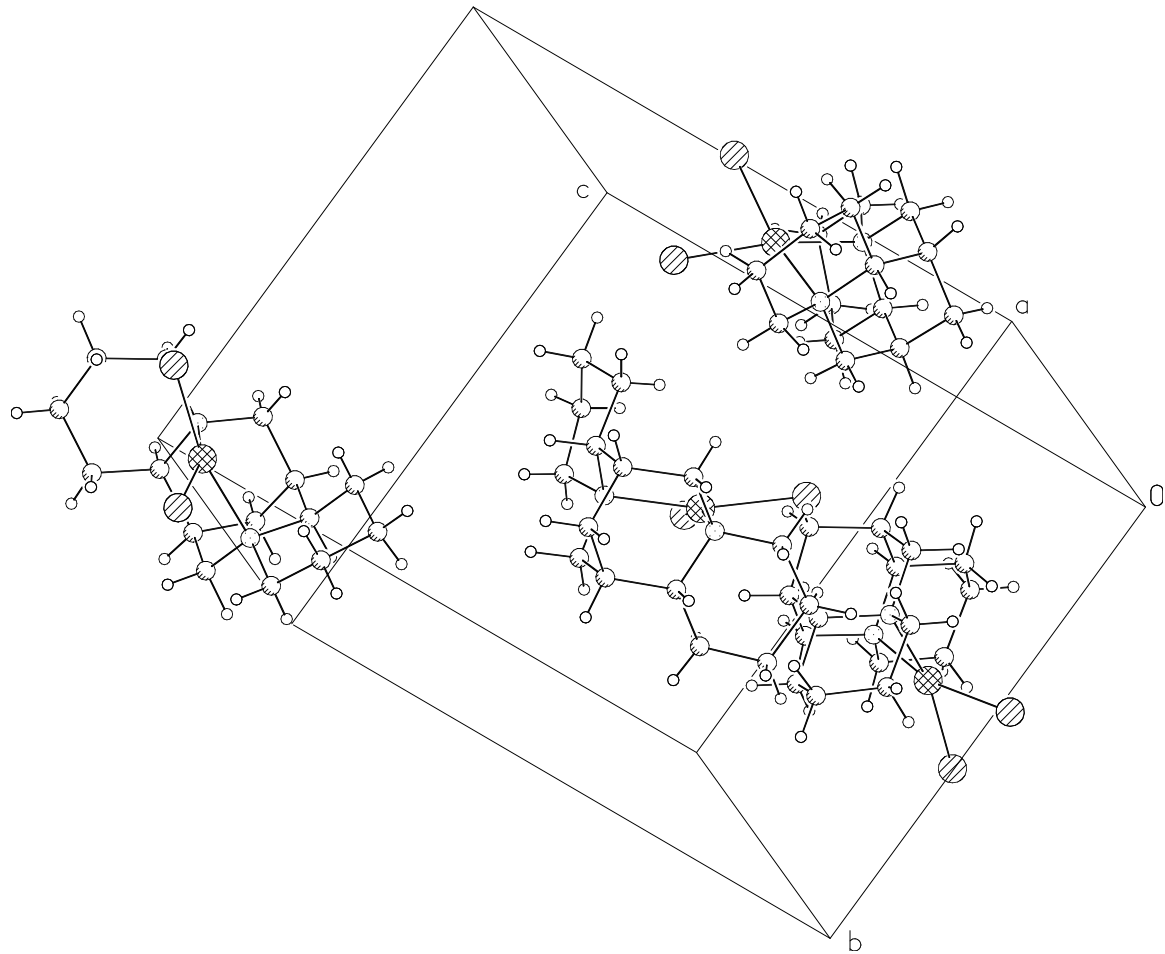


Figure A4.10.3. Unit cell contents of **289**.

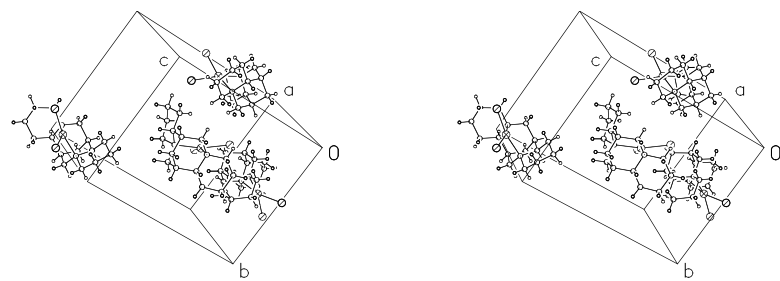


Figure A.4.10.4. Stereo view of unit cell contents of **289**.

Table A4.10.1 Atomic coordinates ( $\times 10^4$ ) and equivalent isotropic displacement parameters ( $\text{\AA}^2 \times 10^3$ ) for **289** (CCDC 223628).  $U(\text{eq})$  is defined as the trace of the orthogonalized  $U^{ij}$  tensor.

	x	y	z	$U_{\text{eq}}$	Occ
Pd	8074(1)	9581(1)	9899(1)	9(1)	
Cl(1)	5914(1)	10226(1)	10509(1)	25(1)	
Cl(2)	8225(1)	8352(1)	11109(1)	17(1)	
N(1)	7712(1)	10349(1)	8651(1)	10(1)	
N(2)	10275(1)	9425(1)	9527(1)	11(1)	
C(1)	6155(2)	10652(2)	8468(1)	16(1)	
C(2)	5171(2)	9593(2)	8410(1)	20(1)	
C(3)	5708(2)	8687(2)	7757(1)	20(1)	
C(4)	7288(2)	8421(1)	7942(1)	16(1)	
C(5)	8165(2)	9540(1)	7909(1)	11(1)	
C(6)	9799(2)	9345(1)	7888(1)	14(1)	
C(7)	10412(2)	8730(1)	8691(1)	15(1)	
C(8)	11240(2)	8851(1)	10201(1)	16(1)	
C(9)	11421(2)	9531(2)	11058(1)	17(1)	
C(10)	11851(2)	10792(1)	10907(1)	15(1)	
C(11)	10843(2)	11343(1)	10230(1)	14(1)	
C(12)	10868(2)	10639(1)	9376(1)	12(1)	
C(13)	10186(2)	11238(1)	8575(1)	15(1)	
C(14)	8566(2)	11450(1)	8618(1)	14(1)	
C(15)	10533(2)	10518(2)	7753(1)	18(1)	

Table A4.10.2 Selected bond lengths [ $\text{\AA}$ ] and angles [ $^\circ$ ] for **289** (CCDC 223628).

Pd-N(1)	2.1091(11)	N(1)-Pd-N(2)	87.23(4)
Pd-N(2)	2.1271(12)	N(1)-Pd-Cl(2)	166.25(4)
Pd-Cl(2)	2.3140(3)	N(2)-Pd-Cl(2)	95.68(3)
Pd-Cl(1)	2.3275(4)	N(1)-Pd-Cl(1)	94.81(3)
		N(2)-Pd-Cl(1)	163.54(3)
		Cl(2)-Pd-Cl(1)	86.205(15)

Table A4.10.3 Bond lengths [ $\text{\AA}$ ] and angles [ $^\circ$ ] for **289** (CCDC 223628).

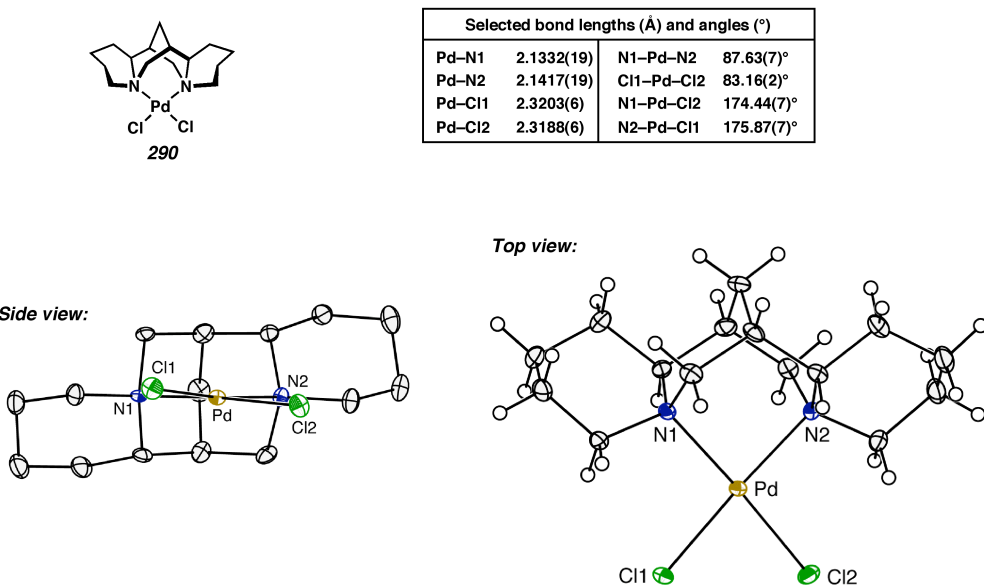
Pd-N(1)	2.1091(11)	N(2)-C(8)	1.5078(18)
Pd-N(2)	2.1271(12)	N(2)-C(12)	1.5166(19)
Pd-Cl(2)	2.3140(3)	C(1)-C(2)	1.524(2)
Pd-Cl(1)	2.3275(4)	C(1)-H(1A)	0.886(18)
N(1)-C(14)	1.493(2)	C(1)-H(1B)	0.896(18)
N(1)-C(1)	1.5118(18)	C(2)-C(3)	1.519(2)
N(1)-C(5)	1.5158(17)	C(2)-H(2A)	0.94(2)
N(2)-C(7)	1.4998(18)	C(2)-H(2B)	0.95(2)

C(3)-C(4)	1.523(2)	N(1)-C(1)-C(2)	113.55(13)
C(3)-H(3A)	0.96(2)	N(1)-C(1)-H(1A)	107.7(11)
C(3)-H(3B)	0.97(2)	C(2)-C(1)-H(1A)	109.5(11)
C(4)-C(5)	1.522(2)	N(1)-C(1)-H(1B)	106.9(12)
C(4)-H(4A)	0.83(2)	C(2)-C(1)-H(1B)	112.8(12)
C(4)-H(4B)	0.960(18)	H(1A)-C(1)-H(1B)	106.1(16)
C(5)-C(6)	1.534(2)	C(3)-C(2)-C(1)	112.83(13)
C(5)-H(5)	0.993(15)	C(3)-C(2)-H(2A)	110.5(12)
C(6)-C(7)	1.515(2)	C(1)-C(2)-H(2A)	111.9(12)
C(6)-C(15)	1.524(2)	C(3)-C(2)-H(2B)	106.9(14)
C(6)-H(6)	0.951(17)	C(1)-C(2)-H(2B)	110.0(15)
C(7)-H(7A)	0.931(17)	H(2A)-C(2)-H(2B)	104.1(18)
C(7)-H(7B)	0.918(18)	C(2)-C(3)-C(4)	109.51(13)
C(8)-C(9)	1.521(2)	C(2)-C(3)-H(3A)	110.5(12)
C(8)-H(8A)	0.954(16)	C(4)-C(3)-H(3A)	108.0(12)
C(8)-H(8B)	0.960(18)	C(2)-C(3)-H(3B)	114.0(13)
C(9)-C(10)	1.519(2)	C(4)-C(3)-H(3B)	109.6(13)
C(9)-H(9A)	0.912(18)	H(3A)-C(3)-H(3B)	104.9(17)
C(9)-H(9B)	0.98(2)	C(5)-C(4)-C(3)	109.83(13)
C(10)-C(11)	1.524(2)	C(5)-C(4)-H(4A)	110.6(16)
C(10)-H(10A)	0.90(2)	C(3)-C(4)-H(4A)	113.9(16)
C(10)-H(10B)	0.958(19)	C(5)-C(4)-H(4B)	107.3(12)
C(11)-C(12)	1.522(2)	C(3)-C(4)-H(4B)	113.6(12)
C(11)-H(11A)	0.984(19)	H(4A)-C(4)-H(4B)	101.3(19)
C(11)-H(11B)	0.926(16)	N(1)-C(5)-C(4)	110.18(11)
C(12)-C(13)	1.530(2)	N(1)-C(5)-C(6)	112.27(11)
C(12)-H(12)	1.005(19)	C(4)-C(5)-C(6)	113.98(12)
C(13)-C(14)	1.525(2)	N(1)-C(5)-H(5)	107.3(9)
C(13)-C(15)	1.527(2)	C(4)-C(5)-H(5)	106.9(9)
C(13)-H(13)	0.948(18)	C(6)-C(5)-H(5)	105.8(9)
C(14)-H(14A)	1.002(18)	C(7)-C(6)-C(15)	110.60(13)
C(14)-H(14B)	1.035(18)	C(7)-C(6)-C(5)	115.02(12)
C(15)-H(15A)	0.914(19)	C(15)-C(6)-C(5)	108.41(12)
C(15)-H(15B)	1.00(2)	C(7)-C(6)-H(6)	106.6(11)
		C(15)-C(6)-H(6)	107.0(10)
N(1)-Pd-N(2)	87.23(4)	C(5)-C(6)-H(6)	108.9(11)
N(1)-Pd-Cl(2)	166.25(4)	N(2)-C(7)-C(6)	113.23(12)
N(2)-Pd-Cl(2)	95.68(3)	N(2)-C(7)-H(7A)	104.9(11)
N(1)-Pd-Cl(1)	94.81(3)	C(6)-C(7)-H(7A)	111.9(11)
N(2)-Pd-Cl(1)	163.54(3)	N(2)-C(7)-H(7B)	106.2(12)
Cl(2)-Pd-Cl(1)	86.205(15)	C(6)-C(7)-H(7B)	109.5(12)
C(14)-N(1)-C(1)	107.82(12)	H(7A)-C(7)-H(7B)	110.9(16)
C(14)-N(1)-C(5)	110.34(11)	N(2)-C(8)-C(9)	114.61(12)
C(1)-N(1)-C(5)	105.75(11)	N(2)-C(8)-H(8A)	108.4(10)
C(14)-N(1)-Pd	107.43(8)	C(9)-C(8)-H(8A)	103.4(10)
C(1)-N(1)-Pd	114.30(8)	N(2)-C(8)-H(8B)	107.5(11)
C(5)-N(1)-Pd	111.15(8)	C(9)-C(8)-H(8B)	109.8(10)
C(7)-N(2)-C(8)	106.63(11)	H(8A)-C(8)-H(8B)	113.2(14)
C(7)-N(2)-C(12)	109.41(11)	C(10)-C(9)-C(8)	112.99(13)
C(8)-N(2)-C(12)	106.75(11)	C(10)-C(9)-H(9A)	116.9(11)
C(7)-N(2)-Pd	110.42(9)	C(8)-C(9)-H(9A)	103.0(11)
C(8)-N(2)-Pd	115.36(9)	C(10)-C(9)-H(9B)	108.9(12)
C(12)-N(2)-Pd	108.11(8)	C(8)-C(9)-H(9B)	109.3(12)

H(9A)-C(9)-H(9B)	105.2(16)	C(14)-C(13)-C(15)	109.20(13)
C(9)-C(10)-C(11)	109.62(12)	C(14)-C(13)-C(12)	116.51(12)
C(9)-C(10)-H(10A)	112.2(13)	C(15)-C(13)-C(12)	108.23(13)
C(11)-C(10)-H(10A)	107.2(13)	C(14)-C(13)-H(13)	102.9(11)
C(9)-C(10)-H(10B)	113.3(12)	C(15)-C(13)-H(13)	114.0(11)
C(11)-C(10)-H(10B)	108.3(12)	C(12)-C(13)-H(13)	106.0(11)
H(10A)-C(10)-H(10B)	105.9(17)	N(1)-C(14)-C(13)	112.95(12)
C(12)-C(11)-C(10)	109.79(12)	N(1)-C(14)-H(14A)	108.7(11)
C(12)-C(11)-H(11A)	110.3(11)	C(13)-C(14)-H(14A)	116.2(11)
C(10)-C(11)-H(11A)	111.9(11)	N(1)-C(14)-H(14B)	103.8(10)
C(12)-C(11)-H(11B)	107.6(12)	C(13)-C(14)-H(14B)	113.9(11)
C(10)-C(11)-H(11B)	109.8(11)	H(14A)-C(14)-H(14B)	99.9(14)
H(11A)-C(11)-H(11B)	107.4(15)	C(6)-C(15)-C(13)	106.02(12)
N(2)-C(12)-C(11)	110.83(11)	C(6)-C(15)-H(15A)	110.8(12)
N(2)-C(12)-C(13)	112.49(12)	C(13)-C(15)-H(15A)	109.4(12)
C(11)-C(12)-C(13)	115.15(12)	C(6)-C(15)-H(15B)	108.0(13)
N(2)-C(12)-H(12)	104.7(11)	C(13)-C(15)-H(15B)	111.3(12)
C(11)-C(12)-H(12)	102.6(11)	H(15A)-C(15)-H(15B)	111.2(17)
C(13)-C(12)-H(12)	110.1(10)		

---



**APPENDIX 4.11***X-ray Crystallographic Data for  
( $\beta$ -isosp)PdCl<sub>2</sub> (**290**)*Figure A4.11.1 ( $\beta$ -isosp)PdCl<sub>2</sub> (**290**).<sup>1,2</sup><sup>1</sup> The protons of the (+)- $\beta$ -sparteine backbone in the side view are not shown.<sup>2</sup> The crystallographic data have been deposited at the Cambridge Database (CCDC), 12 Union Road, Cambridge CB2 1EZ, UK and copies can be obtained on request, free of charge, by quoting the publication citation and the deposition number 294052.

*Crystal data and structure refinement for 290 (CCDC 294052).*

Empirical formula	C <sub>15</sub> H <sub>26</sub> N <sub>2</sub> Cl <sub>2</sub> Pd • CH <sub>2</sub> Cl <sub>2</sub>
Formula weight	496.60
Crystallization solvent	Dichloromethane/pentane
Crystal habit	Fragment
Crystal size	0.26 x 0.20 x 0.11 mm <sup>3</sup>
Crystal color	Orange

#### *Data collection*

Type of diffractometer	Bruker SMART 1000
Wavelength	0.71073 Å MoKα
Data collection temperature	100(2) K
θ range for 11706 reflections used in lattice determination	2.47 to 39.14°
Unit cell dimensions	a = 9.7607(3) Å b = 12.7153(4) Å c = 15.4067(5) Å 1912.13(10) Å <sup>3</sup>
Volume	1912.13(10) Å <sup>3</sup>
Z	4
Crystal system	Orthorhombic
Space group	P2 <sub>1</sub> 2 <sub>1</sub> 2 <sub>1</sub>
Density (calculated)	1.725 Mg/m <sup>3</sup>
F(000)	1008
Data collection program	Bruker SMART v5.630
θ range for data collection	2.08 to 40.49°
Completeness to θ = 40.49°	94.5 %
Index ranges	-12 ≤ h ≤ 17, -22 ≤ k ≤ 22, -25 ≤ l ≤ 28
Data collection scan type	ω scans at 5 φ settings
Data reduction program	Bruker SAINT v6.45A
Reflections collected	35980
Independent reflections	11125 [R <sub>int</sub> = 0.0912]
Absorption coefficient	1.530 mm <sup>-1</sup>
Absorption correction	None
Max. and min. transmission	0.8498 and 0.6918

#### *Structure solution and refinement*

Structure solution program	Bruker XS v6.12
Primary solution method	Direct methods
Secondary solution method	Difference Fourier map
Hydrogen placement	Geometric positions
Structure refinement program	Bruker XL v6.12
Refinement method	Full matrix least-squares on F <sup>2</sup>
Data / restraints / parameters	11125 / 0 / 208
Treatment of hydrogen atoms	Riding
Goodness-of-fit on F <sup>2</sup>	1.108
Final R indices [I>2σ(I), 7904 reflections]	R1 = 0.0466, wR2 = 0.0737
R indices (all data)	R1 = 0.0766, wR2 = 0.0788
Type of weighting scheme used	Sigma
Weighting scheme used	w=1/σ <sup>2</sup> (Fo <sup>2</sup> )
Max shift/error	0.001
Average shift/error	0.000
Absolute structure determination	Anomalous dispersion

Absolute structure parameter	-0.01(3)
Largest diff. peak and hole	2.815 and -2.630 e. $\text{\AA}^{-3}$

#### Special refinement details

All prominent peaks in the final electron density difference Fourier map all lie near the metal center. Refinement of  $F^2$  against ALL reflections. The weighted R-factor ( $wR$ ) and goodness of fit (S) are based on  $F^2$ , conventional R-factors (R) are based on F, with F set to zero for negative  $F^2$ . The threshold expression of  $F^2 > 2\sigma(F^2)$  is used only for calculating R-factors(gt) etc. and is not relevant to the choice of reflections for refinement. R-factors based on  $F^2$  are statistically about twice as large as those based on F, and R-factors based on ALL data will be even larger.

All esds (except the esd in the dihedral angle between two l.s. planes) are estimated using the full covariance matrix. The cell esds are taken into account individually in the estimation of esds in distances, angles and torsion angles; correlations between esds in cell parameters are only used when they are defined by crystal symmetry. An approximate (isotropic) treatment of cell esds is used for estimating esds involving l.s. planes.

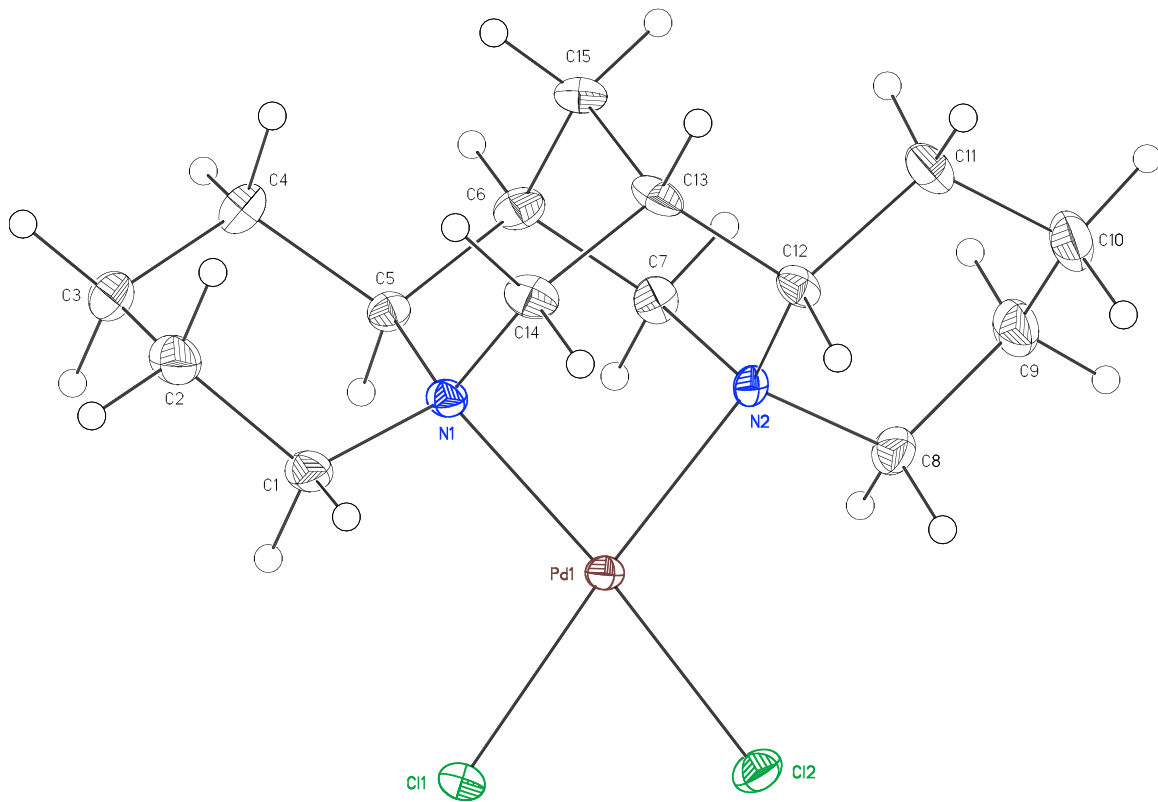


Figure A4.11.2 Molecule of 290.

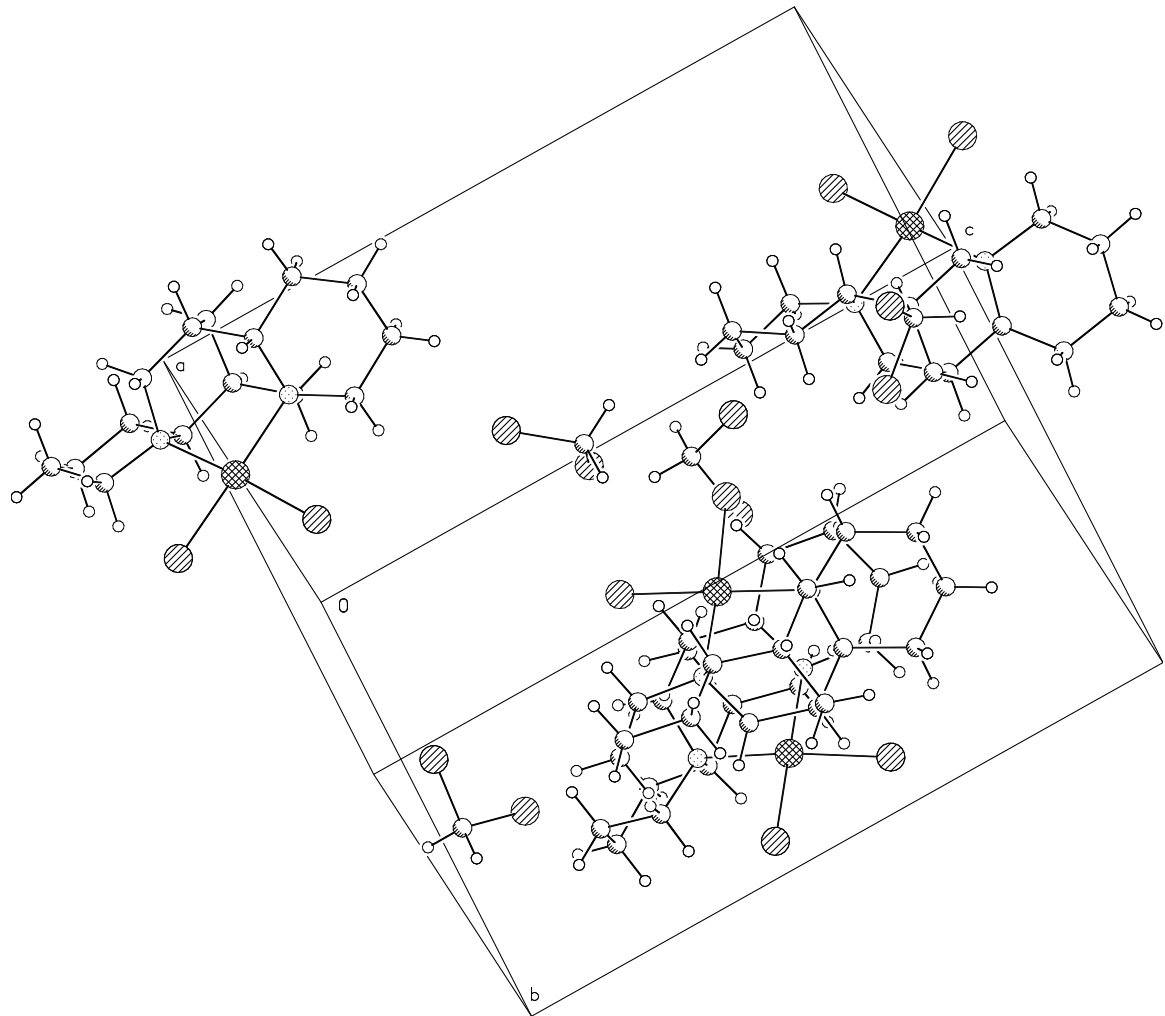


Figure A4.11.3. Unit cell contents of **290**.

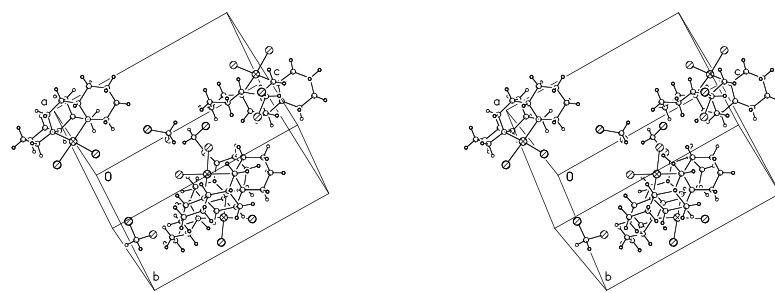


Figure A4.11.4. Stereo view of unit cell contents of **290**.

Table A4.11.1 Atomic coordinates ( $\times 10^4$ ) and equivalent isotropic displacement parameters ( $\text{\AA}^2 \times 10^3$ ) for **290** (CCDC 294052).  $U(\text{eq})$  is defined as the trace of the orthogonalized  $U^{ij}$  tensor.

	x	y	z	$U_{\text{eq}}$	Occ
Pd(1)		4881(1)	2156(1)	9829(1)	10(1)
Cl(1)		4734(1)	554(1)	9114(1)	17(1)
Cl(2)		5018(1)	1099(1)	11053(1)	18(1)
N(1)		4943(3)	3067(1)	8668(1)	12(1)
N(2)		4881(3)	3606(2)	10536(1)	10(1)
C(1)		4896(4)	2372(2)	7869(2)	18(1)
C(2)		5211(3)	2926(2)	7018(2)	21(1)
C(3)		6655(3)	3363(2)	7057(2)	23(1)
C(4)		6732(3)	4144(2)	7809(2)	18(1)
C(5)		6297(3)	3657(2)	8687(2)	13(1)
C(6)		6265(3)	4529(2)	9378(2)	17(1)
C(7)		6208(3)	4133(2)	10316(2)	14(1)
C(8)		4870(4)	3398(2)	11498(2)	17(1)
C(9)		4676(3)	4375(2)	12058(2)	22(1)
C(10)		3336(3)	4922(3)	11835(2)	24(1)
C(11)		3360(3)	5186(2)	10876(2)	20(1)
C(12)		3639(3)	4234(2)	10284(2)	13(1)
C(13)		3746(3)	4621(2)	9340(2)	17(1)
C(14)		3719(3)	3764(2)	8653(2)	16(1)
C(15)		5064(3)	5271(2)	9211(2)	19(1)
Cl(3)		-896(1)	2192(1)	5659(1)	34(1)
Cl(4)		1894(1)	1994(1)	6342(1)	30(1)
C(16)		757(4)	1632(3)	5514(2)	29(1)

Table A4.11.2 Selected bond lengths [ $\text{\AA}$ ] and angles [ $^\circ$ ] for **290** (CCDC 294052).

Pd(1)-N(1)	2.1332(19)	N(1)-Pd(1)-N(2)	87.63(7)
Pd(1)-N(2)	2.1417(19)	N(1)-Pd(1)-Cl(2)	174.44(7)
Pd(1)-Cl(2)	2.3188(6)	N(2)-Pd(1)-Cl(2)	94.93(6)
Pd(1)-Cl(1)	2.3203(6)	N(1)-Pd(1)-Cl(1)	94.60(5)
		N(2)-Pd(1)-Cl(1)	175.87(7)
		Cl(2)-Pd(1)-Cl(1)	83.16(2)

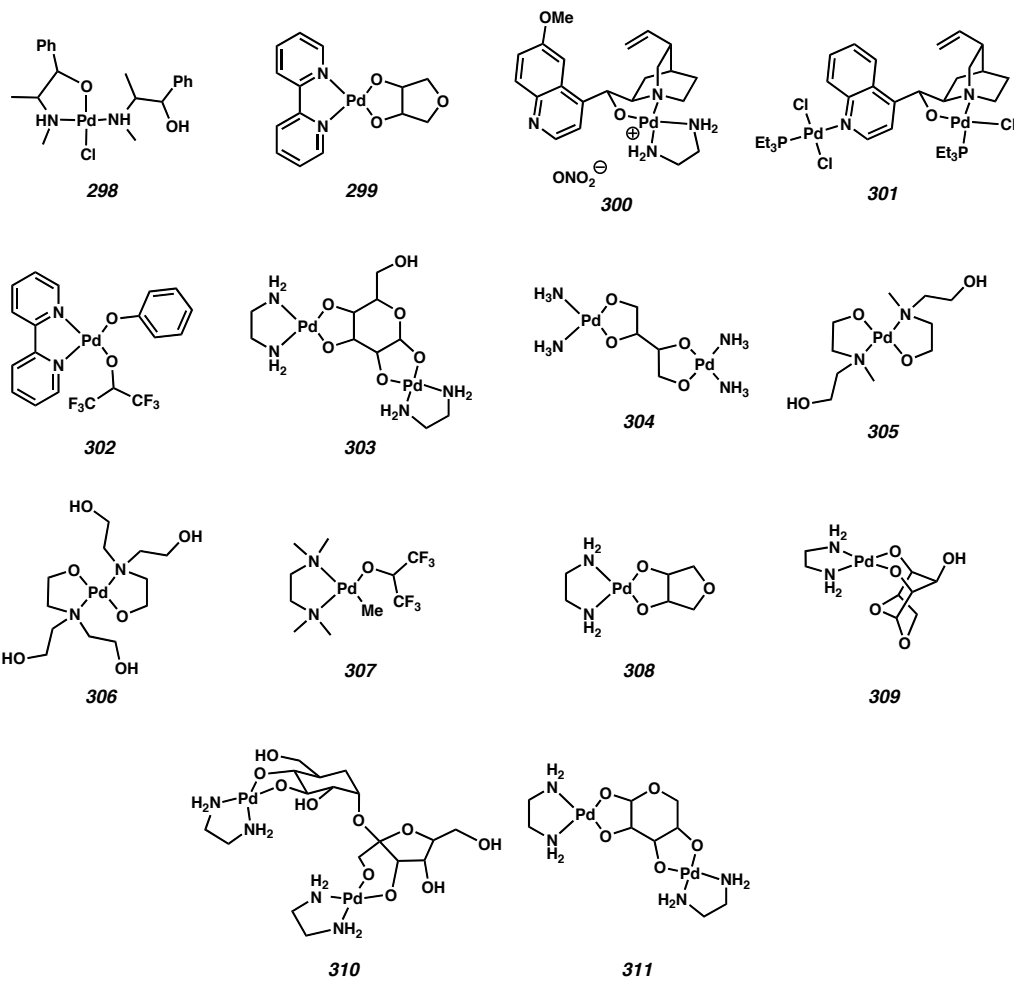
Table A4.11.3 Bond lengths [ $\text{\AA}$ ] and angles [ $^\circ$ ] for **290** (CCDC 294052).

Pd(1)-N(1)	2.1332(19)	N(1)-C(14)	1.488(4)
Pd(1)-N(2)	2.1417(19)	N(1)-C(1)	1.516(3)
Pd(1)-Cl(2)	2.3188(6)	N(1)-C(5)	1.520(4)
Pd(1)-Cl(1)	2.3203(6)	N(2)-C(7)	1.497(3)

N(2)-C(12)	1.502(3)	C(7)-N(2)-C(12)	113.71(18)
N(2)-C(8)	1.506(3)	C(7)-N(2)-C(8)	107.9(2)
C(1)-C(2)	1.519(3)	C(12)-N(2)-C(8)	110.0(2)
C(2)-C(3)	1.517(4)	C(7)-N(2)-Pd(1)	105.71(16)
C(3)-C(4)	1.528(4)	C(12)-N(2)-Pd(1)	109.04(16)
C(4)-C(5)	1.547(4)	C(8)-N(2)-Pd(1)	110.40(14)
C(5)-C(6)	1.538(4)	N(1)-C(1)-C(2)	115.10(19)
C(6)-C(15)	1.526(4)	C(3)-C(2)-C(1)	108.9(2)
C(6)-C(7)	1.532(4)	C(2)-C(3)-C(4)	108.3(2)
C(8)-C(9)	1.525(4)	C(3)-C(4)-C(5)	112.9(2)
C(9)-C(10)	1.521(4)	N(1)-C(5)-C(6)	110.6(2)
C(10)-C(11)	1.515(4)	N(1)-C(5)-C(4)	114.8(2)
C(11)-C(12)	1.540(4)	C(6)-C(5)-C(4)	108.8(2)
C(12)-C(13)	1.540(4)	C(15)-C(6)-C(7)	109.5(2)
C(13)-C(14)	1.519(4)	C(15)-C(6)-C(5)	110.2(2)
C(13)-C(15)	1.541(4)	C(7)-C(6)-C(5)	114.6(2)
Cl(3)-C(16)	1.777(4)	N(2)-C(7)-C(6)	113.1(2)
Cl(4)-C(16)	1.752(4)	N(2)-C(8)-C(9)	114.5(2)
		C(10)-C(9)-C(8)	110.6(3)
N(1)-Pd(1)-N(2)	87.63(7)	C(11)-C(10)-C(9)	107.9(2)
N(1)-Pd(1)-Cl(2)	174.44(7)	C(10)-C(11)-C(12)	114.0(3)
N(2)-Pd(1)-Cl(2)	94.93(6)	N(2)-C(12)-C(13)	111.0(2)
N(1)-Pd(1)-Cl(1)	94.60(5)	N(2)-C(12)-C(11)	114.1(2)
N(2)-Pd(1)-Cl(1)	175.87(7)	C(13)-C(12)-C(11)	108.6(2)
Cl(2)-Pd(1)-Cl(1)	83.16(2)	C(14)-C(13)-C(12)	115.3(2)
C(14)-N(1)-C(1)	108.1(2)	C(14)-C(13)-C(15)	108.1(3)
C(14)-N(1)-C(5)	113.84(18)	C(12)-C(13)-C(15)	110.5(2)
C(1)-N(1)-C(5)	109.3(2)	N(1)-C(14)-C(13)	113.8(2)
C(14)-N(1)-Pd(1)	108.28(18)	C(6)-C(15)-C(13)	106.74(19)
C(1)-N(1)-Pd(1)	111.34(13)	Cl(4)-C(16)-Cl(3)	112.21(18)
C(5)-N(1)-Pd(1)	106.03(16)		

## APPENDIX 4.12

*Tabulation of Palladium Alkoxide Structures Possessing  
 $\beta$ -Hydrogens Reported in the Cambridge Structural Database<sup>1</sup>*



- 
- <sup>1</sup> **298:** Bouquillon, S.; du Moullinet d'Hardemare, A.; Averbuch-Pouchot, M.-T.; Henin, F.; Muzart, J.; Durif, M. *Acta Crystallogr., Sect. C: Cryst. Struct. Commun.* **1999**, *55*, 2028-2030. **299:** Achternbosch, M.; Klufers, P. *Acta Crystallogr., Sect. C: Cryst. Struct. Commun.* **1994**, *50*, 175-178. **300, 301:** Hubel, R.; Polborn, K.; Beck, W. *Eur. J. Inorg. Chem.* **1999**, 471-482. **302:** Kapteijn, G. M.; Grove, D. M.; van Koten, G.; Smeets, W. J. J.; Spek, A. L. *Inorg. Chim. Acta* **1993**, *207*, 131-134. **303:** Klufers, P.; Kunte, T. *Angew. Chem. Int. Ed.* **2001**, *40*, 4210-4212. **304:** Kastele, X.; Klufers, P.; Kunte, T. *Z. Anorg. Allg. Chem.* **2001**, *627*, 2042-2044. **305, 306:** Kapteijn, G. M.; Baesjou, P.; Alsters, P. L.; Grove, D. M.; Smeets, W. J. J.; Kooijman, H.; Spek, A. L.; van Koten, G. *Chem. Ber.* **1997**, *130*, 35-44. **307:** Kapteijn, G. M.; Dervisi, A.; Grove, D. M.; Kooijman, H.; Lakin, M. T.; Spek, A. L.; van Koten, G. *J. Am. Chem. Soc.* **1995**, *117*, 10939-10949. **308, 309, 310:** Ahlrichs, R.; Ballauff, M.; Eichkorn, K.; Hanemann, O.; Kettenbach, G.; Klufers, P. *Chem.-Eur. J.* **1998**, *4*, 835-844. **311:** Klufers, P.; Kunte, T. *Eur. J. Inorg. Chem.* **2002**, 1285-1289.